NOVEL FLAVIN CHEMISTRY INVOLVED IN THE BIOSYNTHESIS OF THE LOWER LIGAND OF VITAMIN B$_{12}$

A Dissertation

by

PREM KUMAR CHANANI

Submitted to the Office of Graduate and Professional Studies of
Texas A&M University
in partial fulfillment of the requirements for the degree of

DOCTOR OF PHILOSOPHY

Chair of Committee,	Tadhg P. Begley
Committee Members,	Frank M. Raushel
	David P. Barondeau
	Paul D. Straight
Head of Department,	Simon W. North

December 2017

Major Subject: Chemistry

ABSTRACT

Vitamin B_{12} or Cobalamin is structurally the most complex of all the vitamins. The entire biosynthetic pathway of cobalamin is well studied except the formation of the lower ligand known as dimethylbenzimidazole (DMB).

In aerobic pathway, BluB catalyzes the formation of DMB using reduced flavin mononucleotide ($FMNH_2$) as its substrate leading to the formation of DMB and erythrose-4-phosphate as the end products. It is a remarkable transformation, wherein, C2 of DMB is derived from C1' of the ribose sugar chain of FMN. However, the fate of the ring C of FMN moiety as well as the overall mechanism of this unique reaction is still unknown. Thus, identification of the final unknown product and a detailed mechanistic study of dimethylbenzimidazole formation is the main focus of this work.

In this dissertation, we have successfully identified alloxan as the end product derived from the third ring of FMN. Water and molecular oxygen have been shown to be the two sources of oxygen atom incorporation in alloxan based on O-18 labeling studies.

A key intermediate in our mechanistic proposal has been successfully trapped in the form of six different shunt products using water, bisulfite and hydride as nucleophiles. Trapping of this intermediate helps us establish that the C-C bond cleavage occurs first forming erythrose-4-phosphate followed by the release of alloxan. Asp-32 has been shown to play an important role in stabilizing this intermediate

Based on stereochemical studies, we have shown that the *pro*-R hydrogen is selectively abstracted from the C1' of the ribityl chain of the substrate. This result helps us

establish that the final oxidation step involved in DMB formation is indeed catalyzed by the enzyme. Formation of a new shunt product was observed on using 8-substituted flavins as substrate analogs for the BluB catalyzed reaction. Characterization of this shunt product provides evidence for the initial fragmentation of the peroxyflavin intermediate involved in the DMB biosynthesis.

All these above observations are consistent with our current mechanistic proposal for the DMB formation. Thus, we have finally unraveled the long unsolved mystery in the Vitamin B_{12} biosynthesis.

To my parents and my wife…..

ACKNOWLEDGEMENTS

First and foremost, I would like to thank my research advisor Dr. Tadhg P. Begley for his continuous guidance and support throughout the course of my research. Thanks a lot, Tadhg for providing me the opportunity to work on this challenging project and the freedom to explore all my thoughts and ideas.

I would also like to acknowledge my committee members, Dr. Frank Raushel, Dr. David Barondeau and Dr. Paul Straight for their valuable advice and insights during all the committee meetings and presentations.

I would like to thank all the Begley group members for being such wonderful colleagues and making my PhD life such a memorable one. Thanks for all the valuable feedback and suggestions on my research. I express my deepest gratitude to Dr. Dinuka Abeydeera and Dr. Bekir Eser for training me during my initial period and for being such amazing mentors. I am thankful to Dr. Sameh Abdelwahed for synthesizing the flavin isotopologues and the initial NMR studies.

I would like to extend my gratitude to Taga group at UC Berkeley for providing me the constructs of BluB and its various mutants. I would also like to thank White group at Virginia Tech and Liu group at UT Austin for providing me the plasmids of the enzymes required for the synthesis of the flavin analogs.

Thanks to all my friends and colleagues and the department faculty and staff for making my time at Texas A&M University such a great experience.

I am really grateful to my parents and my brother for all their encouragement and support. Lastly and most importantly, I am extremely grateful to my wife Sneha for her patience and love. Thanks Sneha for making my research life such a smooth journey. All this would not have been possible without your love and support. Thanks for being by my side for all these years and for many more to come.

CONTRIBUTORS AND FUNDING SOURCES

NOMENCLATURE

FMN	Flavin Mononucleotide
DMB	Dimethylbenzimidazole
FAD	Flavin Adenine Dinucleotide
CIP	Calf Intestinal Phosphatase
CTP	Cytidine Triphosphate
ATP	Adenosine Triphosphate
oPDA	*o*-Phenylenediamine
PFBHA	*o*-(pentafluorobenzyl)hydroxylamine
NADH	Nicotinamide Adenine Dinucleotide (Reduced form)
SAM	S-Adenosyl-L-methionine
NMR	Nuclear Magnetic Resonance
EIC	Extracted Ion Chromatogram
HPLC	High Performance Liquid Chromatography
LC-MS	Liquid Chromatography Mass Spectroscopy

TABLE OF CONTENTS

LIST OF FIGURES

xv

LIST OF TABLES

INTRODUCTION

1.1 Vitamin B$_{12}$

Vitamin B$_{12}$ or Cobalamin (1) is structurally the most complex of all the vitamins and one of the largest non-polymeric natural products[1,2]. The core consists of a modified tetrapyrrole ring, known as the corrin ring, with a cobalt ion chelated at its center (Figure 1). The cobalt ion is coordinated to the four nitrogen atoms of the pyrrole rings along with two other ligands. The upper axial ligand varies, wherein, 5$^{'}$-deoxyadenosyl (adenosylcobalamin), methyl (methylcobalamin) and cyano (cyanocobalamin) groups are usually seen. The lower ligand, covalently attached to the corrin ring by a nucleotide loop, is generally 5,6-dimethylbenzimidazole (DMB).
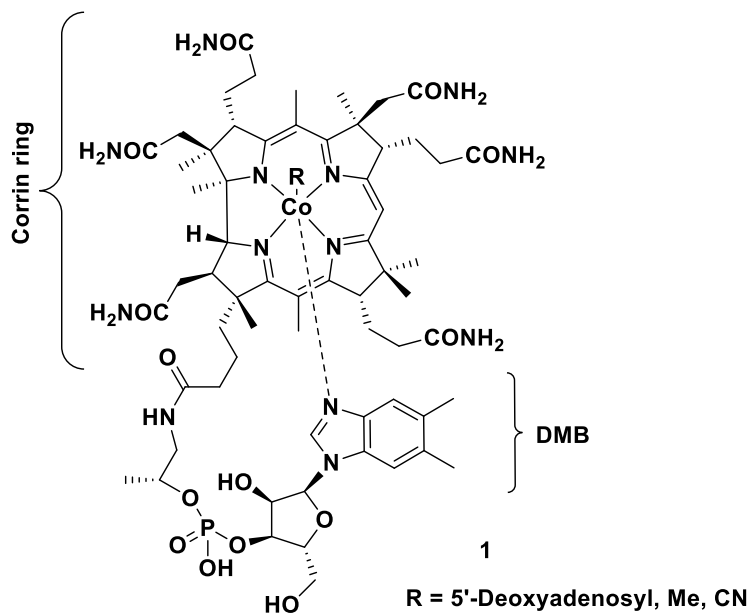
Figure 1. Structure of Vitamin B$_{12}$

Vitamin B_{12} plays a vital role in the proper functioning of the brain and nervous system and is also involved in the fatty and amino acid metabolism. Deficiency of cobalamin leads to pernicious anemia. It is an autoimmune disease in which the parietal cells of the stomach are destroyed. These parietal cells are responsible for secreting the intrinsic factor which plays a major role in the absorption of vitamin B_{12}. Thus, a lack of intrinsic factor leads to vitamin B_{12} deficiency resulting in pernicious anemia.

Cobalamin also acts as an essential co-factor in several enzyme catalyzed reactions. Currently, the B_{12}-dependent enzymes are broadly classified into three groups: isomerases, methyltransferases and dehalogenases[3]. Two of the most notable examples in which vitamin B_{12} acts as a co-factor are shown below in Figure 2.

1. Methylmalonyl CoA mutase: Catalyzes the isomerization of methylmalonyl CoA to succinyl CoA.

2. Methionine synthase: Catalyzes the synthesis of methionine from homocysteine.
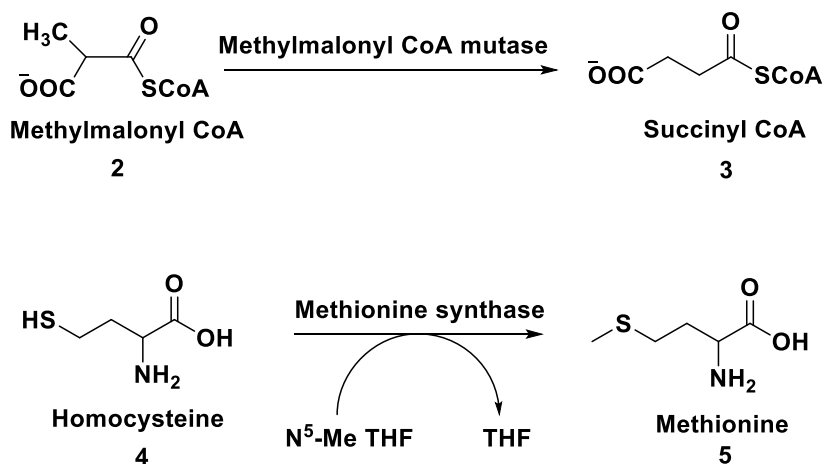
Figure 2. Examples of Vitamin B_{12}-dependent enzymes

1.2 Biosynthesis of dimethylbenzimidazole (DMB)

The entire biosynthetic pathway of cobalamin is well studied except the formation of DMB which is the last unsolved puzzle in vitamin B_{12} biosynthesis[4-8]. Recently, it has been shown that in anaerobic organisms, BzaF is involved in the biosynthesis of benzimidazole[9-12]. BzaF is a radical SAM enzyme which catalyzes the formation of 5-hydroxybenzimidazole (5-HBI, 7) from aminoimidazole ribotide (AIR, 6) (Figure 3)[13,14].
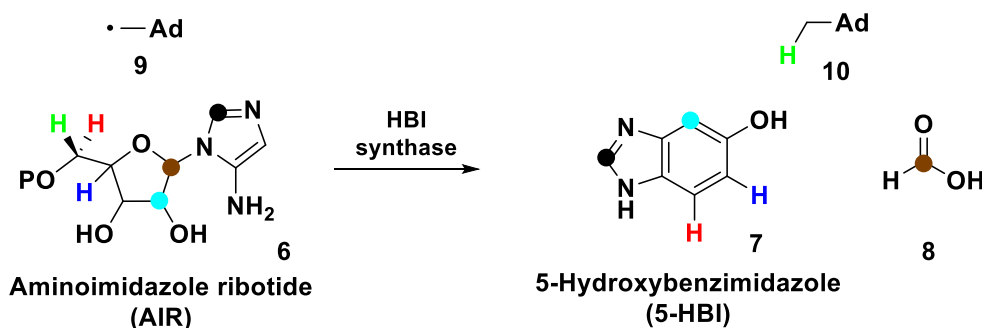
Figure 3. BzaF catalyzed conversion of AIR to 5-HBI

In the aerobic pathway, BluB has been identified as the enzyme which catalyzes the formation of dimethylbenzimidazole (DMB) using reduced flavin mononucleotide (FMNH$_2$, 12) as its substrate[15-17]. BluB catalyzes the unprecedented fragmentation of the flavin molecule in the presence of oxygen leading to the formation of DMB (13) and erythrose-4-phosphate (14) as the end products (Figure 4)[18,19]. It is a remarkable transformation, wherein, C2 of DMB is derived from C1' of the ribose sugar chain of FMN (shown as a black circle) based on previous labeling studies[20-24].
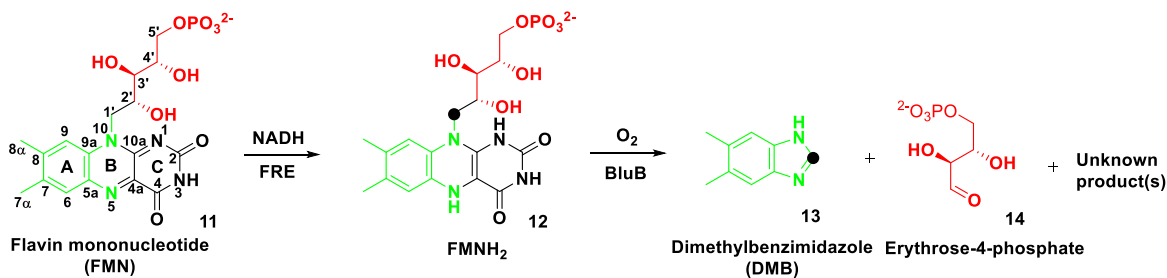
Figure 4. Scheme for BluB catalyzed DMB formation

1.3 Active site structure of BluB

The crystal structure of BluB (PDB code: 2ISL) shows a close resemblance to the flavin oxidoreductase and nitroreductase enzyme superfamily having conserved active site residues[25,26]. In striking contrast to the oxidoreductases and nitroreductases, the active site of BluB consists of an extended lid which completely sequesters FMN from the external solvent. Such a structural motif is also seen in the iodotyrosine deiodinase (IYD) which carries out reductive dehalogenation using reduced FMN (FMNH$_2$) as a cofactor[27]. Though structurally similar, BluB shows completely different function as compared to oxidoreductase, nitroreductase and IYD[28,29].

The key active site residues of BluB and their interactions with the substrate FMNH$_2$ are shown in Figure 5[30]. The phosphate group forms H-bonds with the residues Arg-30 and Arg-31. The active site of BluB consists of residues which are conserved among the BluB orthologs but are absent in oxidoreductases. Asp-32 and Ser-167 are two such residues which are very critical for the catalytic activity of BluB and mutation of these residues results in loss of activity. Oxidoreductase, nitroreductase and IYD enzymes generally have a serine or arginine residue to stabilize the N1 of FMN by H-bonding. In

4

BluB, however, along with Arg-34 there is also Asp-32 which is in proximity to N1 of FMN as well as C1$'$ of the ribityl chain. Ser-167 forms hydrogen bonding with N5 of flavin in the BluB active site. Such an interaction is also seen in IYD where the serine is replaced by threonine. Interestingly, mutation of threonine to alanine in IYD results in a switch of its functionality from being a dehalogenase to a nitroreductase[31]. In oxidoreductases, however, hydrogen bonding to N5 of flavin is achieved by the protein amide backbone. The nature of H-bonding to N5 of flavin, thus, seems to dictate the function carried out by the enzyme. H-bonding between N5 and amide backbone leads to two-electron reduction chemistry (oxidoreductases and nitroreductases) while the bonding with a side chain hydroxyl group results in a one-electron chemistry (BluB and IYD)[32].
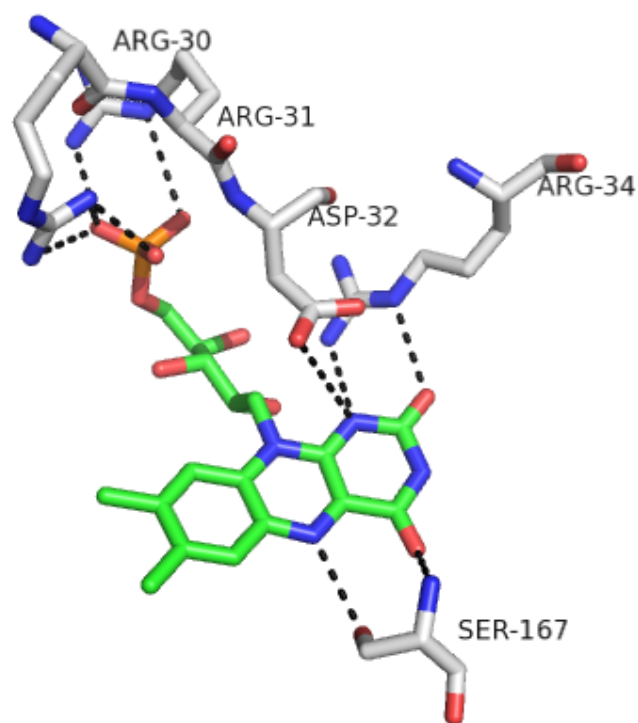
Figure 5. Active site structure of BluB

1.4 Mechanistic proposals for dimethylbenzimidazole formation in the literature

BluB is a unique enzyme, wherein, fragmentation of one cofactor leads to another. The overall transformation from FMN to DMB represents a very complex and unusual reaction. Two mechanistic hypotheses have been proposed in the literature for this remarkable rearrangement[15].

Mechanism A:
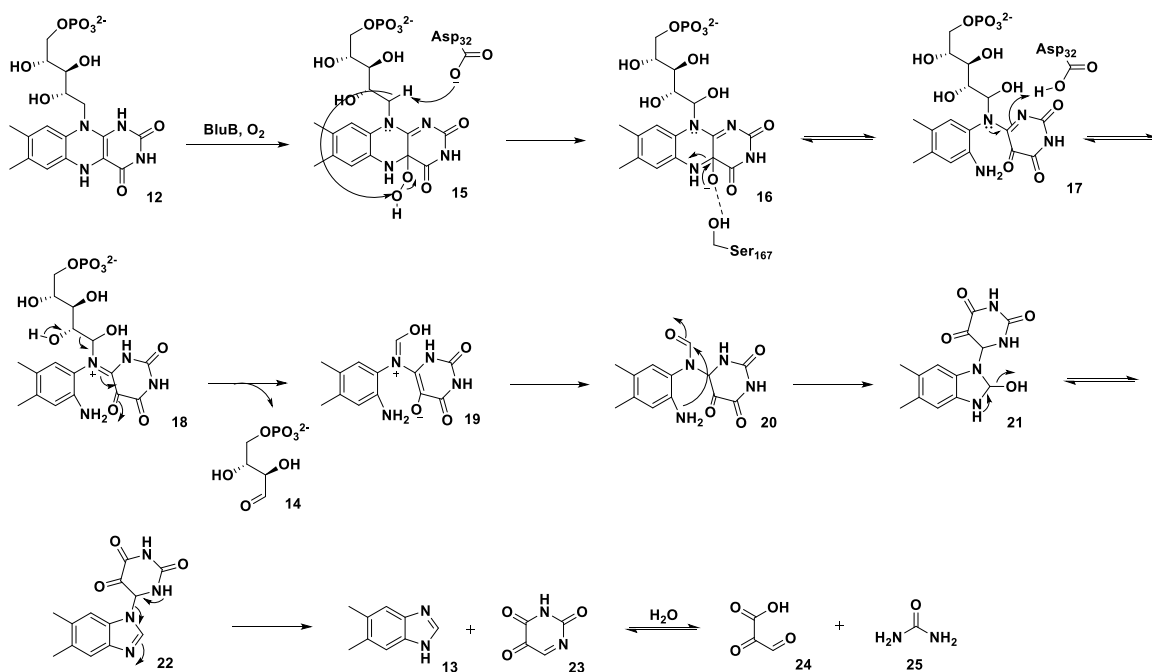
Figure 6. Mechanistic proposal (A) for DMB formation[15]

In mechanism A, the flavin initially reacts with O_2 to form the flavin hydroperoxide (15) which then undergoes hydroxylation at C1' of the ribityl chain assisted by the deprotonation at C1' using the Asp-32 residue (Figure 6). This seems to be a difficult step as hydroxylation at C1' requires a significant conformational change in the active site as

well as the Asp-32 does not appear to be a strong enough base. This hydroxylation step is then followed by the Ser-167 mediated fragmentation of the flavin molecule to form intermediate 17 which then tautomerizes and undergoes C-C bond cleavage between the C1' and C2' of the ribose sugar chain in a retro-aldol fashion forming species 19 and erythrose-4-phosphate (14). The intermediate 19 then cyclizes and ultimately leads to the formation of DMB (13).

Mechanism B:
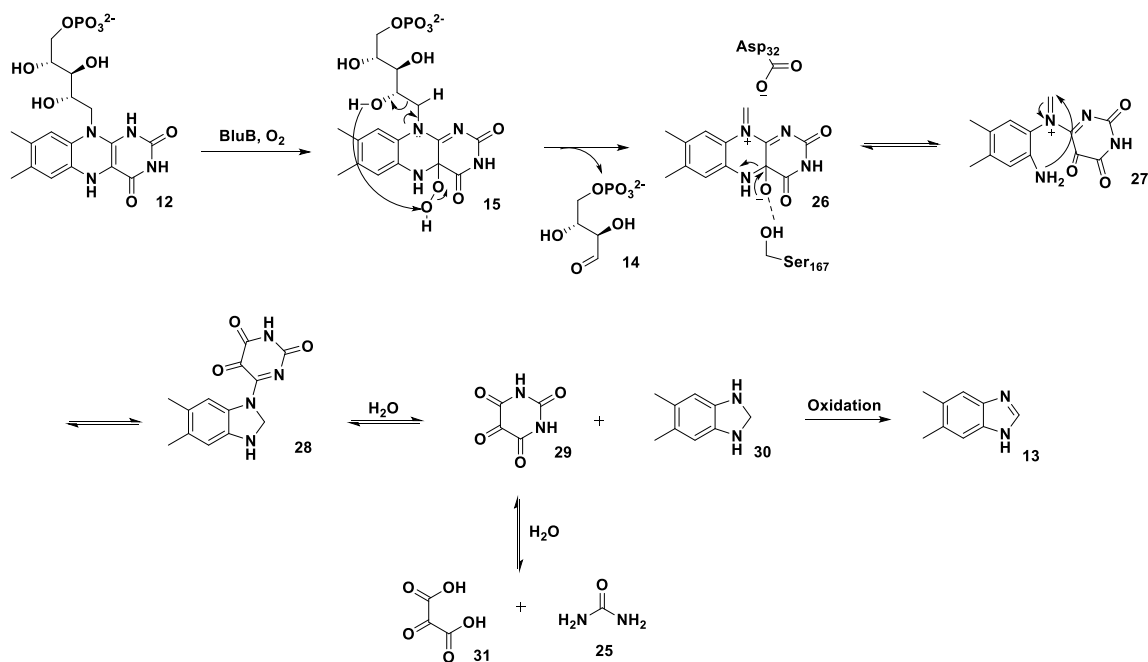
Figure 7. Mechanistic proposal (B) for DMB formation[15]

In mechanism B, the flavin hydroperoxide (15) formed initially is proposed to undergo fragmentation by a hydride transfer from the hydroxyl group at C2' of the ribityl tail leading to the C1' -C2' bond cleavage (Figure 7). Such a hydride transfer is

7

unprecedented, and even the hydroxyl groups are not known to form hydride ions as proposed in this mechanism. This unusual step leads to the formation of erythrose-4-phosphate (14) and the intermediate 26. Asp-32 has been suggested to play a key role in stabilizing the positive charge at C1'position in 26 or the stabilization of the transition state leading to 26. The intermediate 26 is transformed to 27 with the assistance of Ser-167 which then undergoes cyclisation to yield the species 28. Hydrolysis of 28 leads to the formation of alloxan (29) and intermediate 30 which finally undergoes oxidation to yield DMB (13).

The first step in both the above proposals is the formation of the flavin hydroperoxy species (15) from the substrate $FMNH_2$ in the presence of O_2. However, the subsequent fragmentation of the flavin peroxy moiety involves unusual steps which seem to be very challenging in both these mechanisms. Due to this limitation, a third alternate mechanism (Figure 8) has been proposed in the literature based on model chemistry[33,34].

In this proposal, the peroxy flavin (15) undergoes Baeyer-Villiger rearrangement to form the intermediate 32 followed by repeated hydrolysis to form 33. 33 undergoes 2-electron oxidation forming the bisimine (34) followed by a retro-aldol C-C bond cleavage to form 35[35]. Cyclisation followed by oxidation leads to DMB (13) formation.

Mechanism C:
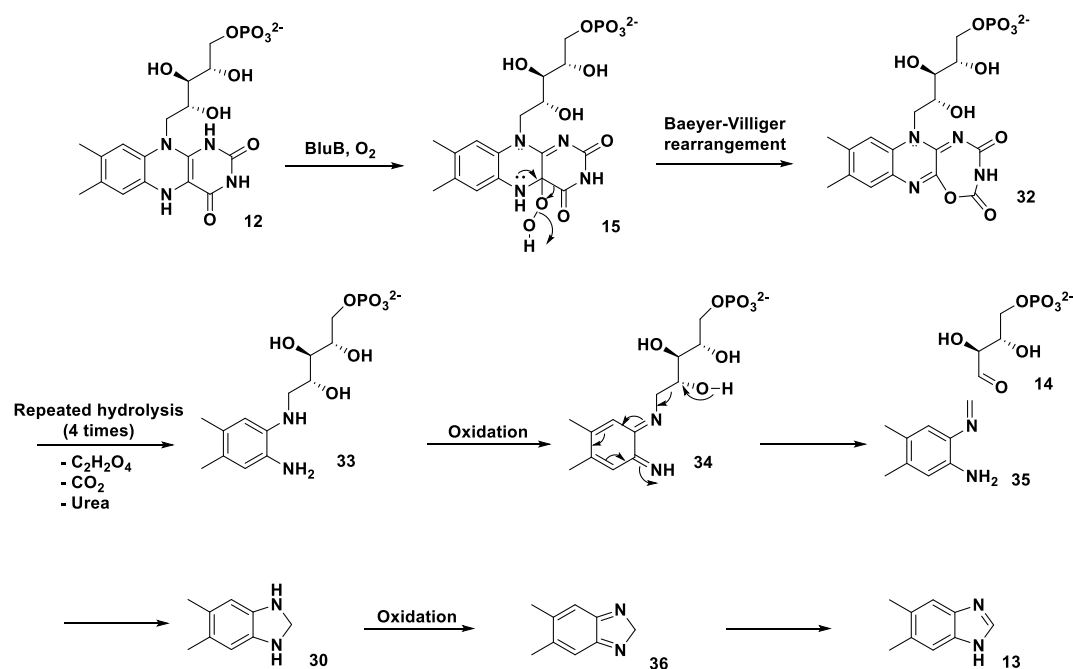
Figure 8. Mechanistic proposal (C) for DMB formation[33,35]

1.5 Research opportunity

Three mechanisms exist in the literature for the BluB catalyzed DMB formation based on the labeling studies and crystal structure. However, the fate of the ring C of the FMN moiety is still unknown, and a complete mechanistic characterization is still desired for this unique transformation.

CHAPTER II

IDENTIFICATION AND CHARACTERIZATION OF THE UNKNOWN PRODUCT

IN THE BLUB CATALYZED REACTION

2.1 Introduction

In aerobic organisms, BluB is involved in the biosynthesis of dimethylbenzimidazole (DMB) using reduced FMN ($FMNH_2$) as its substrate. Oxygen is utmost necessary for the catalytic activity of BluB leading to the formation of DMB and erythrose-4-phosphate as the end products. However, the product(s) derived from the third ring of FMN are still unknown. In the last chapter, we have discussed the three mechanistic hypotheses which have been proposed in the literature for this complex reaction. No evidence has been provided to substantiate these proposals. Thus, along with the identification of the product(s) arising from the third ring of FMN, a detailed study is required to investigate the mechanism of DMB biosynthesis.

2.2 Results and Discussion

2.2.1 Identification of the unknown product(s) based on NMR studies

^{13}C labeled FMN molecules, having the carbons in the third ring as ^{13}C labeled, were designed to figure out the product(s) derived from the ring C of FMN[36]. Thus, three different ^{13}C FMN isotopologues were synthesized: 4a-^{13}C FMN, 2-^{13}C FMN and 4,10a-^{13}C FMN (Figure 9)[37].
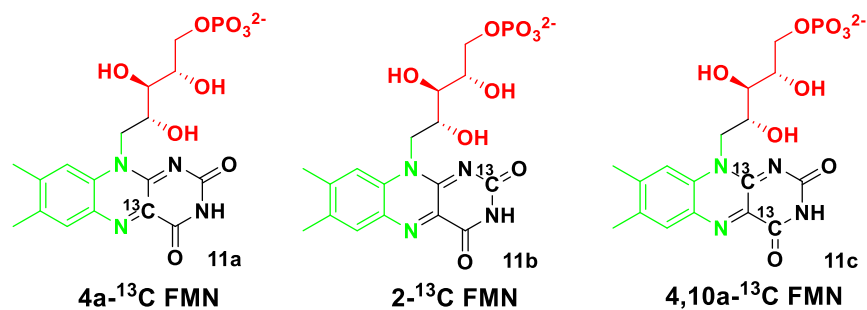
Figure 9. Various ^{13}C FMN isotopologues synthesized

Next, BluB enzymatic reactions were carried out using isotopically labeled FMN as substrate, and the reaction mixture was analyzed by ^{13}C NMR spectroscopy (Figure 10). A new peak was observed at 85.3 ppm in ^{13}C NMR on using [4a-^{13}C] FMN as substrate (Figure 10A). When [2-^{13}C] FMN was used, a new peak was seen at 159.5 ppm (Figure 10B) while on using [4,10a-^{13}C] FMN two new peaks were observed at 171 and 177 ppm (Figure 10C). Several compounds were tested as possible candidates for the new product derived from the ring C such as urea, bicarbonate, oxalic acid, alloxan, alloxanic acid and dialuric acid. Finally, alloxanic acid (37) was found as the unknown product as its ^{13}C NMR spectra aligned exactly with the spectra obtained in case of BluB reactions (Figure 10D). This was further confirmed by spiking the reaction mixture with the alloxanic acid standard (Figure 10E). Thus, alloxanic acid seemed to be the final unknown product in the BluB catalyzed reaction based on the NMR results.
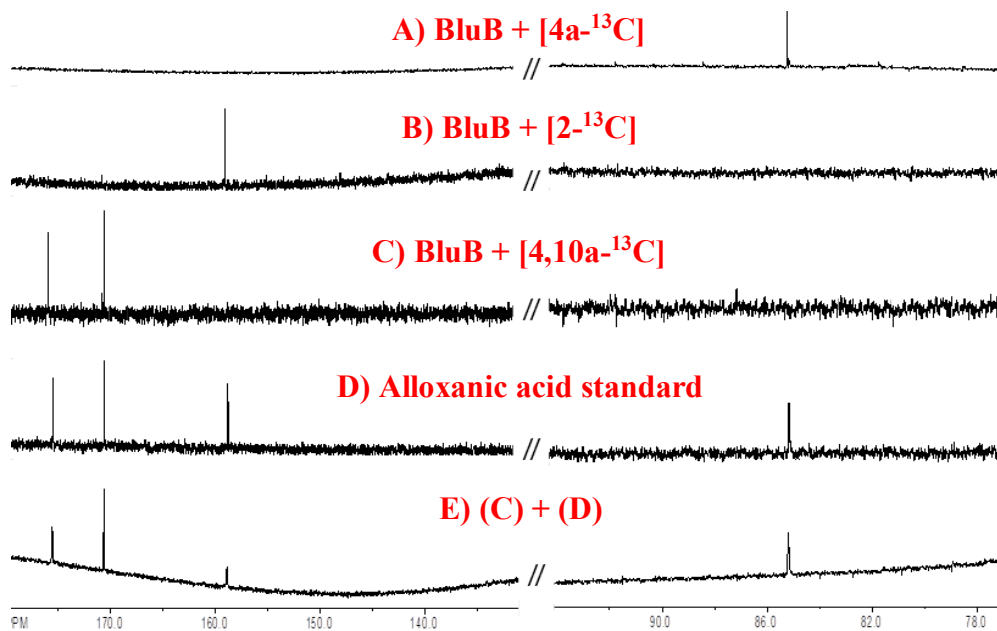
Figure 10. ^{13}C NMR spectra of BluB catalyzed reactions. **(A)** Enzymatic reaction using [4a-^{13}C] FMN **(B)** Enzymatic reaction using [2-^{13}C] FMN **(C)** Enzymatic reaction using [4,10a-^{13}C] FMN **(D)** Alloxanic acid standard **(E)** Enzymatic reaction using [4,10a-^{13}C] FMN spiked with alloxanic acid standard

2.2.2 Identification of the unknown product by derivatization reaction

Alloxan (29) has been reported in the literature to readily undergo rearrangement to alloxanic acid (37) under alkaline conditions (Figure 11)[38-40].
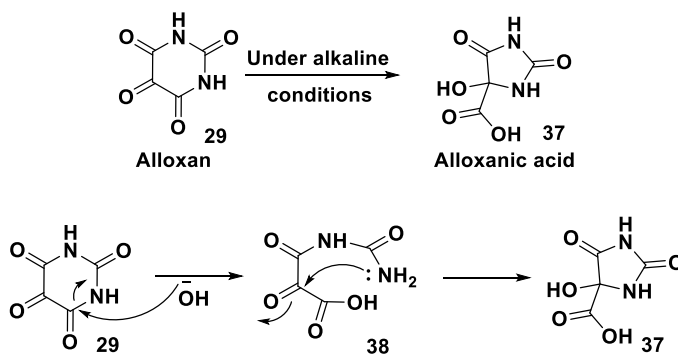
Figure 11. Mechanism of rearrangement of alloxan (29) to alloxanic acid (37)

12

The pH of the phosphate buffer used in our enzymatic reactions was 7.5 which is sufficient to facilitate the rearrangement of alloxan to alloxanic acid. So, the question we had to address was whether alloxan or alloxanic acid is the actual end product of the BluB catalyzed reaction. Alloxan can be easily trapped in the form of an adduct (40) using derivatizing agents such as o-phenylenediamine (oPDA, 39) (Figure 12).
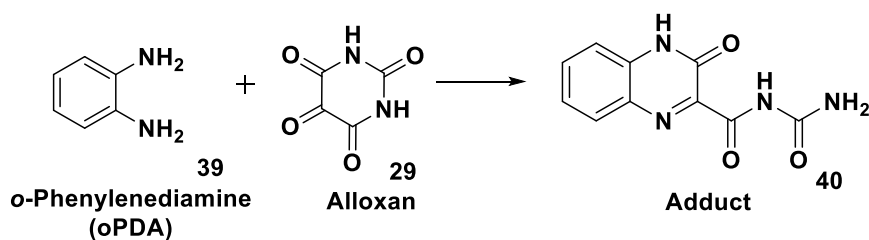
Figure 12. Trapping of alloxan using o-phenylenediamine (oPDA)

Next, enzymatic reactions were carried out in the presence of oPDA and were analyzed for the formation of the alloxan-oPDA adduct. Adduct formation was seen only in case of reaction carried out in the presence of oPDA (blue trace in the HPLC chromatogram, Figure 13A) and was absent in all the controls as well in the reaction carried out in the absence of oPDA (black trace). Formation of the alloxan-oPDA adduct was further confirmed by conducting coelution studies with the synthesized standard (Figure 13B) and by LC-MS analysis (Figure 14)[41].
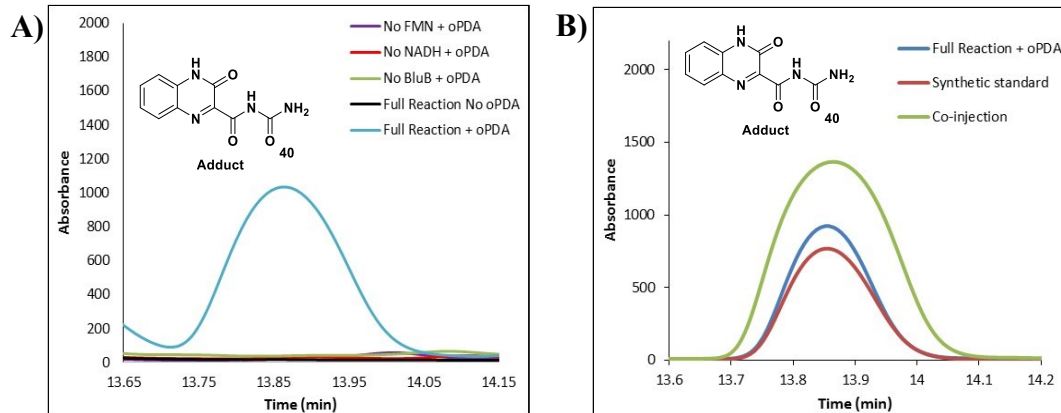
Figure 13. HPLC analysis of BluB catalyzed reactions in presence of *o*-phenylenediamine (oPDA). **(A)** Formation of alloxan-oPDA adduct (40) seen only in case of full reaction carried out in presence of oPDA **(B)** Coelution data for the alloxan-oPDA adduct (40) formation
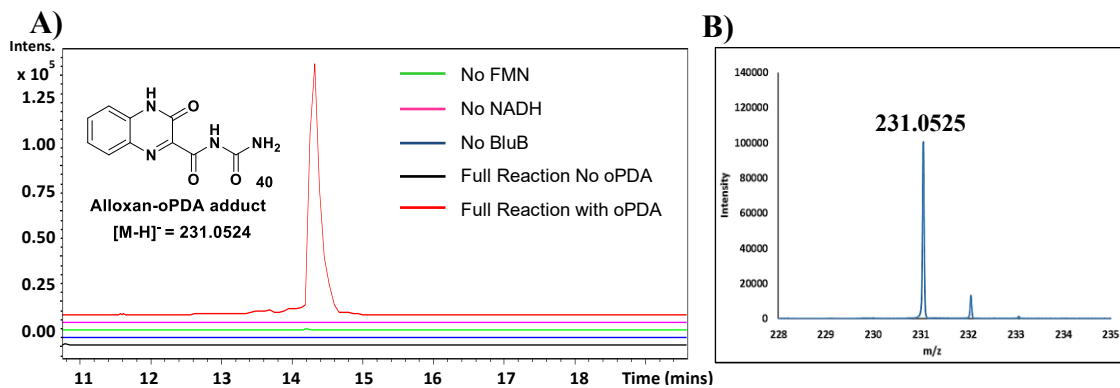
Figure 14. LC-MS analysis of BluB catalyzed reaction in presence of *o*-phenylenediamine (oPDA). **(A)** Extracted Ion Chromatogram (EIC) at m/z 231.0524 showing the formation of alloxan-oPDA adduct only in case of full reaction carried out in presence of oPDA (Red trace) **(B)** ESI-MS of 40 in the negative mode

Based on the results of the derivatization assays using oPDA, we can conclude that alloxan (29) is the actual end product of the BluB catalyzed reaction and was just rearranged to form alloxanic acid (37) in our NMR studies.

Alloxan, being the final end product, has been proposed in only one of the three mechanisms postulated in the literature. In only mechanism B, alloxan has been suggested as the final product though no evidence has been provided for such a proposal while the mechanisms A and C have hypothesized different end products. Identification of alloxan, thus, rules out the mechanisms A and C of the literature. Though mechanism B proposes alloxan as one of the products, the hydride transfer involved in the fragmentation of the flavin peroxy moiety seems to be a difficult step which makes this mechanism implausible.

2.2.3 Trapping of the sugar product, erythrose-4-phosphate (14)

Formation of DMB involves the cleavage of the ribose side chain. The ribose-derived fragment was previously identified as erythrose-4-phosphate (14) by radio TLC and ^{31}P NMR analysis[15]. As radio TLC is a low-resolution separation technique, the analysis was repeated using high resolution LC-MS to be certain of the stereochemical assignment as this is important for the mechanistic analysis. The carbohydrate product was trapped as an oxime using *o*-(pentafluorobenzyl)hydroxylamine (PFBHA, 41) as the derivatizing agent (Figure 15). The corresponding oxime (42) formation was seen only in case of the full reaction and was also confirmed by its standard (Figure 16).
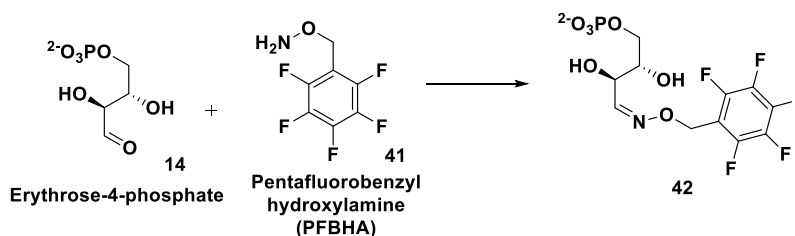
Figure 15. Trapping of erythrose-4-phosphate using PFBHA

15
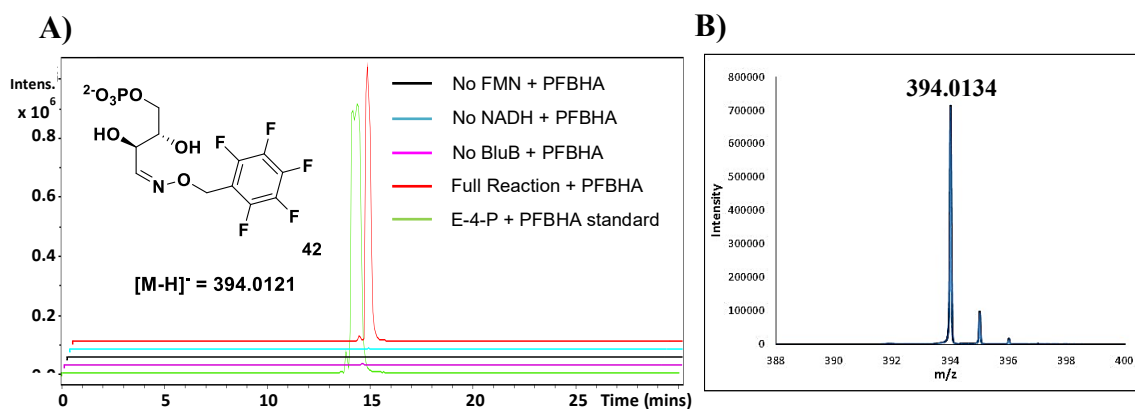
Figure 16. LC-MS analysis for the trapping of erythrose-4-phosphate. **(A)** Extracted Ion Chromatogram (EIC) at m/z 394.0121 corresponding to erythrose-4-phosphate-PFBHA oxime (42) **(B)** ESI-MS of 42 in the negative mode

Thus, the complete scheme for the DMB formation is as illustrated in Figure 17.
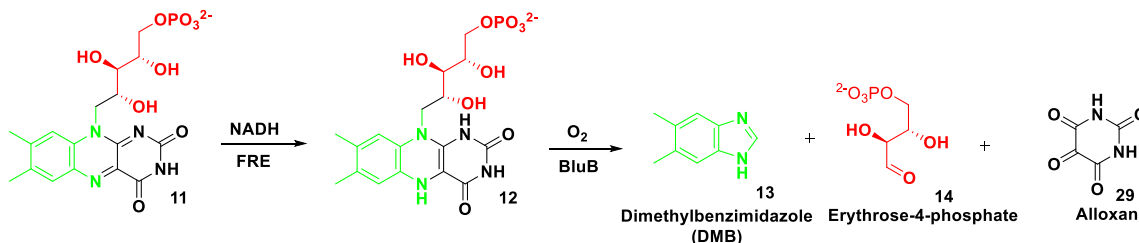
Figure 17. Complete scheme for the formation of Dimethylbenzimidazole

2.2.4 O-18 labeling studies for the source of oxygen incorporation in alloxan

The end product alloxan formed has two additional oxygen atoms incorporated in it as compared to the starting material, FMN. On carrying out the enzymatic reaction in the presence of $^{18}O_2$ gas, no O-18 incorporation was seen in the alloxan-oPDA adduct. However, when the reaction was performed using $H_2^{18}O$ buffer, a 2 Da increase in the

mass of the adduct was observed implying that one of the oxygen atoms in the alloxan is incorporated from water (Figure 18).
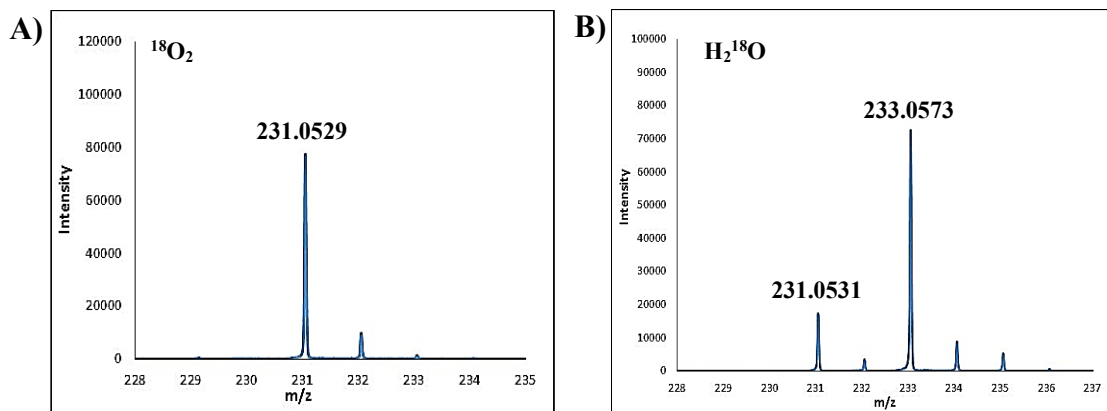
Figure 18. LC-MS analysis of BluB reaction in **(A)** $^{18}O_2$ gas and **(B)** $H_2{}^{18}O$ buffer

We propose that one of the oxygen atoms in alloxan comes from water (atom labeled in pink) whereas the other one is incorporated from oxygen gas (atom labeled in blue) (Figure 19).
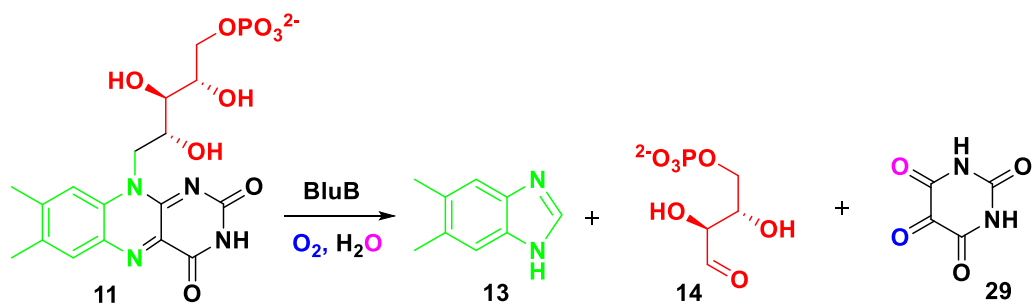
Figure 19. O-18 labeling pattern in alloxan

However, no O-18 incorporation was seen in the adduct on carrying out the reaction using $^{18}O_2$ gas. This result can be attributed to the fact that on trapping alloxan using oPDA, an imine type intermediate (43) is formed first wherein the oxygen atom incorporated from oxygen gas is lost in the form of water. This intermediate further undergoes rearrangement to form the final adduct (40) in which the oxygen atom incorporated from water is still retained as seen in the mass data (Figure 20).
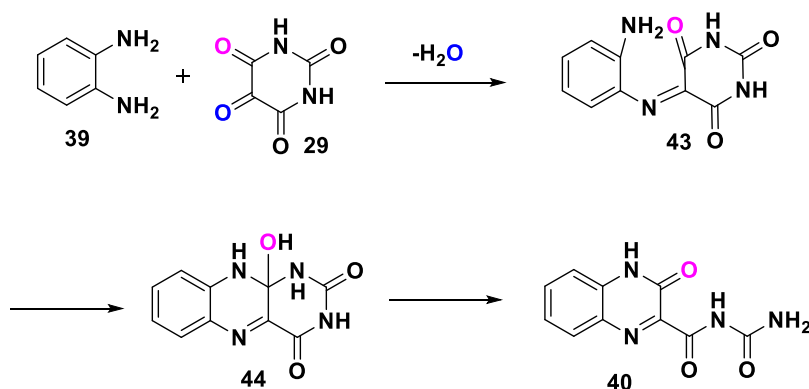
Figure 20. Mechanism of trapping of alloxan using *o*-phenylenediamine (oPDA)

2.2.5 Mechanistic proposal for DMB biosynthesis

Based on all these observations, our current mechanistic proposal for the DMB formation is as shown in Figure 21.

We propose that the reduced flavin (FMNH$_2$, 12) first reacts with molecular oxygen to form the well-characterized species flavin hydroperoxide (15). The flavin hydroperoxide then undergoes fragmentation to form species 46 via 45. The hydroxide released during the peroxide fragmentation (46 to 47) deprotonates the ribose alcohol and triggers a retro-aldol reaction leading to a C-C bond cleavage between the C1' and C2' of

18

the ribose sugar chain to form intermediate 27 with the subsequent release of erythrose-4-phosphate (14) as one of the end products. The species 27 then undergoes hydrolysis to form 48 followed by a C-N bond cleavage to form 35 and alloxan (29). Intermediate 35 finally undergoes cyclization forming 30 followed by oxidation to form the end product dimethylbenzimidazole (13).
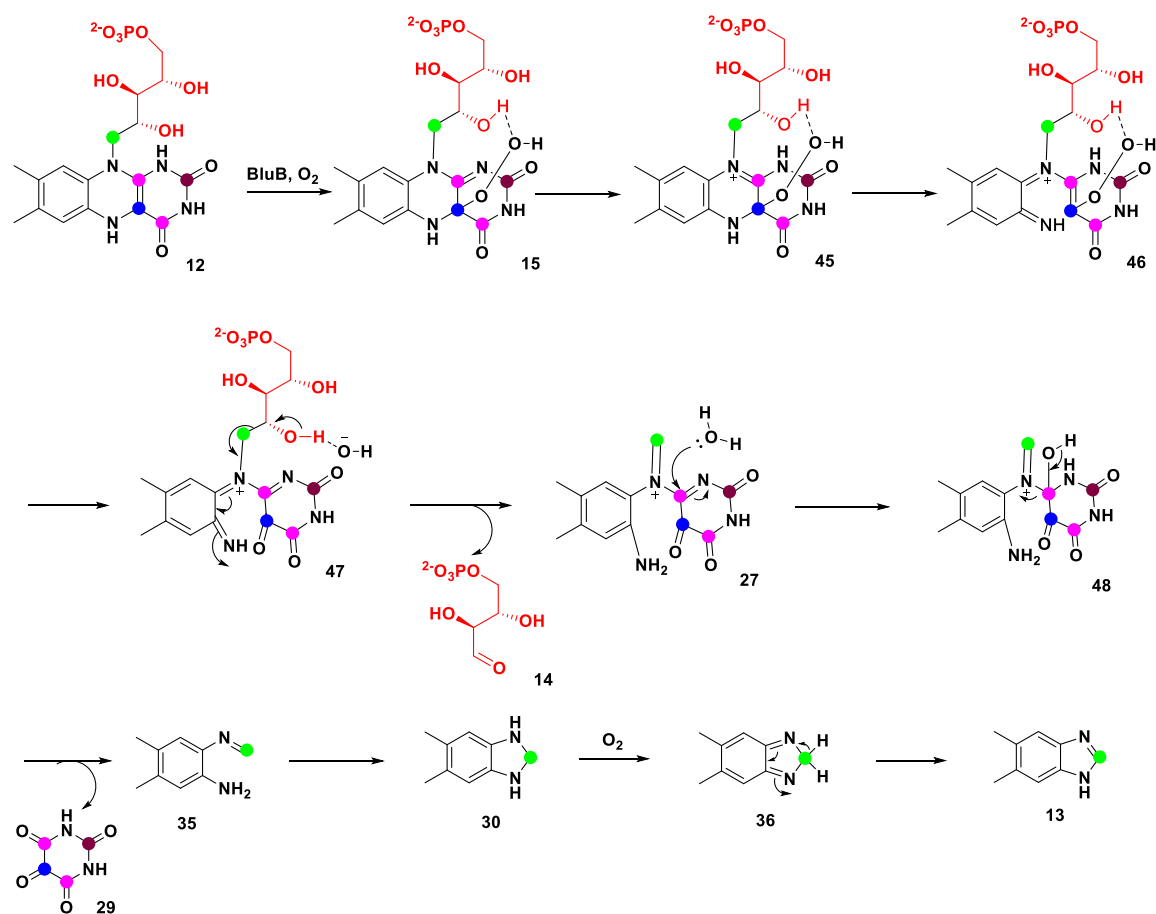
Figure 21. Mechanistic proposal for the formation of dimethylbenzimidazole

2.3 Conclusion

In this chapter, we have successfully identified alloxan as the final unknown product of the BluB catalyzed reaction. We have also been able to establish that water and molecular oxygen are the two sources of oxygen atom incorporation in alloxan. The sugar end product, erythrose-4-phosphate, has been trapped using PFBHA as the derivatizing agent. Finally, a mechanistic hypothesis has been proposed based on our results for the biosynthesis of dimethylbenzimidazole.

2.4 Experimental

2.4.1 Materials

All chemicals were purchased from Sigma-Aldrich unless mentioned otherwise. A dehydrated form of LB medium was purchased from EMD Millipore. IPTG, Kanamycin and Ampicillin were purchased from Lab Scientific Inc. HPLC and LCMS solvents were purchased from EMD and used without any further purification. Histrap column was obtained from GE Healthcare. Amicon ultra centrifugal filters (10,000 MWCO) were purchased from Millipore. Econo-Pack 10DG desalting columns were purchased from Bio-Rad. Protein overexpression was carried out in 2.5L baffled ultra yield flasks obtained from Thomson Instrument Company. $H_2{}^{18}O$ was purchased from Cambridge Isotope Laboratories. ZORBAX Eclipse XDB-C18 column (4.6 x 150 mm, 5μm particles) was obtained from Agilent Technologies.

2.4.2 Overexpression and purification of BluB

The BluB gene, cloned in pET11t vector, was transformed into *Escherichia coli* BL21 (DE3) cell line. A 10 mL starter culture was grown at 37 °C containing 100 μg/mL Ampicillin for 6 hrs. 1.5 liters of LB media was inoculated with this starter culture. The cells were grown at 37 °C with shaking till the OD_{600} reached 0.6. The protein expression was then induced by adding IPTG (final concentration 1 mM) and the culture was incubated at 15 °C for 15 hrs. The cells were then harvested by centrifugation and resuspended in 30 mL of binding buffer (50 mM phosphate buffer containing 150 mM NaCl, 10mM imidazole, pH 7.8). The cells were lysed by sonication followed by centrifugation at 15000 rpm for 45 mins. The supernatant containing the soluble protein was loaded on a Ni-NTA affinity column (Histrap-GE Healthcare) and was then washed with 50 mL of wash buffer (50 mM phosphate buffer containing 150 mM NaCl, 20mM imidazole, pH 7.8). The protein was eluted with the elution buffer (100 mM phosphate buffer containing 100 mM NaCl, 250 mM imidazole, pH 7.8). The eluted protein fractions were pooled and concentrated using 10kDa Amicon ultracentrifugal filters to a final volume of 3 mL. The concentrated protein solution was buffer exchanged into 100 mM phosphate buffer containing 150 mM NaCl and 15% glycerol, pH 7.8 using an Econo-Pac 10DG desalting column.

2.4.3 Over-expression and purification of Riboflavin kinase (RibK)[42,43]

The RibK gene, cloned in pT7-7 vector, was transformed into *Escherichia coli* BL21 (DE3) cell line. A 10 mL starter culture was grown at 37 °C containing 100 μg/mL

ampicillin for 6 hrs. 1.5 liters of LB media was inoculated with this starter culture. The cells were grown at 37 °C with shaking till the OD_{600} reached 0.6. The protein expression was then induced by adding IPTG (final concentration 1 mM) and the culture was incubated at 15 °C for 15 hrs. The cells were then harvested by centrifugation and resuspended in 30 mL of binding buffer (50mM KPi buffer containing 150 mM NaCl, 10mM imidazole, pH 7.8). The cells were lysed by sonication followed by centrifugation at 15000 rpm for 45 mins. The supernatant was heated at 70 °C and the solution was centrifuged. The supernatant containing the soluble protein was concentrated using 10kDa Amicon ultracentrifugal filters to a final volume of 3 mL. The concentrated protein solution was buffer exchanged into 100 mM KPi buffer containing 150 mM NaCl and 15% glycerol, pH 7.8 using an Econo-Pac 10DG desalting column.

2.4.4 HPLC parameters

An Agilent 1260 HPLC equipped with a quaternary pump was used. The system included a diode array UV-Vis detector and eluted compounds were detected using absorbance at 254, 280, 260, 450, 320 and 340 nm. Analysis was performed on a ZORBAX Eclipse XDB-C18 column (4.6 x 150 mm, 5 μm particles, Agilent Technologies).

2.4.5 HPLC conditions

A: Water

B: 10 mM ammonium acetate, pH 6.6

C: Methanol

2.4.6 HPLC method

The following gradient at a flow rate of 1 mL/min was used.

0 min: 90% A, 10% B; 2 min: 90% A, 10% B; 17 min: 15% A, 10% B, 75% C; 23 min: 15% A, 10% B, 75% C; 25 min: 90% A, 10% B; 30 min: 90% A, 10% B.

2.4.7 LC-MS parameters

LC-ESI-TOF-MS was performed using an Agilent 1260 HPLC system equipped with a binary pump and a 1200 series diode array detector followed by a MicroToF-Q II mass spectrometer (Bruker Daltonics) using an ESI source either in positive mode or negative mode. The analysis was performed on a Poroshell 120 EC-C18 column (3.0 x 100 mm, 2.7 μm particles, Agilent Technologies).

2.4.8 LC conditions

A: 5 mM ammonium acetate buffer, pH 6.6

B: 75% Methanol and 25% Water

2.4.9 LC method (for both positive and negative mode on MS)

The following gradient at a flow rate of 0.4 mL/min was used.

0 min: 100% A, 0% B; 2 min: 100% A, 0% B; 12 min: 25% A, 75% B; 17 min: 25% A, 75% B; 18.5 min: 100% A, 0% B; 30 min: 100% A, 0% B.

2.4.10 NMR studies of BluB catalyzed reactions

BluB enzymatic reactions were performed in 100 mM phosphate buffer, pH 7.5 containing BluB (100 μM), ^{13}C labeled FMN (300 μM) and dithionite. The enzymatic reactions were incubated at room temperature for 4 hrs. The protein was removed by heat denaturation and the reaction mixture was analyzed by ^{13}C NMR.

2.4.11 Reconstitution of BluB using Fre-NADH as reducing system

BluB enzymatic reactions were performed in 100 mM phosphate buffer, pH 7.5 containing BluB (100 μM), FMN (500 μM), NADH (2 mM) and *E. coli* flavin reductase, Fre (200 nM). The enzymatic reactions were incubated at room temperature for 4 hrs. The protein was removed by heat denaturation and the reaction mixture was analyzed by HPLC and LC-MS.

2.4.12 BluB reactions in the presence of *o*-phenylenediamine (oPDA) – Trapping of Alloxan

BluB enzymatic reactions were performed in 100 mM phosphate buffer, pH 7.5 containing BluB (100 μM), FMN (500 μM), NADH (2 mM), E. *coli* flavin reductase, Fre (200 nM) and oPDA (2 mM). The enzymatic reactions were incubated at room temperature for 4 hrs. The protein was removed by heat denaturation and the reaction mixture was analyzed by HPLC and LC-MS.

2.4.13 Trapping of the sugar product (14)

BluB enzymatic reactions were performed in 100 mM phosphate buffer, pH 7.5 containing BluB (100 μM), FMN (500 μM), NADH (2 mM) and *E. coli* flavin reductase, Fre (200 nM). The enzymatic reactions were incubated at room temperature for 4 hrs. The protein was removed by heat denaturation and *o*-(pentafluorobenzyl)hydroxylamine (PFBHA) (2mM) was added to the reaction mixture and was heated at 65 °C for 1 hr. The reaction mixture was then analyzed by LC-MS.

2.4.14 BluB reactions in the presence of $^{18}O_2$ and $H_2{}^{18}O$

Two identical samples were prepared each containing BluB (100 μM), FMN (500 μM), NADH (2 mM), E. *coli* flavin reductase, Fre (200 nM) and oPDA (2 mM). One of the samples was prepared using $H_2{}^{18}O$ (final concentration $H_2{}^{18}O:H_2{}^{16}O = 4:1$) while the other which served as a control using $H_2{}^{16}O$. Both the samples were incubated at room temperature for 4 hrs and were then analyzed by LC-MS.

Two identical samples were prepared in an anaerobic glove box each containing BluB (100 μM), FMN (500 μM), NADH (2 mM), E. *coli* flavin reductase, Fre (200 nM) and oPDA (2 mM). One of the samples was exposed to $^{18}O_2$ while the other, serving as a control, to $^{16}O_2$. Both the samples were incubated at room temperature for 4 hrs and were then analyzed by LC-MS.

2.4.15 Synthesis of ^{13}C labeled FMN isotopologues[36,37]

The general synthetic scheme for ^{13}C labeled FMN is shown in Figure 22. Dr.

Sameh H. Abdelwahed synthesized the ^{13}C labeled FMN isotopologues (11a-c).
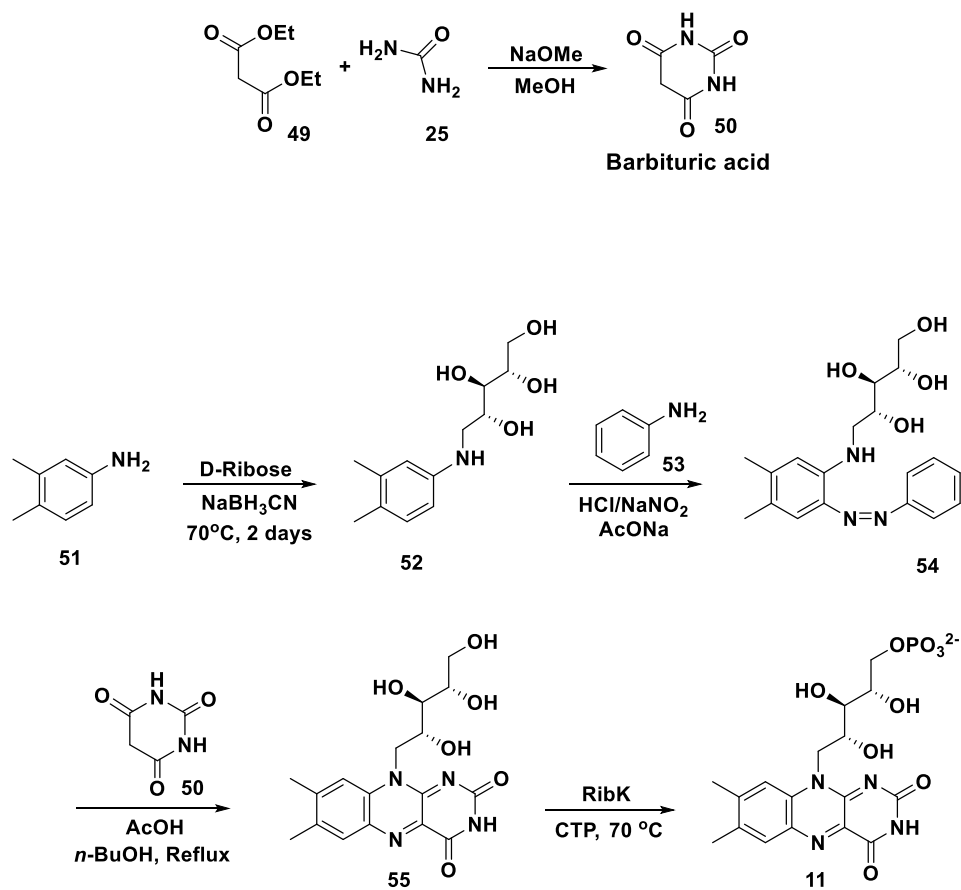
Figure 22. Scheme for the synthesis of ^{13}C labeled FMN

The scheme for the synthesis of ^{13}C labeled FMN isotopologues: 4a-^{13}C FMN, 2-^{13}C FMN and 4,10a-^{13}C FMN is shown in Figure 23.
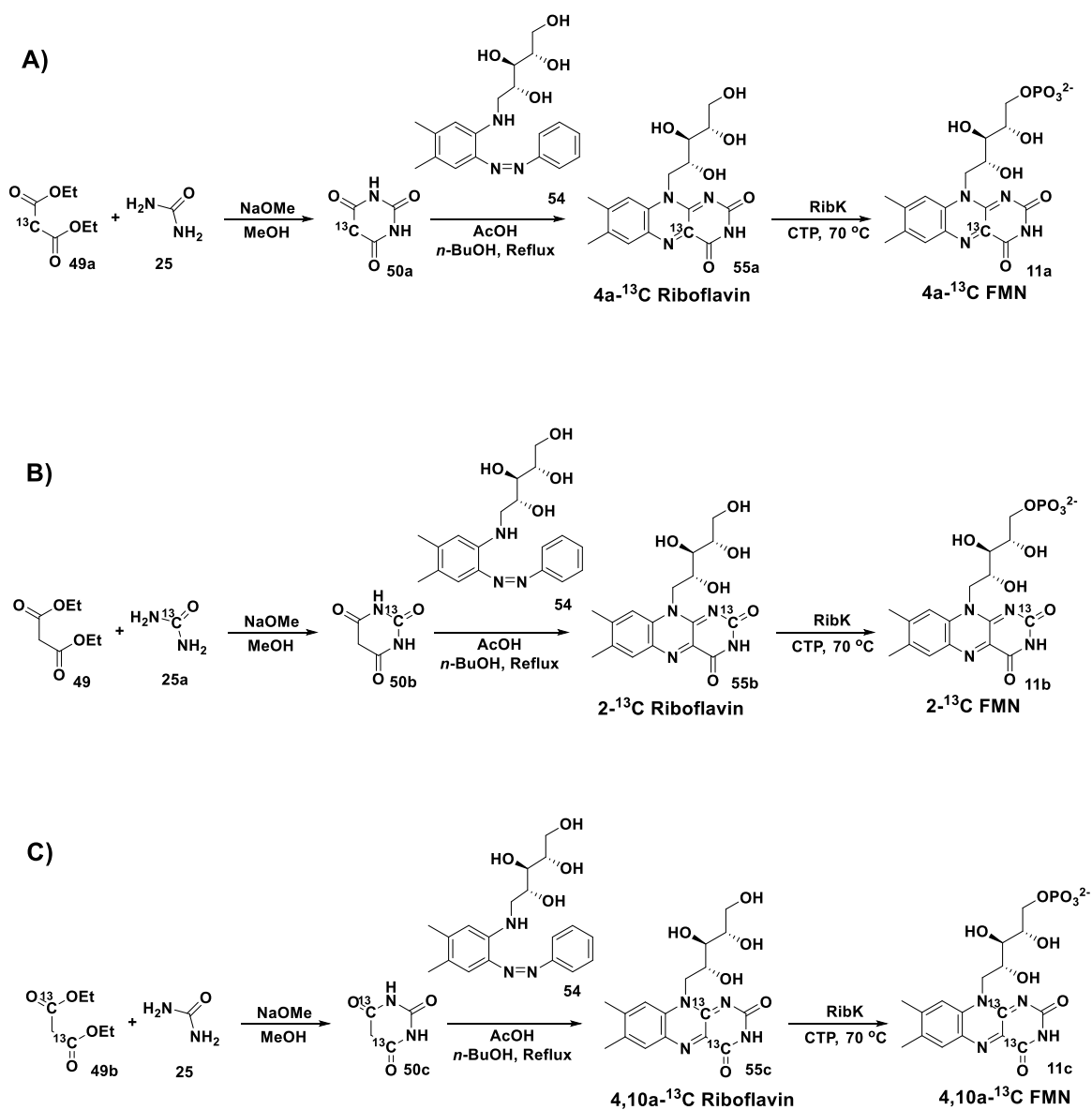
Figure 23. Scheme for the synthesis of ^{13}C labeled FMN isotopologues **(A)** 4a-^{13}C FMN **(B)** 2-^{13}C FMN **(C)** 4,10a-^{13}C FMN

Procedure

Synthesis of N-(D-ribityl)-3,4-dimethylaniline **(52):** 3,4-Dimethylaniline, 51 (152 mg, 1.0 equiv.), D-ribose (450 mg, 3.0 equiv.) and sodium cyanoborohydride (126 mg, 2.0 equiv.) were dissolved in anhydrous MeOH (15 mL). The mixture was refluxed at 80 °C for 2 days under argon atmosphere. Then the solvent was removed under reduced pressure and excess NaBH₃CN was quenched using 1M HCl. The resulting mixture was neutralized using saturated NaHCO₃ solution and concentrated under reduced pressure. The residue was purified by silica gel column chromatography using chloroform/methanol (98:2 to 80:20). Yield: 74%. ^{1}H NMR (400 MHz, CD₃OD): δ 2.12 (s, 3H), 2.17 (s, 3H), 3.08 (dd, 1H), 3.43 (dd, 1H), 3.60-3.81 (m, 4H), 3.91 (dd, 1H), 6.47 (dd, 1H), 6.55 (d, 1H), 6.88 (d, 1H) ppm.

Synthesis of N-(D-ribityl)-2-phenylazo-4,5-dimethylaniline **(54):** A solution of 1.05 g (0.01 mole) of aniline (53) in 3 ml of 12 N hydrochloric acid and 10 mL of water was cooled to 0 °C. A total of 0.80 g of solid sodium nitrite was added at a rate such that the temperature of the solution did not exceed 3 °C. After the sodium nitrite had been added, the solution was kept at 0 °C for half an hour. To a suspension of 2.15 g (0.09 mole) of N-(D-ribityl)-3,4-dimethylaniline (52) in 20 mL of water, 6.1 mL of 12 N hydrochloric acid and 6.06 g of sodium acetate was added. The mixture was cooled to -5 °C and the diazotized aniline solution prepared above was added. The resulting solution was stirred at -5 °C for 1.5 hours and then at 0 to 5 °C for another 1.5 hours. After warming to 20 °C, a solution of 3.0 g of sodium acetate in 20 mL of water was added at a rate such that the pH remained between 3-3.5 and the temperature between 17-20 °C. After stirring the

resultant mixture overnight, water was removed under vacuum and the crude residue was purified by column chromatography. Yield: 45%. ^{1}H NMR (400 MHz, CD$_3$OD): δ ppm 2.17 (s, 3H), 2.20 (s, 3H), 3.3-3.42 (m, 1H), 3.81−3.56 (m, 5H), 4.01 (m, 1H), 6.78 (s, 1H), 7.4-7.6 (m, 4H), 7.82 (d, 2H) ppm.

***Synthesis of barbituric acid* (50):** In 25 mL bottomed flask fitted with a reflux condenser under argon atmosphere, 0.06 g of sodium was dissolved in 10 mL of dry methanol. To this solution, 0.4 g (0.5 moles) of diethyl malonate (49) was added followed by 0.15 g (0.025 moles) of dry urea (25) dissolved in 10 mL of dry methanol. The mixture was stirred and refluxed for 4 hrs. A white solid separated out rapidly. After the completion of the reaction, 20 mL of hot water (50 °C) was added followed by enough hydrochloric acid to make the solution acidic. The resulting clear solution was filtered, cooled and kept in the fridge overnight. The white product thus obtained was filtered and washed with 20 mL of cold water and dried. Yield: 72–78 %.

[5-^{13}C] Barbituric acid: ^{1}H NMR (400 MHz, CD$_3$OD): H is exchangeable by deuterium. ^{13}C NMR (100 MHz, CD$_3$OD): δ 39.90 ppm (^{13}C enriched C).

[2-^{13}C] Barbituric acid: ^{1}H NMR (400 MHz, CD$_3$OD): H is exchangeable by deuterium. ^{13}C NMR (100 MHz, CD$_3$OD): δ 151.80 ppm (^{13}C enriched C).

[4,6-^{13}C] Barbituric acid: ^{1}H NMR (400 MHz, CD$_3$OD): H is exchangeable by deuterium. ^{13}C NMR (100 MHz, CD$_3$OD): δ 168.85 ppm (^{13}C enriched C).

***Synthesis of Riboflavin* (55):** To N-ribityl-2-phenylazo-4,5-dimethyl aniline, 54 (35 mg, 0.1 mmol) in a 10 mL round bottomed flask, 2 mL of *n*-butanol, barbituric acid (20 mg, 0.15 mmol), and 0.5 mL of AcOH was added. The mixture was stirred and heated

to reflux for 5 hrs. Solvents were dried under vacuum and the crude yellow solid was purified by column chromatography. Yield: 42-47 %.

4a-^{13}C Riboflavin: ^{1}H NMR (400 MHz, CD$_3$OD): δ 2.23 (s, 3H), 2.34 (s, 3H), 3.73-3.97 (m, 4H), 4.23-4.37 (m, 2H) 4.48 (m, 1H), 7.36 (s, 1H), 7.39 (s, 1H) ppm. ^{13}C NMR (100 MHz, DMSO-d_6): δ 137.59 ppm (^{13}C enriched C).

2-^{13}C Riboflavin: ^{1}H NMR (400 MHz, CD$_3$OD): δ 2.23 (s, 3H), 2.34 (s, 3H), 3.73-3.97 (m, 4H), 4.23-4.37 (m, 2H) 4.48 (m, 1H), 7.36 (s, 1H), 7.39 (s, 1H) ppm. ^{13}C NMR (100 MHz, DMSO-d_6): δ 159.60 ppm (^{13}C enriched C).

4,10a-^{13}C Riboflavin: ^{1}H NMR (400 MHz, CD$_3$OD): δ 2.23 (s, 3H), 2.34 (s, 3H), 3.73-3.97 (m, 4H), 4.23-4.37 (m, 2H) 4.48 (m, 1H), 7.36 (s, 1H), 7.39 (s, 1H) ppm. ^{13}C NMR (100 MHz, DMSO-d_6): δ 151.30, 162.95 ppm (^{13}C enriched C).

***Synthesis of FMN* (11):** Riboflavin (55) was converted to FMN (11) enzymatically using RibK from *Methanocaldococcus jannaschii*. Riboflavin was incubated for 30 mins at 70 °C with 5 mM CTP, 20 mM MgCl$_2$ and RibK in 100 mM potassium phosphate buffer, pH 7.5. The reaction mixture was passed through a 10kDa cut-off filter and purified by reverse phase high performance liquid chromatography.

2.4.16 Synthesis of N-[(3-Oxo-3,4-dihydroquinoxalin-2-yl)carbonyl]urea (Alloxan-oPDA adduct, 40)[41]

The synthetic scheme for the alloxan-oPDA adduct is shown in Figure 24.
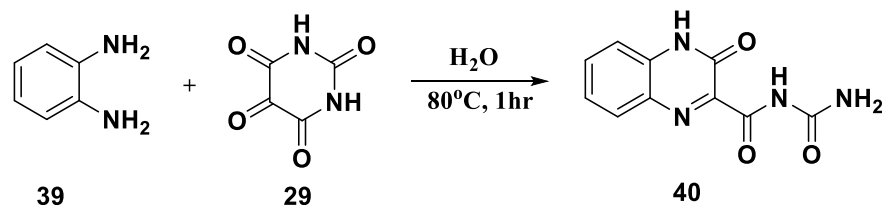
Figure 24. Scheme for the synthesis of alloxan-oPDA adduct (40)

Procedure

Synthesis of N-[(3-Oxo-3,4-dihydroquinoxalin-2-yl)carbonyl]urea (Alloxan-oPDA adduct (40): *o*-Phenylenediamine, 39 (108 mg, 1.0 equiv.) was dissolved in 10 mL of water and was then added to the aqueous solution of alloxan, 29 (160 mg, 1.0 equiv. in 10 mL). A yellow precipitate was immediately formed. The reaction mixture was heated at 80 °C for an hour and was then filtered followed by washing with hot water to yield the final compound. Yield: 70%, ESI-MS *m/z* 233.1 (M+H). ^{1}H NMR (400 MHz, CDCl₃/CF₃COOH): δ 7.1 (br, 1H), 7.54 (d, 1H), 7.68 (t, 1H), 7.91 (t, 1H), 8.14 (d, 1H), 8.65 (br, 1H) ppm. ^{13}C NMR (100 MHz, CDCl₃/CF₃COOH): δ 116.7, 128.1, 131.2, 132.0, 133.3, 137.1, 139.9, 156.4, 157.2, 163.0 ppm.

CHAPTER III

TRAPPING OF KEY REACTION INTERMEDIATES IN THE BLUB CATALYZED

DIMETHYLBENZIMIDAZOLE FORMATION

3.1 Introduction

In the last chapter, we have successfully identified alloxan as the product derived

from the third ring of FMN. Molecular oxygen and water have been shown to be the two

sources of oxygen atom incorporation in the alloxan. Based on our observations, a

mechanism has been proposed which is consistent with all our experimental data.

In a complex multi-step reaction, it is highly likely that some of the reactive

intermediates may be trapped in the form of shunt products. Thus, in pursuit of the

intermediates proposed in our mechanistic hypothesis, we looked for the formation of

shunt products in the BluB catalyzed reaction. Several new products were seen to be

formed only in case of full reaction in the HPLC and LC-MS analysis of the enzymatic

reactions. All these new products were formed on carrying out the reactions with wild type

BluB using the native substrate FMN.

3.2 Results and Discussion

3.2.1 Identification of the shunt product 56

BluB catalyzed reactions were carried out and analyzed in the HPLC and LC-MS.

A new peak was seen to be formed only in case of full reaction at 320 nm in the HPLC

chromatogram (Figure 25A). LCMS analysis of the new compound showed that the new

product has a mass of 232 Da (Figure 26). Based on the mass and MS-MS fragmentation pattern (Figure 27), we proposed 56 as the possible structure of the new compound. The proposed structure for the new compound was confirmed by synthesizing a standard and carrying out a coelution experiment (Figure 25B)[44,45].
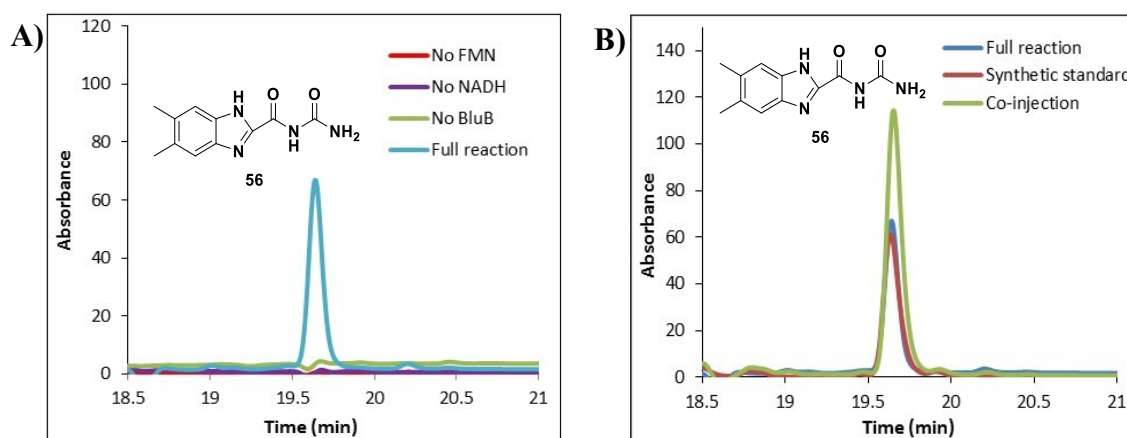
Figure 25. Identification of the shunt product 56. (A) HPLC chromatogram showing the formation of shunt product 56 (B) Coelution study for the formation of 56
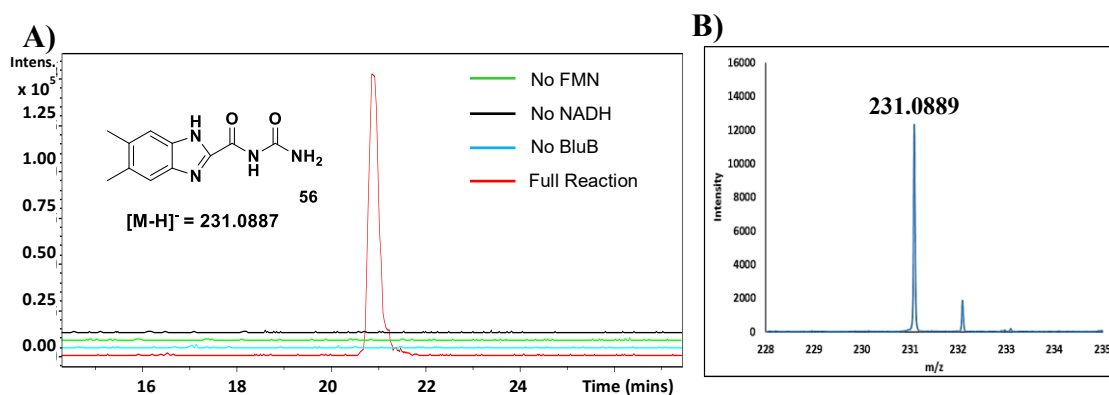
Figure 26. LC-MS analysis of the formation of the shunt product 56. **(A)** Extracted Ion Chromatogram (EIC) at m/z 231.0887 showing the formation of 56 only in case of full reaction (Red trace) **(B)** ESI-MS of 56 in the negative mode
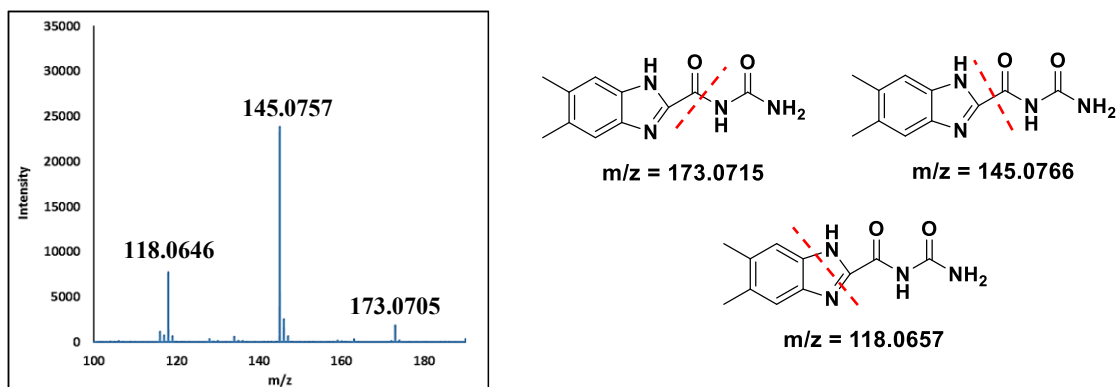
Figure 27. MS-MS fragmentation pattern of 56 in the positive mode

3.2.2 Labeling pattern for the shunt product 56

Labeling studies were done to figure out the origin of various atoms in the shunt product 56. On carrying out the reaction with FMN labeled as 13C at the C1' of the ribose sugar chain, no increment in mass was observed for the new product indicating that the carbon at C1' is not incorporated (Figure 28A & B). Only one of the two carbons labeled at 4 and 10a positions was seen to be incorporated as a 1Da increase in mass was observed (Figure 28C & D). Both the carbons labeled at 2 (Figure 28E & F) and 4a (Figure 28G & H) positions were incorporated and in both the cases a 1Da increment was seen in the mass of the new shunt product (56).

34
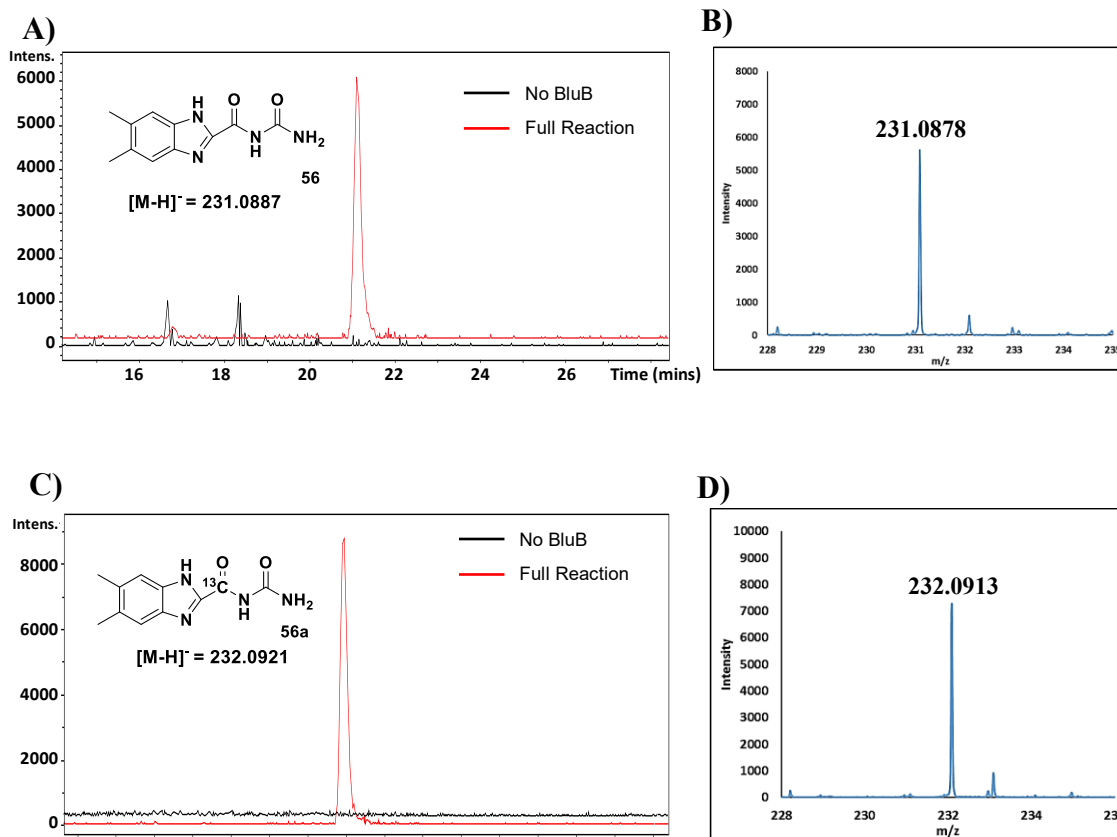
Figure 28. LC-MS analysis of the labeling pattern for the shunt product 56. **(A)** EIC at m/z 231.0887 showing that the carbon at C1′ position of the ribose sugar chain of FMN is not incorporated in 56 when FMN labeled as ^{13}C at C1′ position of ribose is used as substrate **(B)** ESI-MS of 56 formed on using FMN labeled as ^{13}C at C1′ position of ribose as substrate in the negative mode **(C)** EIC at m/z 232.0921 showing that only one of the two carbons at 4,10a positions of FMN is incorporated in 56 when 4,10a-^{13}C FMN is used as substrate **(D)** ESI-MS of 56 formed on using 4,10a-^{13}C FMN as substrate in the negative mode **(E)** EIC at m/z 232.0921 showing that the carbon at 2 position of FMN is incorporated in 56 when 2-^{13}C FMN is used as substrate **(F)** ESI-MS of 56 formed on using 2-^{13}C FMN as substrate in the negative mode **(G)** EIC at m/z 232.0921 showing that the carbon at 4a position of FMN is incorporated in 56 when 4a-^{13}C FMN is used as substrate **(H)** ESI-MS of 56 formed on using 4a-^{13}C FMN as substrate in the negative mode

E)

F)

G)

H)
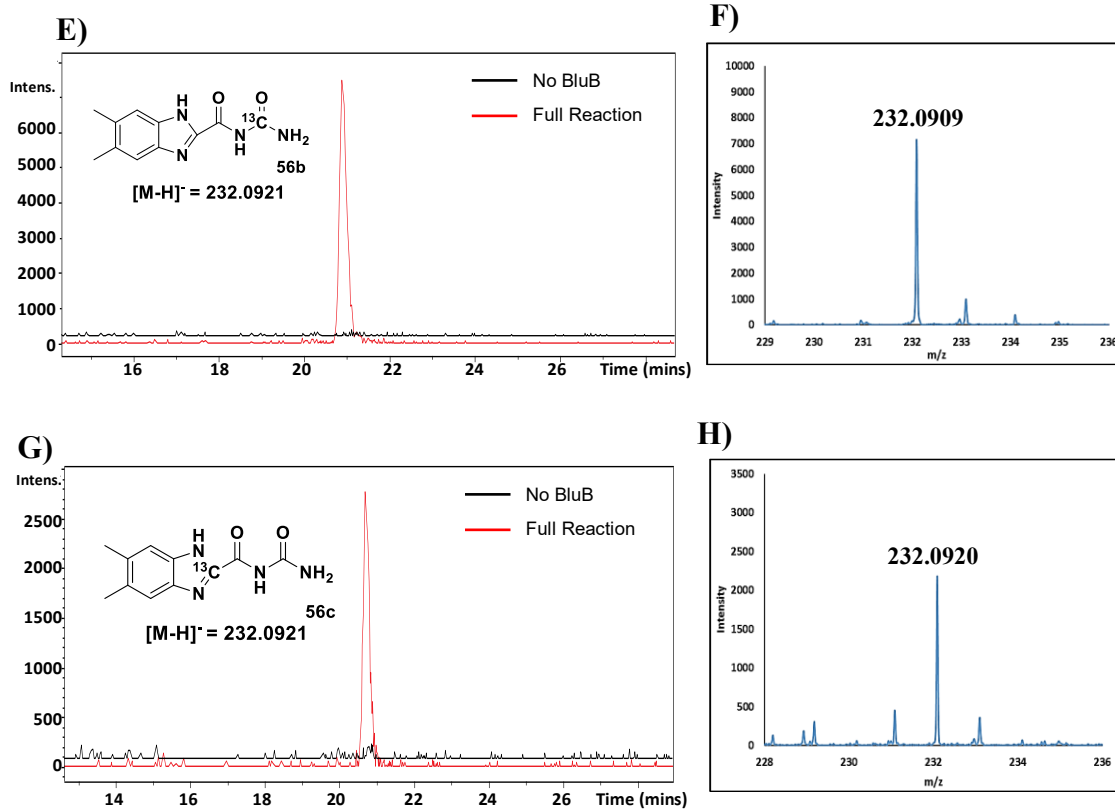
Figure 28. Continued

Substrate	Mass obtained
FMN	231.1
C1' (Ribose) ^{13}C FMN	231.1
4,10a-^{13}C FMN	232.1
2-^{13}C FMN	232.1
4a-^{13}C FMN	232.1

Table 1. Labeling study for the formation of shunt product 56

The results of the labeling studies for shunt product 56 have been summarized in Table 1.

Based on all these results, we propose the labeling pattern for the shunt product 56 to be as shown in figure 29.
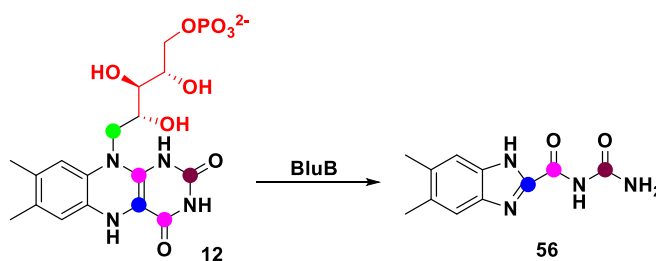
Figure 29. Labeling pattern for the shunt product 56

3.2.3 Identification of the shunt product 57

On reducing the substrate FMN chemically, using sodium dithionite instead of the enzymatic system comprising NADH/Fre, led to the formation of a new peak observed at 320 nm in the HPLC chromatogram (Figure 30). Based on the mass and fragmentation pattern, we assigned 57 to be the structure for the new peak formed (Figure 31).
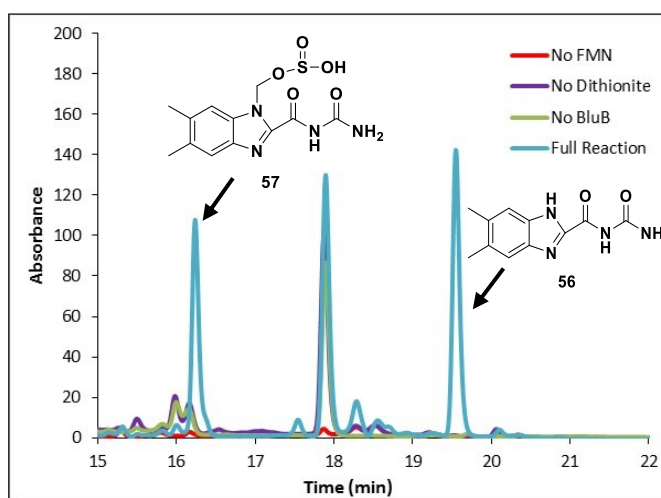
Figure 30. Formation of shunt product 57 on carrying out reactions using dithionite as the reducing agent
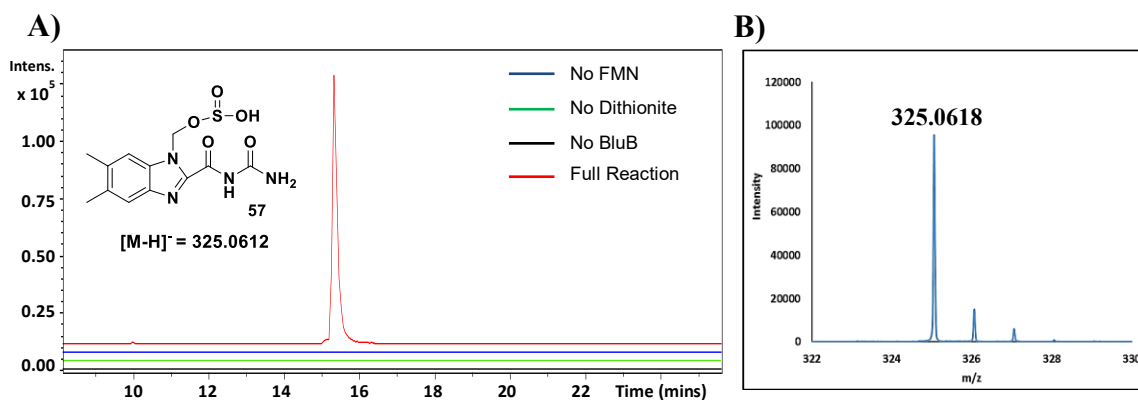
Figure 31. LC-MS analysis of the formation of the shunt product 57. **(A)** Extracted Ion Chromatogram (EIC) at m/z 325.0612 showing the formation of 57 only in case of full reaction (Red trace) **(B)** ESI-MS of 57 in the negative mode

3.2.4 Labeling pattern for the shunt product 57

Labeling studies were performed using ^{13}C labeled FMN isotopologues to figure out the origin of various atoms in the shunt product 57. On carrying out the reaction with FMN labeled as 13C at the C1' of the ribose sugar chain, a 1Da increment in mass was observed for the new product indicating the carbon at C1' is incorporated (Figure 32A & B). Only one of the two carbons labeled at 4 and 10a positions was seen to be incorporated as a 1Da increase in mass was observed (Figure 32C & D). Both the carbons labeled at 2 (Figure 32E & F) and 4a (Figure 32G & H) positions were incorporated as in both the cases a 1Da increment was observed.
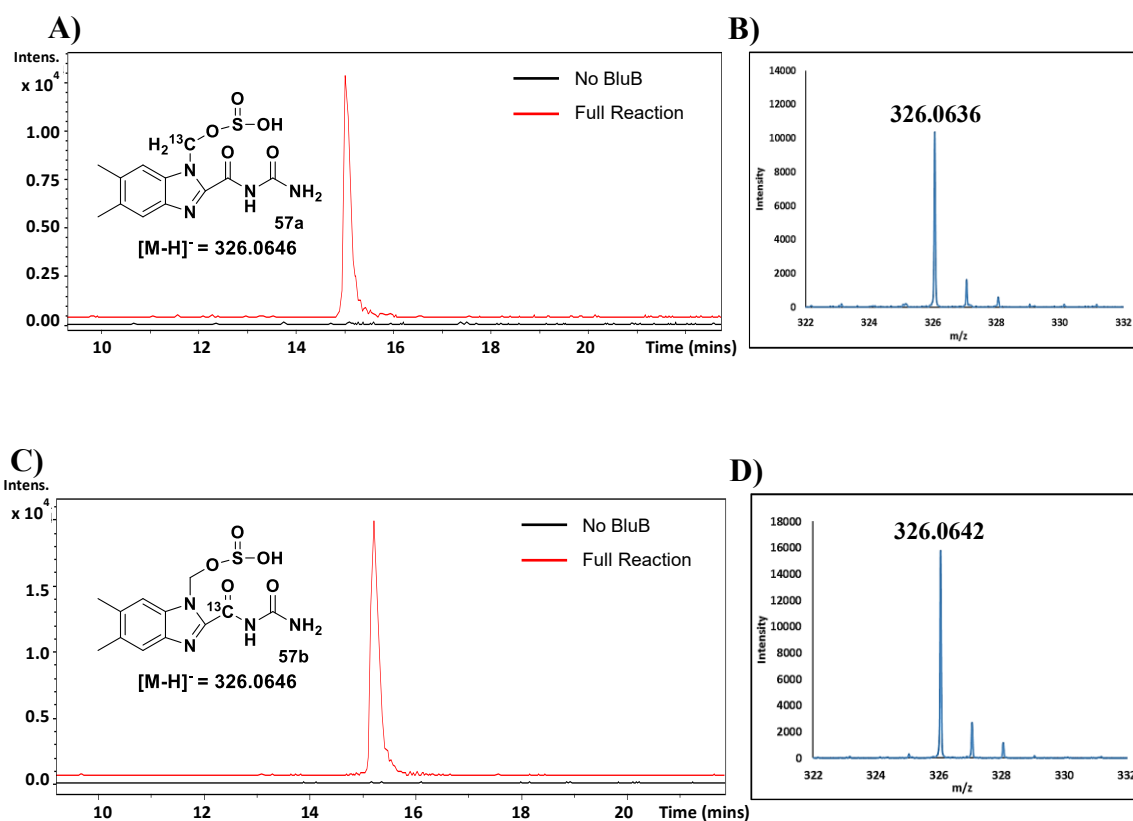
Figure 32. LC-MS analysis of the labeling pattern of the shunt product 57. **(A)** EIC at m/z 326.0646 showing that the carbon at C1′ position of the ribose sugar chain of FMN is incorporated in 57 when FMN labeled as ^{13}C at C1′ position of ribose is used as substrate **(B)** ESI-MS of 57 formed on using FMN labeled as ^{13}C at C1′ position of ribose as substrate in the negative mode **(C)** EIC at m/z 326.0646 showing that only one of the two carbons at 4,10a positions of FMN is incorporated in 57 when 4,10a-^{13}C FMN is used as substrate **(D)** ESI-MS of 57 formed on using 4,10a-^{13}C FMN as substrate in the negative mode **(E)** EIC at m/z 326.0646 showing that the carbon at 2 position of FMN is incorporated in 57 when 2-^{13}C FMN is used as substrate **(F)** ESI-MS of 57 formed on using 2-^{13}C FMN as substrate in the negative mode **(G)** EIC at m/z 326.0646 showing that the carbon at 4a position of FMN is incorporated in 57 when 4a-^{13}C FMN is used as substrate **(H)** ESI-MS of 57 formed on using 4a-^{13}C FMN as substrate in the negative mode

E)

F)
326.0645

G)

H)
326.0647
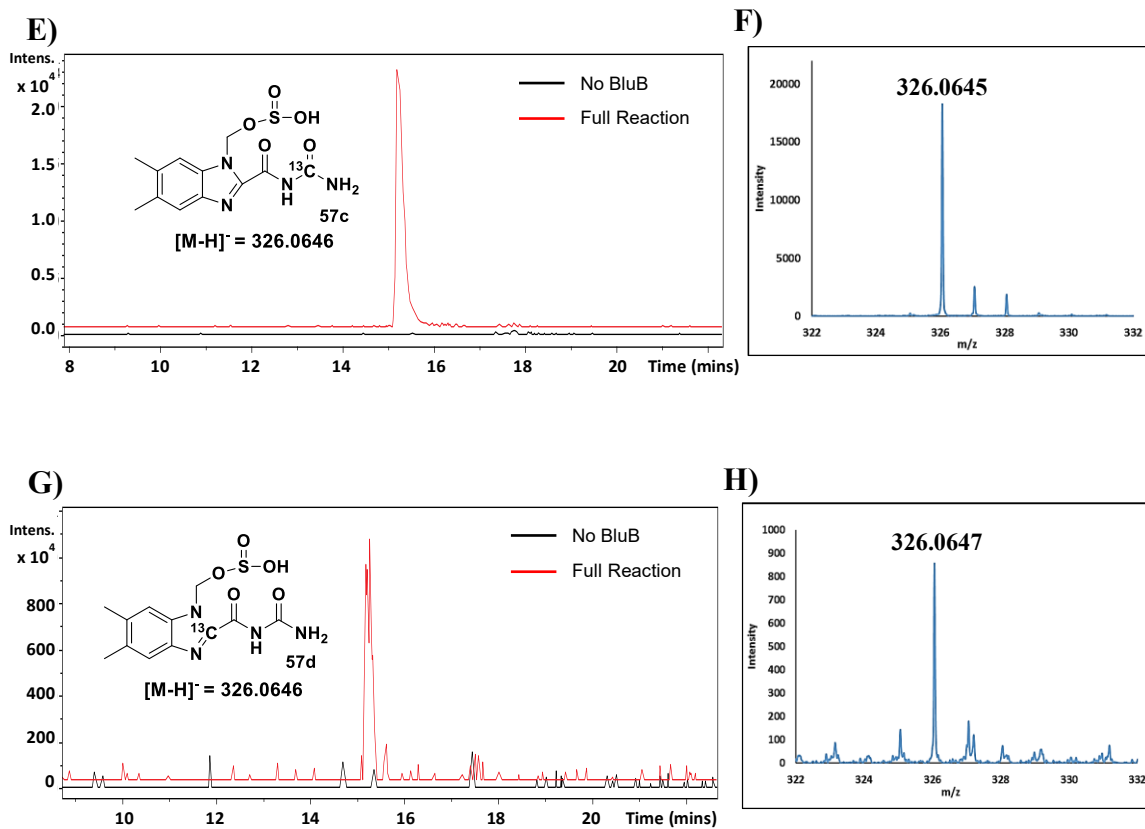
Figure 32. Continued

Substrate	Mass obtained
FMN	325.1
C1$'$ (Ribose)-^{13}C FMN	326.1
4,10a-^{13}C FMN	326.1
2-^{13}C FMN	326.1
4a-^{13}C FMN	326.1

Table 2. Summary of the labeling studies for the shunt product 57

The results of the labeling studies for shunt product 57 have been summarized in Table 2.

Thus, based on the above results, the labeling pattern for the shunt product 57 is as shown in figure 33.
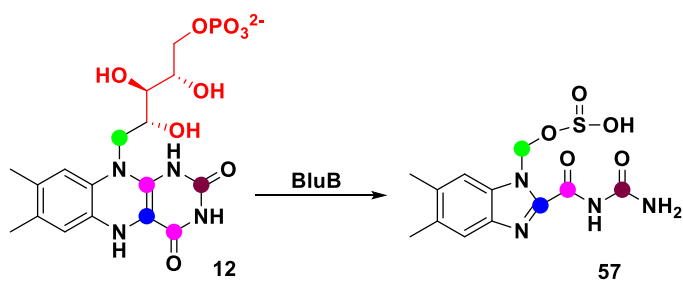
Figure 33. Labeling pattern for the shunt product 57

3.2.5 Formation of the shunt product 57 in presence of sodium bisulfite

The formation of the shunt product 57 was observed on carrying out BluB catalyzed reactions using dithionite as the reducing agent. The shunt product 57, thus, formed seems to be a dithionite adduct of one of the intermediates in our mechanistic proposal for DMB formation. Our hypothesis is that the reduction of flavin with dithionite forms bisulfite as a by-product which subsequently acts as a nucleophile and traps one of the reaction intermediates in the form of an adduct (57). To test this, BluB catalyzed reactions were carried out in presence of sodium bisulfite using NADH/Fre as the reducing agent instead of dithionite. We observed the formation of the same shunt product (57) as seen in case of reactions carried out using dithionite as the reducing agent (Figure 34). The formation of 57, however, was not observed in the absence of bisulfite.

41
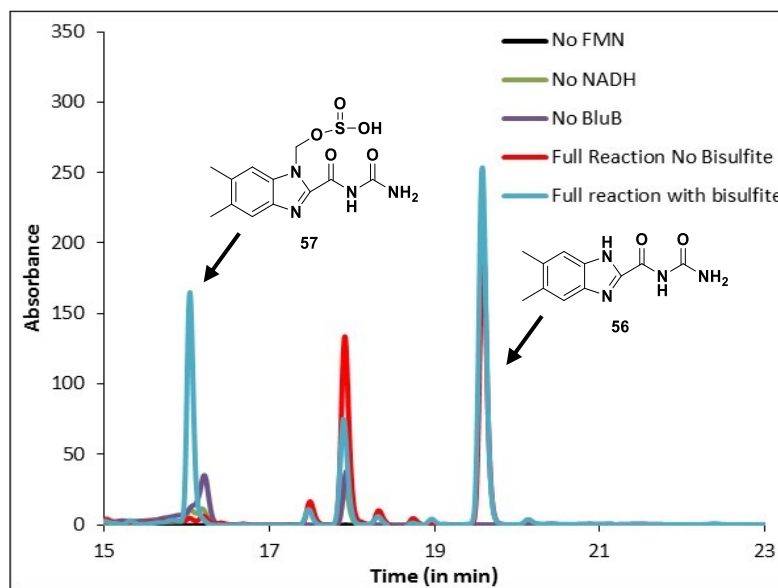
Figure 34. Formation of 57 in the BluB catalyzed reactions in the presence of sodium bisulfite

Formation of 57 was also confirmed by LC-MS analysis, wherein, the shunt product was only seen in the enzymatic reaction carried out in the presence of sodium bisulfite (Figure 35).
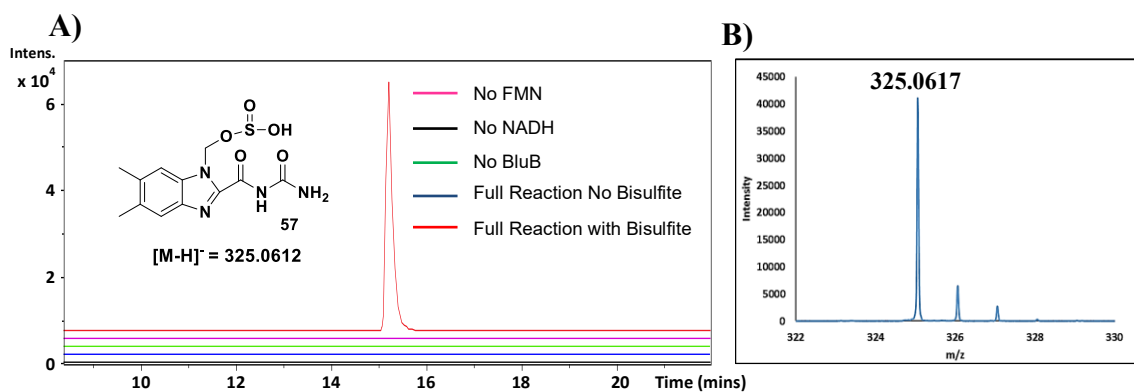
Figure 35. LC-MS analysis of BluB catalyzed reactions in presence of sodium bisulfite. **(A)** Extracted Ion Chromatogram (EIC) at m/z 325.0612 showing the formation of the shunt product 57 only in case of full reaction carried out in presence of bisulfite (Red trace) **(B)** ESI-MS of 57 in the negative mode

42

Usually, bisulfite forms adduct through an attack from the sulfur center leading to a C-S bond. However, in the case of shunt product 57, MS-MS fragmentation pattern indicates the attack occurs through the oxygen atom forming a C-O linkage as the nucleophilic attack from the sulfur center may be hindered due to steric effect (Figure 36).
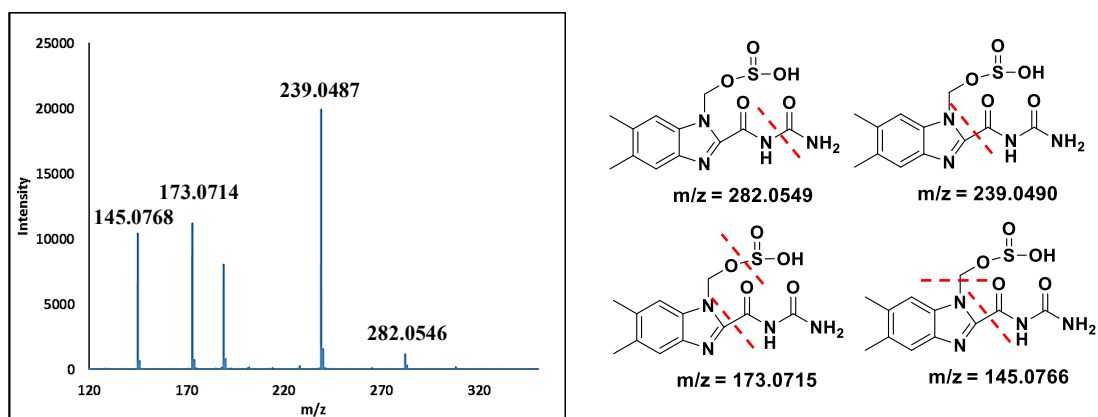
Figure 36. MS-MS fragmentation analysis of 57 in the negative mode

3.2.6 Identification of the shunt product 58 in the presence of sodium cyanoborohydride

The results obtained indicate that the intermediate trapped by bisulfite may contain a reactive imine or carbonyl functional group as bisulfite is known to form stable adducts with compounds containing either an imine or a carbonyl moiety. To figure this out, we performed BluB reactions in the presence of sodium cyanoborohydride which can potentially reduce these functional groups. On carrying out reactions using cyanoborohydride, we observed the formation of a new peak (58) (Figure 37A) whose

structure was confirmed by coelution studies (Figure 37B) and LC-MS analysis (Figure 38)[46,47].
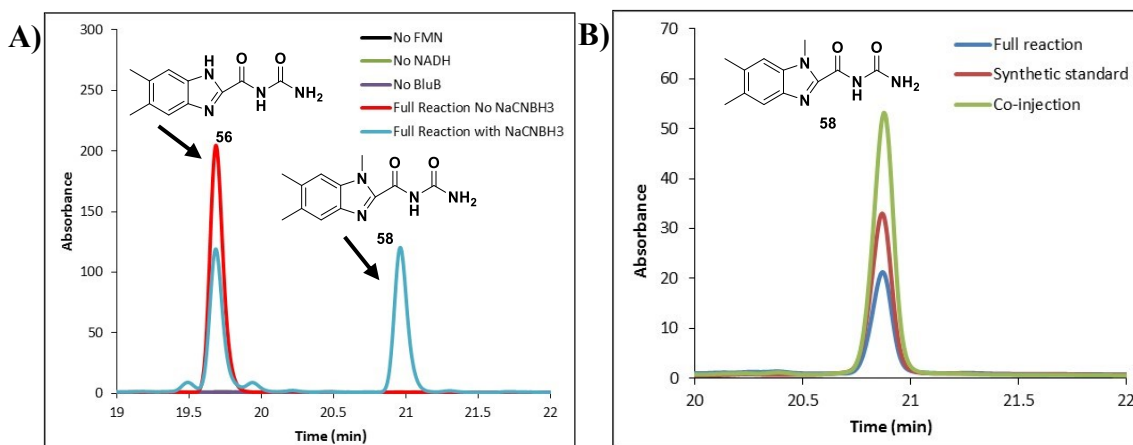
Figure 37. BluB catalyzed reactions in presence of sodium cyanoborohydride. **(A)** HPLC Chromatogram showing the formation of the shunt product 58 **(B)** Coelution study for formation of product 58
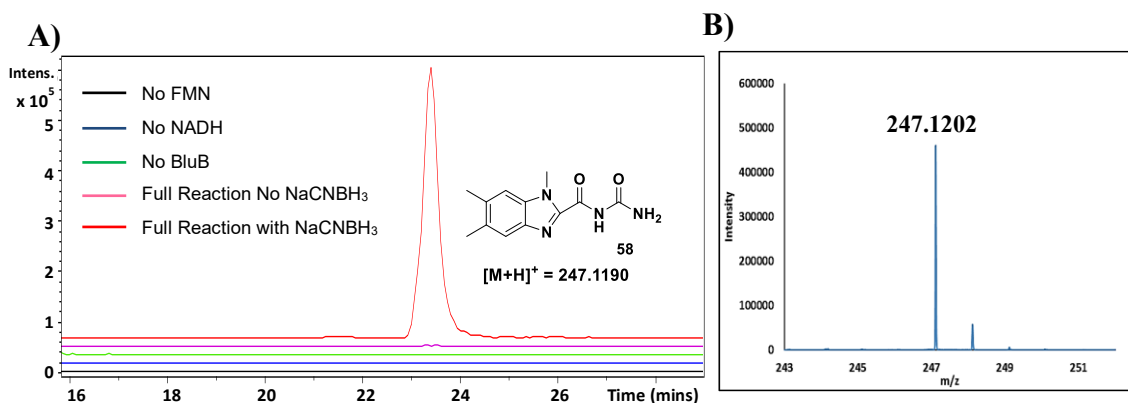
Figure 38. LC-MS analysis of BluB catalyzed reaction in presence of sodium cyanoborohydride. **(A)** Extracted Ion Chromatogram (EIC) at m/z 247.1190 showing the formation of the shunt product 58 only in case of full reaction carried out in presence of cyanoborohydride (Red trace) **(B)** ESI-MS of 58 in the positive mode **(C)** MS-MS fragmentation pattern of 58 in the positive mode
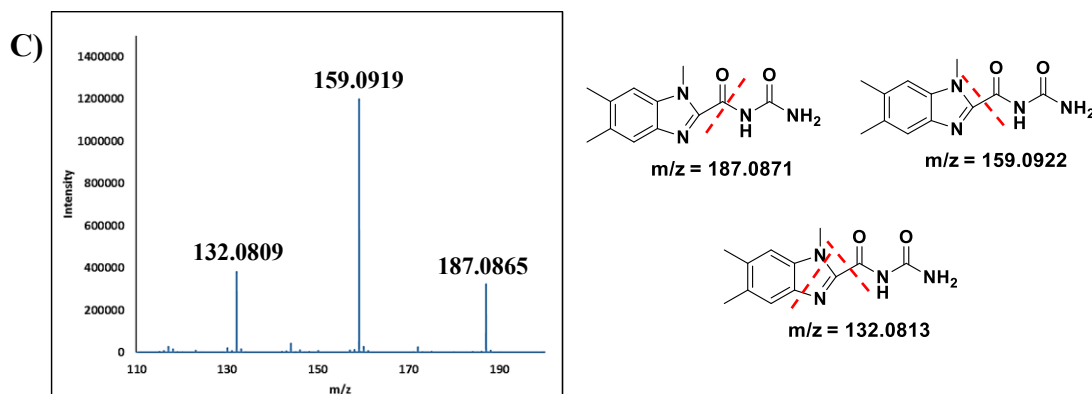
Figure 38. Continued

These results confirm that the intermediate trapped contains an imine moiety which gets reduced in the presence of cyanoborohydride forming 58. This was further confirmed by using cyanoborodeuteride wherein a 1Da increment in mass was observed (Figure 39).
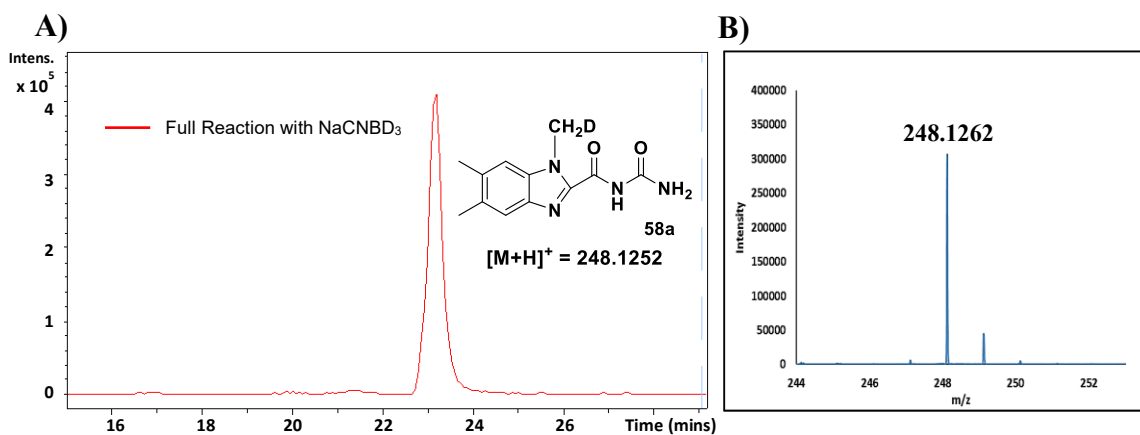
Figure 39. Deuterium incorporation studies in the shunt product 58. **(A)** EIC at m/z 248.1252 showing the incorporation of deuterium in 58 in presence of cyanoborodeuteride **(B)** ESI-MS of 58a in the positive mode

3.2.7 Labeling pattern for the shunt product 58

Labeling studies were done to figure out the origin of various atoms in the shunt product 58. On carrying out the reaction with FMN labeled as 13C at the C1' of the ribose sugar chain, a 1Da increment in mass was observed indicating that the carbon at C1' is incorporated (Figure 40A & B). Only one of the two carbons labeled at 4 and 10a positions was seen to be incorporated as only a 1Da increase in mass was observed (Figure 40C & D). The carbon labeled at 2 position was also incorporated with a 1Da increment seen in the mass of the shunt product 58 (Figure 40E & F).
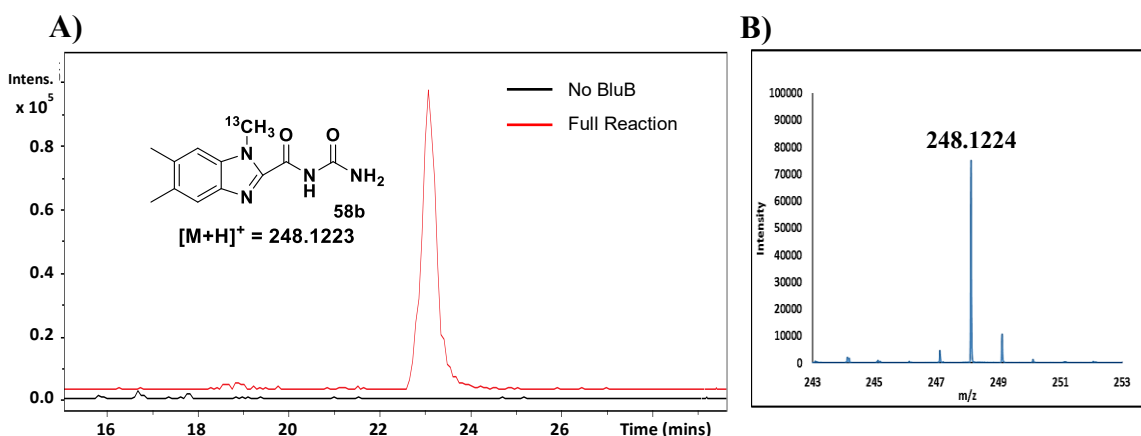
Figure 40. LC-MS analysis of the labelling pattern of the shunt product 58. **(A)** EIC at m/z 248.1223 showing that the carbon at C1' position of the ribose sugar chain of FMN is incorporated in 58 when FMN labeled as ^{13}C at C1' position of ribose is used as substrate **(B)** ESI-MS of 58 formed on using FMN labeled as ^{13}C at C1' position of ribose as substrate in the positive mode **(C)** EIC at m/z 248.1223 showing that only one of the two carbons at 4,10a positions of FMN is incorporated in 58 when 4,10a-^{13}C FMN is used as substrate **(D)** ESI-MS of 58 formed on using 4,10a-^{13}C FMN as substrate in the positive mode **(E)** EIC at m/z 248.1223 showing that the carbon at 2 position of FMN is incorporated in 58 when 2-^{13}C FMN is used as substrate **(F)** ESI-MS of 58 formed on using 2-^{13}C FMN as substrate in the positive mode

C)

D)

E)

F)
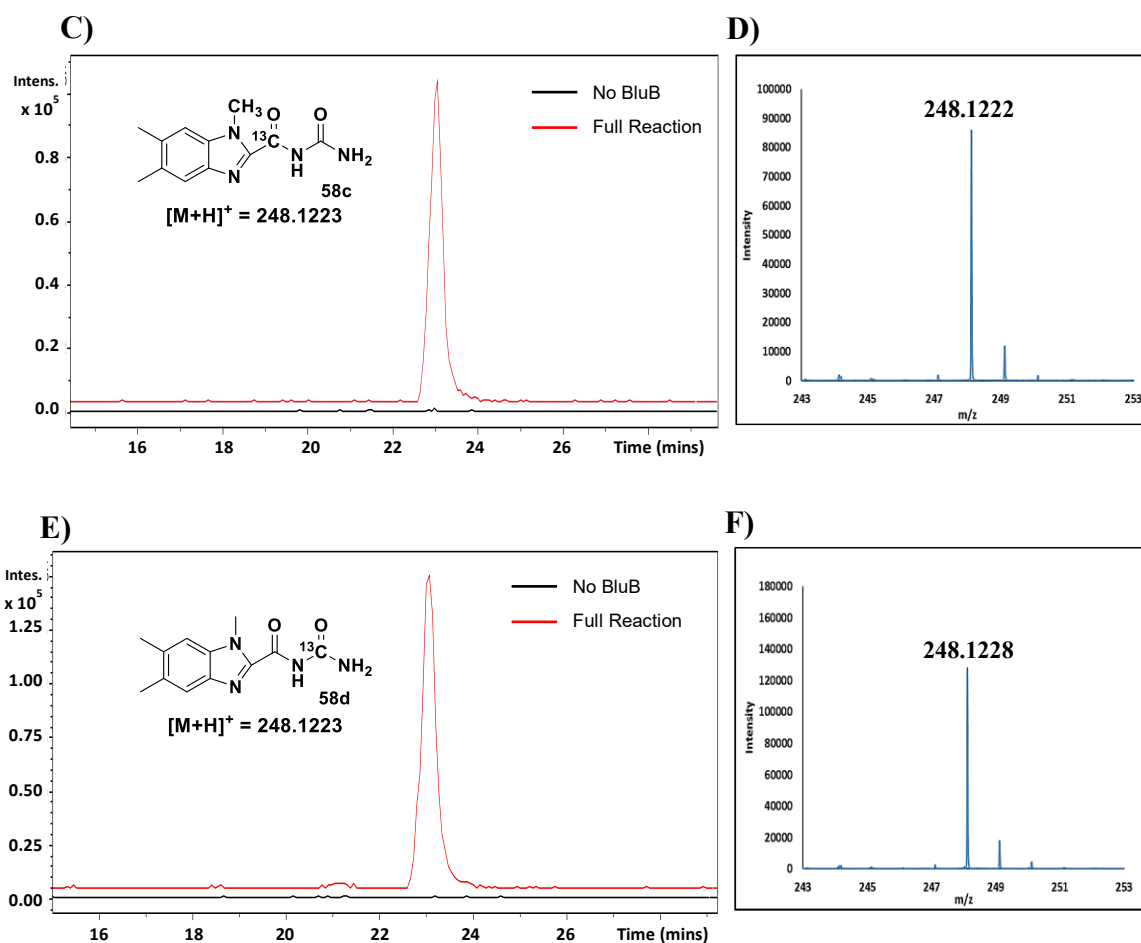
Figure 40. Continued

Substrate	Mass obtained
FMN	247.1
C1' (Ribose)-^{13}C FMN	248.1
4,10a-^{13}C FMN	248.1
2-^{13}C FMN	248.1

Table 3. Summary of the labeling studies for the shunt product 58

The summary of the labeling studies for the shunt product 58 is shown in Table 3.

Thus, based on the above data, the labeling pattern for the shunt product 58 is as shown in Figure 41.
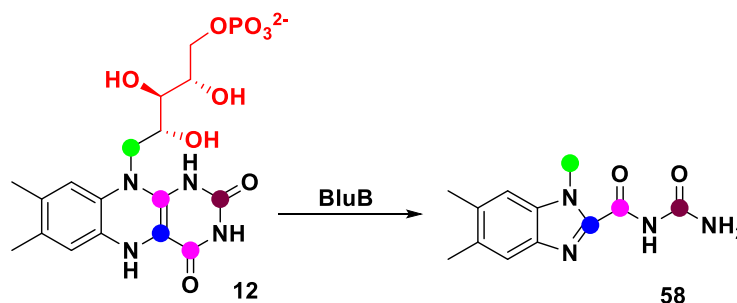
Figure 41. Labeling pattern for the shunt product 58

3.2.8 Mechanistic proposal for the formation of the shunt products (56, 57 and 58)

We have thus successfully identified and characterized three shunt products (56, 57 and 58). Our hypothesis is that these products are formed by trapping the reaction intermediate 27 (in Figure 21) in our mechanistic proposal for DMB biosynthesis. All the three above-mentioned shunt products are pretty closely related to one another in terms of their structure and thus must be formed following a common mechanism by trapping the intermediate 27 using various nucleophiles as shown in Figure 42.

We propose that the intermediate 27, formed by a C-C bond cleavage between the C1$'$ and C2$'$ of the ribose sugar chain, can react with various nucleophiles such as water, bisulfite and hydride apart from undergoing the usual chemistry to form DMB. This is due to the presence of a highly reactive imine moiety in 27 which is quite susceptible to attack by nucleophiles. Intermediate 27 can thus react with nucleophiles forming species 59

48

which can undergo similar chemistry to the alloxan/alloxanic acid rearrangement (Figure 11) to form 60 which is then followed by ring closure to form 62. Addition of water to C10a triggers a ring contraction to give 64. This can be followed by a decarboxylation step to loss CO_2 in a conjugated fashion forming 65 which can finally oxidize to yield the shunt product 67. When X is water, one can expect a loss of formaldehyde forming the product 56, X being bisulfite will lead to compound 57 and on X being hydride product 58 will be formed.
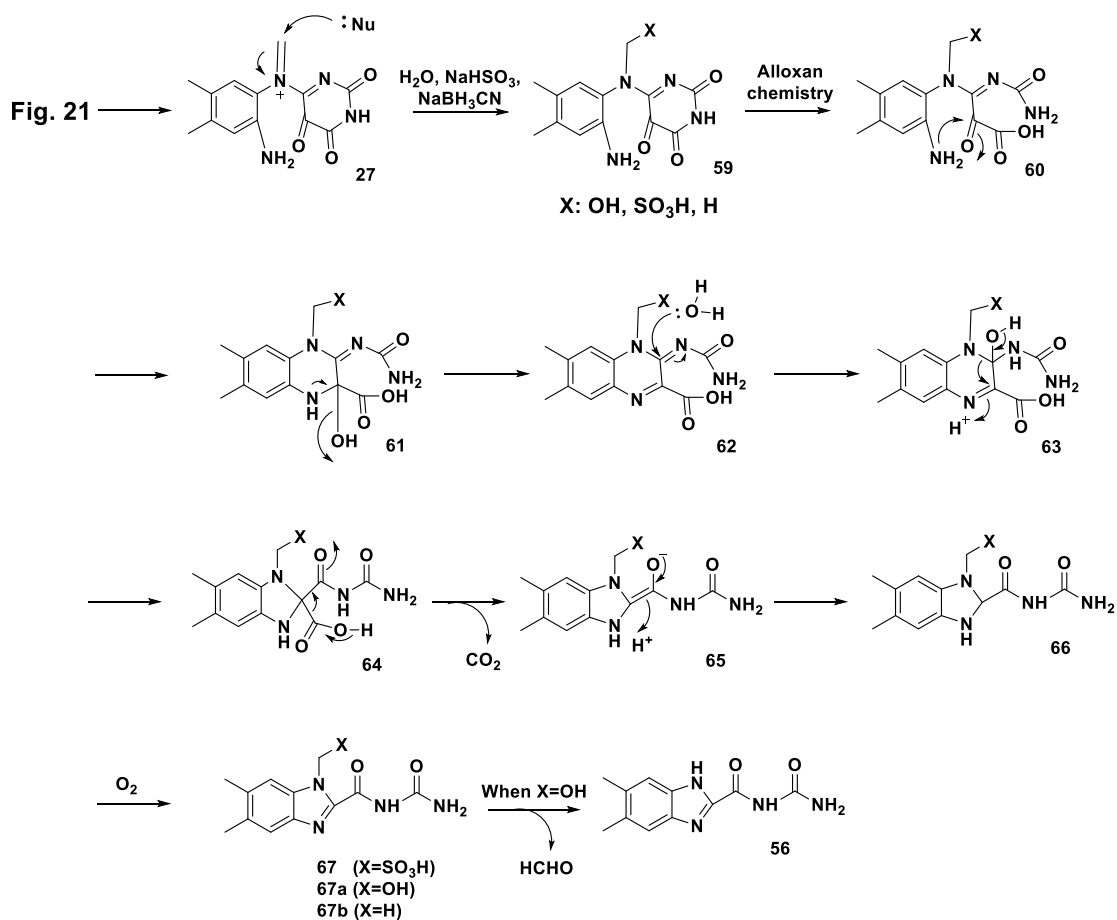
Figure 42. Mechanistic proposal for the formation of shunt products 56, 57 and 58

3.2.9 Identification of lumichrome based shunt products as further evidence for the intermediate 27

Having successfully identified and characterized the three shunt products, we next explored the possibility for the formation of any cyclic lumichrome derived shunt products which can again arise from the same reaction intermediate 27 (in Figure 21). We were indeed successful in identifying three more shunt products. One of these newly identified shunt products is a bisulfite adduct of lumichrome (68) formed only in reactions carried out using dithionite as the reducing agent (Figure 43).
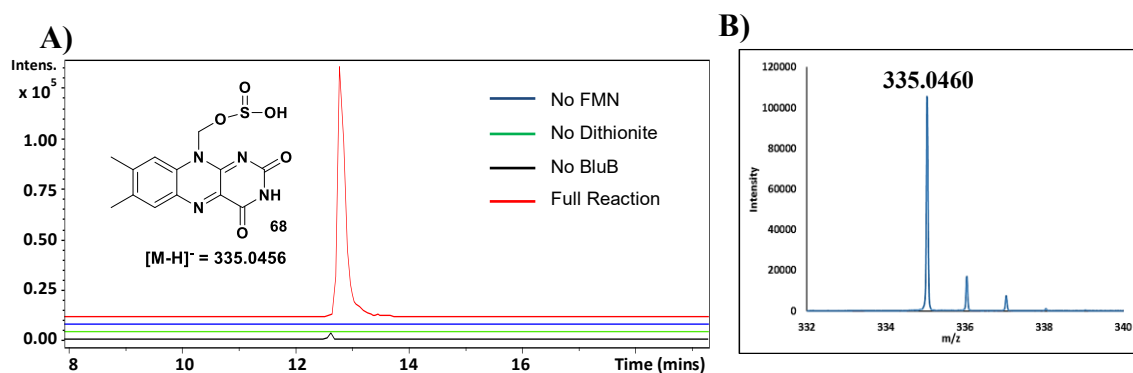
Figure 43. LC-MS analysis of the formation of the shunt product 68. **(A)** Extracted Ion Chromatogram (EIC) at m/z 335.0456 showing the formation of 68 only in case of full reaction (Red trace) **(B)** ESI-MS of 68 in the negative mode

3.2.10 Labeling pattern for the shunt product 68

Labeling studies were done to figure out the origin of various atoms in the shunt product 68. Both the carbons labeled at 4 and 10a positions were seen to be incorporated as a 2Da increase in mass was observed (Figure 44A & B). The carbons labeled at 2 (Figure

50

44C & D) as well as 4a (Figure 44E & F) positions were also incorporated with a 1Da increment seen in the mass of the shunt product 68 in both the cases.
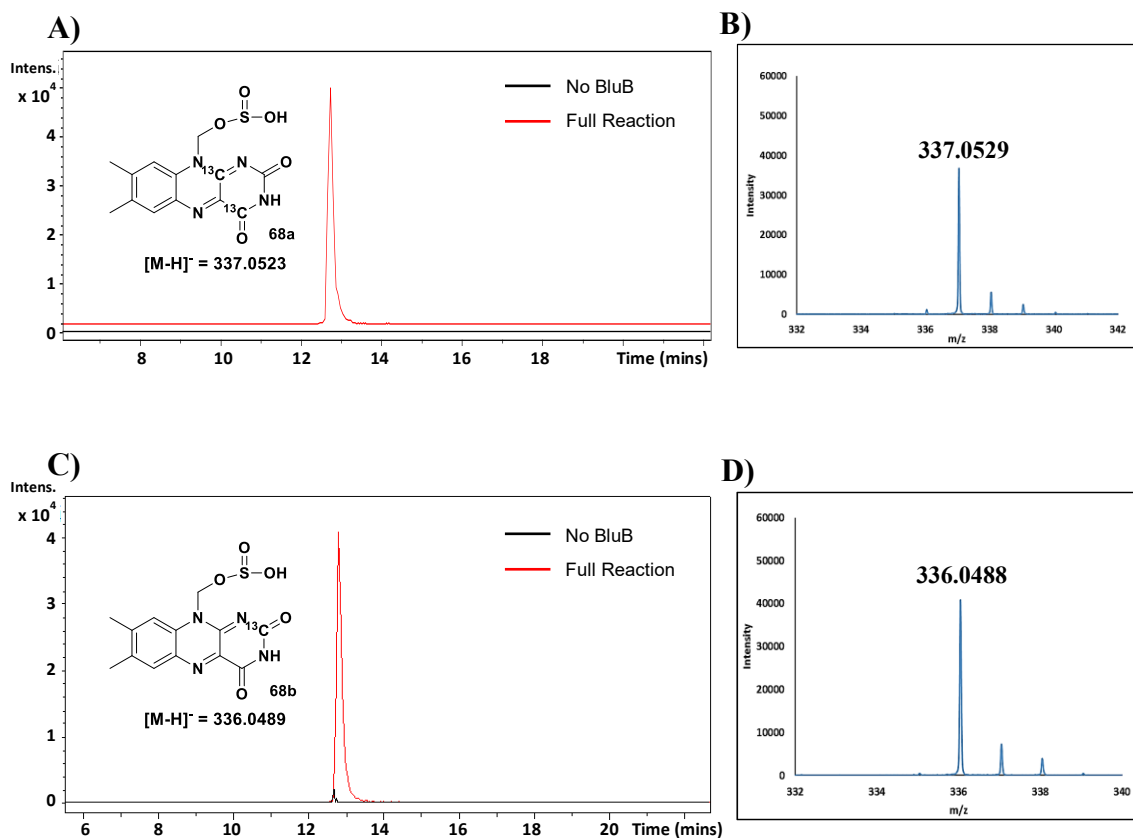

Figure 44. LC-MS analysis of the labelling pattern of the shunt product 68. **(A)** EIC at m/z 337.0523 showing that both the carbons at 4,10a positions of FMN are incorporated in 68 when 4,10a-^{13}C FMN is used as substrate **(B)** ESI-MS of 68 formed on using 4,10a-^{13}C FMN as substrate in the negative mode **(C)** EIC at m/z 336.0489 showing that the carbon at 2 position of FMN is incorporated in 68 when 2-^{13}C FMN is used as substrate **(D)** ESI-MS of 68 formed on using 2-^{13}C FMN as substrate in the negative mode **(E)** EIC at m/z 336.0489 showing that the carbon at 4a position of FMN is incorporated in 68 when 4a-^{13}C FMN is used as substrate **(F)** ESI-MS of 68 formed on using 4a-^{13}C FMN as substrate in the negative mode
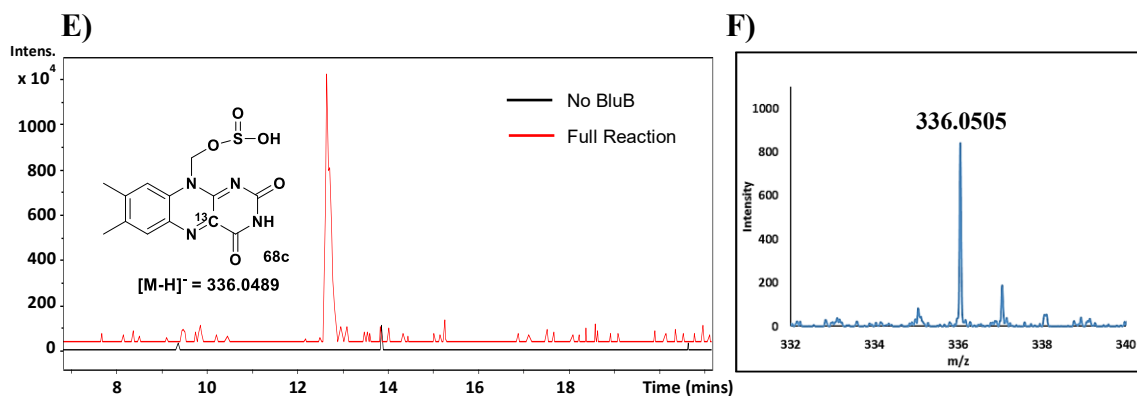
Figure 44. Continued

The summary of the labeling studies for shunt product 68 is shown in Table 4.

Substrate	Mass obtained
FMN	335.1
4,10a-^{13}C FMN	337.1
2-^{13}C FMN	336.1
4a-^{13}C FMN	336.1

Table 4. Labeling study for the formation of shunt product 68

Thus, based on these results, the labeling pattern for the shunt product 68 is as shown in Figure 45.
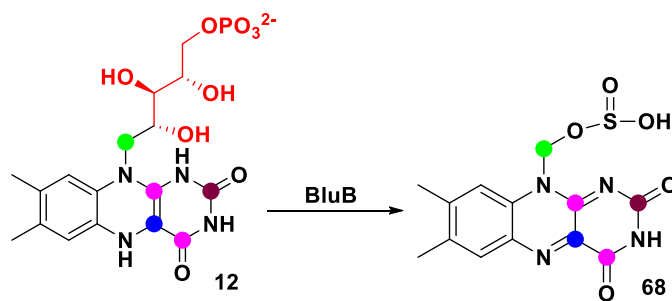
Figure 45. Labeling pattern for the shunt product 68

3.2.11 Formation of lumiflavin as a shunt product

Lumiflavin (69) formation was observed on carrying out the BluB catalyzed reaction using cyanoborohydride (Figure 46). Formation of 69 was confirmed by coelution and deuterium incorporation studies (Figure 47).
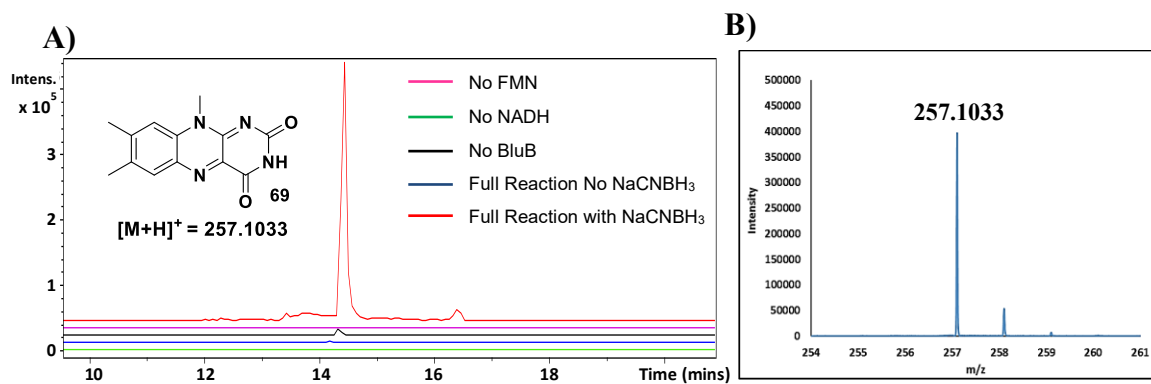
Figure 46. LC-MS analysis of the formation of the shunt product-lumiflavin (69). **(A)** EIC at m/z 257.1033 showing the formation of lumiflavin (69) only in case of full reaction carried out in presence of cyanoborohydride (Red trace) **(B)** ESI-MS of 69 in the positive mode
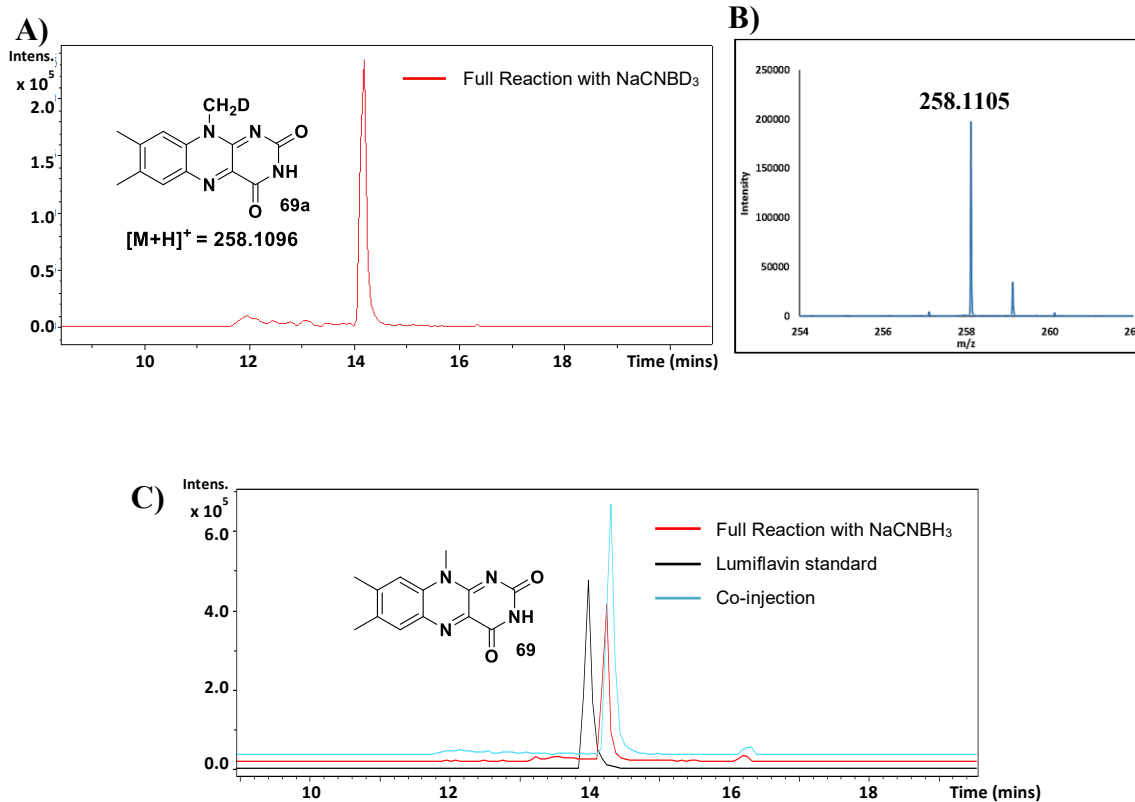
Figure 47. Deuterium and coelution studies for lumiflavin formation. **(A)** EIC at m/z 258.1096 showing the incorporation of deuterium in lumiflavin in presence of cyanoborodeuteride **(B)** ESI-MS of 69a in the positive mode **(C)** Coelution data for the formation of lumiflavin (69)

3.2.12 Formation of lumichrome as a shunt product

Having identified bisulfite adduct of lumichrome (68) and lumiflavin (69) as shunt products in BluB catalyzed reactions, we investigated further to look for the formation of lumichrome itself in the full reaction. The native substrate FMN undergoes slight degradation forming lumichrome which cannot be avoided even after HPLC purification. So, we used 8-substituted FMN analogs (8-OH FMN and 8-NH$_2$ FMN) for this purpose to explore the possibility of formation of any corresponding 8-substituted lumichrome (8-OH

lumichrome and 8-NH$_2$ lumichrome, 70). In both the cases, the lumichrome formation was seen only in case of full reaction (Figure 48A) which was confirmed by coelution studies (Figure 48B).
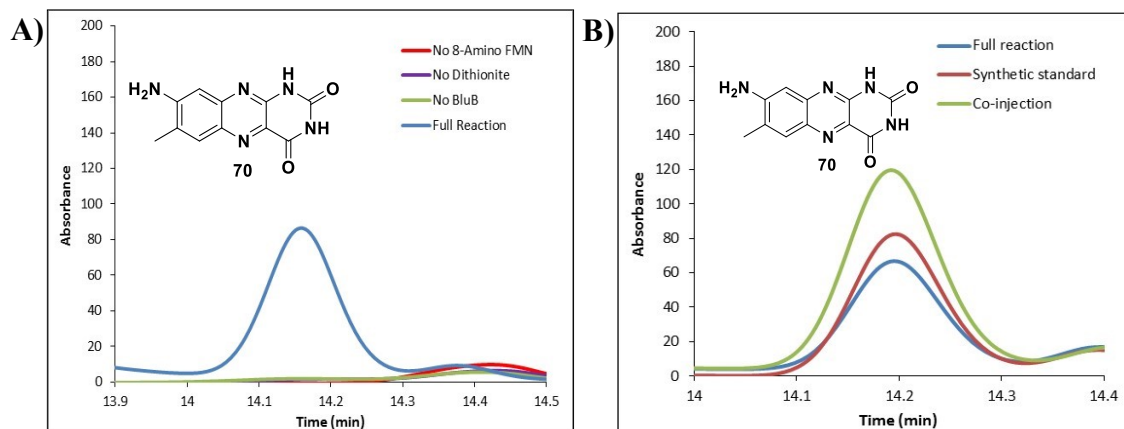
Figure 48. HPLC analysis of the lumichrome formation. **(A)** HPLC chromatogram showing the formation of 8-NH$_2$ lumichrome (70) **(B)** Coelution data for the formation of 70

3.2.13 Mechanistic proposal for the formation of lumichrome based shunt products

Similar to the formation of 56, 57 and 58, we propose a common mechanism for the formation of the three shunt products 68, 69 and 70 as shown in Figure 49. We propose that these three products are also formed by trapping the intermediate 27 (in Figure 21) using different nucleophiles such as water, bisulfite and hydride leading to the formation of species 59 which can readily cyclize to form the final shunt product 71.
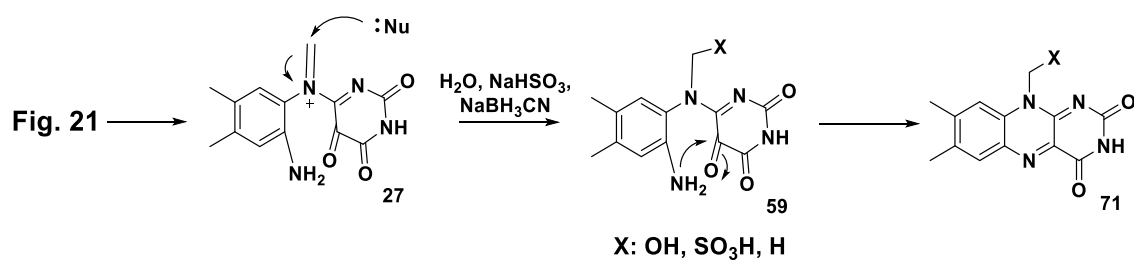
Figure 49. Mechanistic hypothesis for formation of 68, 69 and 70

When X is water, one can readily lose formaldehyde to form lumichrome, X being bisulfite will lead to the formation of 68 and finally when X is hydride one will observe the formation of lumiflavin (69).
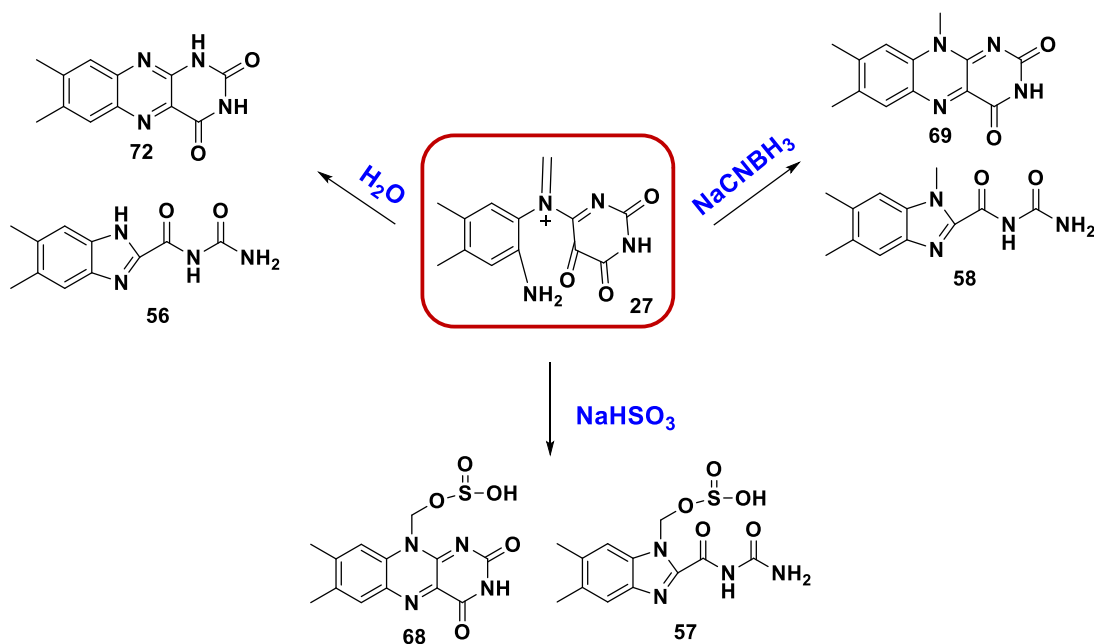
Figure 50. Summary of the formation of different shunt products

Thus, we have successfully trapped one of the key reaction intermediates (27) in the DMB formation in the form of six different shunt products using water, bisulfite and hydride as nucleophiles (Figure 50). In the case of water, we observed the formation of the shunt products 56 and lumichrome (72), in case of bisulfite products 57 and 68 are formed while in the presence of cyanoborohydride as the hydride donor formation of 58 and lumiflavin (69) is seen.

The identification and characterization of these six shunt products, thus, provide evidence for the existence of the intermediate 27 in our mechanistic proposal. Trapping of 27 also establishes the actual sequence of the release of the products in the DMB formation. The intermediate 27 still has the alloxan moiety attached to it and thus we can conclude that the release of the sugar (erythrose-4-phosphate, 14) occurs first followed by the formation of alloxan (29).

3.2.14 Trapping of the intermediate 35 in the form of the shunt product 73

In pursuit of the late intermediates proposed in our mechanistic hypothesis, we were able to identify the formation of a new shunt product seen only in full reaction at 320 nm in HPLC chromatogram (Figure 51A). Based on the mass observed in the LC-MS analysis (Figure 52), we proposed 73 as the possible structure for the new compound which was further confirmed by synthesizing a standard and carrying out a coelution experiment (Figure 51B)[41].
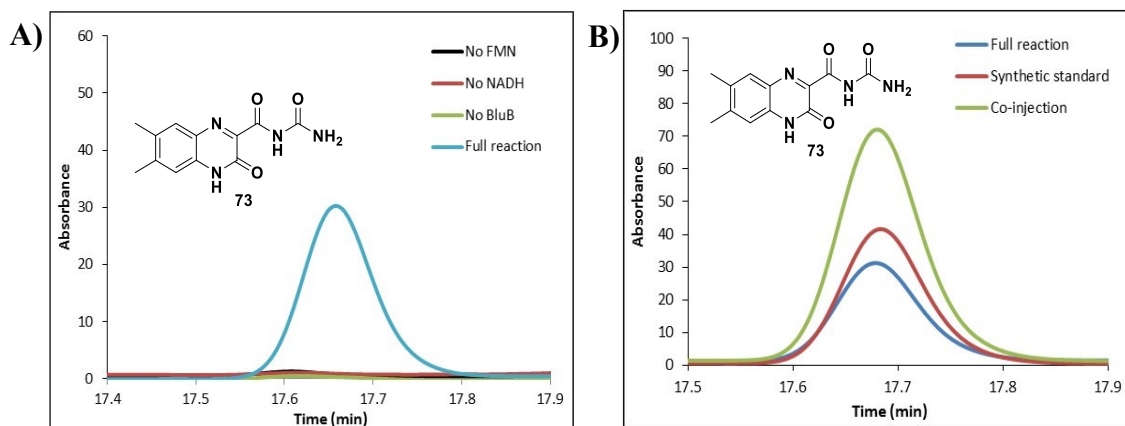
Figure 51. Identification of the shunt product 73. **(A)** HPLC chromatogram for the formation of the shunt product 73 **(B)** Coelution study for 73
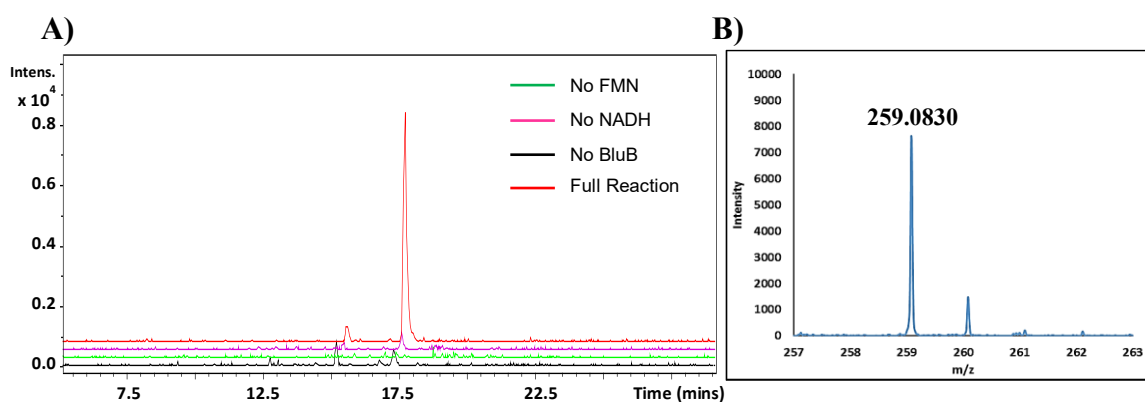
Figure 52. LC-MS analysis of the formation of the shunt product 73. **(A)** EIC at m/z 259.0837 showing the formation of 73 only in case of full reaction (Red trace) **(B)** ESI-MS of 73 in the negative mode

3.2.15 Mechanistic proposal for the formation of the shunt product 73

Our proposal for the formation of 73 is that it arises from the reaction of alloxan (29) with the hydrolyzed product of intermediate 35 (in Figure 21) in our mechanistic hypothesis for DMB formation (Figure 53). The intermediate 35 formed undergoes

58

cyclisation and oxidation to form the native product DMB. It can, however, also undergo hydrolysis to form 74 followed by loss of formaldehyde to give 4,5-Dimethyl-1,2-phenylenediamine (75) which can further react with alloxan, 29 (already present in the reaction mixture as one of the products of DMB biosynthesis) forming shunt product 73.
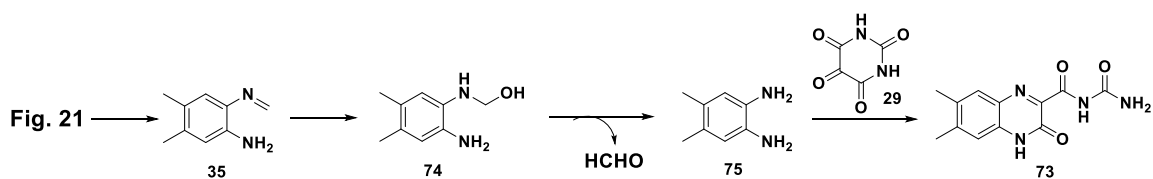
Figure 53. Mechanistic proposal for the formation of 73

The identification of the shunt product 73, thus, proves the intermediacy of 35 in our hypothesis for the biosynthesis of DMB. It also helps us establish the sequence of events, wherein, alloxan is released first followed by the cyclisation step in DMB formation.

3.3 Conclusion

We have successfully identified and characterized the formation of several shunt products during the biosynthesis of dimethylbenzimidazole.

A key intermediate (27) in our mechanistic proposal has been successfully trapped in the form of six different shunt products using water, bisulfite and hydride as nucleophiles. Presence of the imine functionality in the intermediate 27 was confirmed by trapping it with bisulfite as well as reducing it with cyanoborohydride and deuterium

studies. Trapping of 27 also helps us establish the sequence of the release of the products during DMB formation, wherein, the C-C bond cleavage occurs first forming erythrose-4-phosphate followed by the release of alloxan.

Characterization of the shunt product 73 provides evidence for the intermediacy of 35 in our mechanistic hypothesis.

3.4 Experimental

3.4.1 Over-expression and purification of FAD synthetase[48]

The FAD synthetase gene, cloned in a pET24b vector with a C-terminal His-tag, was transformed into *Escherichia coli* BL21 (DE3) cell line. A 10 mL starter culture was grown at 37 °C containing 40 μg/mL kanamycin for 6 hrs. 1.5 liters of LB media was inoculated with this starter culture. The cells were grown at 37 °C with shaking till the OD_{600} reached 0.6. The protein expression was then induced by adding IPTG (final concentration 1 mM) and the culture was incubated at 15 °C for 15 hrs. The cells were then harvested by centrifugation and resuspended in 30 mL of binding buffer (50 mM KPi buffer containing 150 mM NaCl, 10mM imidazole, pH 7.8). The cells were lysed by sonication followed by centrifugation at 15000 rpm for 45 mins. The supernatant containing the soluble protein was loaded on a Ni-NTA affinity column (Histrap-GE Healthcare) and was then washed with 50 mL of wash buffer (50 mM KPi buffer containing 150 mM NaCl, 20mM imidazole, pH 7.8). The protein was eluted with the elution buffer (100 mM KPi buffer containing 100 mM NaCl, 250 mM imidazole, pH 7.8). The eluted protein fractions were pooled and concentrated using 10kDa Amicon

ultracentrifugal filters to a final volume of 3 mL. The concentrated protein solution was buffer exchanged into 100 mM KPi buffer containing 150 mM NaCl and 15% glycerol, pH 7.8 using an Econo-Pac 10DG desalting column.

3.4.2 Reconstitution of BluB using dithionite as reducing system

BluB enzymatic reactions were performed in 100 mM phosphate buffer, pH 7.5 containing BluB (100 μM), FMN (500 μM) and dithionite. The enzymatic reactions were incubated at room temperature for 4 hrs. The protein was removed by heat denaturation and the reaction mixture was analyzed by HPLC and LC-MS.

3.4.3 BluB reactions in the presence of sodium bisulfite

BluB enzymatic reactions were performed in 100 mM phosphate buffer, pH 7.5 containing BluB (100 μM), FMN (500 μM), NADH (2 mM), *E. coli* flavin reductase, Fre (200 nM) and 10 mM sodium bisulfite. The enzymatic reactions were incubated at room temperature for 4 hrs. The protein was removed by heat denaturation and the reaction mixture was analyzed by HPLC and LC-MS.

3.4.4 BluB reactions in the presence of sodium cyanoborohydride

BluB enzymatic reactions were performed in 100 mM phosphate buffer, pH 7.5 containing BluB (100 μM), FMN (500 μM), NADH (2 mM), *E. coli* flavin reductase, Fre (200 nM) and 10 mM sodium cyanoborohydride. The enzymatic reactions were incubated

at room temperature for 4 hrs. The protein was removed by heat denaturation and the reaction mixture was analyzed by HPLC and LC-MS.

3.4.5 Synthesis of the shunt product 56

The synthetic scheme for the shunt product 56 is shown in the Figure 54[44,45].
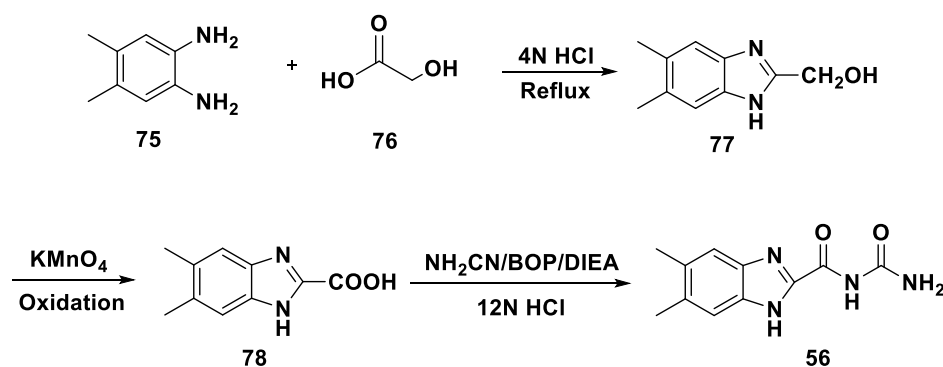
Figure 54. Scheme for the synthesis of 56

Procedure

Synthesis of 5,6-Dimethyl-2-hydroxymethylbenzimidazole (**77**): 4,5-Dimethyl-*o*-phenylenediamine, 75 (136 mg, 1.0 equiv.), glycolic acid, 76 (114 mg, 1.5 equiv.), 4(N) HCl (10 mL) and water (10 mL) were all taken in a round bottom flask and the mixture was refluxed overnight. After cooling, the solution was neutralized slowly with NaOH and the precipitate thus formed was collected by filtration. Yield: 80%, ESI-MS *m/z* 177.1 (M+H). ^{1}H NMR (400 MHz, CD$_3$OD): δ 2.32 (s, 6H), 4.77 (s, 2H), 7.27 (s, 2H) ppm. ^{13}C NMR (100 MHz, CD$_3$OD): δ 20.3, 59.0, 115.8, 132.3, 138.0, 155.1 ppm.

***Synthesis of 5,6-Dimethylbenzimidazole-2-carboxylic acid* (78):** Compound 5,6-Dimethyl-2-hydroxymethylbenzimidazole, 77 (176 mg, 1 equiv.) and Na_2CO_3 (1.06 g, 10 equiv.) were added to 10 mL of boiling water followed by the addition of potassium permanganate (237 mg, 1.5 equiv) in small portions. The mixture was refluxed overnight. The hot solution was filtered and the precipitate of MnO_2 was washed with hot water. The filtrate was cooled and carefully neutralized with hydrochloric acid. The precipitated 5,6-Dimethylbenzimidazole-2-carboxylic acid (78) was collected by filtration. LC-MS *m/z* 191.1 (M+H).

***Synthesis of N-Carbamoyl-5,6-dimethylbenzimidazole-2-carboxamide* (56):** 5,6-Dimethylbenzimidazole-2-carboxylic acid, 78 (1 equiv.), BOP (1.2 equiv.), cyanamide (1.5 equiv) and DIEA (3 equiv.) were dissolved in DMF (5 mL) and the reaction mixture was stirred at rt for 16 hrs. 12(N) HCl (2 mL) was added to the reaction mixture and it was further stirred at rt for another 16 hrs. The desired compound thus formed was purified by reverse phase high performance liquid chromatography. LC-MS *m/z* 233.1 (M+H). ^{1}H NMR (400 MHz, DMSO-*d_6*/CD_3OD): δ 2.33 (s, 6H), 7.45 (s, 2H) ppm. ^{13}C NMR (100 MHz, DMSO-*d_6*/CD_3OD): δ 20.0, 116.1, 134.0, 136.6, 142.4, 152.3, 158.3 ppm.

3.4.6 Synthesis of the shunt product 58

The synthetic scheme for the shunt product 58 is shown in the Figure 55[46,47].
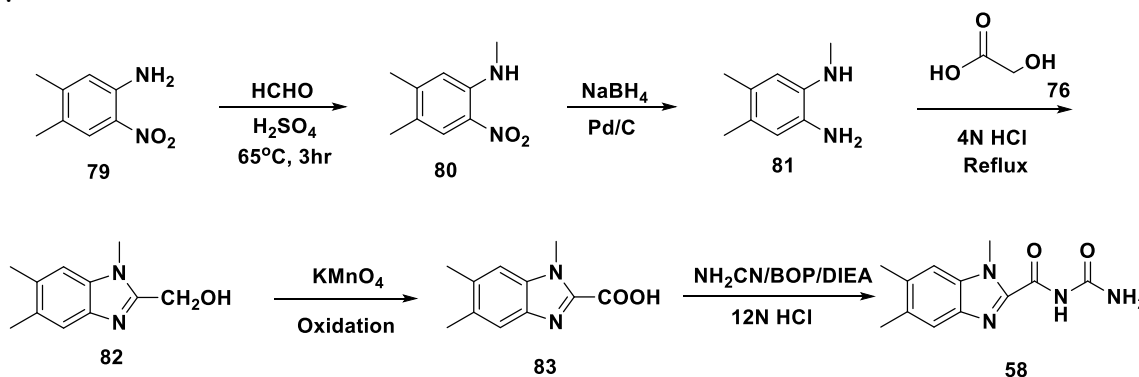
Figure 55. Scheme for the synthesis of 58

Procedure

Synthesis of N-Methyl-4,5-dimethyl-2-nitrobenzenamine **(80):** Aqueous formaldehyde (10 mL, 37%) was added slowly in a dropwise manner to a mixture of 4,5-Dimethyl-2-nitroaniline, 79 (1 g) and conc. H_2SO_4 (10 mL). The mixture was then heated for 3 hrs at 65 °C, cooled and poured into ice water (500 mL). The solid was collected by filtration and was then dissolved in ethyl acetate. The solution was then washed with saturated $NaHCO_3$ and was dried using Na_2SO_4. The resulting solution was filtered and evaporated to give the desired compound in the form of a red-orange solid. Yield: 90%, LC-MS m/z 181.1 (M+H). ^{1}H NMR (400 MHz, CDCl$_3$): δ 2.16 (s, 3H), 2.26 (s, 3H), 2.98 (s, 3H), 6.59 (s, 1H), 7.90 (s, 1H) ppm. ^{13}C NMR (100 MHz, CDCl$_3$): δ 18.5, 20.7, 29.7, 113.7, 124.3, 126.4, 145.0, 147.3 ppm.

Synthesis of N-Methyl-4,5-dimethylbenzene-1,2-diamine **(81):** Catalytic reduction of N-Methyl-4,5-dimethyl-2-nitrobenzenamine, 80 (1 equiv.) was carried out using 10% Pd/C (4% Pd w/w) and $NaBH_4$ (3 equiv.) in MeOH under argon at rt. After 40 mins, the reaction mixture was filtered through celite and washed with MeOH. The filtrate was evaporated to give the desired compound. Yield: 90%, LC-MS *m/z* 151.1 (M+H). ^{1}H NMR (400 MHz, CD_3OD): δ 2.22 (s, 3H), 2.26 (s, 3H), 2.91 (s, 3H), 6.53 (s, 1H), 6.65 (s, 1H) ppm. ^{13}C NMR (100 MHz, CD_3OD): δ 18.9, 19.3, 31.7, 114.4, 119.3, 126.7, 128.4, 133.2, 137.5 ppm.

Synthesis of 1,5,6-Trimethyl-2-hydroxymethylbenzimidazole **(82):** N-Methyl-4,5-dimethylbenzene-1,2-diamine, 81 (150 mg, 1.0 equiv.), glycolic acid, 76 (114 mg, 1.5 equiv.), 4(N) HCl (10 mL) and water (10 mL) were all taken in a round bottom flask and the mixture was refluxed overnight. After cooling, the solution was neutralized slowly with NaOH and the precipitate thus formed was collected by filtration. Yield: 80%, LC-MS *m/z* 191.1 (M+H). ^{1}H NMR (400 MHz, DMSO-*d6*): δ 2.28 (s, 3H), 2.32 (s, 3H), 3.75 (s, 3H), 4.66 (s, 2H), 7.25 (s, 1H), 7.33 (s, 1H) ppm. ^{13}C NMR (100 MHz, DMSO-*d6*): δ 19.8, 20.0, 29.7, 56.3, 109.8, 119.0, 129.4, 130.5, 134.6, 140.3, 153.0 ppm.

Synthesis of 1,5,6-Trimethylbenzimidazole-2-carboxylic acid **(83):** Compound 1,5,6-trimethyl-2-hydroxymethylbenzimidazole, 82 (190 mg, 1 equiv.) and Na_2CO_3 (1.06 g, 10 equiv.) were added to 10 mL of boiling water followed by the addition of potassium permanganate (237 mg, 1.5 equiv) in small portions. The mixture was refluxed overnight. The hot solution was filtered and the precipitate of MnO_2 was washed with hot water. The filtrate was cooled and carefully neutralized with hydrochloric acid. The precipitated N-

Methyl-5,6-dimethylbenzimidazole-2-carboxylic acid (83) was collected by filtration. LC-MS *m/z* 203.1 (M-H). ^{1}H NMR (400 MHz, DMSO-*d₆*): δ 2.29 (s, 3H), 2.33 (s, 3H), 4.05 (s, 3H), 7.25 (s, 1H), 7.37 (s, 1H) ppm. ^{13}C NMR (100 MHz, DMSO-*d₆*): δ 19.9, 20.1, 31.4, 110.5, 119.5, 129.9, 131.2, 134.6, 139.3, 150.2, 162.3 ppm.

***Synthesis of N-Carbamoyl-1,5,6-trimethylbenzimidazole-2-carboxamide* (58):** Compound 1,5,6-Trimethylbenzimidazole-2-carboxylic acid, 83 (1 equiv.), BOP (1.2 equiv.), cyanamide (1.5 equiv) and DIEA (3 equiv.) were dissolved in DMF/MeOH (5 mL) and the reaction mixture was stirred at rt for 16 hrs. 12(N) HCl (2 mL) was added to the reaction mixture and it was further stirred at rt for another 16 hrs. The desired compound thus formed was purified by reverse phase high performance liquid chromatography. LC-MS *m/z* 247.1 (M+H). ^{1}H NMR (400 MHz, CD₃OD): δ 2.39 (s, 3H), 2.44 (s, 3H), 4.16 (s, 3H), 7.39 (s, 1H), 7.53 (s, 1H) ppm.

3.4.7 Synthesis of ^{13}C labeled FMN (Labeled at C1′ position of ribose)[49,50]

The synthetic scheme for 11d is shown in Figure 56.
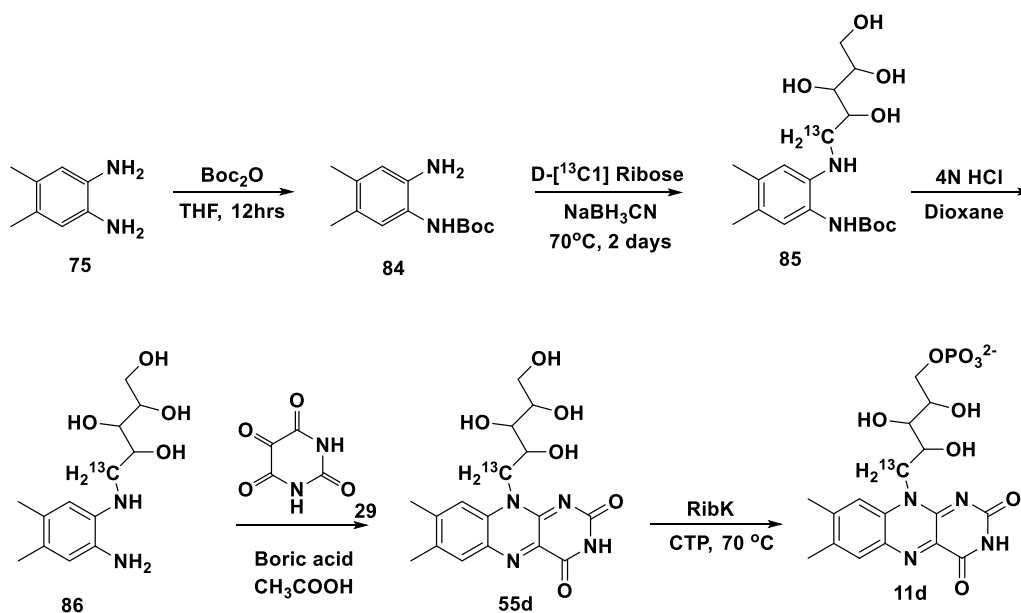
Figure 56. Scheme for the synthesis of 11d

Procedure

Synthesis of 2-(Boc)amino-4,5-dimethylaniline (84): 4,5-Dimethylbenzene-1,2-diamine, 75 (272 mg, 1 equiv.), Boc$_2$O (218, 0.5 equiv.) and NaHCO$_3$ (84 mg, 1 equiv.) were dissolved in 1:1 water-dioxane mixture (25 mL). The reaction mixture was stirred at rt for 5 hrs. The mixture was then diluted with water (30 mL) and extracted with DCM. The organic phase was then washed with saturated NaHCO$_3$ solution followed by brine, dried over Na$_2$SO$_4$ and was concentrated. The residue was purified by silica gel column chromatography using chloroform/methanol. Yield: 90%. ^{1}H NMR (400 MHz, CD$_3$OD):

δ 1.49 (s, 9H), 2.11 (s, 3H), 2.13 (s, 3H), 6.61 (s, 1H), 6.87 (s, 1H) ppm. ^{13}C NMR (100 MHz, CD$_3$OD): δ 18.8, 19.3, 28.7, 80.8, 119.9, 123.5, 127.9, 135.5, 140.0, 156.7 ppm.

Synthesis of 85: Boc-protected aniline, 84 (1 equiv.), D-[^{13}C1] ribose (3.0 equiv.) and sodium cyanoborohydride (2.0 equiv.) were dissolved in anhydrous MeOH (15 mL). The mixture was refluxed at 80 °C for 2 days under argon atmosphere. Then the solvent was removed under reduced pressure and excess NaBH$_3$CN was quenched using 1M HCl. The resulting mixture was neutralized using saturated NaHCO$_3$ solution and concentrated under reduced pressure. The residue was purified by silica gel column chromatography using chloroform/methanol. Yield: 80%, ESI-MS *m/z* 372.2 (M+H). ^{1}H NMR (400 MHz, CD$_3$OD): δ 1.44 (s, 9H), 2.07 (s, 3H), 2.13 (s, 3H), 3.26 (m, 1H), 3.58 (m, 3H), 3.71 (m, 2H), 3.88 (m, 1H), 6.56 (s, 1H), 6.85 (s, 1H) ppm.

Synthesis of 86: Boc-protected riboaniline, 85 (100 mg) was stirred in 4(N) HCl/dioxane mixture (5 mL) for 4 hrs. The solvent was removed under reduced pressure and the remaining mixture was diluted with water followed by extraction with ether. The aqueous layer was concentrated to yield the desired product. Yield: 90%. ^{1}H NMR (400 MHz, CD$_3$OD): δ 2.31 (s, 3H), 2.32 (s, 3H), 3.52 (m, 1H), 3.86 (m, 5H), 4.11 (br, 1H), 7.44 (s, 1H), 7.52 (s, 1H) ppm.

Synthesis of 55d: Compound 86 (1 equiv.), alloxan monohydrate (3 equiv.) and boric acid (2 equiv.) were dissolved in 20 mL of acetic acid. The reaction mixture was stirred overnight under argon atmosphere and the desired ^{13}C labeled riboflavin (55d) was purified by reverse phase high performance liquid chromatography. LC-MS *m/z* 378.1 (M+H) (Figure 57).

Synthesis of 11d: Compound 55d was converted to ^{13}C labeled FMN enzymatically using RibK from *Methanocaldococcus jannaschii*. 55d was incubated for 30 mins at 70 °C with 5 mM CTP, 20 mM MgCl$_2$ and RibK in 100 mM potassium phosphate buffer, pH 7.5. The reaction mixture was passed through a 10kDa cut-off filter and purified by reverse phase high performance liquid chromatography. LC-MS *m/z* 458.1 (M+H) (Figure 58).
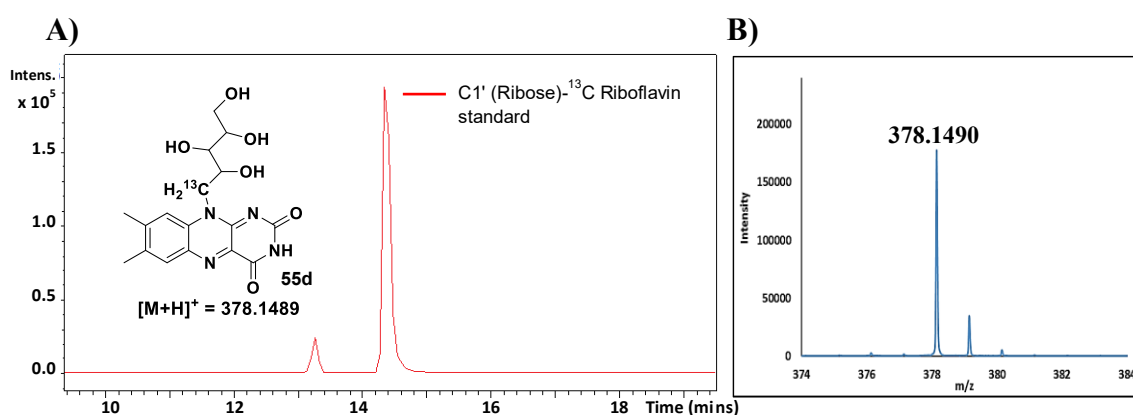
Figure 57. LCMS analysis of the synthesized ^{13}C labeled riboflavin 55d (Labeled at C1' position of ribose). **(A)** EIC at m/z 378.1489 showing the formation of ^{13}C labeled riboflavin **(B)** ESI-MS of 55d in the positive mode
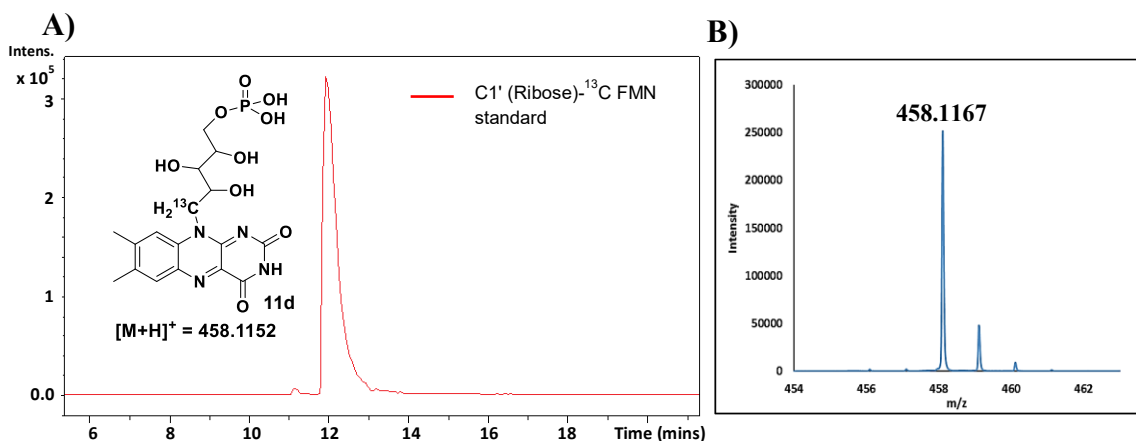
Figure 58. LCMS analysis of the synthesized ^{13}C labeled FMN 11d (Labeled at C1' position of ribose). **(A)** EIC at 458.1152 showing the formation of ^{13}C labeled FMN **(B)** ESI-MS of 11d in the positive mode

3.4.8 Synthesis of 8-NH$_2$ FMN (93)[51,52]

The synthetic scheme for 8-NH$_2$ FMN (93) is shown in Figure 59.
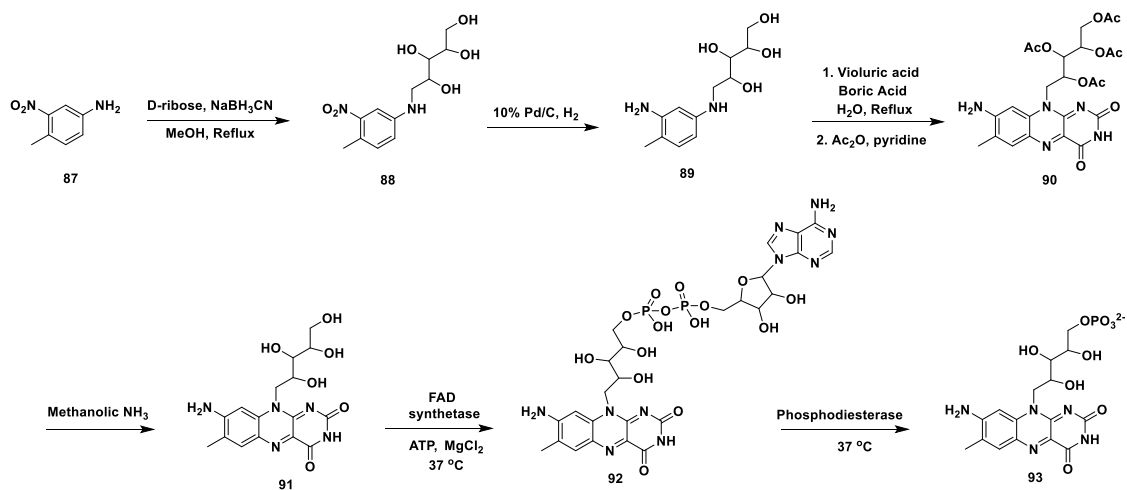
Figure 59. Scheme for the synthesis of 8-NH$_2$ FMN (93)

Procedure

Synthesis of 5-((4-Methyl-3-nitrophenyl)amino)pentane-1,2,3,4-tetraol (88): Methyl-3-nitrophenylamine, 87 (152 mg, 1.0 equiv.), D-ribose (450 mg, 3.0 equiv.) and sodium cyanoborohydride (126 mg, 2.0 equiv.) were dissolved in anhydrous MeOH (15 mL). The mixture was refluxed at 80 °C for 2 days under argon atmosphere. Then the solvent was removed under reduced pressure and excess NaBH$_3$CN was quenched using 1M HCl. The resulting mixture was neutralized using saturated NaHCO$_3$ solution and concentrated under reduced pressure. The residue was purified by silica gel column chromatography using chloroform/methanol (98:2 to 80:20). Yield: 50%, LC-MS *m/z* 285.1 (M-H). ^{1}H NMR (400 MHz, CD$_3$OD): δ 2.36 (s, 3H), 3.15-3.21 (m, 1H), 3.45 (dd,

1H), 3.61-3.67 (m, 2H), 3.72-3.80 (m, 2H), 3.89-3.94 (m, 1H), 6.87 (dd, 1H), 7.08 (d, 1H), 7.21 (d, 1H) ppm. ^{13}C NMR (100 MHz, CD$_3$OD): δ 19.2, 47.1, 64.4, 72.1, 74.1, 74.4, 108.3, 119.0, 121.2, 133.9, 149.3, 151.0 ppm.

Synthesis of 5-((3-Amino-4-methylphenyl)amino)pentane-1,2,3,4-tetraol **(89):** Compound 88 (100 mg) was dissolved in 50 mL MeOH and passed through a Thalesnano H-cube hydrogenator with 10% Pd/C catalyst at 40 °C and 1 bar hydrogen gas pressure at a flow rate of 1.0 mL/min. The solution was then concentrated under reduced pressure and the resulting compound 89 was used for the next coupling step without further purification. Yield: 90%, LC-MS *m/z* 255.1 (M-H). ^{1}H NMR (400 MHz, CD$_3$OD): δ 2.02 (s, 3H), 3.39 (dd, 1H), 3.44-3.51 (m, 1H), 3.61-3.68 (m, 2H), 3.74-3.80 (m, 2H), 3.88-3.92 (m, 1H), 6.09 (dd, 1H), 6.16 (d, 1H), 6.75 (d, 1H) ppm. ^{13}C NMR (100 MHz, CD$_3$OD): δ 16.5, 48.1, 64.4, 72.1, 74.1, 74.8, 102.7, 106.2, 114.1, 131.7, 146.6, 148.9 ppm.

Synthesis of 8-Aminoriboflavintetraacetate **(90):** To a solution of 89 in 15 mL of water, violuric acid monohydrate (175 mg) and boric acid (62 mg) were added. The mixture was refluxed at 105 °C for 12 hours and was then concentrated under reduced pressure. The crude product was dissolved in 8 mL of pyridine. 1 mL of acetic anhydride was added to the mixture and was stirred at RT for 6 hrs. The solvent was then removed under reduced pressure with toluene. The residue was purified by silica gel column chromatography using chloroform/methanol (95:5 to 80:20). LC-MS *m/z* 544.2 (M-H). ^{1}H NMR (400 MHz, CD$_3$OD): δ 1.98 (s, 3H), 2.01 (s, 3H), 2.14 (s, 3H), 2.18 (s, 3H), 2.28 (s, 3H), 4.24 (dd, 2H), 4.48 (dd, 1H), 5.37-5.41 (m, 2H), 5.48 (t, 1H), 5.63-5.67 (m, 1H), 6.81 (s, 1H), 7.61 (s, 1H) ppm. ^{13}C NMR (100 MHz, CD$_3$OD): δ 17.1, 20.4, 20.6, 20.7, 20.9,

45.9, 62.9, 70.4, 71.0, 72.0, 96.0, 127.8, 127.9, 132.9, 134.8, 137.4, 152.4, 158.3, 158.7, 163.4, 171.4, 171.6, 171.9, 172.4 ppm.

***Synthesis of 8-Aminoriboflavin* (91):** Compound 90 was converted to compound 91 by overnight stirring in ammonia (7N in methanol). LC-MS *m/z* 376.1 (M-H) (Figure 60A and B).

***Synthesis of 8-Aminoflavinadeninedinucleotide* (92):** Compound 91 was converted to 8-NH$_2$ FAD (92) enzymatically using FAD synthetase enzyme from *Corynebacterium ammoniagenes.* 8-NH$_2$ riboflavin (91) was incubated overnight at 37 $^{\circ}$C with 5 mM ATP, 20 mM MgCl$_2$ and FAD synthetase in 100 mM potassium phosphate buffer, pH 7.5. The reaction mixture was passed through a 10kDa cut-off filter and purified by reverse phase high performance liquid chromatography. LC-MS *m/z* 785.1 (M-H) (Figure 60 C and D).

***Synthesis of 8-Aminoflavinmononucleotide* (93):** 8-NH$_2$ FAD (92) purified by HPLC was incubated overnight at 37 $^{\circ}$C with 2-3 mg of phosphodiesterase I from *Crotalus atrox* (Western Diamondback Rattlesnake) in 10 mL of 100 mM potassium phosphate buffer, pH 7.5. The reaction mixture was passed through a 10kDa cut-off filter and then purified by reverse phase high performance liquid chromatography to yield the final compound 8-NH$_2$ FMN (93)**.** LC-MS *m/z* 456.1 (M-H) (Figure 60E and F). ^{1}H NMR (400 MHz, CD$_3$OD): δ 2.18 (s, 3H), 3.91-3.94 (m, 1H), 3.99-4.03 (m, 2H), 4.05-4.10 (m, 1H), 4.29-4.31 (m, 1H), 4.40 (d, 1H), 4.75-4.82 (m, 1H), 6.66 (s, 1H), 7.34 (s, 1H). ^{13}C NMR (100 MHz, CD$_3$OD): δ 16.4, 47.2, 66.1, 69.1, 71.2, 71.3, 72.8, 95.1, 124.3, 128.9, 132.6, 132.7, 136.2, 150.4, 157.3, 158.1, 162.5 ppm.
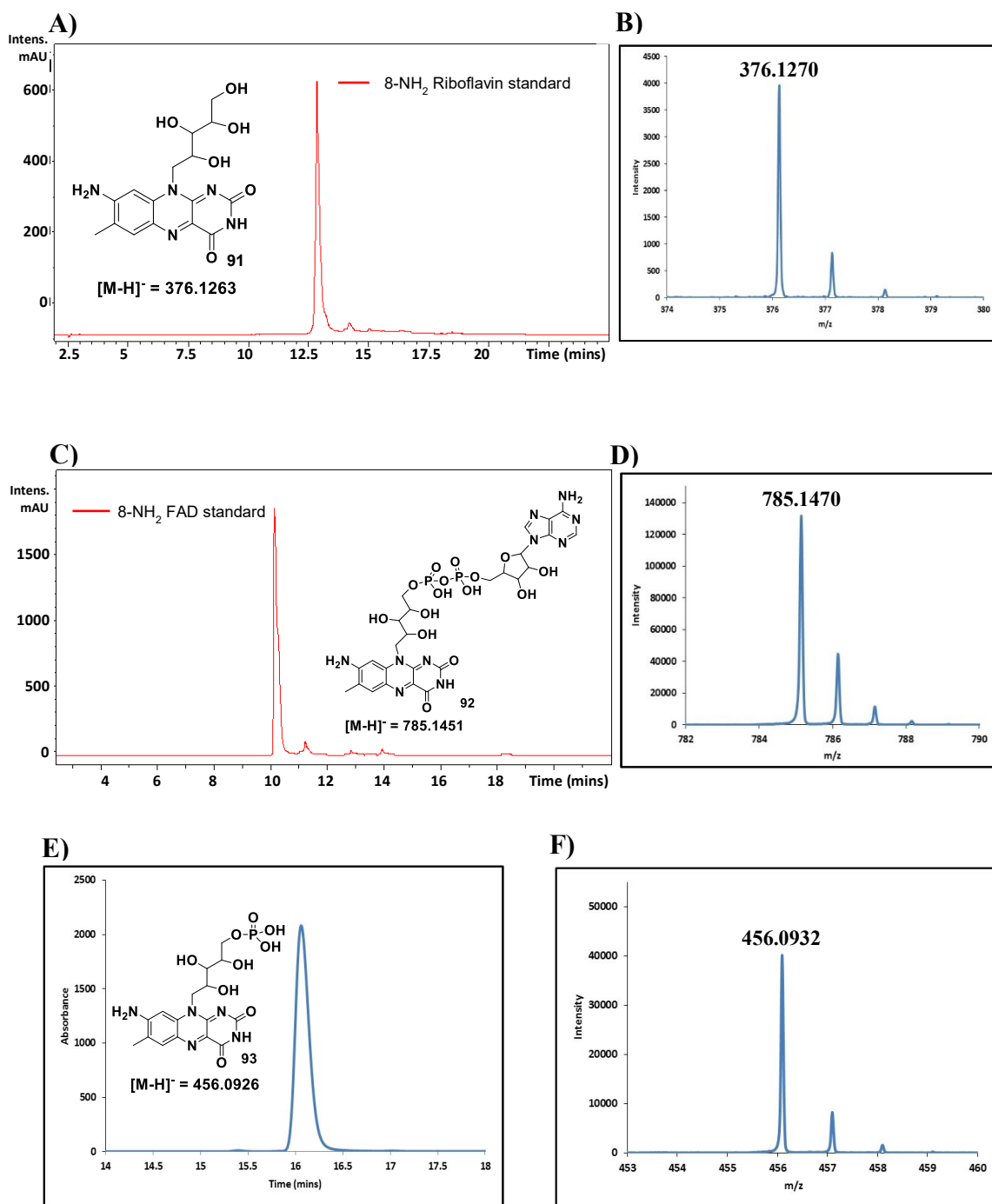
**Figure 60.** HPLC and LC-MS analysis of the synthesized 8-NH$_2$ FMN (93). **(A)** UV chromatogram at 450 nm showing the formation of 8-NH$_2$ Riboflavin **(B)** ESI-MS of 91 in the negative mode **(C)** UV chromatogram at 450 nm showing the formation of 8-NH$_2$ FAD **(D)** ESI-MS of 92 in the negative mode **(E)** UV chromatogram at 450 nm showing the formation of 8-NH$_2$ FMN **(F)** ESI-MS of 93 in the negative mode

3.4.9 Synthesis of 8-NH$_2$ lumichrome (70)

The synthetic scheme for 8-NH$_2$ lumichrome (70) is shown in Figure 61.
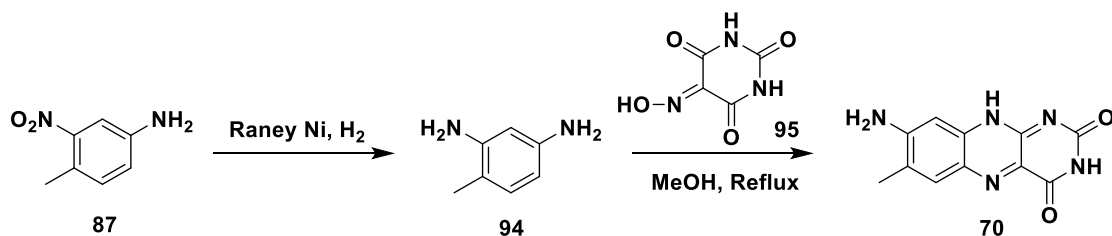
Figure 61. Scheme for the synthesis of 8-NH$_2$ lumichrome (70)

Procedure

Synthesis of 4-Methylbenzene-1,3-diamine **(94):** 4-Methyl-3-nitroaniline, 87 (100 mg) was dissolved in 50 mL MeOH and passed through a Thalesnano H-cube hydrogenator with 10% Pd/C catalyst at 40 ºC and 1 bar hydrogen gas pressure at a flow rate of 1.0 mL/min. The solution was then concentrated under reduced pressure and the resulting compound 94 was used for the next coupling step without further purification. Yield: 90%. ^{1}H NMR (400 MHz, CD$_3$OD): δ 2.03 (s, 3H), 6.09 (dd, 1H), 6.17 (d, 1H), 6.72 (d, 1H) ppm. ^{13}C NMR (100 MHz, CD$_3$OD): δ 16.6, 104.7, 108.1, 114.9, 131.7, 146.7, 146.9 ppm.

Synthesis of 8-Aminolumichrome **(70):** To a solution of 4-Methylbenzene-1,3-diamine, 94 (122 mg, 1 equiv.) in 15 mL of water, violuric acid monohydrate (175 mg, 1 equiv.) and boric acid (62 mg, 1 equiv.) were added. The mixture was refluxed at 105 ºC for 12 hours and was then concentrated under reduced pressure and purified. Yield: 40%.

^{1}H NMR (400 MHz, DMSO-d_6): δ 2.28 (s, 3H), 6.51 (s, 2H), 6.78 (s, 1H), 7.65 (s, 1H), 11.33 (s, 1H), 11.46 (s, 1H) ppm. ^{13}C NMR (100 MHz, DMSO-d_6): δ 17.6, 101.9, 123.6, 129.5, 130.0, 134.6, 144.7, 146.7, 150.0, 153.3, 160.8 ppm.

3.4.10 Synthesis of the shunt product 73[41]

The synthetic scheme for the shunt product 73 is shown in Figure 62.
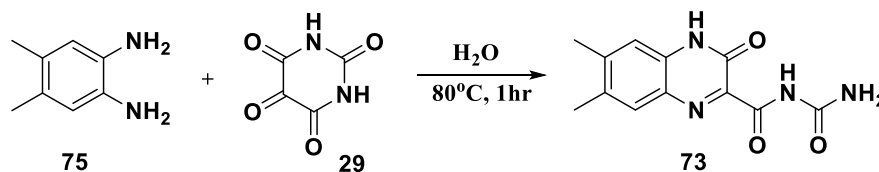
Figure 62. Scheme for the synthesis of the shunt product 73

Procedure

Synthesis of N-[(6,7-Dimethyl-3-oxo-3,4-dihydroquinoxalin-2-yl)carbonyl]urea **(73):** 4,5-Dimethyl-*o*-phenylenediamine, 75 (136 mg, 1.0 equiv.) was dissolved in 10 mL of water and was then added to the aqueous solution of alloxan, 29 (160 mg, 1.0 equiv. in 10 mL). A precipitate was immediately formed. The reaction mixture was then heated at 80 °C for an hour and was then filtered followed by washing with hot water to yield the final compound. Yield: 65%, LC-MS *m/z* 259.1 (M-H). ^{1}H NMR (400 MHz, CDCl$_3$/CF$_3$COOH): δ 2.44 (s, 3H), 2.51 (s, 3H), 7.1 (br, 1H), 7.31 (s, 1H), 7.86 (s, 1H), 8.64 (br, 1H) ppm. ^{13}C NMR (100 MHz, CDCl$_3$/CF$_3$COOH): δ 19.6, 20.9, 116.4, 130.4, 132.3, 137.8, 138.7, 149.9, 156.3, 157.0, 163.1 ppm.

CHAPTER IV

ROLE OF THE ASPARTATE RESIDUE (ASP-32)

4.1 Introduction

The active site of BluB consists of residues which are well conserved among the BluB orthologs but are found absent in oxidoreductases. Asp-32 is one such residue which has been shown to be very critical for the catalytic activity of BluB[15]. Mutation of Asp-32 residue to alanine (Ala) or asparagine (Asn) results in loss of enzymatic activity. Typically, serine or arginine residue is seen to stabilize the N1 of FMN by H-bonding in the active sites of oxidoreductase, nitroreductase and IYD enzymes[32]. Interestingly, in BluB along with Arg-34, there is also Asp-32 which is in proximity to N1 of FMN as well as to the C1$'$ of the ribityl chain of FMN[30]. Aspartate has never been seen at this position in the other enzymes which are structurally similar to BluB. In fact, the presence of aspartate at this position would be expected to destabilize the BluB-FMNH$_2$ complex as the N1 of the reduced flavin often exists in the deprotonated form. Thus, the Asp-32 residue can be postulated to play an important role in stabilizing a reactive intermediate during the DMB formation in BluB.

4.2 Results and Discussion

4.2.1 Activity of D32N mutant and its comparison with the wild type enzyme

A closer look at the crystal structure of BluB revealed that the Asp-32 residue is well placed to undergo interaction with the C1$'$ of the ribityl tail with the distance being

3.2 Å (Figure 63). To explore the role of the Asp-32 residue, it was mutated to asparagine and the corresponding D32N mutant was used for BluB enzymatic reactions.
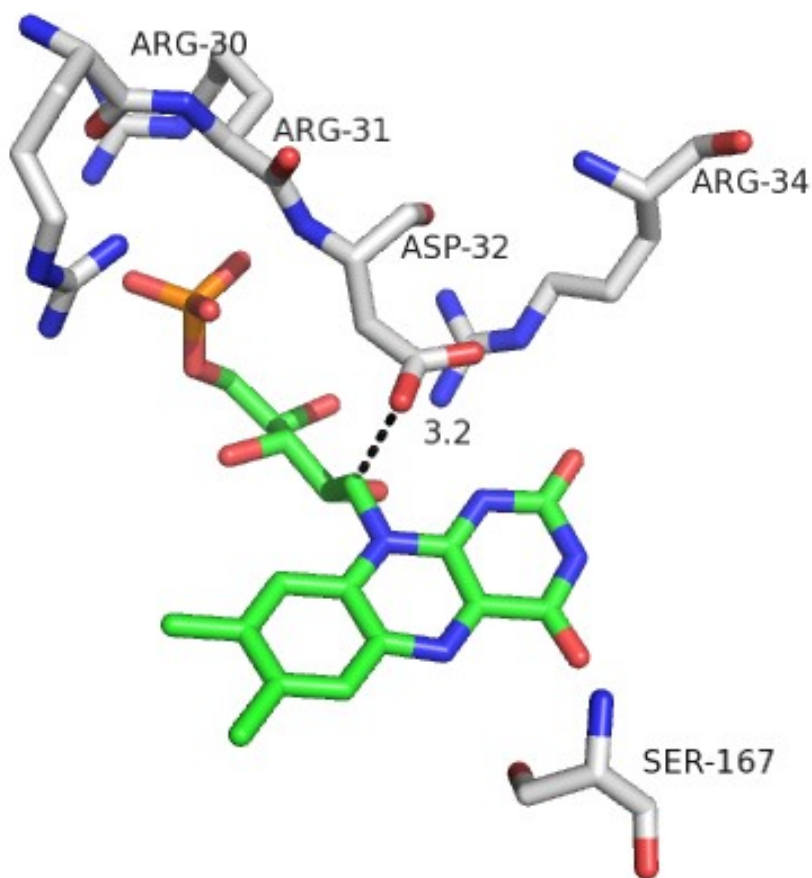

Figure 63. Interaction of Asp 32 residue with C1' of the ribityl tail

D32N mutant was found to be almost inactive towards the formation of the native product as only negligible amounts of DMB (13) formation was observed (Figure 64). Interestingly with the D32N mutant, shunt product 56 was seen to be formed in much greater amounts as compared to wild type BluB (Figure 65).
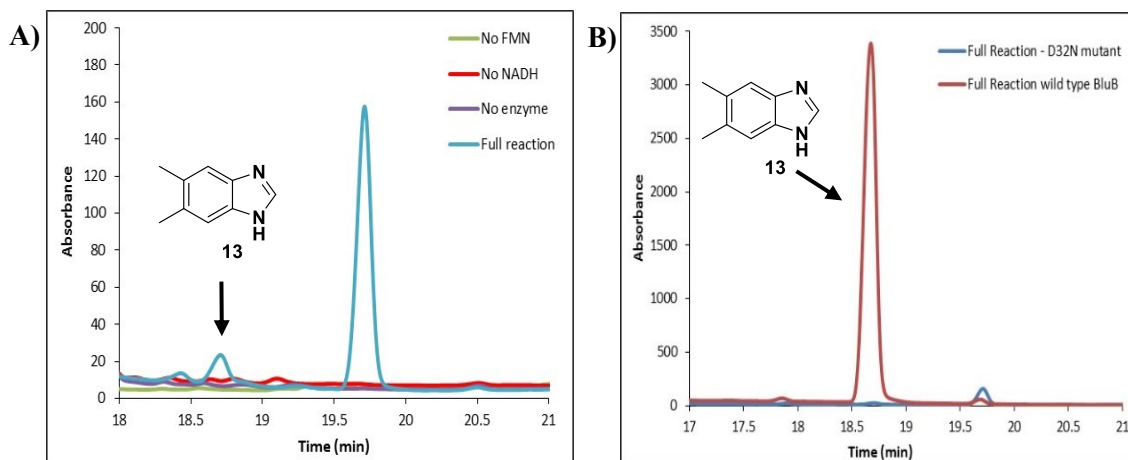
Figure 64. HPLC analysis of the activity of D32N BluB mutant and its comparison with that of wild type BluB for the formation of DMB. **(A)** HPLC chromatogram at 280 nm showing the formation of DMB (13) using the D32N mutant **(B)** Comparison of activities of wild type BluB and D32N mutant towards DMB (13) formation
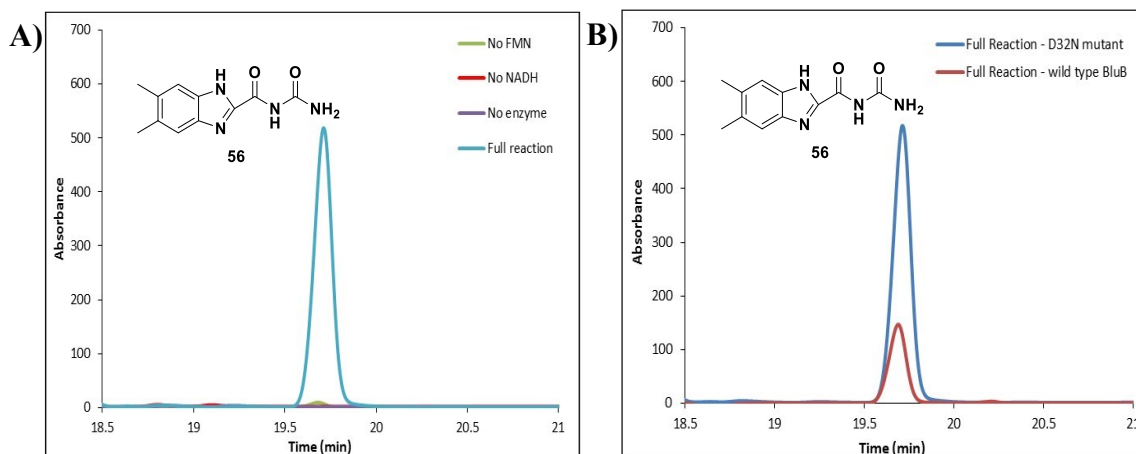

Figure 65. HPLC analysis of the activity of D32N BluB mutant and its comparison with that of wild type BluB for the shunt product 56 formation. **(A)** HPLC chromatogram at 320 nm showing the formation of the shunt product 56 using the D32N mutant **(B)** Comparison of activities of wild type BluB and D32N mutant towards the formation of 56

78

We next checked the activity of the D32N mutant for the formation of the other shunt products (57 and 58). Similar results were also obtained for the shunt products 57 and 58 which were again seen to be formed in larger amounts compared to the wild type enzyme (Figure 66).
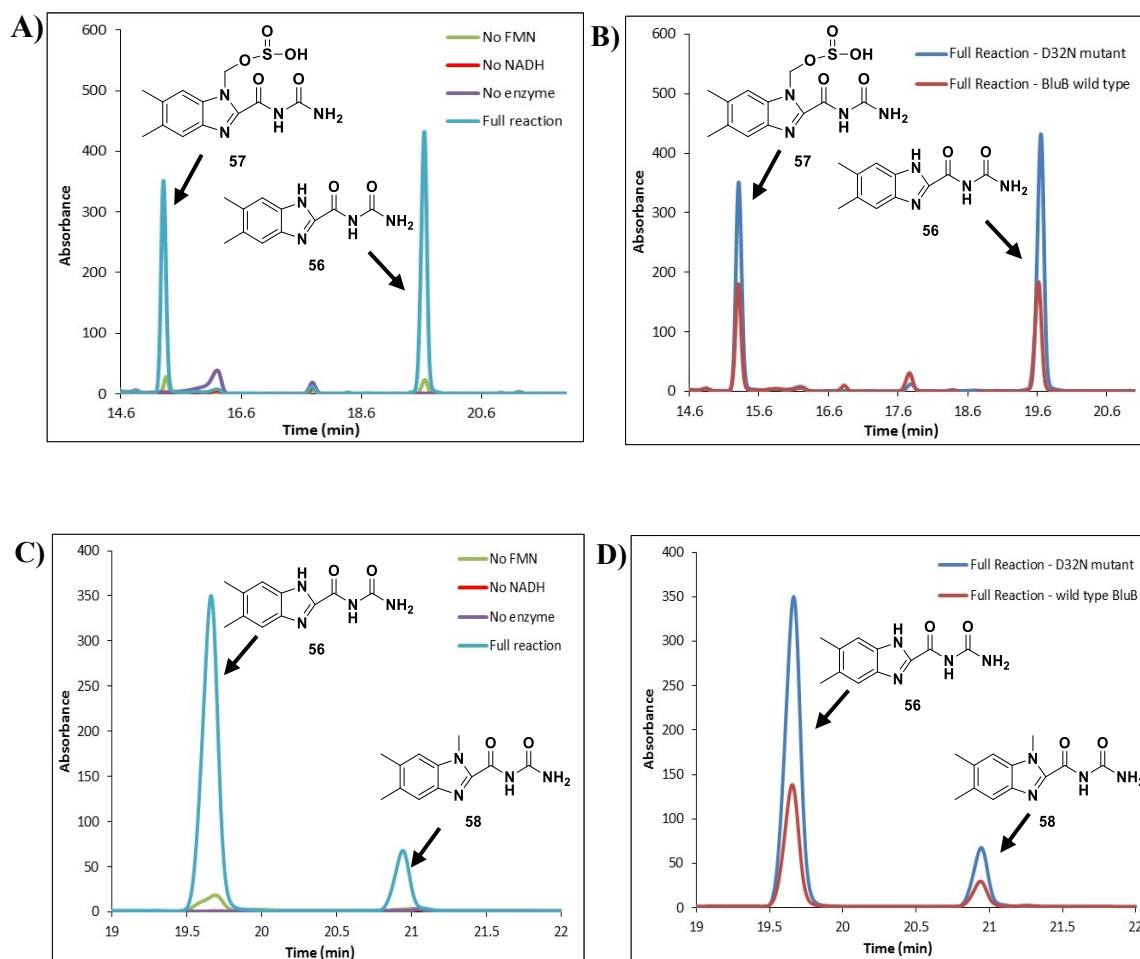
Figure 66. HPLC analysis of the activity of D32N BluB mutant and its comparison with that of wild type BluB. **(A)** HPLC chromatogram at 320 nm showing the formation of the shunt product 57 using the D32N mutant **(B)** Comparison of activities of wild type BluB and D32N mutant towards the formation of 57 **(C)** HPLC chromatogram at 320 nm showing the formation of the shunt product 58 using the D32N mutant **(D)** Comparison of activities of wild type BluB and D32N mutant towards the formation of 58

4.2.2 Revised mechanistic proposal for DMB biosynthesis

The results obtained with the D32N mutant suggest that the residue Asp 32 plays a key role in stabilizing the key intermediate 27 (in Figure 21) during the formation of DMB. Based on this, our revised proposal for DMB formation is as shown in Figure 67.
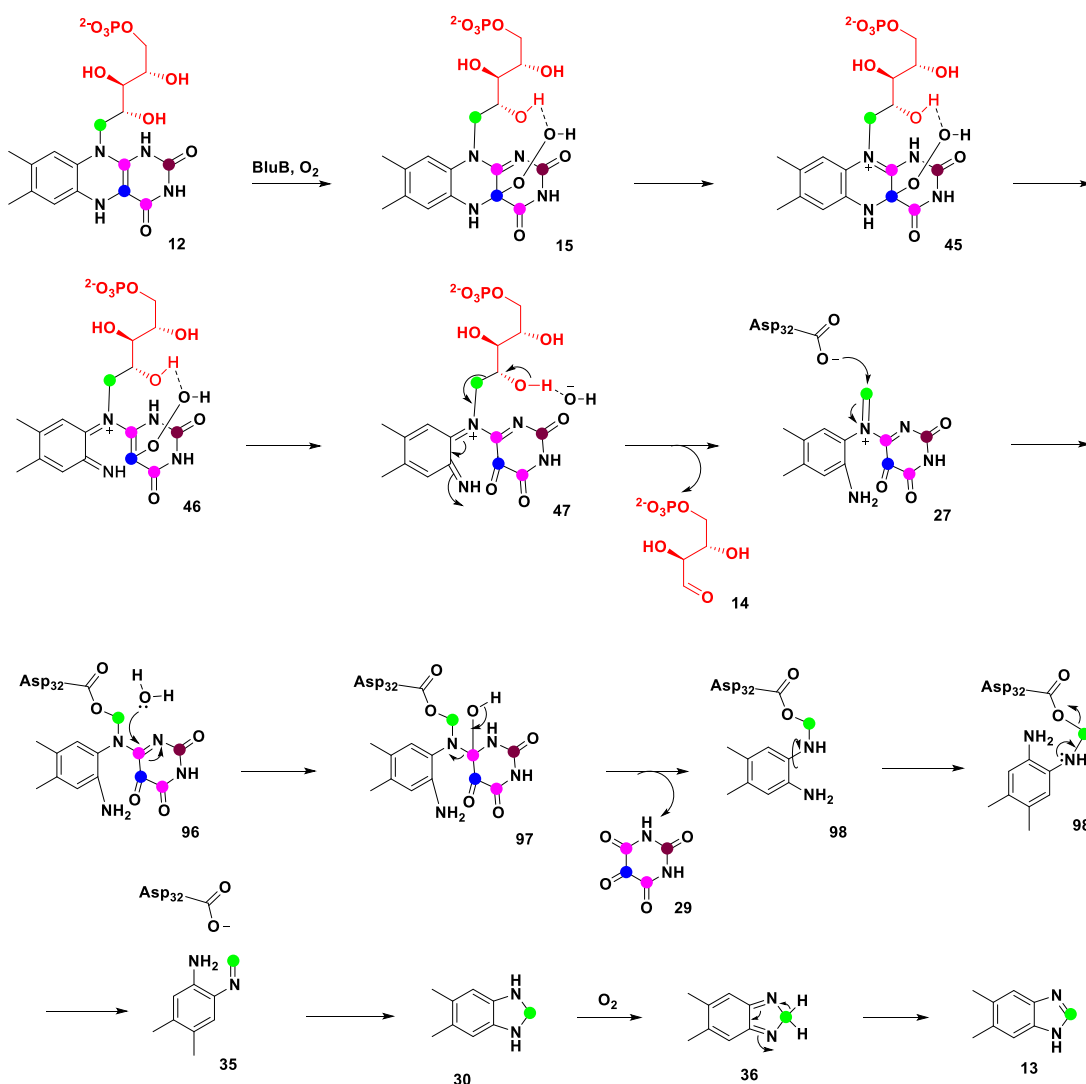

Figure 67. Revised mechanistic proposal for DMB formation

We propose that the residue Asp 32 forms an adduct (96) with intermediate 27, thereby, preventing it from getting hydrolyzed. The adduct 96 then undergoes hydrolysis to form 97 which subsequently undergoes C-N bond cleavage forming 98 with the release of alloxan (29). Flipping of the aryl ring is followed by elimination of Asp 32 to give the iminium ion 35. Cyclisation followed by oxidation leads to the formation of the final product DMB (13). Asp 32 thus plays an important role by protecting the reactive intermediate 27 in the form of an adduct. In the absence of this key residue, intermediate 27 undergoes reactions with the various nucleophiles present leading to the formation of the shunt products exclusively as seen in case of D32N mutant.

A closer look at the surface view of BluB (Figure 68) further helps us in explaining the formation of all the observed shunt products.
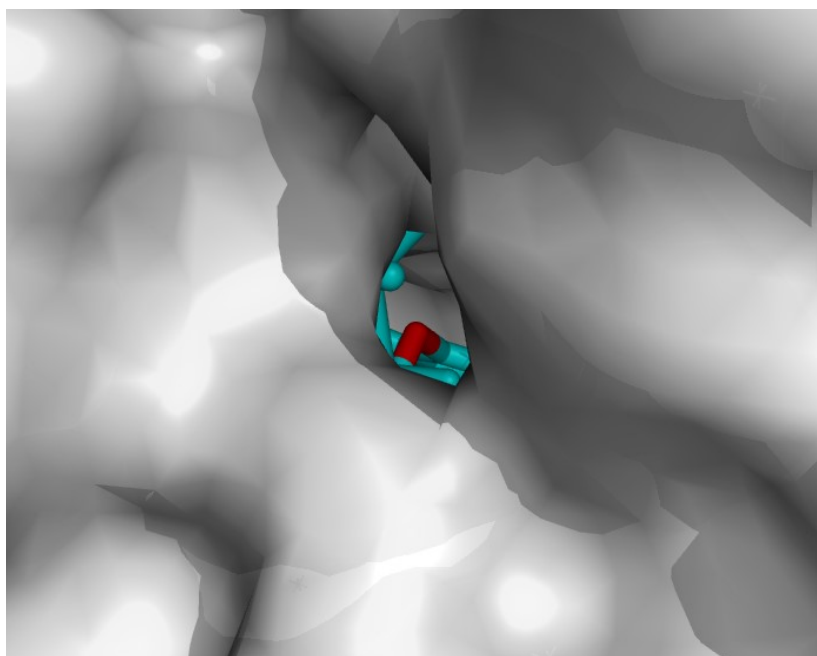

Figure 68. Surface view showing the C1' (in red) of the ribityl chain of FMN being exposed to the solvent

The surface view structure shows that the substrate $FMNH_2$ is deeply buried inside the active site pocket which is pretty much closed. Only a small opening is observed through which the substrate can have interaction with the external solvent. Looking closely, we observed that the C1' (shown in red color in Figure 68) of the ribityl tail is directly facing this opening. This explains the fact that once the intermediate 27 is formed having an imine moiety at the C1' position, it can readily undergo interaction with the external solvent and nucleophiles through this opening leading to the formation of the various shunt products. This observation, thus, helps us rationalize the different shunt products observed during the biosynthesis of dimethylbenzimidazole.

4.3 Conclusion

In this chapter, we have demonstrated that the Asp 32 residue plays a key role during the DMB formation. It helps in the stabilization of the intermediate 27. Asp 32 forms an adduct with 27 and thus shields it from getting hydrolyzed. Based on all these observations, a revised mechanism has been proposed for BluB catalyzed DMB biosynthesis. Mutation of Asp 32 to asparagine (D32N mutant) leads to a loss in activity with regards to the DMB formation. However, greater amounts of the various shunt products are seen to be formed with the D32N mutant. Surface view of BluB further helps in explaining the formation of the different shunt products observed.

STEREOCHEMISTRY OF PROTON ABSTRACTION FROM THE C1'POSITION OF THE RIBOSE SUGAR CHAIN OF FMN

5.1 Introduction

Biosynthesis of DMB involves a novel transformation, wherein, the C1' of the sugar side chain in FMN is incorporated at the C2 position in the product, DMB[20,21]. One of the hydrogen is lost from the C1' of the sugar (highlighted in a blue circle) and only one is retained at the C2 position in DMB (Figure 69).
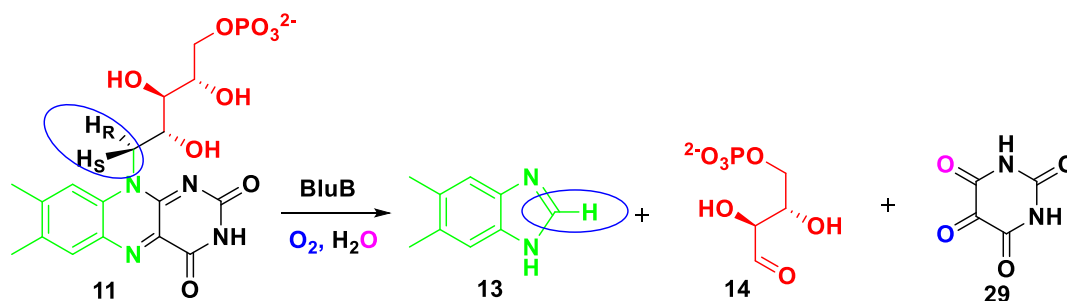

Figure 69. Overall scheme for the DMB formation

Renz and co-workers have previously reported that the *pro*-S hydrogen of C1' of the sugar in FMN is retained in the DMB formed[53]. They concluded this based on their deuterium labeling studies wherein they observed 27% deuterium incorporation in the DMB formed on using flavin which contained 25% deuterium at 1'S position. However, on using the substrate flavin containing 75% deuterium at 1'S position, they only observed

46% deuterium incorporation in DMB which is pretty low. They attributed this low incorporation to the fact that a part of the deuterium may be incorporated in some other product derived from the substrate. Thus, the second result does not support the findings of the first based on which was concluded that the *pro*-S hydrogen at the C1′ of FMN is retained in the final product, DMB.

In our mechanistic hypothesis, we propose a final oxidation step in which the intermediate 30 (in Figure 67) is oxidized to form the final product, DMB. So, stereochemical studies were carried out to establish whether the proposed last step is an enzymatic or non-enzymatic process and whether there is any selectivity in the abstraction of one of the hydrogens from the C1′ of the ribityl chain of FMN.

5.2 Results and discussion

We synthesized deuterated forms of FMN, wherein, deuterium was incorporated at the C1′ of the sugar side chain. Two forms of deuterated flavin were synthesized. One of the deuterated flavin synthesized had deuterium in the ratio of 3:1 in favor of R:S isomer at C1′ position whereas the other form had it in the ratio of 1:3 in favor of R:S isomer at C1′ position. These deuterated forms of FMN were used as substrates for BluB catalyzed reactions and the reaction mixture was analyzed by LC-MS to calculate the amount of deuterium incorporated in the DMB formed.

On using the substrate containing 25% deuterium at 1′ S position, we observed 24.5% deuterium incorporation in the final product, DMB (Figure 70B). This data indicated that the *pro*-S hydrogen of the C1′ of the sugar is retained in the DMB formed.

This was further confirmed by carrying out BluB reactions with the substrate containing 75% deuterium at 1'S position. We observed 71% deuterium incorporation in DMB this time on using FMN containing 75% deuterium at 1'S position (Figure 70C).
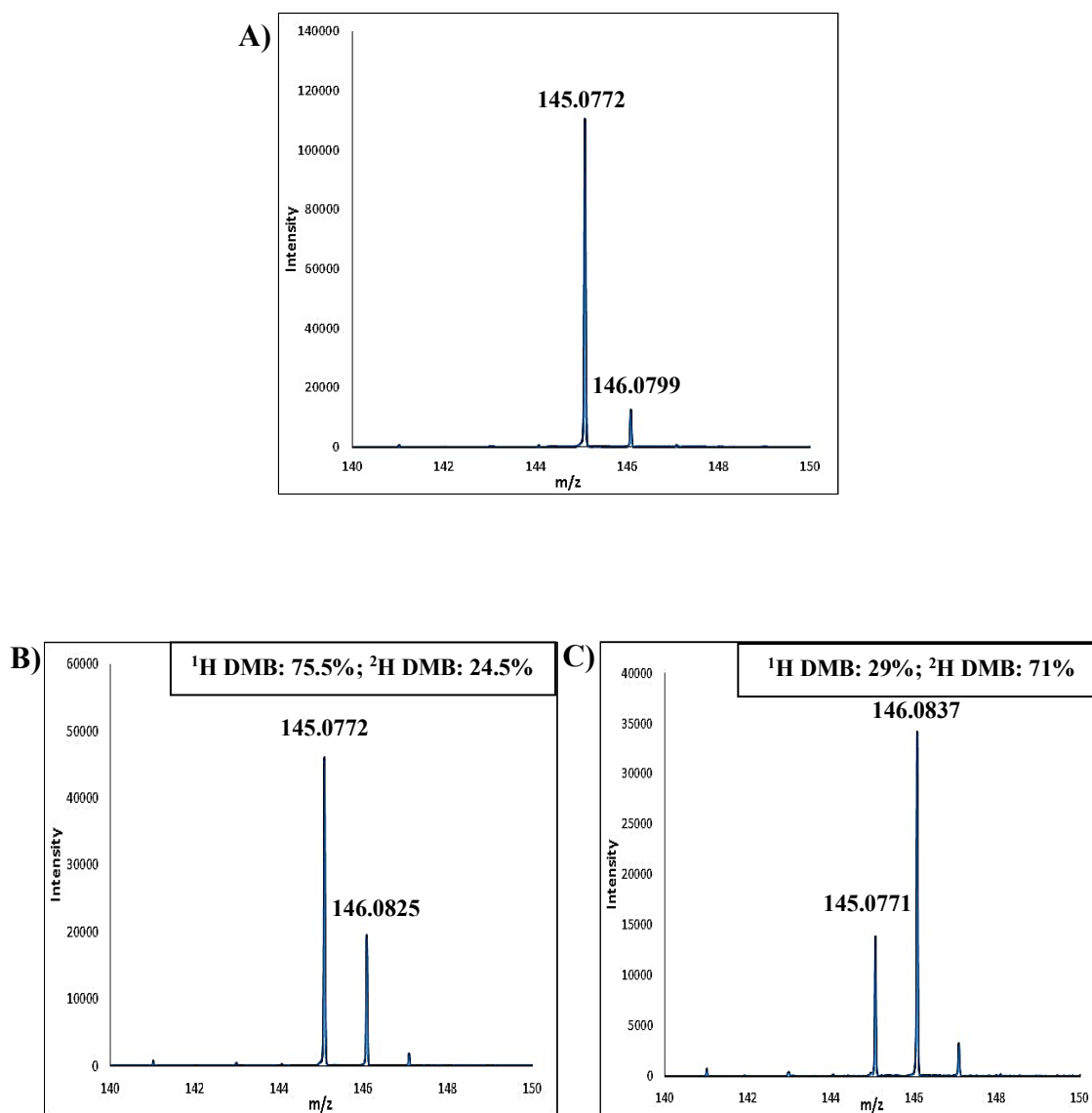

Figure 70. LC-MS analysis of the deuterium incorporation in DMB on using **(A)** Unlabeled FMN **(B)** Deuterated FMN (25% deuterium at 1'S position) **(C)** Deuterated FMN (75% deuterium at 1'S position)

85

The results of the deuterium incorporation studies have been summarised in Table 5.

Substrate (Deuterated FMN)	^{1}H DMB	^{2}H DMB
75% R – 25% S	75.5%	24.5%
25% R – 75% S	29.0%	71.0%

Table 5. Summary of the deuterium incorporation studies in DMB

Based on both these above results, we can safely conclude that it is the *pro*-S hydrogen at the C1' of FMN which is retained in the DMB formed. Thus, we observe a selective abstraction of the *pro*-R hydrogen from the C1' position of the ribose side chain. These results thus help us infer that the proposed final oxidation step in DMB biosynthesis is indeed an enzymatic process.

5.3 Conclusion

In this chapter, we have successfully demonstrated that there is a selectivity in the proton abstraction from the C1' position of the ribityl side chain. We have been able to show that the *pro-R* hydrogen is abstracted while the pro-S hydrogen is retained based on stereochemical studies. Thus, we have been able to establish that the final oxidation step involved in the DMB biosynthesis is enzyme catalyzed occurring in the active site of BluB.

5.4 Experimental

5.4.1 Synthesis of deuterated FMN (R:S::3:1)[53,54]

The synthetic scheme for 11e is shown in Figure 71.
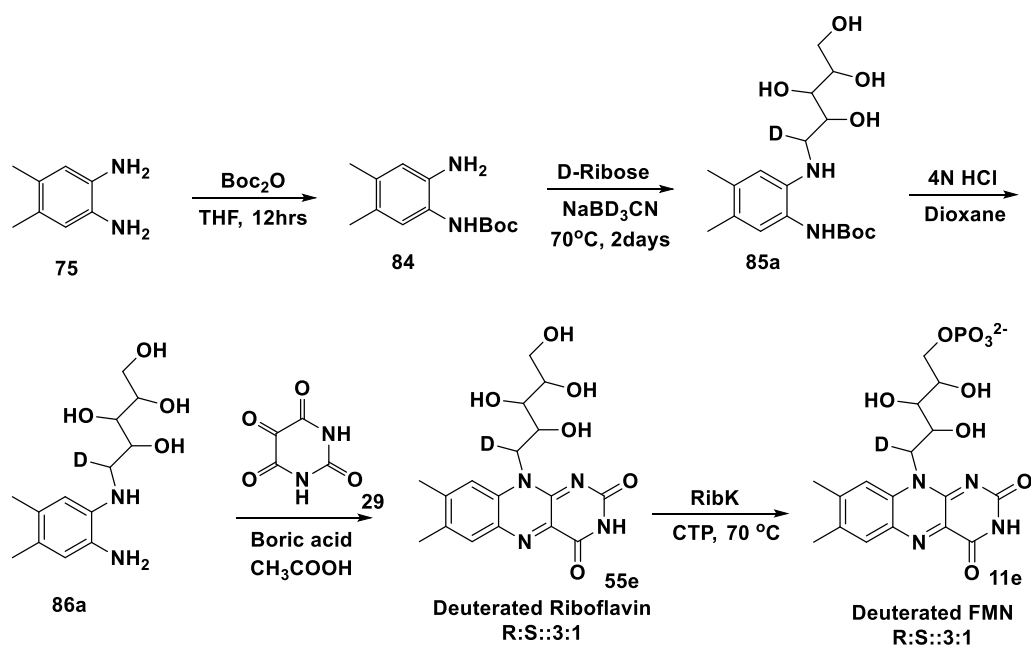
Figure 71. Scheme for the synthesis of 11e

Procedure

Synthesis of 2-(Boc)amino-4,5-dimethylaniline (84): Compound 84 was synthesized following the same procedure used during the synthesis of ^{13}C labeled FMN 11d (Labeled at C1' position of ribose).

Synthesis of 85a: Boc-protected aniline, 84 (1 equiv.), D-ribose (3.0 equiv.) and sodium cyanoborodeuteride (2.0 equiv.) were dissolved in anhydrous MeOH (15 mL). The mixture was refluxed at 80 °C for 2 days under argon atmosphere. Then the solvent was

removed under reduced pressure and excess $NaBD_3CN$ was quenched using 1M HCl. The resulting mixture was neutralized using saturated $NaHCO_3$ solution and concentrated under reduced pressure. The residue was purified by silica gel column chromatography using chloroform/methanol. Yield: 80%, ESI-MS *m/z* 372.2 (M+H). ^{1}H NMR (400 MHz, CD_3OD): δ 1.49 (s, 9H), 2.12 (s, 3H), 2.18 (s, 3H), 3.64 (m, 3H), 3.76 (m, 2H), 3.92 (m, 1H), 6.61 (s, 1H), 6.87 (s, 1H) ppm.

Synthesis of 86a: Boc-protected riboaniline, 85a (100 mg) was stirred in 4(N) HCl/dioxane mixture (5 mL) for 4 hrs. The solvent was removed under reduced pressure and the remaining mixture was diluted with water followed by extraction with ether. The aqueous layer was concentrated to yield the desired product. Yield: 90%. ^{1}H NMR (400 MHz, CD_3OD): δ 2.30 (s, 3H), 2.31 (s, 3H), 3.62 (m, 1H), 3.72 (m, 4H), 4.08 (m, 1H), 7.21 (s, 1H), 7.29 (s, 1H) ppm.

Synthesis of 55e: Compound 86a (1 equiv.), alloxan monohydrate (3 equiv.) and boric acid (2 equiv.) were dissolved in 20 mL of acetic acid. The reaction mixture was stirred overnight under argon atmosphere and the desired ^{13}C labeled riboflavin (55e) was purified by reverse phase high performance liquid chromatography. LC-MS *m/z* 378.1 (M+H) (Figure 72).

Synthesis of 11e: Compound 55e was converted to deuterated FMN (11e) enzymatically using RibK from *Methanocaldococcus jannaschii*. Compound 55e was incubated for 30 mins at 70 °C with 5 mM CTP, 20 mM $MgCl_2$ and RibK in 100 mM potassium phosphate buffer, pH 7.5. The reaction mixture was passed through a 10kDa

cut-off filter and purified by reverse phase high performance liquid chromatography. LC-MS m/z 458.1 (M+H) (Figure 73).
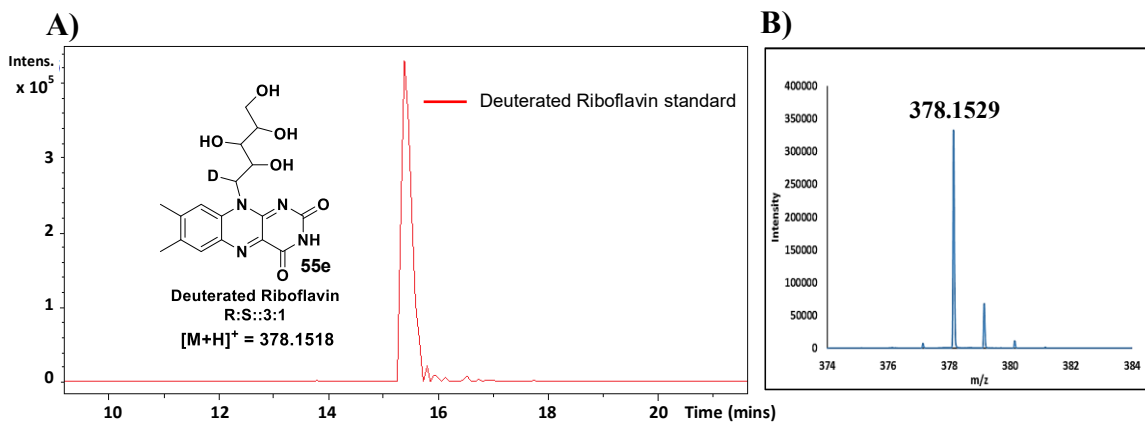

Figure 72. LC-MS analysis of the synthesized deuterated riboflavin (R:S::3:1). **(A)** EIC at m/z 378.1518 showing the formation of deuterated riboflavin **(B)** ESI-MS of 55e in the positive mode
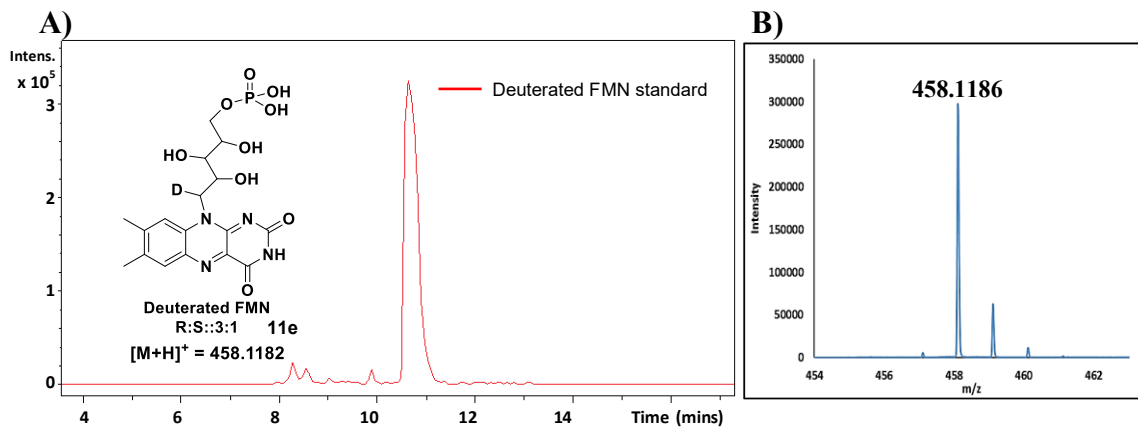

Figure 73. LC-MS analysis of the synthesized deuterated FMN (R:S::3:1). **(A)** EIC at 458.1182 showing the formation of deuterated FMN **(B)** ESI-MS of 11e in the positive mode

5.4.2 Synthesis of deuterated FMN (R:S::1:3)

The synthetic scheme for 11f is shown in the Figure 74.
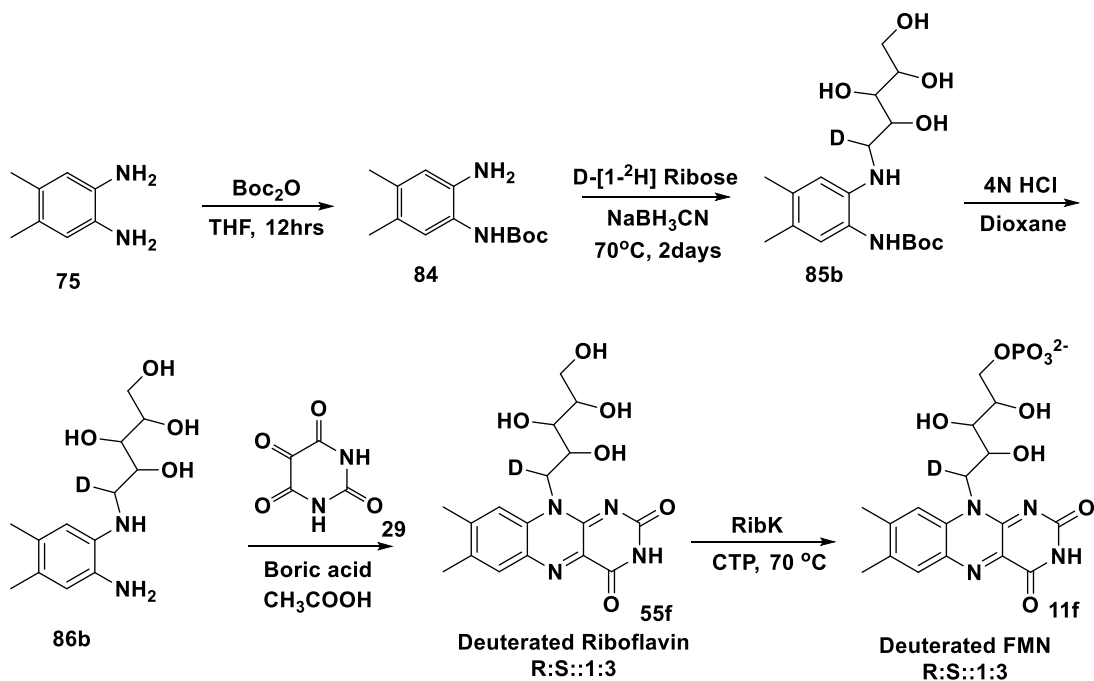
Figure 74. Scheme for the synthesis of 11f

Procedure

Synthesis of 2-(Boc)amino-4,5-dimethylaniline **(84):** Compound 84 was synthesized following the same procedure used during the synthesis of ^{13}C labeled FMN 11d (Labeled at C1' position of ribose).

Synthesis of 85b: Boc-protected aniline, 84 (1 equiv.), D-[1-^{2}H] ribose (3.0 equiv.) and sodium cyanoborohydride (2.0 equiv.) were dissolved in anhydrous MeOH (15 mL). The mixture was refluxed at 80 °C for 2 days under argon atmosphere. Then the solvent

was removed under reduced pressure and excess NaBH$_3$CN was quenched using 1M HCl. The resulting mixture was neutralized using saturated NaHCO$_3$ solution and concentrated under reduced pressure. The residue was purified by silica gel column chromatography using chloroform/methanol. Yield: 80%, ESI-MS *m/z* 372.2 (M+H). ^{1}H NMR (400 MHz, CD$_3$OD): δ 1.49 (s, 9H), 2.11 (s, 3H), 2.18 (s, 3H), 3.40 (m, 1H), 3.63 (m, 2H), 3.76 (m, 2H), 3.92 (m, 1H), 6.60 (s, 1H), 6.87 (s, 1H) ppm.

Synthesis of 86b: Boc-protected riboaniline, 85b (100 mg) was stirred in 4(N) HCl/dioxane mixture (5 mL) for 4 hrs. The solvent was removed under reduced pressure and the remaining mixture was diluted with water followed by extraction with ether. The aqueous layer was concentrated to yield the desired product. Yield: 90%. ^{1}H NMR (400 MHz, CD$_3$OD): δ 2.33 (s, 3H), 2.34 (s, 3H), 3.71 (m, 3H), 3.77 (m, 2H), 4.09 (m, 1H), 7.34 (s, 1H), 7.43 (s, 1H) ppm.

Synthesis of 55f: Compound 86b (1 equiv.), alloxan monohydrate (3 equiv.) and boric acid (2 equiv.) were dissolved in 20 mL of acetic acid. The reaction mixture was stirred overnight under argon atmosphere and the desired ^{13}C labeled riboflavin (55f) was purified by reverse phase high performance liquid chromatography. LC-MS *m/z* 378.1 (M+H) (Figure 75).

Synthesis of 11f: Compound 55f was converted to deuterated FMN (11f) enzymatically using RibK from *Methanocaldococcus jannaschii*. Compound 55f was incubated for 30 mins at 70 °C with 5 mM CTP, 20 mM MgCl$_2$ and RibK in 100 mM potassium phosphate buffer, pH 7.5. The reaction mixture was passed through a 10kDa

91

cut-off filter and purified by reverse phase high performance liquid chromatography. LC-MS m/z 458.1 (M+H) (Figure 76).
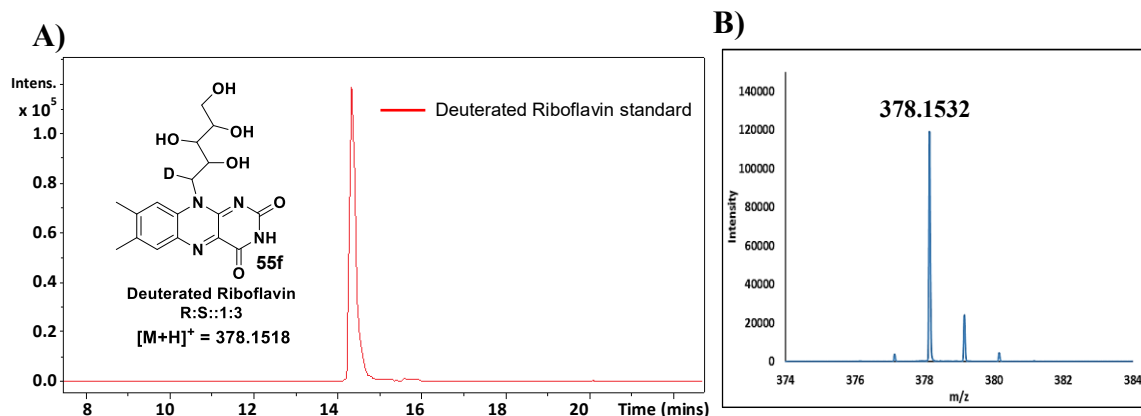

Figure 75. LC-MS analysis of the synthesized deuterated riboflavin (R:S::1:3). **(A)** EIC at m/z 378.1518 showing the formation of deuterated riboflavin **(B)** ESI-MS of 55f in the positive mode
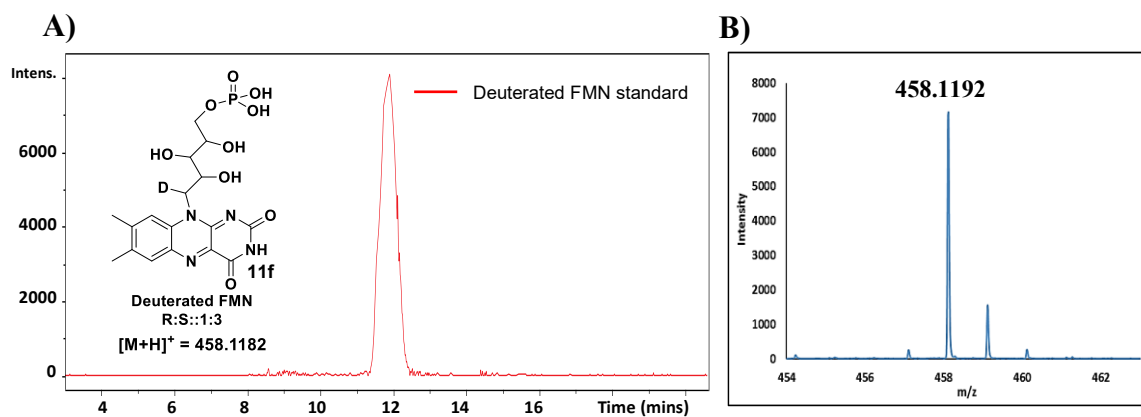

Figure 76. LC-MS analysis of the synthesized deuterated FMN (R:S::1:3). **(A)** EIC at 458.1182 showing the formation of deuterated FMN **(B)** ESI-MS of 11f in the positive mode

CHAPTER VI

SUBSTRATE ANALOG STUDIES WITH 8-SUBSTITUTED FLAVIN

6.1 Introduction

The formation of flavin hydroperoxide (15) has been proposed as the first step in DMB biosynthesis in all the mechanistic proposals in the literature based on the BluB crystal structure. Evidence for its formation has been provided using stopped-flow studies. It has been reported that the peroxyflavin formation in BluB is both enzyme and oxygen dependent[55]. The formation of flavin peroxide intermediate has been observed to be very rapid (in the order of milliseconds) whereas its decay is seen to be comparatively slower being in the order of seconds. It has also been reported that the decay occurs in a biphasic manner as the peroxy species decays in productive (leading to DMB formation) as well as non-productive manner (giving back oxidized flavin).

The flavin hydroperoxide (15) thus formed undergoes unusual fragmentation leading to a C-C bond cleavage between the C1' and C2' of the ribose sugar chain. In the mechanism A proposed in the literature (Figure 6), the fragmentation is initiated by hydroxylation at C1' of the ribityl chain assisted by the deprotonation at C1' using the Asp-32 residue. This seems to be very difficult as a large conformational change in the active site would be required for hydroxylation at C1' and even the Asp-32 is not a strong enough base to carry out this transformation. On the other hand, in the mechanism B (Figure 7), fragmentation of the peroxy moiety occurs by a hydride transfer from the hydroxyl group at C2' position of the ribityl tail. Such a hydride transfer is highly unlikely as the hydroxyl

groups are typically not known to form hydride ions. Thus, the fragmentation steps proposed in both these mechanisms seem to be very difficult and challenging[15].

In our current mechanistic hypothesis (Figure 67), we have proposed that the flavin hydroperoxide (15) undergoes fragmentation forming the intermediate 47 followed by C-C bond cleavage and further chemistry to ultimately form DMB. To explore this unusual fragmentation of the flavin, substrate analog studies were done using 8-substituted flavins.

6.2 Results and discussion

6.2.1 Identification of the shunt product 100

Enzymatic reactions with the 8-substituted flavins (8-OH FMN and 8-NH$_2$ FMN) provided interesting results. Formation of the usual products (5-OH DMB (99), erythrose-4-phosphate and alloxan) following the native chemistry was observed on carrying out BluB catalyzed reactions using 8-OH FMN (Figure 77).
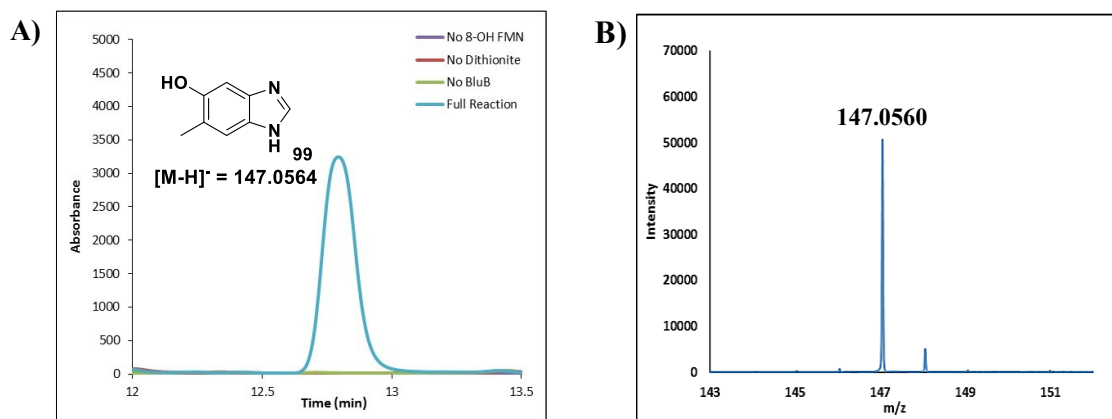
Figure 77. BluB catalyzed reaction with 8-OH FMN. **(A)** HPLC chromatogram at 280 nm showing the formation of 5-OH DMB (99) **(B)** ESI-MS of 99 in the negative mode

The formation of 5-OH DMB (99) was confirmed by co-eluting it with a synthesized standard (Figure 78)[56].
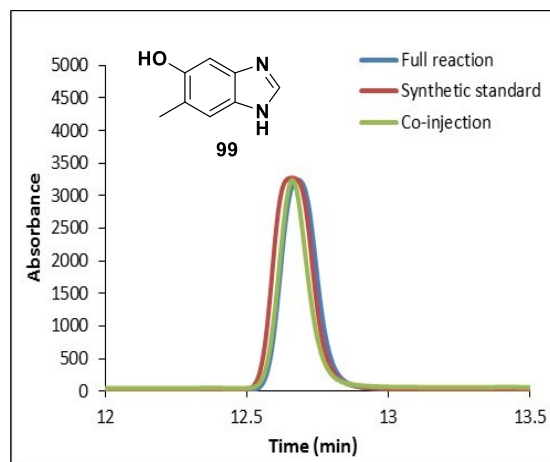
Figure 78. Co-elution data for the formation of 5-OH DMB using 8-OH FMN as substrate analog

Along with the formation of the native products, a new peak was also observed at 450 nm in the HPLC analysis of the BluB catalyzed reactions using 8-OH FMN (Figure 79A). The new peak had a UV-Vis spectrum similar to that of the substrate (8-OH FMN) and a mass corresponding to 316 Da (Figure 79B). Based on the mass and MS-MS fragmentation pattern (Figure 80), we assigned 100 to be the structure for the new shunt product formed.
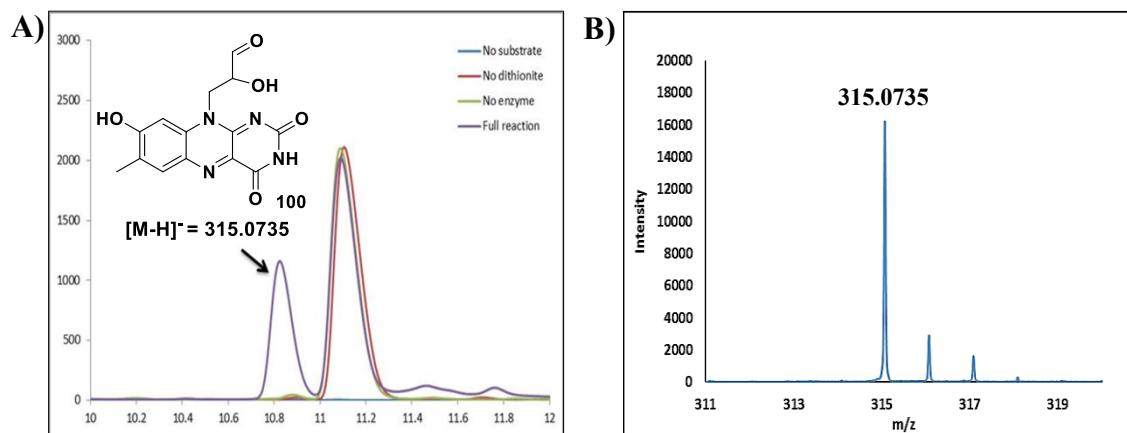
Figure 79. BluB catalyzed reaction with 8-OH FMN. **(A)** Formation of the shunt product 100 using 8-OH FMN as substrate **(B)** ESI-MS of 100 in the negative mode
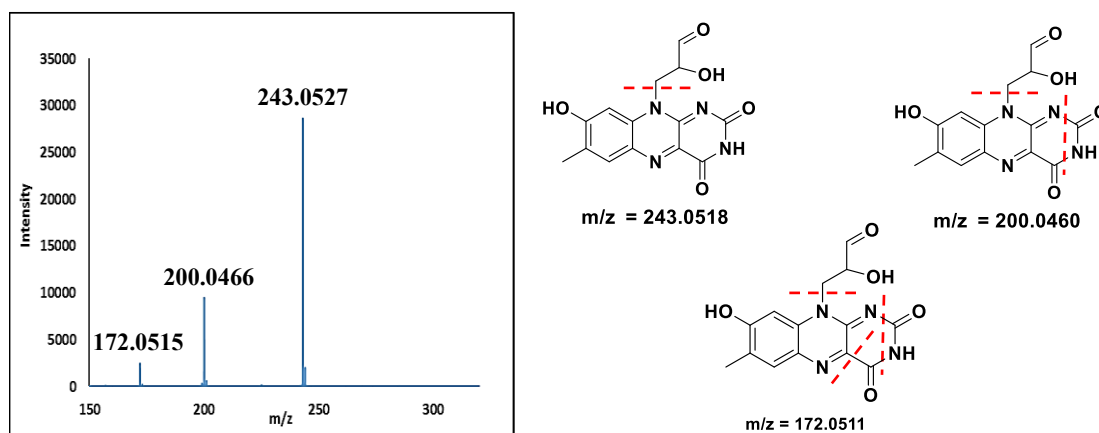
Figure 80. MS-MS fragmentation pattern of 100 in the negative mode

To confirm the structure of 100, the new shunt product formed was collected, treated with sodium borohydride and was then coeluted with the synthesized alcohol standard, 101 (Figure 81).
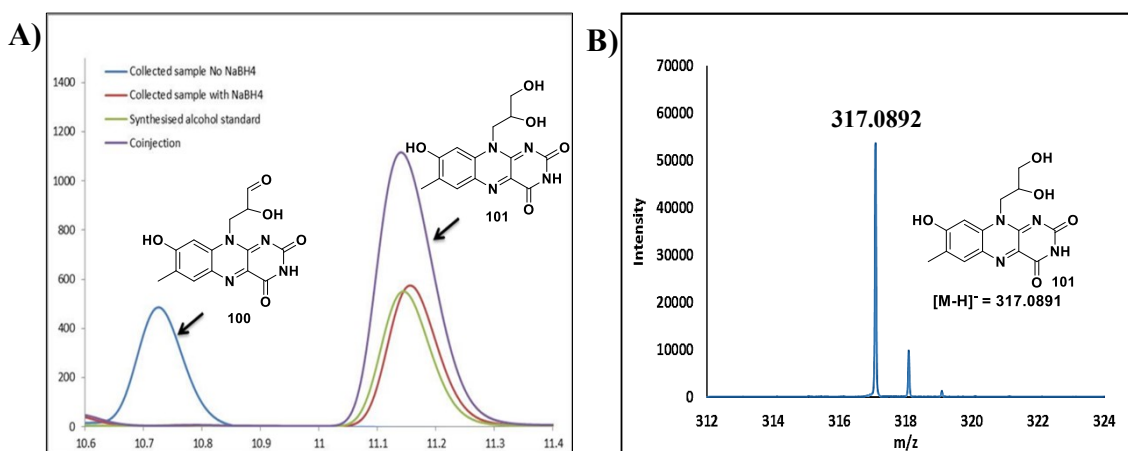
Figure 81. Coelution data for the shunt product 100. **(A)** Coelution study after borohydride treatment of 100 **(B)** ESI-MS of the compound (101) formed on borohydride reduction of 100 in the negative mode

To establish the presence of an aldehyde group in 100, the reaction mixture was derivatized using *o*-pentafluorobenzylhydroxylamine (PFBHA) to convert 100 into its corresponding oxime (102). Formation of 102 was seen only in case of the full reaction treated with PFBHA and was absent in all the other controls (Figure 82) which confirms that the shunt product 100 contains an aldehydic group.
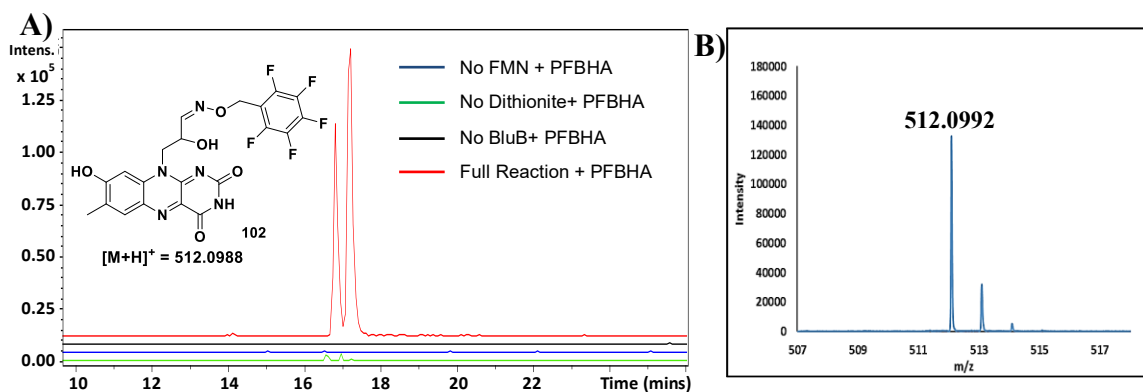
Figure 82. LC-MS analysis of the derivatization of the shunt product 100. **(A)** EIC at m/z 512.0988 showing the derivatization of 100 using PFBHA into its corresponding oxime (102) only in case of full reaction (Red trace) **(B)** ESI-MS of 102 in the positive mode

6.2.2 Identification and trapping of glycolaldehyde-2-phosphate (105)

The shunt compound 100 thus formed contains only three carbons in the sugar side chain as compared to five carbons in the ribose chain of the substrate, 8-OH FMN. The remaining two carbon fragment was identified as glycolaldehyde-2-phosphate (105) using a similar strategy of trapping it in its corresponding oxime form (103) using PFBHA (Figure 83).
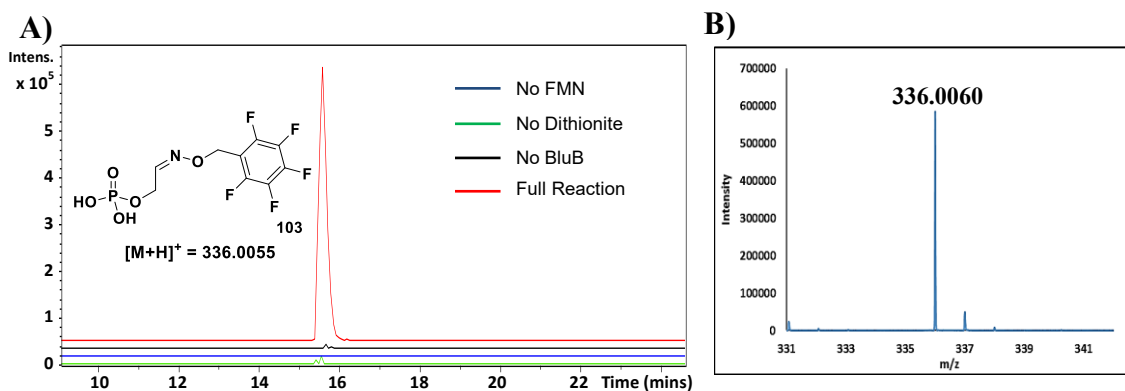

Figure 83. LC-MS analysis for the trapping of glycolaldehyde-2-phosphate. **(A)** EIC at 336.0055 showing the trapping of glycolaldehyde-2-phosphate using PFBHA in the form of oxime (103) only in case of full reaction (Red trace) **(B)** ESI-MS of 103 in the positive mode

Formation of glycolaldehyde-2-phosphate (105) was further confirmed by carrying out CIP treatment of the reaction mixture treated with PFBHA (Figure 84) and then coeluting it with the synthesized standard 104 (Figure 85)[57].
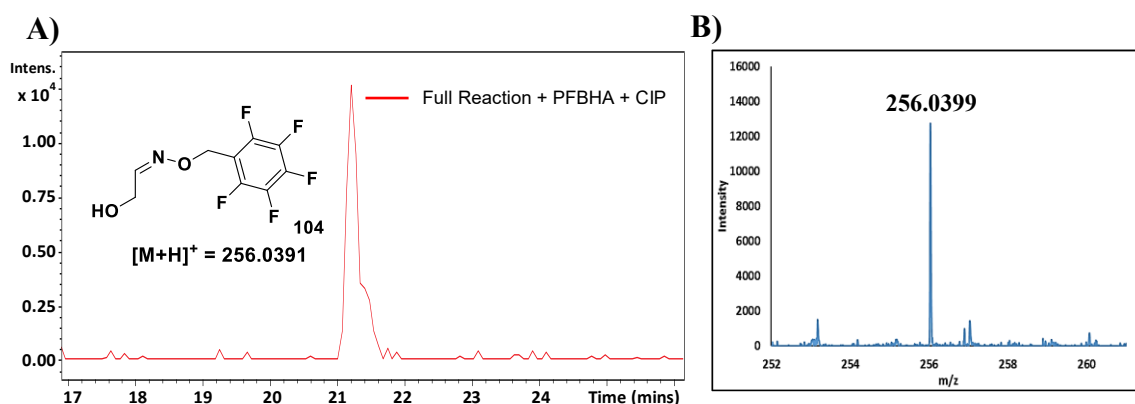
Figure 84. LC-MS analysis after the CIP treatment of 103. **(A)** EIC at 256.0391 showing the loss of the phosphate group on CIP treatment of glycolaldehyde-2-phosphate – PFBHA oxime (103) **(B)** ESI-MS of 104 in the positive mode
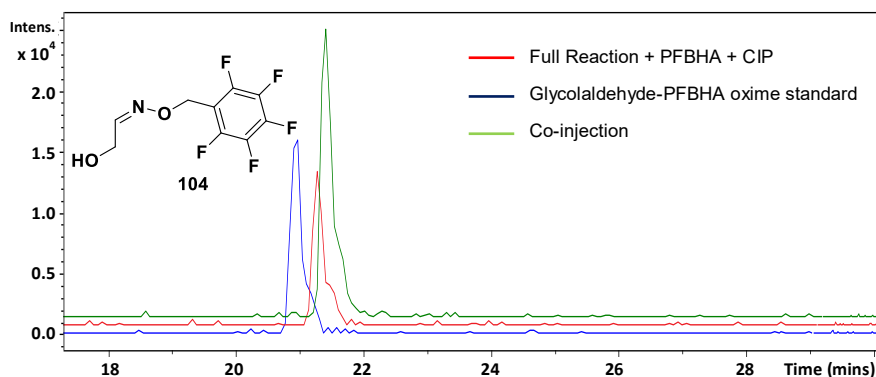

Figure 85. LCMS analysis for the coelution of PFBHA derivatized oxime of glycolaldehyde (104)

6.2.3 Summary of the BluB reaction with 8-OH FMN

Thus, the reaction of BluB with 8-OH FMN leads to the formation of 100 and 105 following an unusual C-C bond fragmentation between the C3$'$ and C4$'$ of the ribose sugar chain apart from forming the usual products (Figure 86). Similar results were also obtained on using 8-NH$_2$ FMN as a substrate analog.
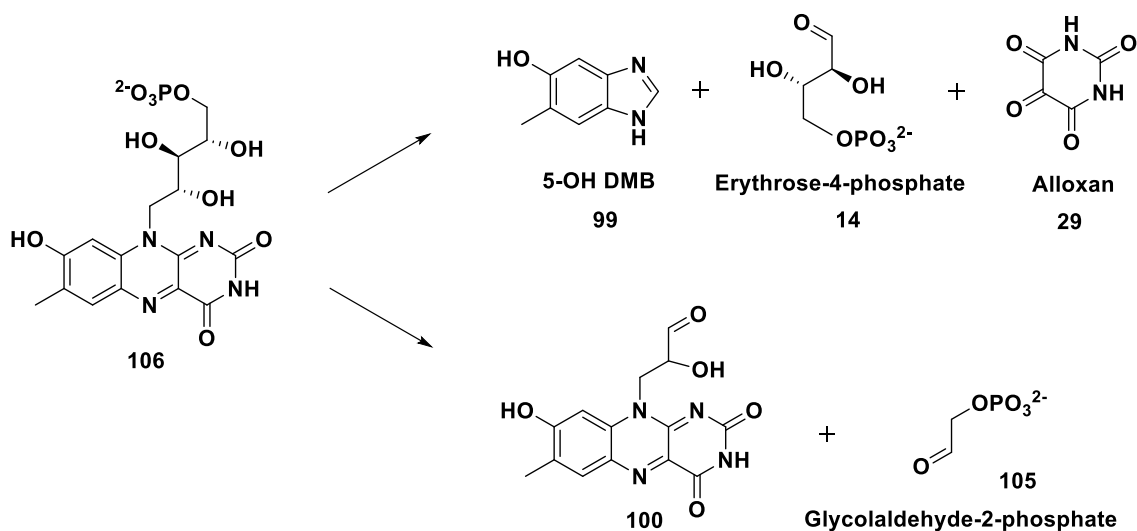
Figure 86. Summary of the BluB catalyzed reaction with 8-OH FMN (106)

6.2.4 Mechanistic proposal for the formation of the shunt product 100

Our current mechanistic hypothesis for the formation of the shunt product 100 is shown in Figure 87. Our proposal is that the reduced form of 8-OH FMN (107) first reacts with oxygen to form the flavin hydroperoxide intermediate (108) which undergoes fragmentation to form 110 via intermediate 109. The peroxide fragmentation forms the intermediate 111 which undergoes the usual C-C bond fragmentation between the C1' and C2' of the ribose sugar chain forming the native products (5-OH DMB (99), erythrose-4-phosphate and alloxan). However, 111 can also tautomerize to form 113 via 112 which further undergoes keto-enol tautomerization to form intermediate 114. 114 then undergoes a C-C bond fragmentation between the C3' and C4' of the sugar chain in a retro-aldol manner forming glycolaldehyde-2-phosphate (105) and 115. The intermediate 115 tautomerizes to form 116 which finally cyclizes forming the shunt product 100.

100
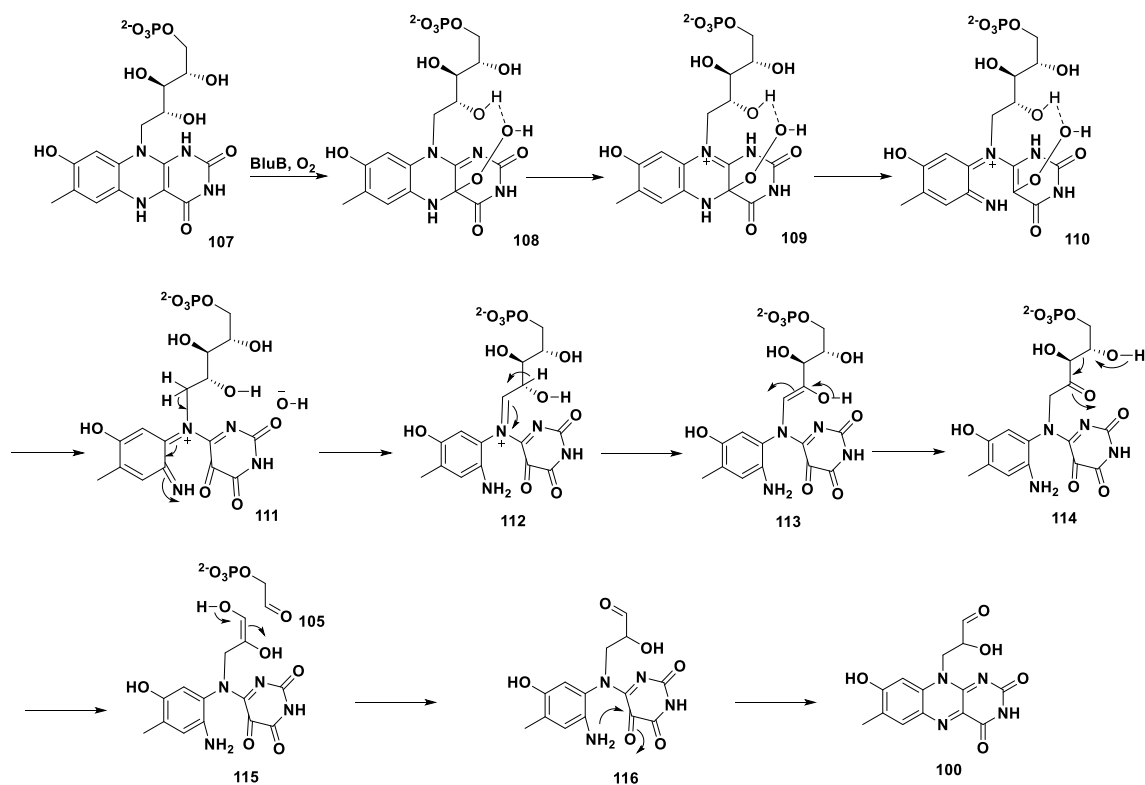
Figure 87. Mechanistic proposal for the formation of 100

We propose that the substitution of the methyl with a hydroxyl group at the 8 position of the substrate leads to a conformational change in the active site of the enzyme. This leads to the unusual fragmentation between the C3' and C4' of the sugar chain besides the usual C-C bond cleavage chemistry leading to DMB.

The identification and characterization of the shunt product 100 help us provide evidence for the existence of the intermediate 47 (Figure 21) which is formed from the fragmentation of the peroxyflavin moiety (15) during DMB formation. This serves as

evidence for the initial fragmentation step of the flavin peroxide intermediate involved in the DMB biosynthesis.

6.3 Conclusion

BluB catalyzed reactions using 8-substituted flavin as substrate yielded unusual results. Along with the formation of the native products, a new shunt product (100) was also observed. The observed shunt product is formed as a result of a C-C bond fragmentation between the C3$'$ and C4$'$ of the ribose sugar chain. The identification of this shunt product provides evidence for the initial peroxyflavin fragmentation step involved in the formation of dimethylbenzimidazole.

6.4 Experimental

6.4.1 PFBHA derivatization of shunt product 100 and glycolaldehyde-2-phosphate

BluB enzymatic reactions were performed in 100 mM phosphate buffer, pH 7.5 containing BluB (100 μM), 8-OH FMN (300 μM) and dithionite. The enzymatic reactions were incubated at room temperature for 4 hrs. The protein was then removed by heat denaturation and *o*-(pentafluorobenzyl)hydroxylamine (PFBHA) (2mM) was added to the reaction mixture and was heated at 65 °C for 1 hr. The reaction mixture was then analyzed by LC-MS.

6.4.2 Borohydride reduction of the shunt product 100

The shunt product 100 was collected in the HPLC and was then lyophilized. The sample was then dissolved in anhydrous THF and was treated with sodium borohydride at room temperature. After 2 hrs, the solvent THF was removed under vacuum and the sample was dissolved back in phosphate buffer. The reaction mixture was then analyzed by HPLC and LC-MS.

6.4.3 CIP treatment of glycolaldehyde-2-phosphate – PFBHA oxime (103)

BluB enzymatic reactions were performed in 100 mM phosphate buffer, pH 7.5 containing BluB (100 µM), 8-OH FMN (300 µM) and dithionite. The enzymatic reactions were incubated at room temperature for 4 hrs. The protein was removed by heat denaturation and o-(pentafluorobenzyl)hydroxylamine (PFBHA) (2mM) was added to the reaction mixture and was heated at 65 °C. After an hour, the reaction mixture was incubated with CIP at 37 °C for 2 hrs. The reaction mixture was then analyzed by LC-MS.

6.4.4 Synthesis of 8-OH FMN (106)[58]

The synthetic scheme for 8-OH FMN (106) is shown in Figure 88.
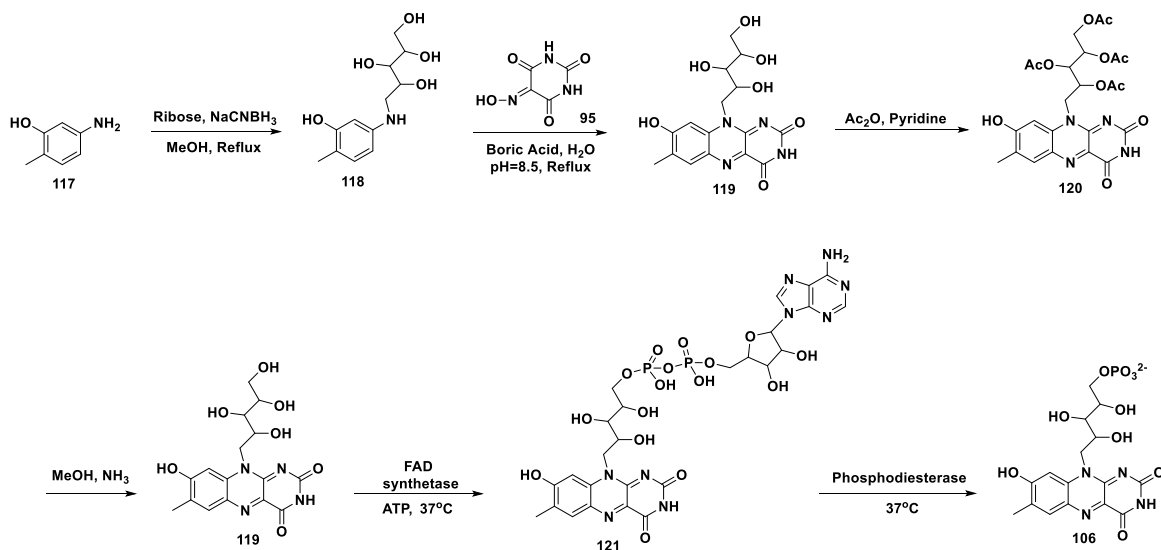
Figure 88. Scheme for the synthesis of 8-OH FMN (106)

Procedure

Synthesis of 5-((3-Hydroxy-4-methylphenyl)amino)pentane-1,2,3,4-tetraol **(118):** 5-Amino-2-methylphenol, 117 (123 mg, 1.0 equiv.), D-ribose (450 mg, 3.0 equiv.) and sodium cyanoborohydride (126 mg, 2.0 equiv.) were dissolved in anhydrous MeOH (15 mL). The mixture was refluxed at 80 °C for 2 days under argon atmosphere. Then the solvent was removed under reduced pressure and excess NaBH$_3$CN was quenched using 1M HCl. The resulting mixture was neutralized using saturated NaHCO$_3$ solution and concentrated. The residue was purified by silica gel column chromatography using chloroform/methanol. Yield: 65%, LC-MS *m/z* 258.1 (M+H). ^{1}H NMR (400 MHz, CD$_3$OD): δ 2.04 (s, 3H), 3.39 (dd, 1H), 3.64 (m, 3H), 3.78 (m, 2H), 3.90 (m, 1H), 6.16

(dd, 1H), 6.21 (d, 1H), 6.79 (d, 1H), 7.80 (s, 1H) ppm. ^{13}C NMR (100 MHz, CD$_3$OD): δ 15.3, 64.2, 72.0, 73.9, 74.7, 79.3, 102.0, 106.8, 114.9, 131.9, 149.0, 156.6 ppm.

Synthesis of 8-Hydroxyriboflavintetraacetate (120): To a solution of 118 (258 mg, 1 equiv.) in 15 mL of water, violuric acid monohydrate (175 mg, 1 equiv.) and boric acid (62 mg, 1 equiv.) were added. The mixture was refluxed at 105 °C for 12 hours and was then concentrated under reduced pressure. The crude product was dissolved in 8 mL of pyridine. 1 mL of acetic anhydride was added to the mixture and was stirred at rt for 6 hrs. The solvent was then removed under reduced pressure with toluene. The residue was purified by silica gel column chromatography using chloroform/methanol. LC-MS *m/z* 547.2 (M+H). ^{1}H NMR (400 MHz, CD$_3$OD): δ 1.73 (s, 3H), 2.01 (s, 3H), 2.14 (s, 3H), 2.20 (s, 3H), 2.30 (s, 3H), 3.49 (m, 1H), 3.59 (q, 1H), 4.09 (q, 1H), 4.26 (dd, 1H), 4.46 (dd, 1H), 5.38 (m, 1H), 5.50 (m, 1H), 5.70 (m, 1H), 6.95 (s, 1H), 7.78 (s, 1H) ppm.

Synthesis of 8-Hydroxyriboflavin (119): Compound 120 was converted to 8-Hydroxyriboflavin (119) by overnight stirring in ammonia (7N in methanol) and was purified by reverse phase high performance liquid chromatography. LC-MS *m/z* 379.1 (M+H) (Figure 89A and B).

Synthesis of 8-Hydroxyflavinadeninedinucleotide (121): Compound 119 was converted to 8-OH FAD (121) enzymatically using FAD synthetase from *Corynebacterium ammoniagenes.* 8-OH riboflavin was incubated overnight at 37 °C with 5 mM ATP, 20 mM MgCl$_2$ and FAD synthetase in 100 mM phosphate buffer, pH 7.5. The reaction mixture was passed through a 10kDa cut-off filter and purified by reverse phase high performance liquid chromatography. LC-MS *m/z* 788.1 (M+H) (Figure 89C and D).

***Synthesis of 8-Hydroxyflavinmononucleotide* (106):** 8-OH FAD (121) purified by HPLC was incubated for 2 hrs at 37 °C with 2-3 mg of phosphodiesterase I from *Crotalus atrox* (Western Diamondback Rattlesnake) in 10 mL of 100 mM potassium phosphate buffer, pH 7.5. The reaction mixture was passed through a 10kDa cut-off filter and then purified by reverse phase high performance liquid chromatography to yield the final compound 8-OH FMN (106). LC-MS *m/z* 459.1 (M+H) (Figure 90).
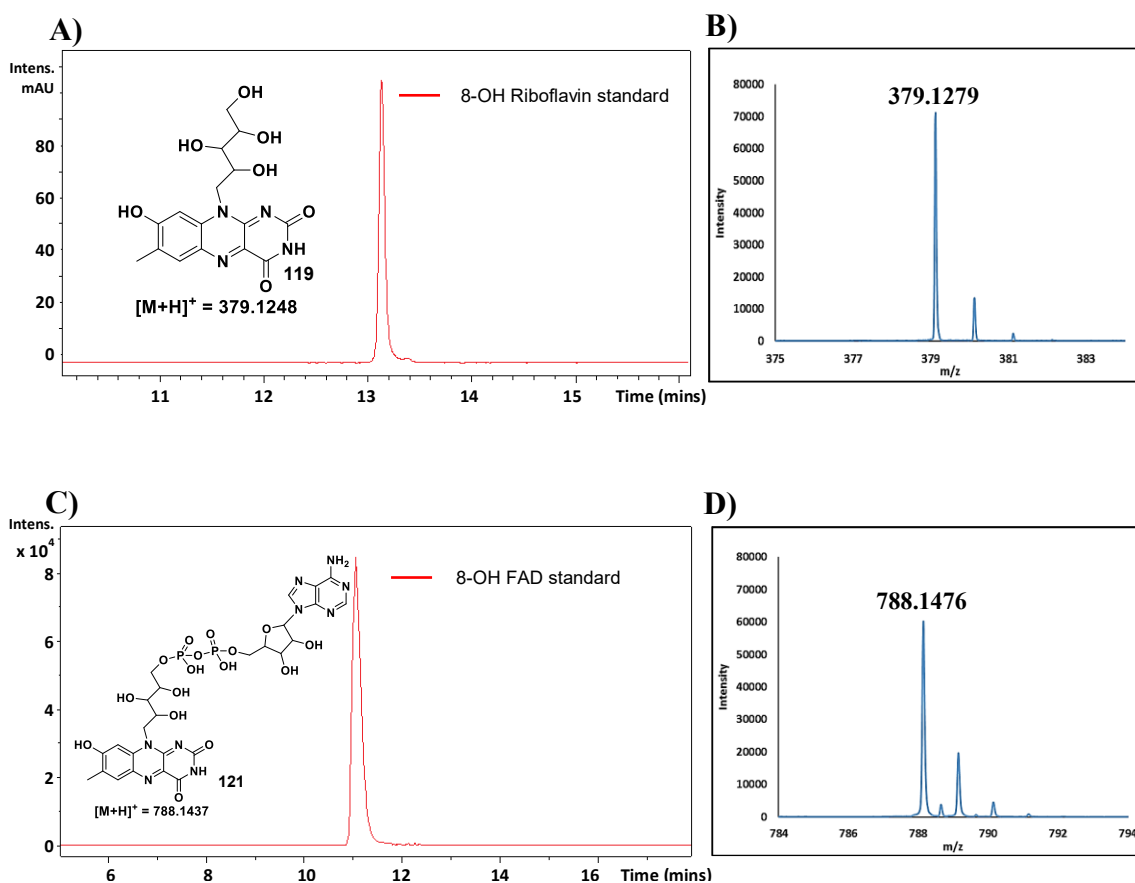

Figure 89. LC-MS analysis of the synthesized 8-OH Riboflavin and 8-OH FAD. **(A)** UV chromatogram at 450 nm showing the formation of 8-OH Riboflavin **(B)** ESI-MS of 119 in the positive mode **(C)** EIC at m/z 788.1437 showing the formation of 8-OH FAD **(D)** ESI-MS of 121 in the positive mode
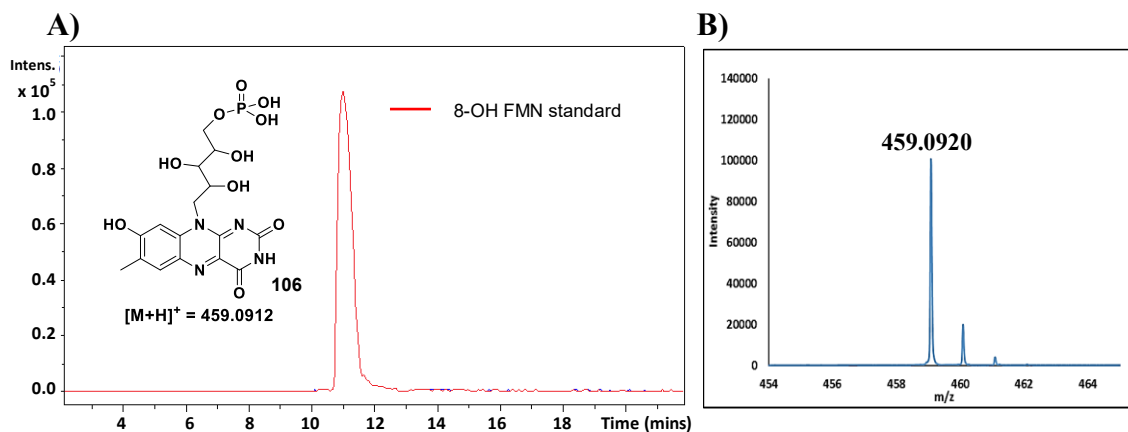
Figure 90. LC-MS analysis of the synthesized 8-OH FMN. **(A)** EIC at m/z 459.0912 showing the formation of 8-OH FMN **(B)** ESI-MS of 106 in the positive mode

6.4.5 Synthesis of 5-OH DMB (99)[56]

The synthetic scheme for 5-OH DMB (99) is shown in Figure 91.
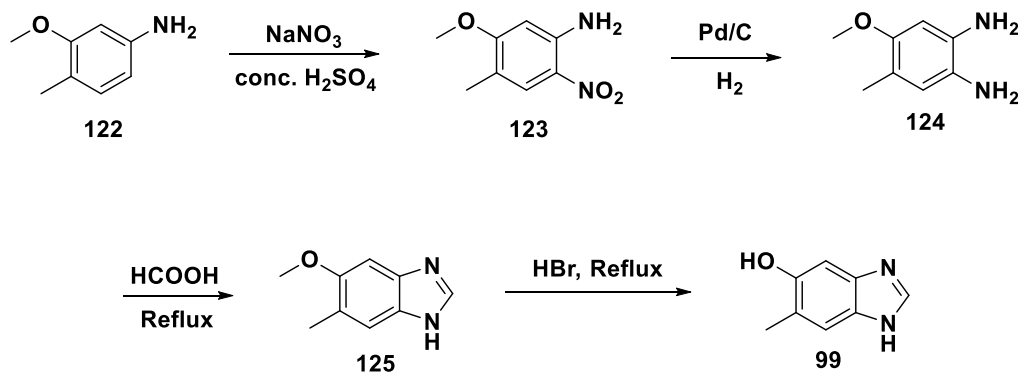
Figure 91. Scheme for the synthesis of 5-OH DMB (99)

107

Procedure

***Synthesis of 5-Methoxy-4-methyl-2-nitroaniline* (123):** 3-Methoxy-4-methylaniline, 122 (137 mg, 1.0 equiv.) was dissolved in 5 mL of conc. H_2SO_4 and the solution was cooled to -5 °C. To this, a solution of $NaNO_3$ (85 mg, 1.0 equiv.) in 2.5 mL of conc. H_2SO_4 was slowly added with the temperature being maintained below -3 °C. After stirring the mixture for 15 mins, it was poured on ice and 25 mL of water was then added to it. The precipitate was collected by filtration. Yield: 40%, LC-MS *m/z* 183.1 (M+H). ^{1}H NMR (400 MHz, CDCl$_3$): δ 2.07 (s, 3H), 3.82 (s, 3H), 5.57 (s, 2H), 6.12 (s, 1H), 7.86 (s, 1H) ppm. ^{13}C NMR (100 MHz, CDCl$_3$): δ 15.2, 55.8, 98.0, 118.5, 126.2, 127.3, 144.9, 164.1 ppm.

***Synthesis of 4-Methoxy-5-methylbenzene-1,2-diamine* (124):** 5-Methoxy-4-methyl-2-nitroaniline, 123 (100 mg) was dissolved in 50 mL MeOH and passed through a Thalesnano H-cube hydrogenator with 10% Pd/C catalyst at 40 °C and 1 bar hydrogen gas pressure at a flow rate of 1.0 mL/min. The solution was then concentrated under reduced pressure and the resulting compound was used for the next step without further purification. Yield: 85%, LC-MS *m/z* 153.1 (M+H). ^{1}H NMR (400 MHz, CD$_3$OD): δ 2.01 (s, 3H), 3.68 (s, 3H), 6.36 (s, 1H), 6.51 (s, 1H) ppm.

***Synthesis of 5-Methoxy-6-methylbenzimidazole* (125):** 4-Methoxy-5-methylbenzene-1,2-diamine (124) was dissolved in 2 mL of HCOOH and the solution was refluxed for 2 hrs. The reaction mixture was then diluted with water and extracted with CHCl$_3$. The pH of the aqueous phase was adjusted to 8 using ammonium hydroxide and was then extracted with CHCl$_3$. The organic phase was concentrated under reduced

pressure and purified by silica gel column chromatography. Yield: 35%, LC-MS *m/z* 163.1 (M+H). ^{1}H NMR (400 MHz, CD$_3$OD): δ 2.26 (s, 3H), 3.83 (s, 3H), 7.04 (s, 1H), 7.32 (s, 1H), 7.98 (s, 1H) ppm. ^{13}C NMR (100 MHz, CD$_3$OD): δ 17.1, 56.1, 96.5, 117.0, 124.5, 132.7, 137.3, 140.9, 156.6 ppm.

***Synthesis of 5-Hydroxy-6-methylbenzimidazole* (99):** 5-Methoxy-6-methyl benzimidazole (125) was dissolved in 2.5 mL of hydrobromic acid and the solution was refluxed for 1 hr. The reaction mixture was then diluted with water and the pH was adjusted to 8 using ammonium hydroxide followed by purification using silica gel column chromatography. Yield: 80%, LC-MS *m/z* 149.1 (M+H). ^{1}H NMR (400 MHz, CD$_3$OD): δ 2.27 (s, 3H), 7.04 (s, 1H), 7.31 (s, 1H), 8.04 (s, 1H) ppm. ^{13}C NMR (100 MHz, CD$_3$OD): δ 17.0, 99.7, 117.0, 123.1, 132.5, 136.4, 140.8, 153.4 ppm.

6.4.6 Synthesis of the compound 101

The synthetic scheme for 101 is shown in Figure 92.
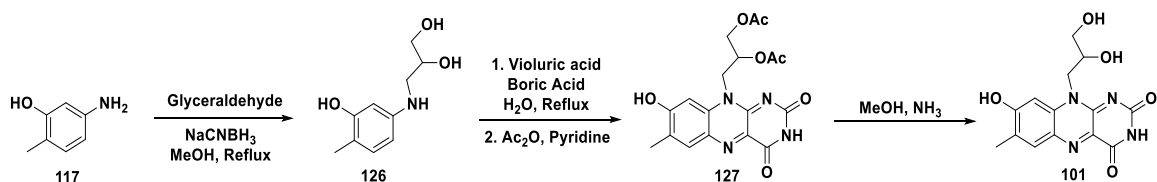
Figure 92. Scheme for the synthesis of 101

109

Procedure

Synthesis of 3-((3-Hydroxy-4-methylphenyl)amino)propane-1,2-diol **(126):** 5-Amino-2-methylphenol, 117 (123 mg, 1.0 equiv.), glyceraldehyde (270 mg, 3.0 equiv.) and sodium cyanoborohydride (126 mg, 2.0 equiv.) were dissolved in anhydrous MeOH (15 mL). The mixture was refluxed at 80 °C for 2 days under argon atmosphere. Then the solvent was removed under reduced pressure and excess $NaCNBH_3$ was quenched using 1M HCl. The resulting mixture was neutralized using saturated $NaHCO_3$ solution and concentrated under reduced pressure. The residue was purified by silica gel column chromatography using chloroform/methanol. Yield: 60%, LC-MS *m/z* 198.1 (M+H). ^{1}H NMR (400 MHz, CD_3OD): δ 2.05 (s, 3H), 2.99 (dd, 1H), 3.19 (dd, 1H), 3.57 (m, 2H), 3.81 (p, 1H), 6.13 (dd, 1H), 6.18 (d, 1H), 6.80 (d, 1H) ppm. ^{13}C NMR (100 MHz, CD_3OD): δ 15.3, 48.3, 65.5, 71.6, 101.7, 106.5, 114.7, 132.0, 149.1, 156.6 ppm.

Synthesis of 127: To a solution of 126 (197 mg, 1 equiv.) in 15 mL of water, violuric acid monohydrate (175 mg, 1 equiv.) and boric acid (62 mg, 1 equiv.) were added. The mixture was refluxed at 105 °C for 12 hours and was then concentrated under reduced pressure. The crude product was dissolved in 8 mL of pyridine. 1 mL of acetic anhydride was added to the mixture and was stirred at rt for 6 hrs. The solvent was then removed under reduced pressure with toluene. The residue was purified by silica gel column chromatography using chloroform/methanol. LC-MS *m/z* 401.1 (M-H). ^{1}H NMR (400 MHz, CD_3OD): δ 1.78 (s, 3H), 2.09 (s, 3H), 2.21 (s, 3H), 4.38 (m, 2H), 4.69 (m, 1H), 5.56 (m, 1H), 5.70 (br, 1H), 6.78 (s, 1H), 7.61 (s, 1H) ppm. ^{13}C NMR (100 MHz, CD_3OD): δ

16.5, 20.5, 20.6, 46.2, 64.5, 70.3, 100.9, 126.0, 134.0, 134.2, 134.9, 138.0, 152.0, 159.1, 163.5, 163.9, 171.9, 172.4 ppm.

Synthesis of 101: Compound 127 was converted to compound 101 by overnight stirring in ammonia (7N in methanol) and was purified by reverse phase high performance liquid chromatography. LC-MS *m/z* 317.1 (M-H) (Figure 93).
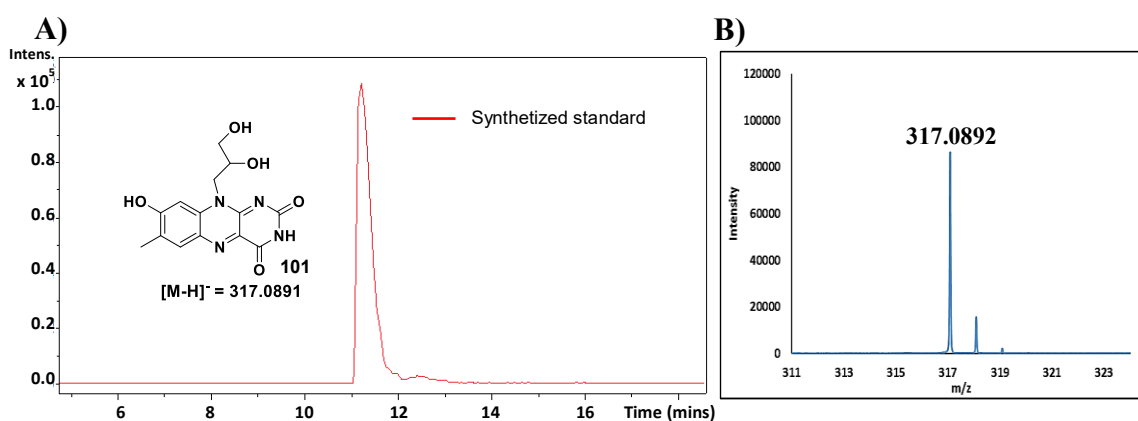
Figure 93. LC-MS analysis of the synthesized compound 101. **(A)** EIC at m/z 317.0891 showing the formation of 101 **(B)** ESI-MS of 101 in the negative mode

6.4.7 Synthesis of glycolaldehyde-PFBHA oxime (104)[57]

The synthetic scheme for the glycolaldehyde-PFBHA oxime (104) is shown in Figure 94.
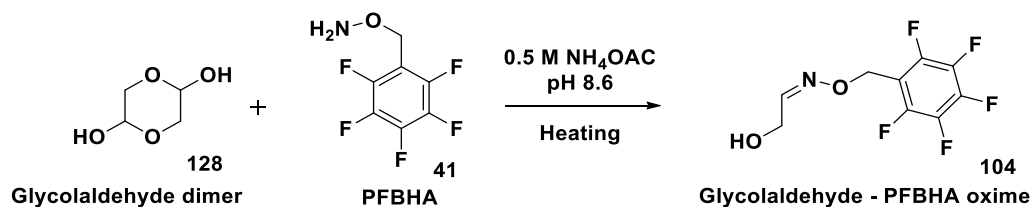
Figure 94. Scheme for the synthesis of glycolaldehyde-PFBHA oxime (104)

111

Procedure

***Synthesis of glycolaldehyde-PFBHA oxime* (104):** Glycolaldehyde dimer, 128 (1 mM) and *o*-(pentafluorobenzyl)hydroxylamine (PFBHA, 41) (2mM) were mixed in 500 mM NH$_4$OAc buffer, pH 8.6. The reaction mixture was heated at 65 °C for 1 hr and was then analyzed by LC-MS (Figure 95).
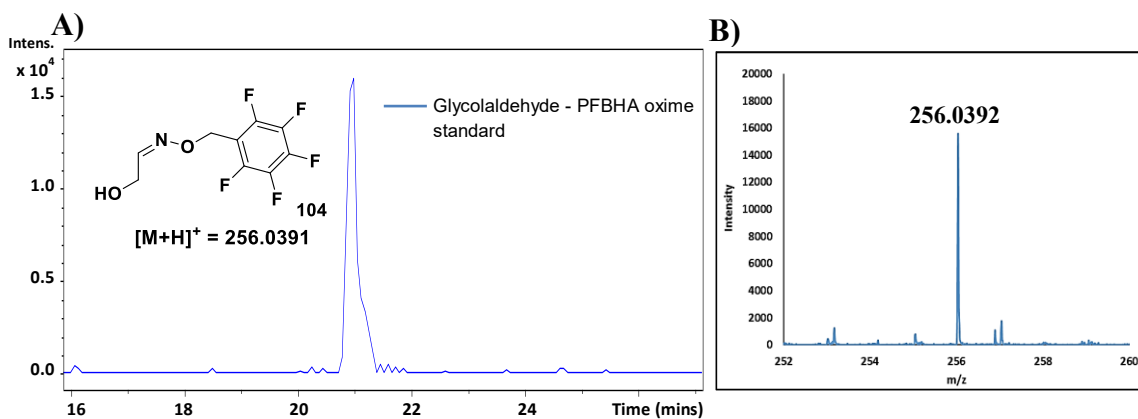
Figure 95. LC-MS analysis for the synthesized glycolaldehyde - PFBHA oxime (104). **(A)** EIC at 256.0391 showing the formation of the glycolaldehyde – PFBHA oxime standard **(B)** ESI-MS of 104 in the positive mode

CHAPTER VII

SUMMARY

BluB catalyzes the oxygen dependent biosynthesis of Dimethylbenzimidazole (DMB) from reduced FMN. It involves a remarkable rearrangement in which the C1$'$ of the ribityl side chain of FMN is incorporated at C2 of the product, DMB (13).

In this dissertation, we have successfully identified alloxan (29) as the final end product derived from the ring C of FMN. Formation of alloxan was confirmed by trapping it as an adduct using the derivatizing agent oPDA. Water and oxygen gas have been shown to be the two sources of oxygen atom incorporation in the alloxan based on O-18 labeling studies. The sugar end product, erythrose-4-phosphate (14) was successfully derivatized using PFBHA in the form of its corresponding oxime.

A key intermediate (27) in our mechanistic proposal has been successfully trapped in the form of six different shunt products using water, bisulfite and hydride as nucleophiles. Presence of the imine functionality in the intermediate 27 was confirmed by trapping it with bisulfite as well as reducing it with cyanoborohydride and deuterium studies. Detailed characterization of the various shunt products was done by coelution and labeling studies.

Trapping of the intermediate 27 helps us establish the actual sequence of the release of the different products in the BluB catalyzed reaction. Presence of the alloxan moiety in 27 proves that the C-C bond cleavage occurs first forming erythrose-4-phosphate (14) followed by the release of alloxan (29).

Asp-32 has been shown to play an important role in stabilizing this intermediate by forming an adduct and its mutation to asparagine (D32N mutant) leads to the exclusive formation of the different shunt products.

Characterization of the shunt product 73 provides evidence for the intermediate 35 in our mechanistic hypothesis. It also helps us establish that the alloxan is released first followed by the cyclization and oxidation steps leading to the formation of DMB.

Based on the stereochemical studies, we have successfully shown that the *pro*-R hydrogen is abstracted from the C1' of the ribose sugar chain of the substrate and the *pro*-S hydrogen is retained in the final product, DMB. Thus, there exists a selectivity in the abstraction of the proton from the C1' of the ribityl chain of FMN. This result helps us establish that the final oxidation step leading to DMB is indeed catalyzed by the enzyme.

Substrate analog studies were also performed for the BluB catalyzed reaction. Interesting results were obtained on using 8-substituted flavins as substrates. Along with the formation of the native products, a new shunt product (100) was observed in the BluB reactions with 8-OH FMN. An unusual C-C bond fragmentation between C3' and C4' of the ribose sugar chain of FMN leads to the formation of the shunt product 100 along with glycolaldehyde-2-phosphate as the other fragment. Characterization of 100 provides evidence for the initial fragmentation of the peroxyflavin intermediate involved in the biosynthesis of dimethylbenzimidazole.

All these above observations are consistent with our current mechanistic proposal for the DMB biosynthesis as shown in Figure 96.
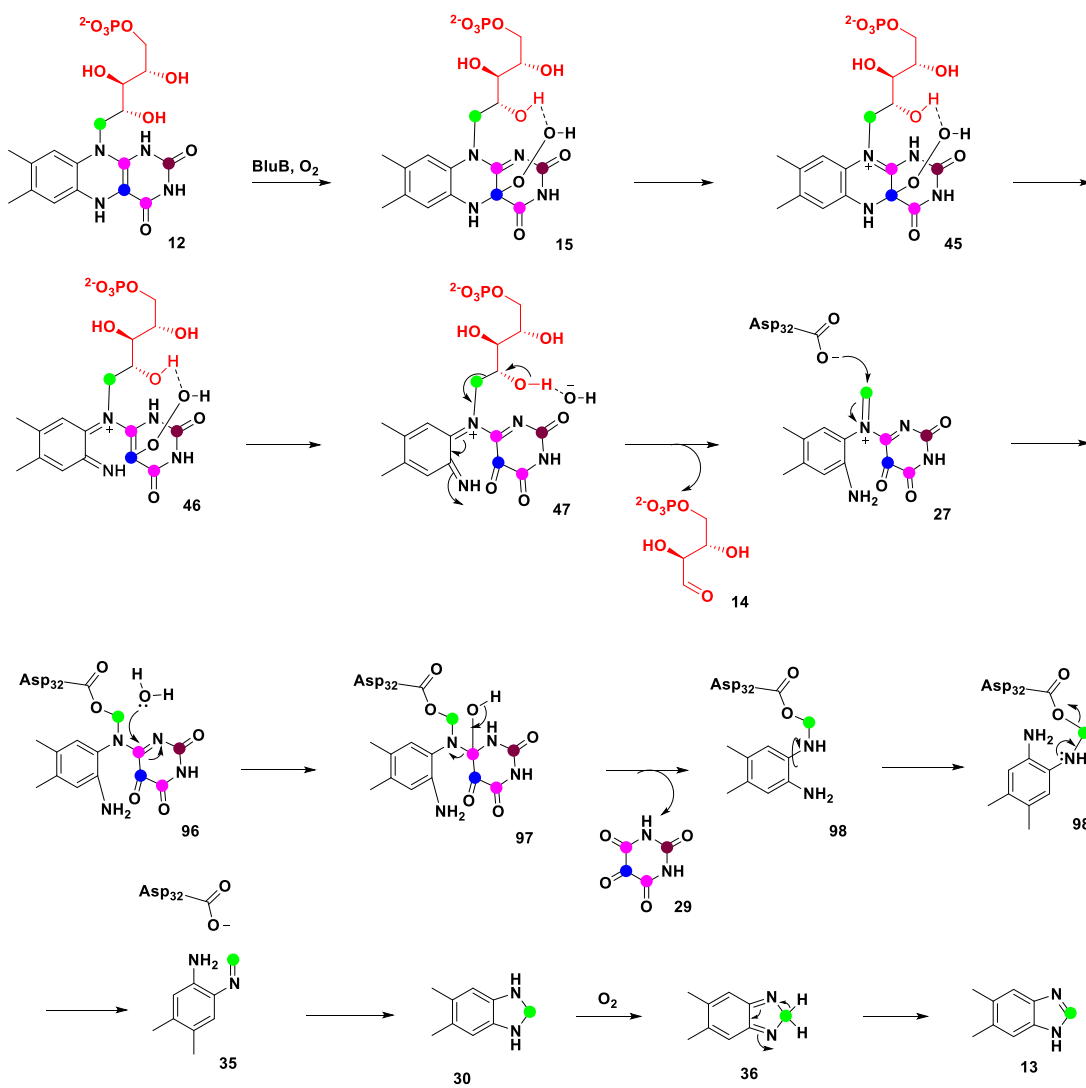
Figure 96. Final mechanistic proposal for the formation of Dimethylbenzimidazole

Thus, we have been thus able to provide multiple pieces of evidence in support of our mechanistic proposal for DMB formation and have finally unraveled the long unsolved mystery in the vitamin B_{12} biosynthesis.

Interestingly, the two pathways involved in the DMB formation are distinctly different. In the anaerobic organisms, BzaF carries out the benzimidazole formation involving complex radical mediated chemistry. Identification and successful reconstitution of BzaF is a major stepping stone in the anaerobic biosynthesis of benzimidazole. On the other hand, in the aerobic pathway BluB is responsible for the DMB biosynthesis involving unique flavochemistry. Reduced FMN is the substrate of BluB which undergoes unprecedented rearrangement to form DMB. It is a unique example, wherein, destruction of one cofactor leads to another.

It is amazing to see how subtle changes in the active site leads to an entirely different functionality. Though being structurally similar to the flavin reductase superfamily, BluB carries out completely different chemistry as compared to the oxidoreductases and nitroreductases.

In general, identification of the various shunt products formed can help us provide snapshots of the reaction coordinates in a multi-step reaction. With the advancement in the field of mass spectrometry, the characterization of these shunt products is no longer difficult. BluB, serves as a good example, wherein, identification of the various shunt products helped us decode the complex transformation involved in DMB biosynthesis. This can serve as a general tool to elucidate the detailed mechanism involved in various complex enzymatic reactions.

REFERENCES

1.   Raux, E., Schubert, H. L. & Warren, M. J. Biosynthesis of cobalamin (vitamin B_{12}): a bacterial conundrum. *Cellular and molecular life sciences : CMLS* **57**, 1880-1893 (2000).

2.   Roth, J. R., Lawrence, J. G. & Bobik, T. A. Cobalamin (coenzyme B_{12}): synthesis and biological significance. *Annual review of microbiology* **50**, 137-181 (1996).

3.   Banerjee, R. & Ragsdale, S. W. The many faces of vitamin B_{12}: catalysis by cobalamin-dependent enzymes. *Annual review of biochemistry* **72**, 209-247 (2003).

4.   Scott, A. I. Discovering Nature's Diverse Pathways to Vitamin B_{12}: A 35-Year Odyssey. *The Journal of Organic Chemistry* **68**, 2529-2539 (2003).

5.   Warren, M. J. Finding the final pieces of the vitamin B_{12} biosynthetic jigsaw. *Proc Natl Acad Sci U S A* **103**, 4799-4800 (2006).

6.   Warren, M. J., Raux, E., Schubert, H. L. & Escalante-Semerena, J. C. The biosynthesis of adenosylcobalamin (vitamin B_{12}). *Natural product reports* **19**, 390-412 (2002).

7.   Renz, P. in *Chemistry and Biochemistry of B_{12}* (ed. Banerjee, R.) 557-575 (John Wiley & Sons, New York,1999).

8.   Höllriegl, V., Lamm, L., Rowold, J., Hörig, J. & Renz, P. Biosynthesis of vitamin B_{12}. *Archives of microbiology* **132**, 155-158 (1982).

9.   Munder, M., Vogt, J. R. A., Vogler, B. & Renz, P. Biosynthesis of vitamin B_{12} in anaerobic bacteria. *European journal of biochemistry* **204**, 679-683 (1992).

10.   Renz, P., Endres, B., Kurz, B. & Marquart, J. Biosynthesis of vitamin B_{12} in anaerobic bacteria. *European journal of biochemistry* **217**, 1117-1121 (1993).

11.   Schulze, B., Vogler, B. & Renz, P. Biosynthesis of vitamin B_{12} in anaerobic bacteria--experiments with *Eubacterium limosum* on the transformation of 5-hydroxy-6-methyl-benzimidazole, its nucleoside, its cobamide, and of 5-hydroxybenzimidazolylcobamide in vitamin B_{12}. *European journal of biochemistry* **254**, 620-625 (1998).

12.   Vogt, J. R. & Renz, P. Biosynthesis of vitamin B-12 in anaerobic bacteria. Experiments with *Eubacterium limosum* on the origin of the amide groups of the

corrin ring and of *N-3* of the 5,6-dimethylbenzimidazole part. *European journal of biochemistry* **171**, 655-659 (1988).

13. Hazra, A. B. *et al.* Anaerobic biosynthesis of the lower ligand of vitamin B_{12}. *Proc Natl Acad Sci U S A* **112**, 10792-10797 (2015).

14. Mehta, A. P. *et al.* Anaerobic 5-Hydroxybenzimidazole Formation from Aminoimidazole Ribotide: An Unanticipated Intersection of Thiamin and Vitamin B_{12} Biosynthesis. *Journal of the American Chemical Society* **137**, 10444-10447 (2015).

15. Taga, M. E., Larsen, N. A., Howard-Jones, A. R., Walsh, C. T. & Walker, G. C. BluB cannibalizes flavin to form the lower ligand of vitamin B_{12}. *Nature* **446**, 449-453 (2007).

16. Campbell, G. R. O. *et al.* Sinorhizobium meliloti bluB is necessary for production of 5,6-dimethylbenzimidazole, the lower ligand of B_{12}. *Proceedings of the National Academy of Sciences of the United States of America* **103**, 4634-4639 (2006).

17. Gray, M. J. & Escalante-Semerena, J. C. Single-enzyme conversion of $FMNH_2$ to 5,6-dimethylbenzimidazole, the lower ligand of B_{12}. *Proceedings of the National Academy of Sciences* **104**, 2921-2926 (2007).

18. Wang, X.-L. & Quan, J.-M. Intermediate-Assisted Multifunctional Catalysis in the Conversion of Flavin to 5,6-Dimethylbenzimidazole by BluB: A Density Functional Theory Study. *Journal of the American Chemical Society* **133**, 4079-4091 (2011).

19. Cooper, A. J. L. & Pinto, J. T. BluB cannibalizes flavin to form the lower ligand of vitamin B_{12}. *Chemtracts* **19**, 474-481 (2006).

20. Renz, P. & Weyhenmeyer, R. Biosynthesis of 5,6-dimethylbenzimidazole from riboflavin Transformation of C-1′ of riboflavin into C-2 of 5,6-dimethylbenzimidazole. *FEBS Letters* **22**, 124-126 (1972).

21. Renz, P., Wurm, R. & Hörig, J. Nonenzymatic Transformation of Riboflavin into 5,6-Dimethylbenzimidazole. *Zeitschrift für Naturforschung C* **32,** 523-527 (1977).

22. Horig, J. A. & Renz, P. Biosynthesis of vitamin B_{12}. Some properties of the 5,6-dimethylbenzimidazole-forming system of *Propionibacterium freudenreichii* and *Propionibacterium shermanii*. *European journal of biochemistry* **105**, 587-592 (1980).

23. Keck, B., Munder, M. & Renz, P. Biosynthesis of cobalamin in *Salmonella typhimurium*: transformation of riboflavin into the 5,6-dimethylbenzimidazole moiety. *Archives of microbiology* **171**, 66-68 (1998).

24. Renz, P. Riboflavin as precursor in the biosynthesis of the 5,6-Dimethylbenzimidazole-moiety of vitamin B_{12}. *FEBS Letters* **6**, 187-189 (1970).

25. Race, P. R. *et al.* Structural and Mechanistic Studies of *Escherichia coli* Nitroreductase with the Antibiotic Nitrofurazone: Reversed binding orientations in different redox states of the enzyme. *Journal of Biological Chemistry* **280**, 13256-13264 (2005).

26. Tanner, J. J., Lei, B., Tu, S. C. & Krause, K. L. Flavin reductase P: structure of a dimeric enzyme that reduces flavin. *Biochemistry* **35**, 13531-13539 (1996).

27. Thomas, S. R., McTamney, P. M., Adler, J. M., LaRonde-LeBlanc, N. & Rokita, S. E. Crystal Structure of Iodotyrosine Deiodinase, a Novel Flavoprotein Responsible for Iodide Salvage in Thyroid Glands. *The Journal of Biological Chemistry* **284**, 19659-19667 (2009).

28. Koike, H. *et al.* 1.8 Å crystal structure of the major NAD(P)H:FMN oxidoreductase of a bioluminescent bacterium, *Vibrio fischeri*: overall structure, cofactor and substrate-analog binding, and comparison with related flavoproteins. *Journal of molecular biology* **280**, 259-273 (1998).

29. Lovering, A. L., Hyde, E. I., Searle, P. F. & White, S. A. The structure of *Escherichia coli* nitroreductase complexed with nicotinic acid: three crystal forms at 1.7 Å, 1.8 Å and 2.4 Å resolution. *Journal of molecular biology* **309**, 203-213 (2001).

30. Yu, T.-Y. *et al.* Active site residues critical for flavin binding and 5,6-dimethylbenzimidazole biosynthesis in the flavin destructase enzyme BluB. *Protein Science* **21**, 839-849 (2012).

31. Mukherjee, A. & Rokita, S. E. Single Amino Acid Switch between a Flavin-Dependent Dehalogenase and Nitroreductase. *Journal of the American Chemical Society* **137**, 15342-15345 (2015).

32. Sun, Z., Su, Q. & Rokita, S. E. The distribution and mechanism of iodotyrosine deiodinase defied expectations. *Archives of biochemistry and biophysics* (2017).

33. Ealick, S. E. & Begley, T. P. Biochemistry: Molecular cannibalism. *Nature* **446**, 387-388 (2007).

34.   Maggio-Hall, L. A., Dorrestein, P. C., Escalante-Semerena, J. C. & Begley, T. P. Formation of the Dimethylbenzimidazole Ligand of Coenzyme B_{12} under Physiological Conditions by a Facile Oxidative Cascade. *Organic Letters* **5**, 2211-2213 (2003).

35.   Begley, T. P., Chatterjee, A., Hanes, J. W., Hazra, A. & Ealick, S. E. Cofactor biosynthesis – still yielding fascinating new biological chemistry. *Current opinion in chemical biology* **12**, 118-125 (2008).

36.   Yagi, K., Ohishi, N., Takai, A., Kawano, K. & Kyogoku, Y. Carbon-13-NMR study of flavins. *Flavins and Flavoproteins* (ed. Singer, T. P.) 775-781 (Amsterdam, Elsevier, 1976).

37.   Neti, S. S. & Poulter, C. D. Site-Selective Synthesis of ^{15}N- and ^{13}C-Enriched Flavin Mononucleotide Coenzyme Isotopologues. *The Journal of Organic Chemistry* **81**, 5087-5092 (2016).

38.   Clark-Lewis, J. W. & Edgar, J. A. Ring contractions of alloxan with alicyclic secondary amines: formation of amine salts of alloxanic acid. *Journal of the Chemical Society (Resumed)*, 3887-3889 (1962).

39.   Kwart, H. & Sarasohn, I. M. Studies on the Mechanism of the Benzilic Acid Rearrangement; the Rearrangement of Alloxan (I). *Journal of the American Chemical Society* **83**, 909-919 (1961).

40.   Kwart, H., Spayd, R. W. & Collins, C. J. Evidence for nitrogen migration in the benzilic acid rearrangement of alloxan and derivatives. *Journal of the American Chemical Society* **83**, 2579-2580 (1961).

41.   Kaupp, G. & Naimi-Jamal, M. R. Quantitative Cascade Condensations between *o*-Phenylenediamines and 1,2-Dicarbonyl Compounds without Production of Wastes. *European Journal of Organic Chemistry* **2002**, 1368-1373 (2002).

42.   Ammelburg, M. *et al.* A CTP-Dependent Archaeal Riboflavin Kinase Forms a Bridge in the Evolution of Cradle-Loop Barrels. *Structure* **15**, 1577-1590 (2007).

43.   Mashhadi, Z., Zhang, H., Xu, H. & White, R. H. Identification and characterization of an archaeon-specific riboflavin kinase. *Journal of bacteriology* **190**, 2615-2618 (2008).

44.   Prasad A. Thakurdesai, S. G. W., Chandrabhan T. Chopade. Synthesis and anti-inflammatory activity of some benzimidazole-2-carboxylic acids. *Pharmacologyonline* **1**, 314-329 (2007).

45. Xiao, Z., Yang, M. G., Tebben, A. J., Galella, M. A. & Weinstein, D. S. Novel two-step, one-pot synthesis of primary acylureas. *Tetrahedron Letters* **51**, 5843-5844 (2010).

46. Imada, Y., Iida, H., Ono, S., Masui, Y. & Murahashi, S.-I. Flavin-Catalyzed Oxidation of Amines and Sulfides with Molecular Oxygen: Biomimetic Green Oxidation. *Chemistry – An Asian Journal* **1**, 136-147 (2006).

47. Valdez-Padilla, D. *et al.* Synthesis and antiprotozoal activity of novel 1-methylbenzimidazole derivatives. *Bioorganic & Medicinal Chemistry* **17**, 1724-1730 (2009).

48. Thibodeaux, C. J., Chang, W.-c. & Liu, H.-w. Linear Free Energy Relationships Demonstrate a Catalytic Role for the Flavin Mononucleotide Coenzyme of the Type II Isopentenyl Diphosphate:Dimethylallyl Diphosphate Isomerase. *Journal of the American Chemical Society* **132**, 9994-9996 (2010).

49. Carlson, E. E. & Kiessling, L. L. Improved Chemical Syntheses of 1- and 5-Deazariboflavin. *The Journal of Organic Chemistry* **69**, 2614-2617 (2004).

50. Mansurova, M., Koay, M. S. & Gärtner, W. Synthesis and Electrochemical Properties of Structurally Modified Flavin Compounds. *European Journal of Organic Chemistry* **2008**, 5401-5406 (2008).

51. Jhulki, I., Chanani, P. K., Abdelwahed, S. H. & Begley, T. P. A Remarkable Oxidative Cascade That Replaces the Riboflavin C8 Methyl with an Amino Group during Roseoflavin Biosynthesis. *J Am Chem Soc* **138**, 8324-8327 (2016).

52. Sabu, K., J., F. B. & Kunio, M. An Improved Synthesis of 8-Amino-8-demethylriboflavin. *Bulletin of the Chemical Society of Japan* **60**, 3041-3042 (1987).

53. Lingens, B., Schild, T. A., Vogler, B. & Renz, P. Biosynthesis of vitamin B_{12}. Transformation of riboflavin ^{2}H-labeled in the 1'R position or 1'S position into 5,6-dimethylbenzimidazole. *European journal of biochemistry* **207**, 981-985 (1992).

54. Keller, P. J. *et al.* Biosynthesis of riboflavin: mechanism of formation of the ribitylamino linkage. *Biochemistry* **27**, 1117-1120 (1988).

55. Collins, H. F. *et al. Bacillus megaterium* Has Both a Functional BluB Protein Required for DMB Synthesis and a Related Flavoprotein That Forms a Stable Radical Species. *PLOS ONE* **8**, e55708 (2013).

56. Renz, P., Endres, B., Kurz, B. & Marquart, J. Biosynthesis of vitamin B_{12} in anaerobic bacteria. Transformation of 5-hydroxybenzimidazole and 5-hydroxy-6-

methylbenzimidazole into 5,6-dimethylbenzimidazole in *Eubacterium limosum*. *European journal of biochemistry* **217**, 1117-1121 (1993).

57.   Mathis, J. B. & Brown, G. M. The Biosynthesis of Folic Acid: XI. Purification and properties of dihydroneopterin aldolase. *Journal of Biological Chemistry* **245**, 3015-3025 (1970).

58.   Ghisla, S. & Mayhew, S. G. Isolation, synthesis, and properties of 8-hydroxyflavins. *Methods in Enzymology* **66**, 241-253 (1980).

APPENDIX
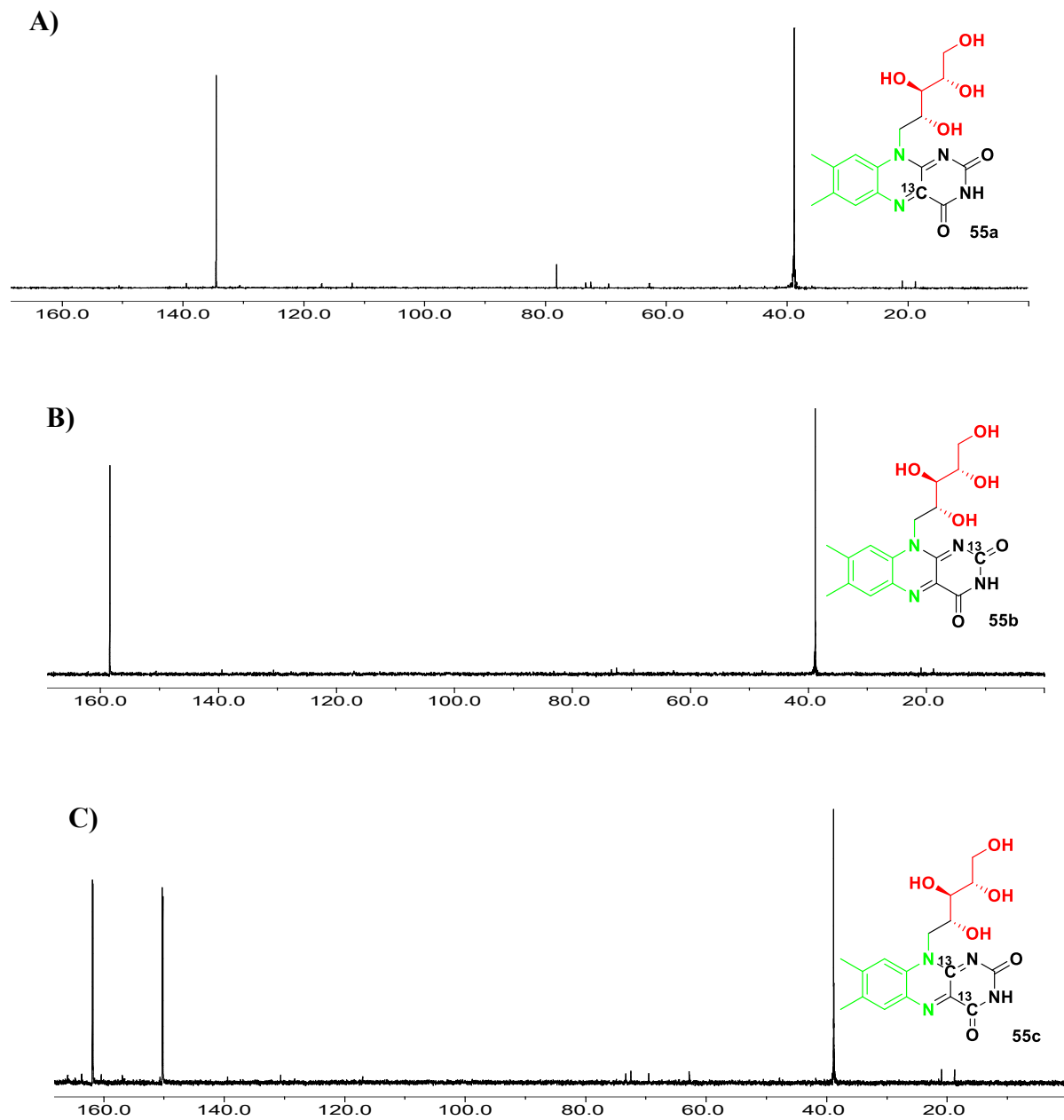
Figure A1. ^{13}C NMR of Riboflavin isotopologues **(A)** 4a-[13]C Riboflavin (55a) **(B)** 2-[13]C Riboflavin (55b) **(C)** 4,10a-[13]C Riboflavin (55c)
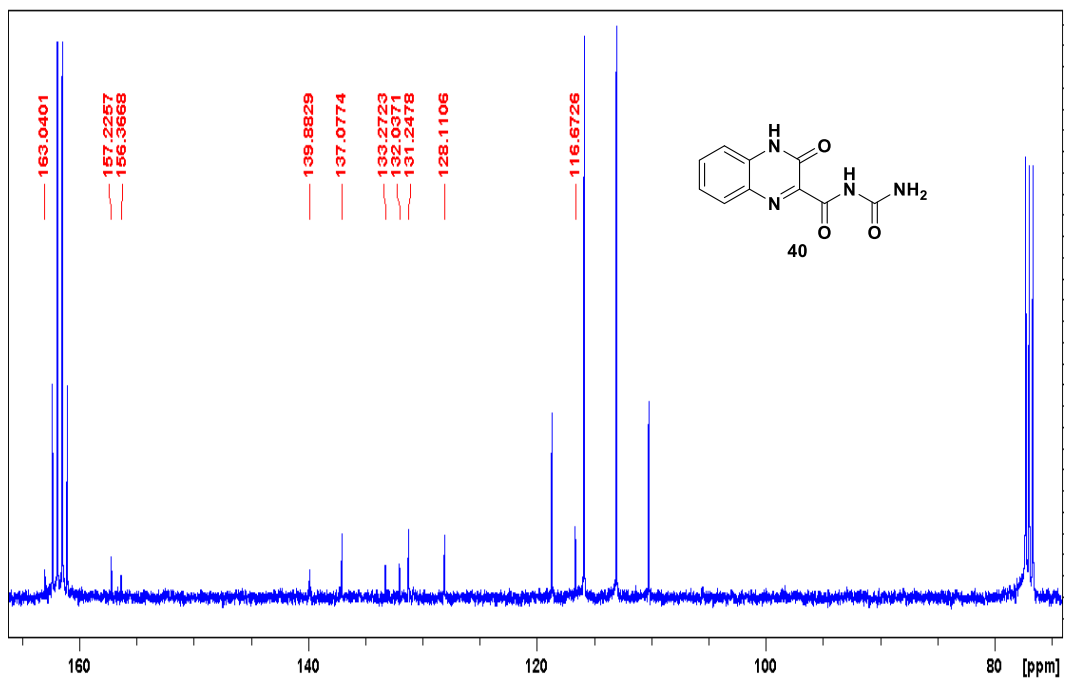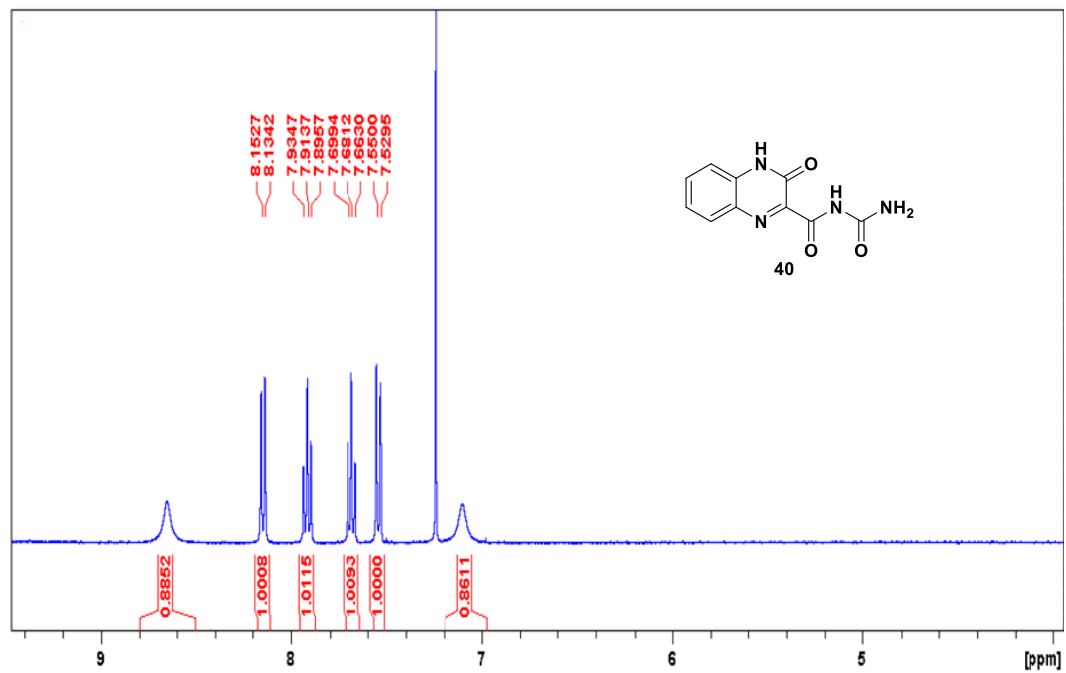
Figure A2. ^{1}H and ^{13}C NMR of alloxan-oPDA adduct (40)

124
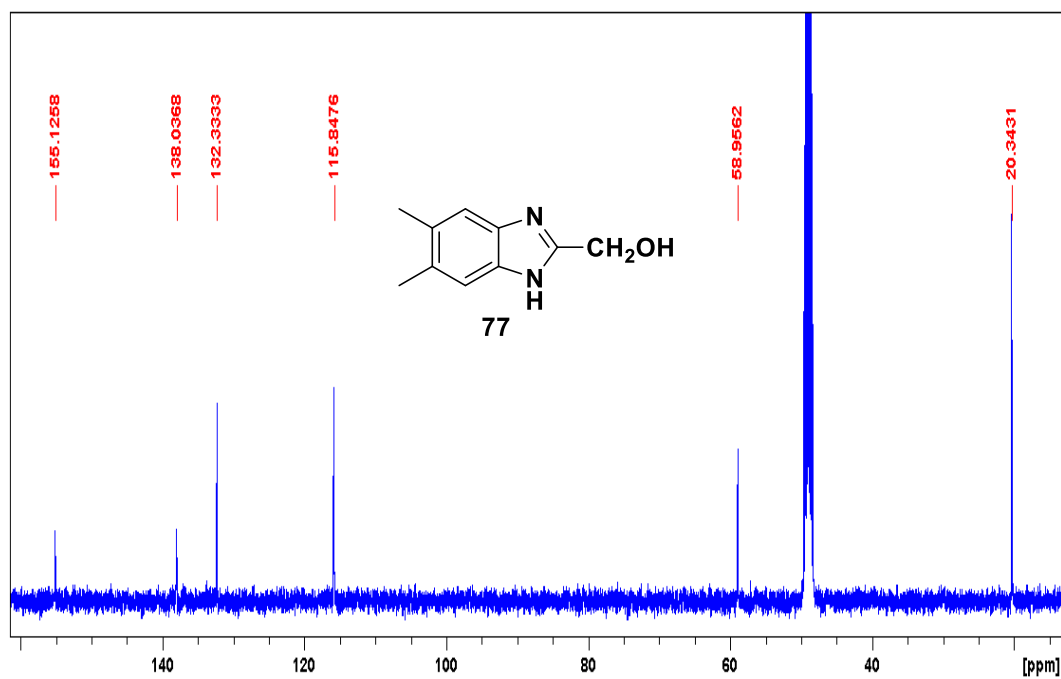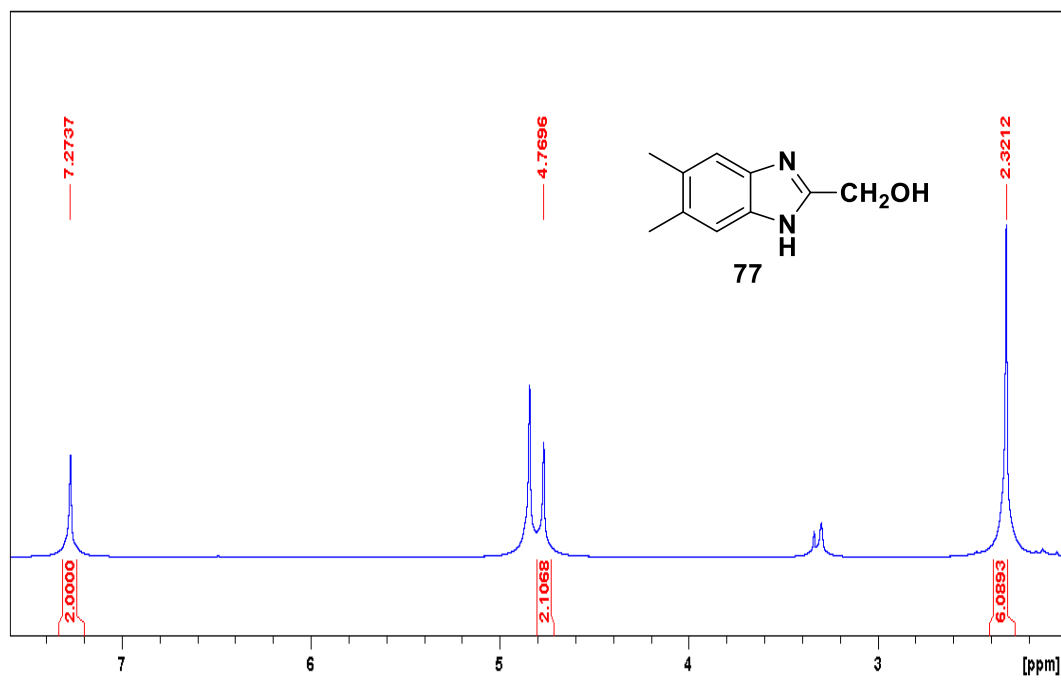
Figure A3. ^{1}H and ^{13}C NMR of 5,6-Dimethyl-2-hydroxymethylbenzimidazole (77)
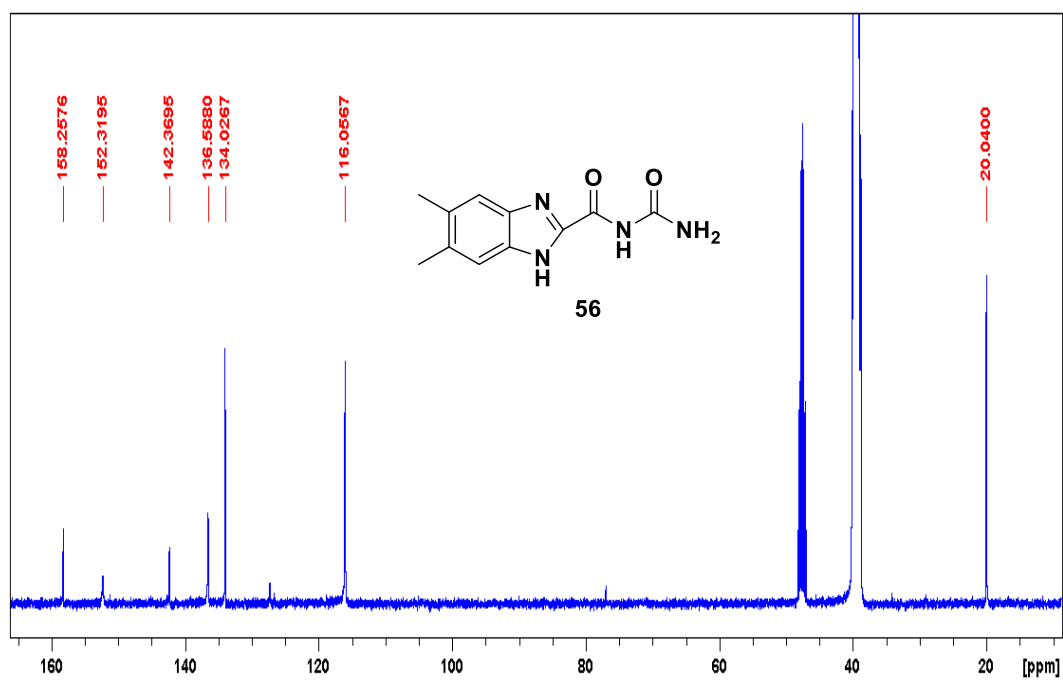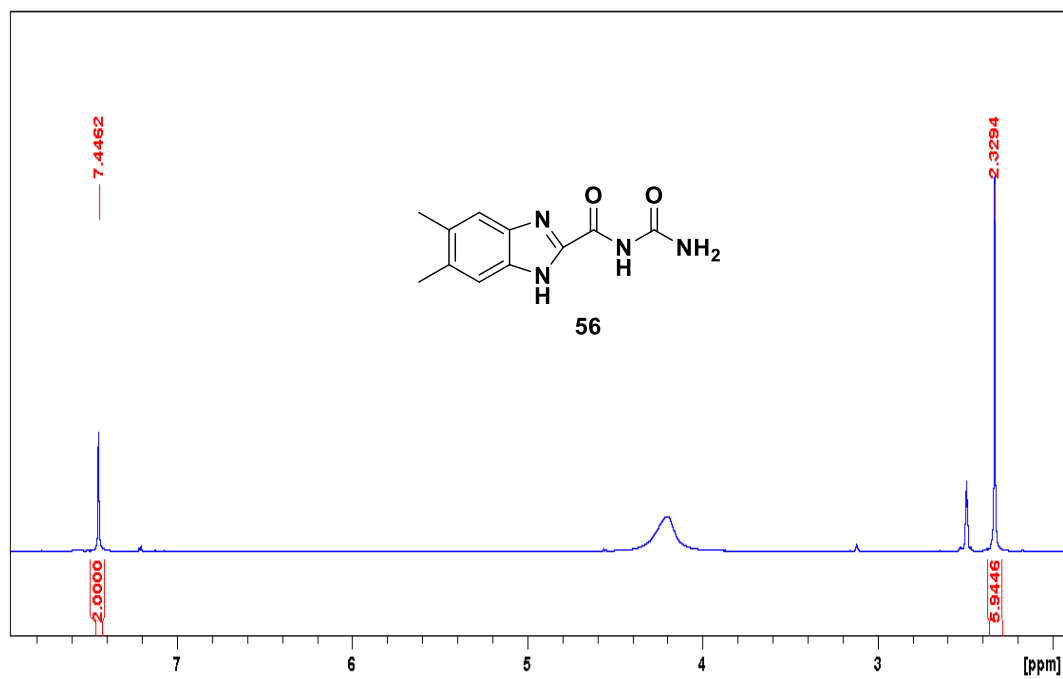
Figure A4. ^{1}H and ^{13}C NMR of N-Carbamoyl-5,6-dimethylbenzimidazole-2-carboxamide (56)
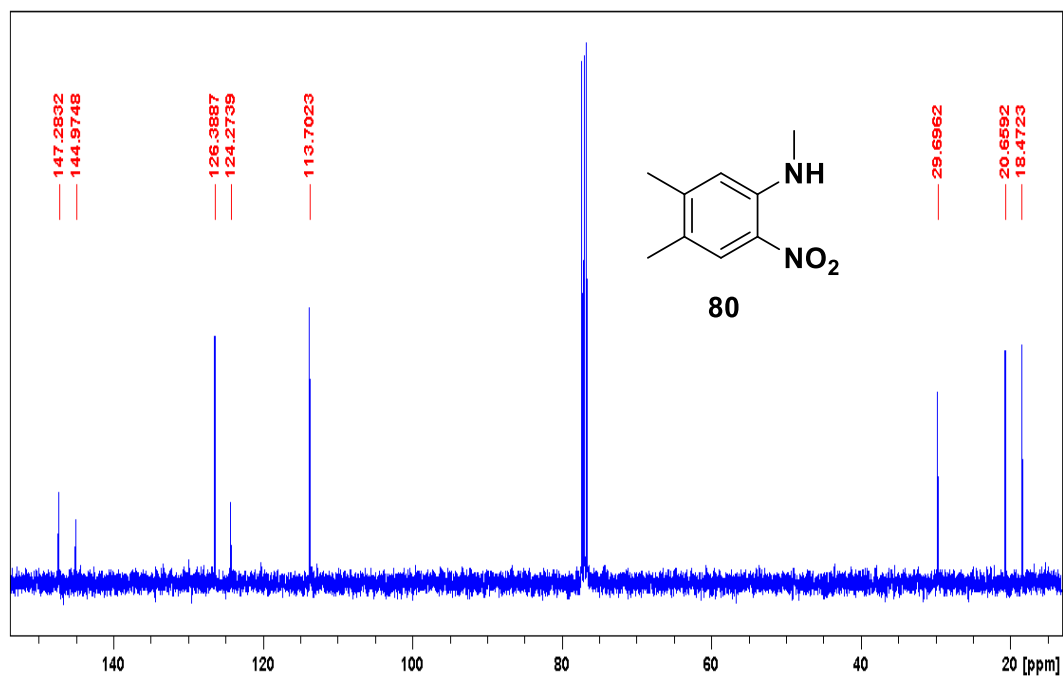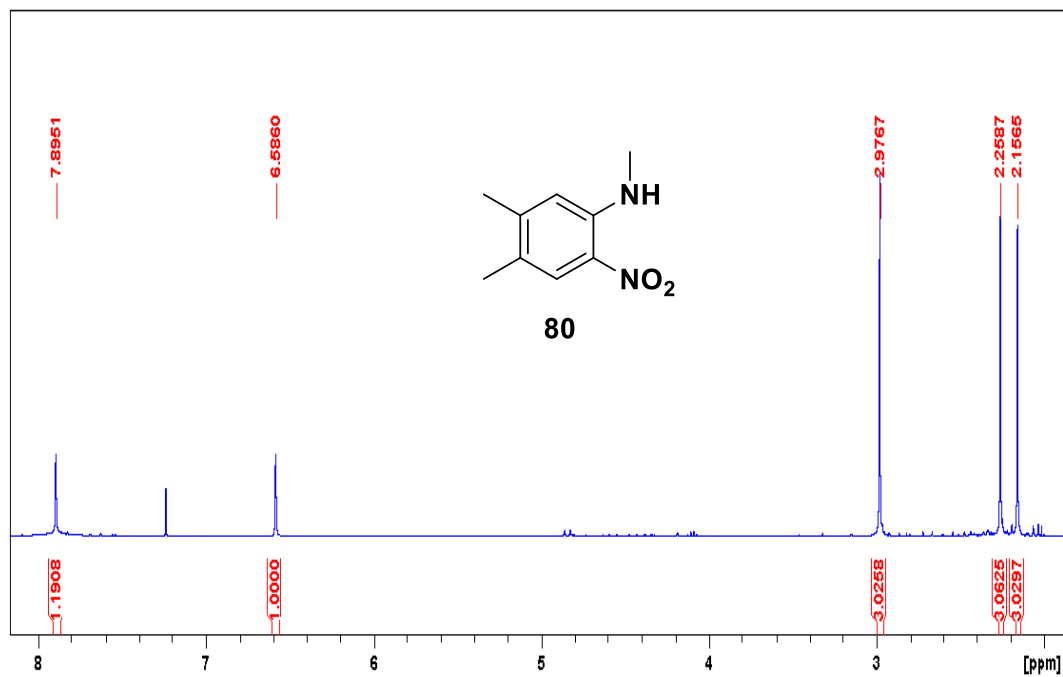
Figure A5. ^{1}H and ^{13}C NMR of N-Methyl-4,5-dimethyl-2-nitrobenzenamine (80)
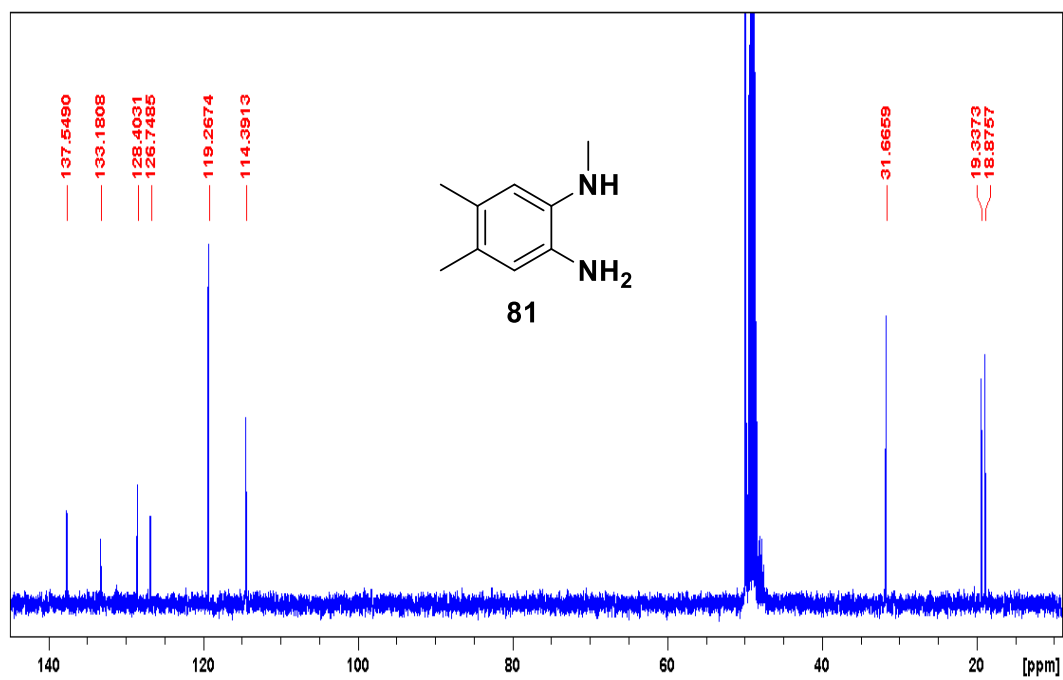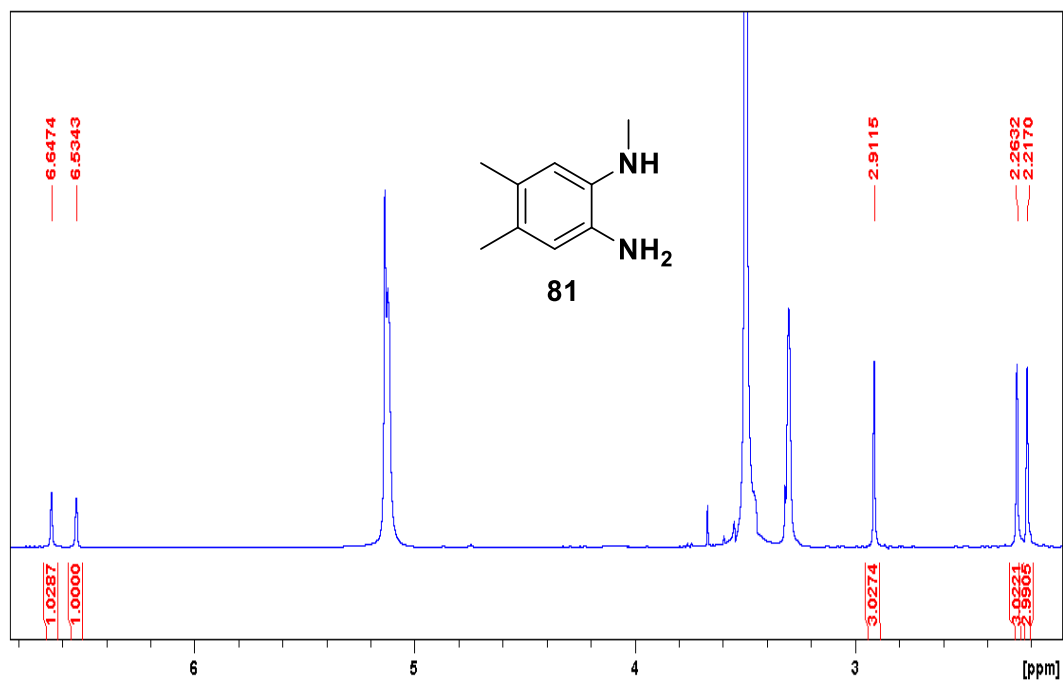
Figure A6. ^{1}H and ^{13}C NMR of N-Methyl-4,5-dimethylbenzene-1,2-diamine (**81**)
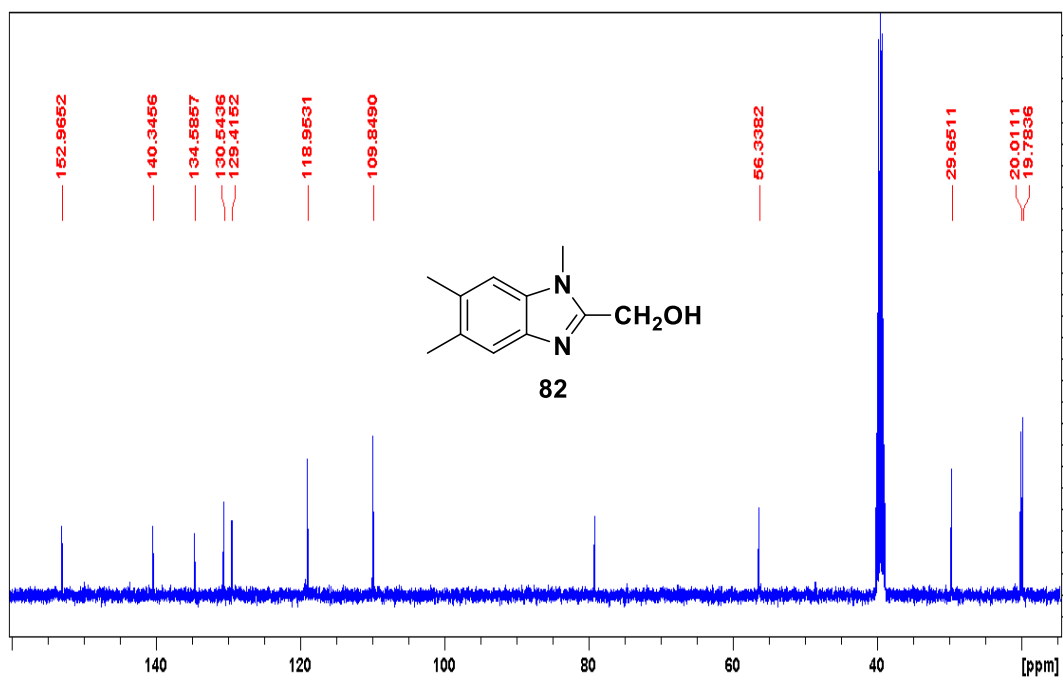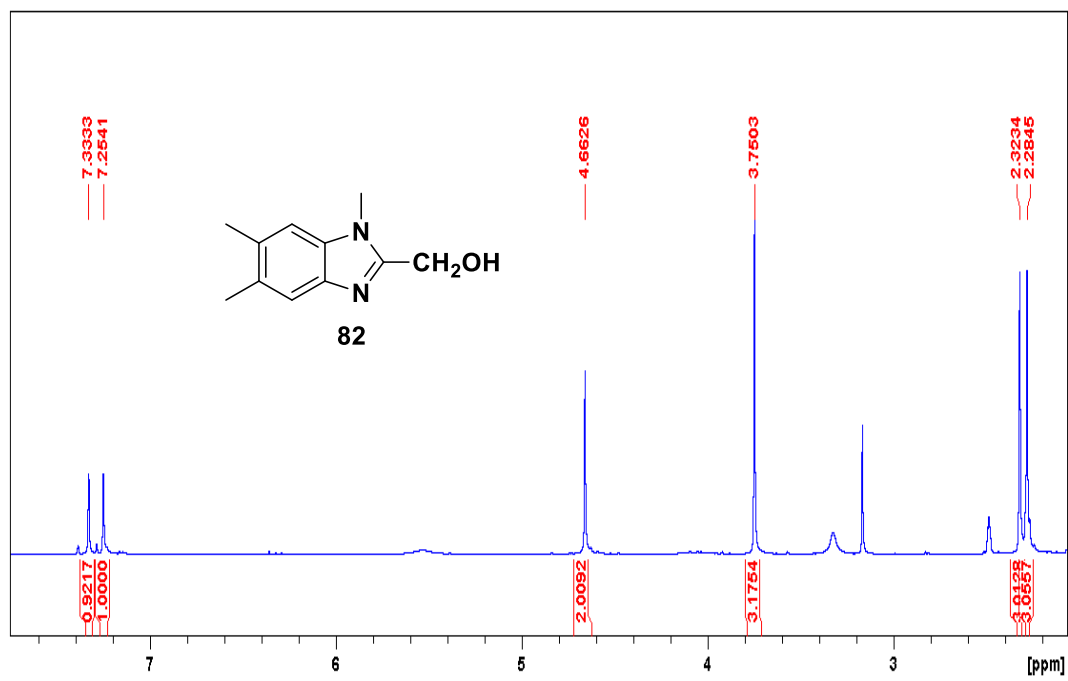
Figure A7. ^{1}H and ^{13}C NMR of 1,5,6-Trimethyl-2-hydroxymethylbenzimidazole (82)
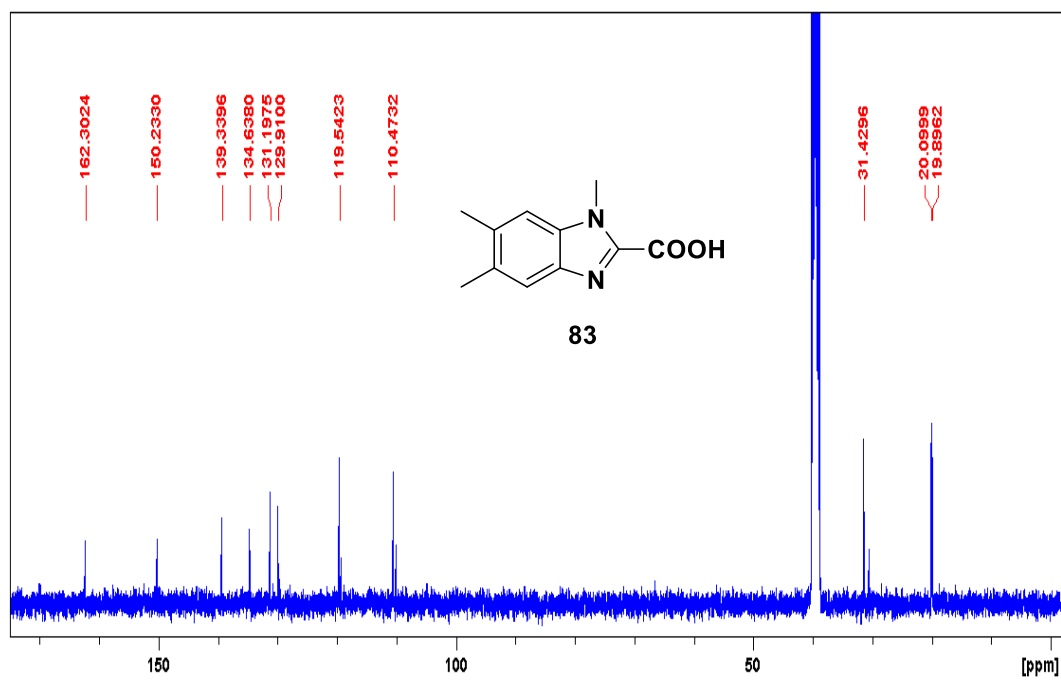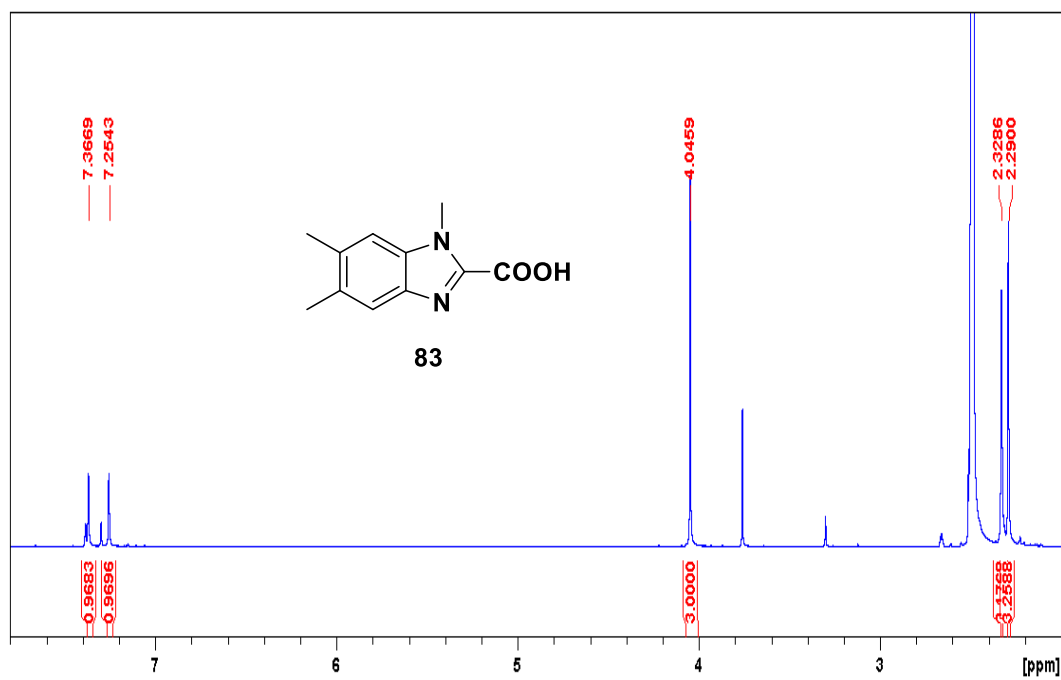
Figure A8. ^{1}H and ^{13}C NMR of 1,5,6-Trimethylbenzimidazole-2-carboxylic acid (83)
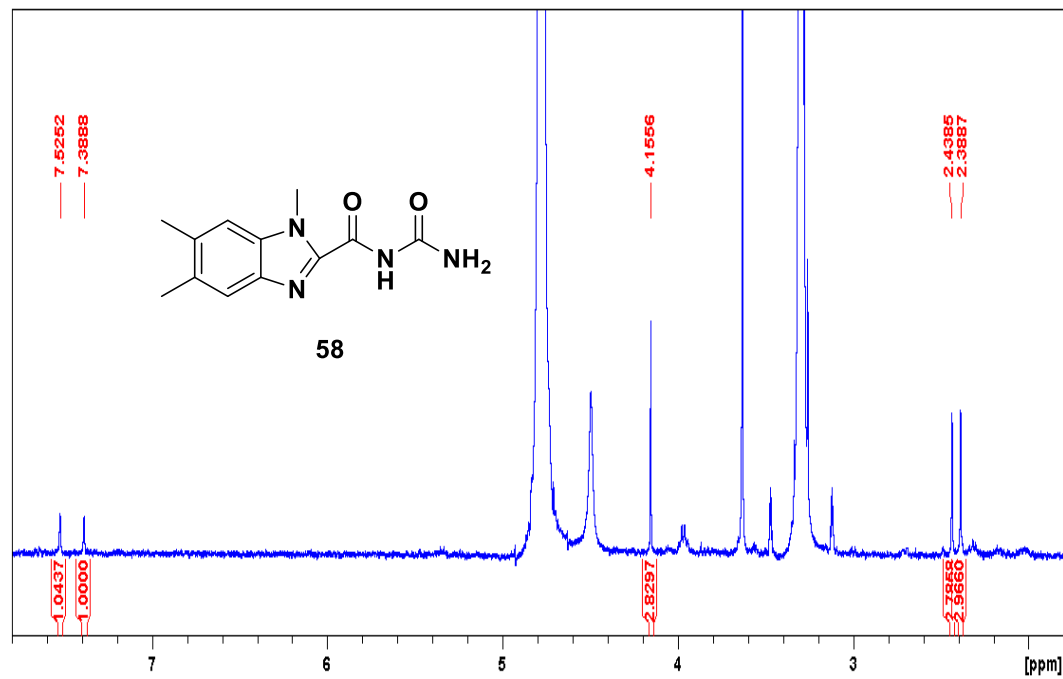
Figure A9. ^{1}H NMR of N-Carbamoyl-1,5,6-trimethylbenzimidazole-2-carboxamide (58)
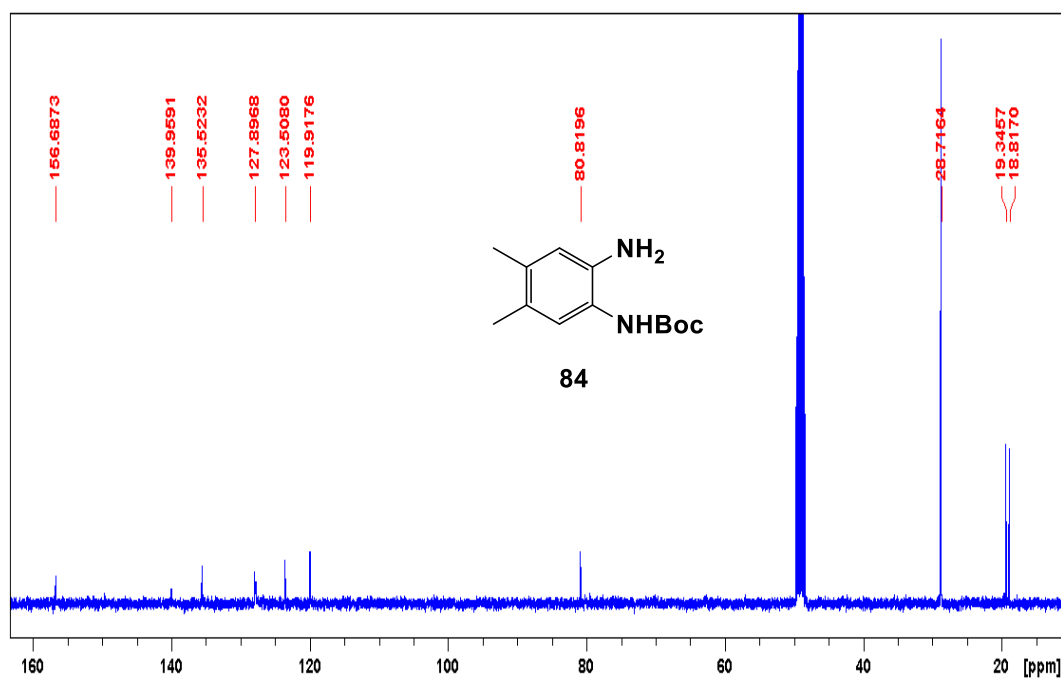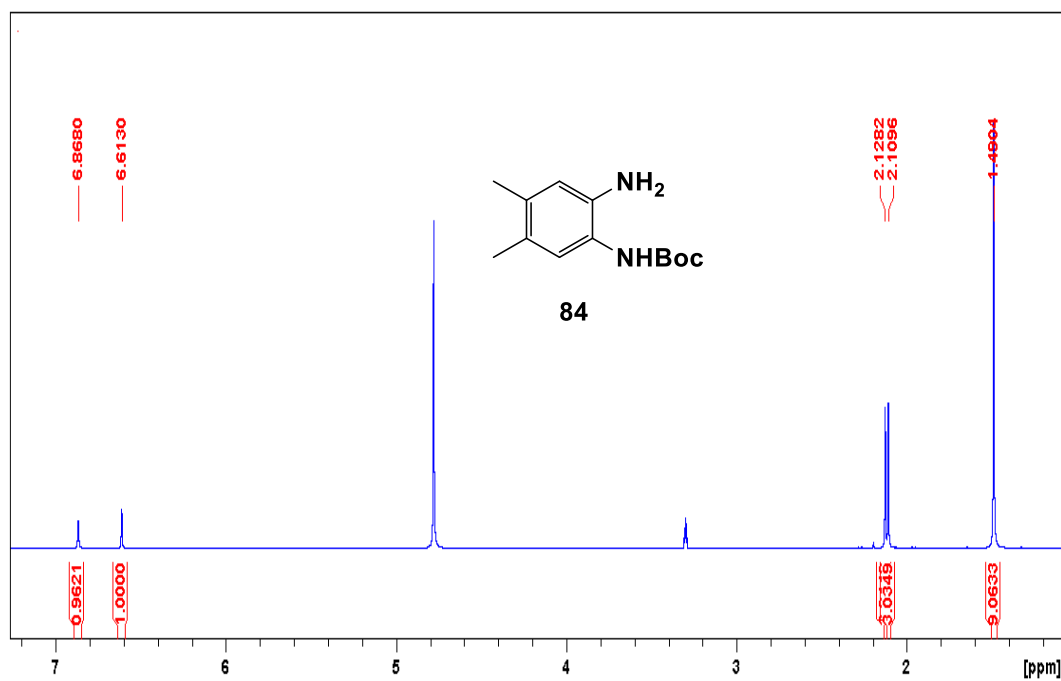
Figure A10. ^{1}H and ^{13}C NMR of 2-(Boc)amino-4,5-dimethylaniline (84)
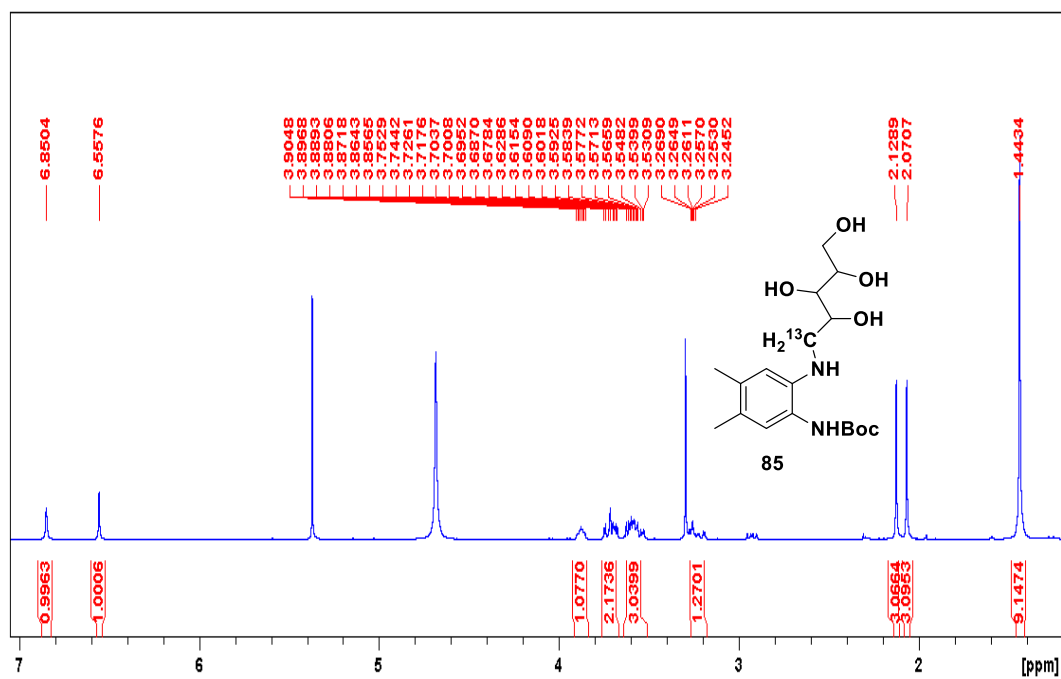
Figure A11. ^{1}H NMR of 85
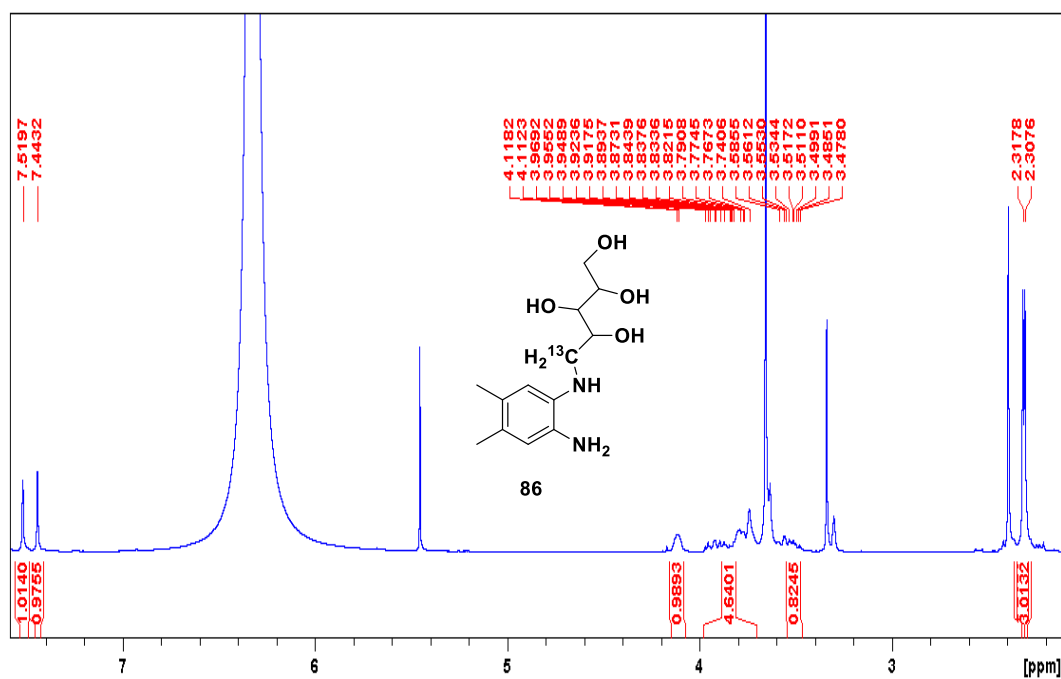
Figure A12. ^{1}H NMR of 86
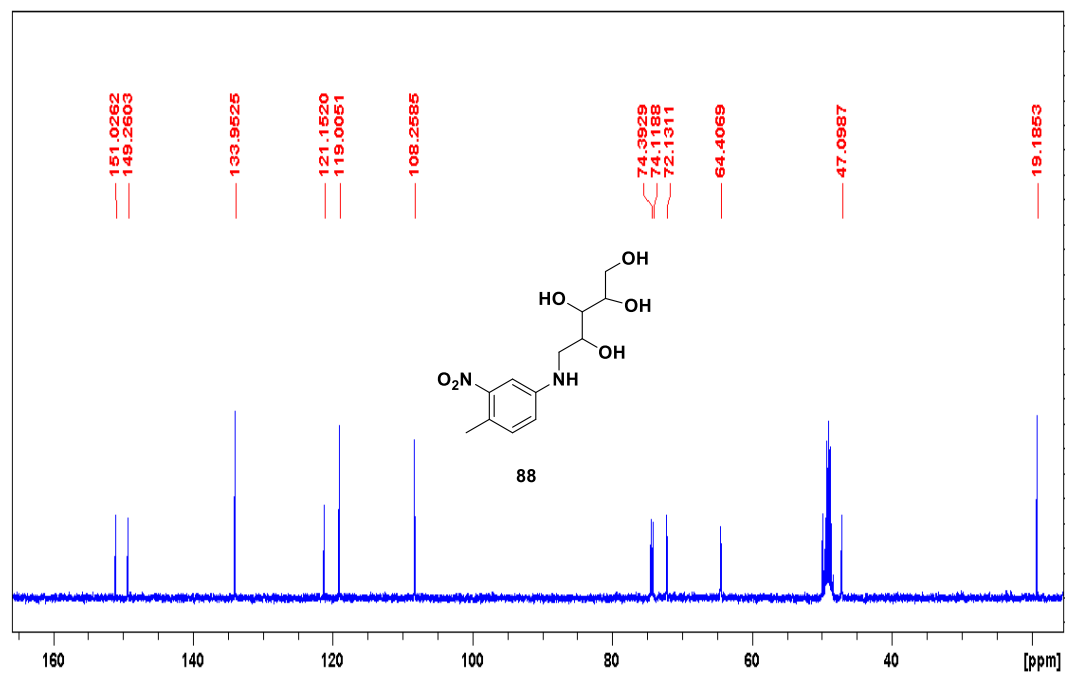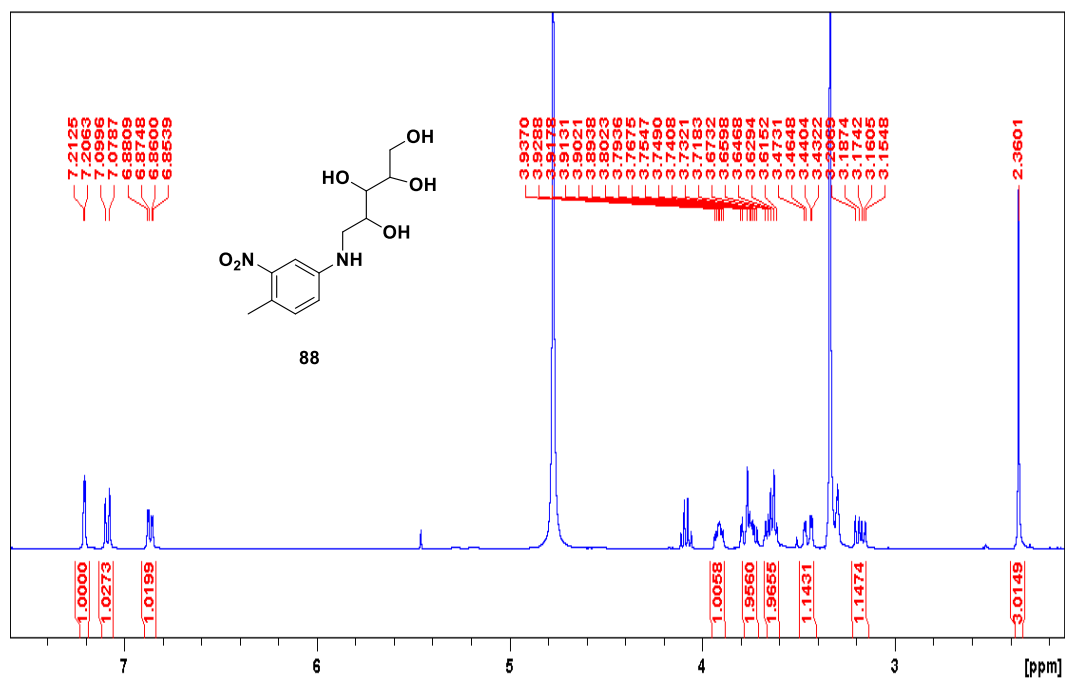
Figure A13. ^{1}H and ^{13}C NMR of 88
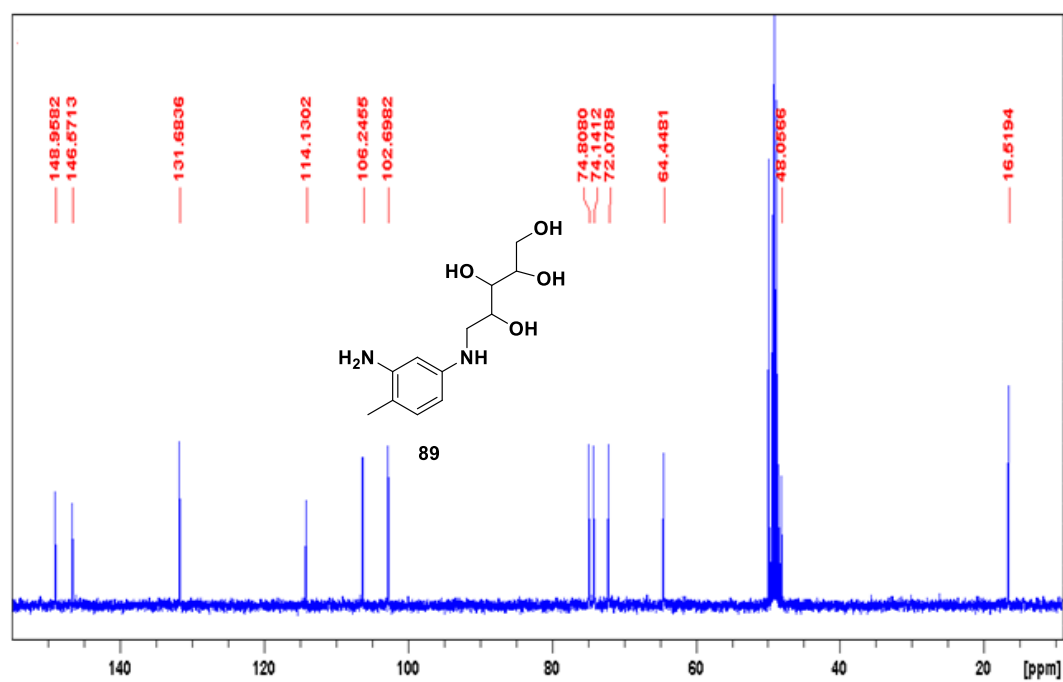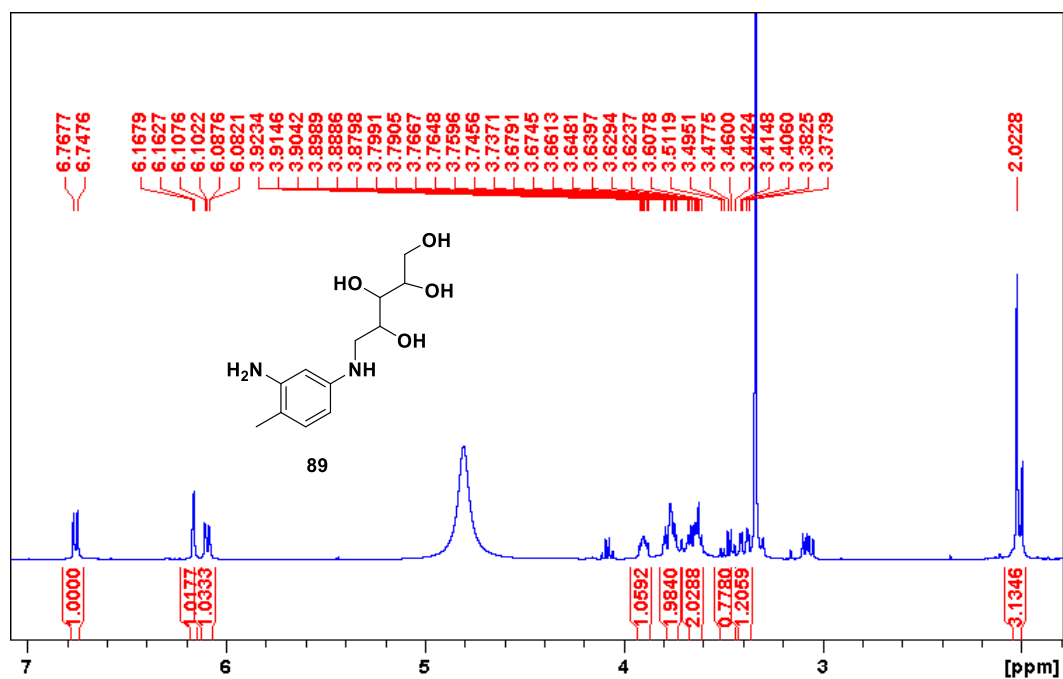
Figure A14. ^{1}H and ^{13}C NMR of 89
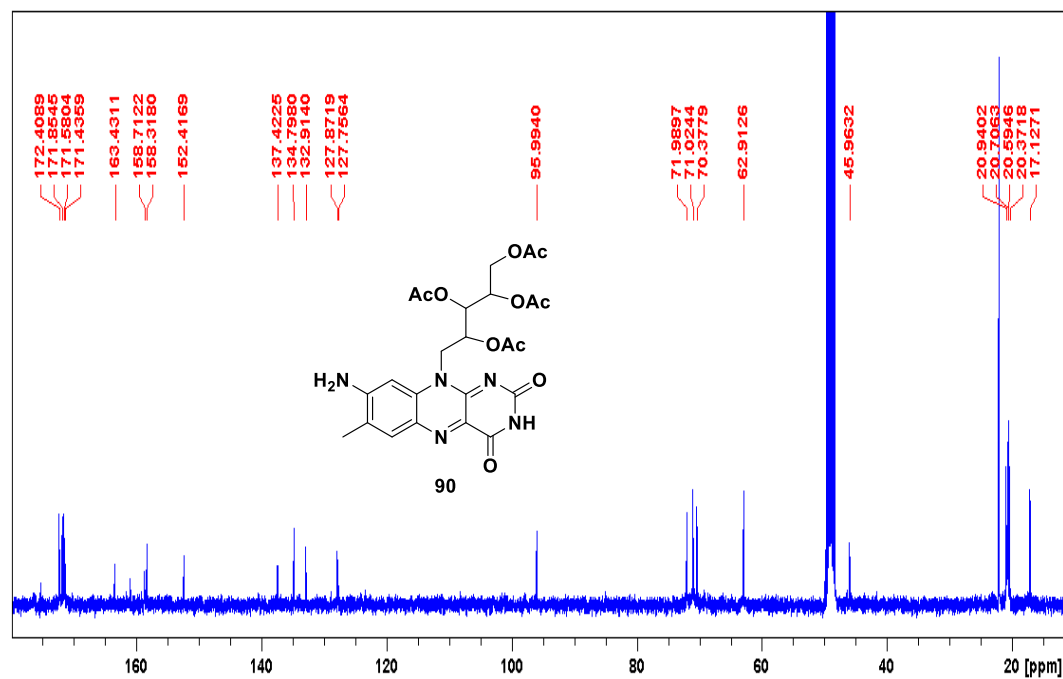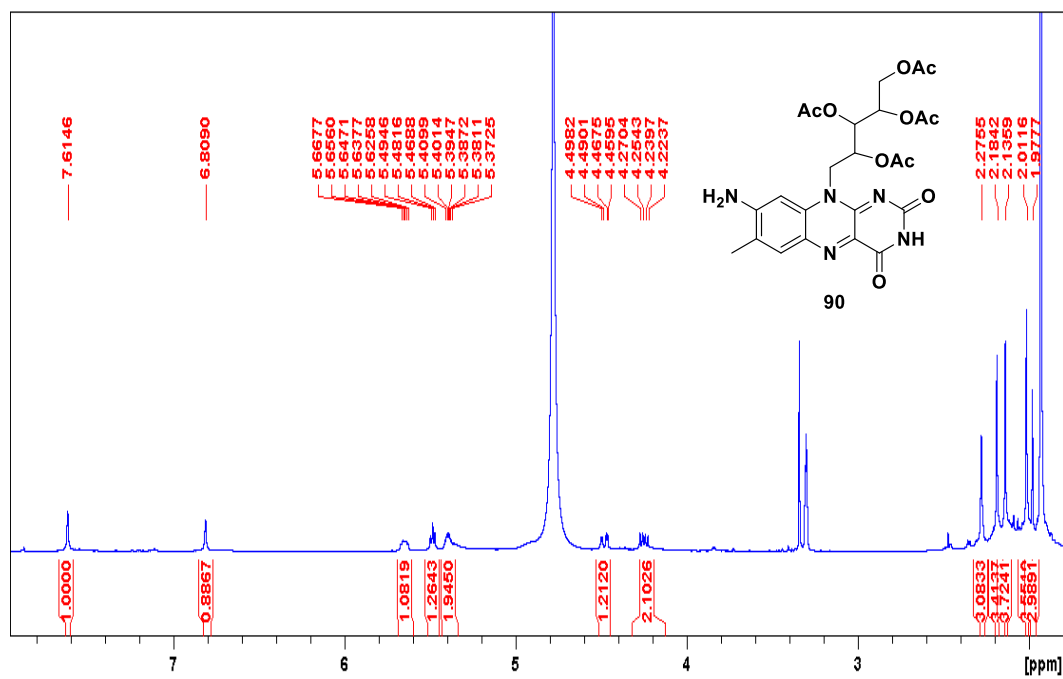
Figure A15. ^{1}H and ^{13}C NMR of 8-Aminoriboflavintetraacetate (90)
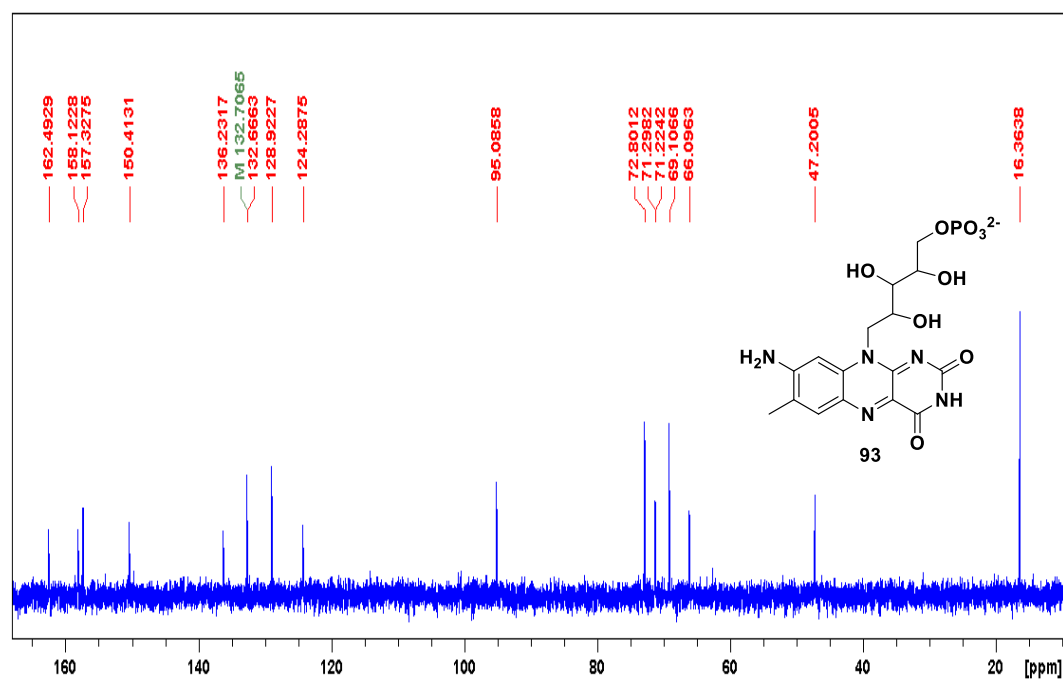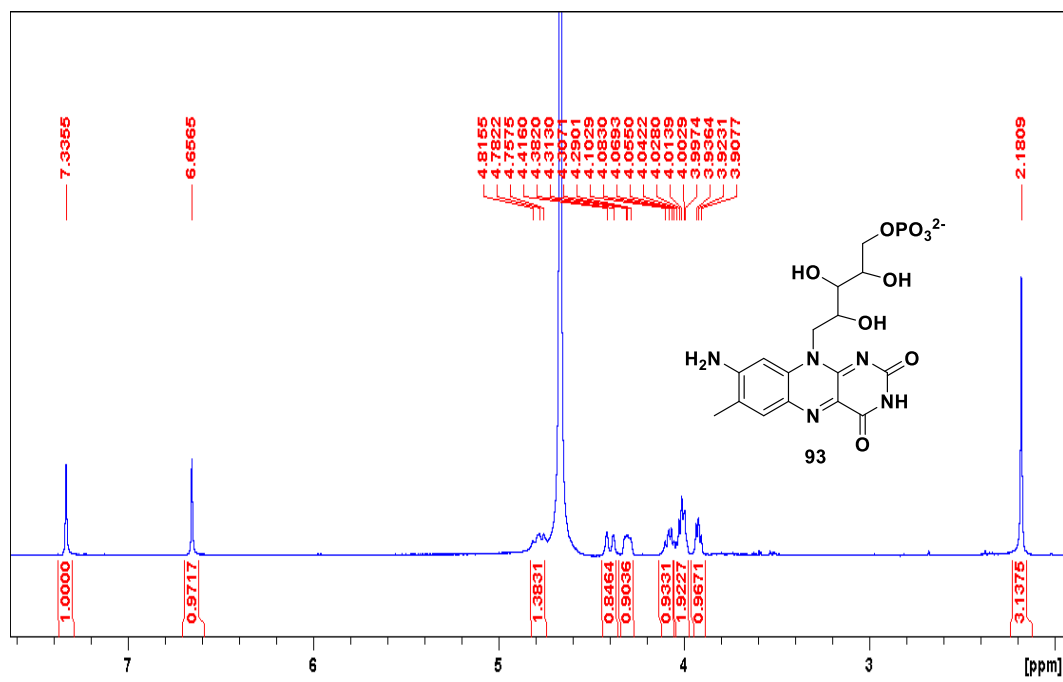
Figure A16. ^{1}H and ^{13}C NMR of 8-Aminoflavinmononucleotide (93)
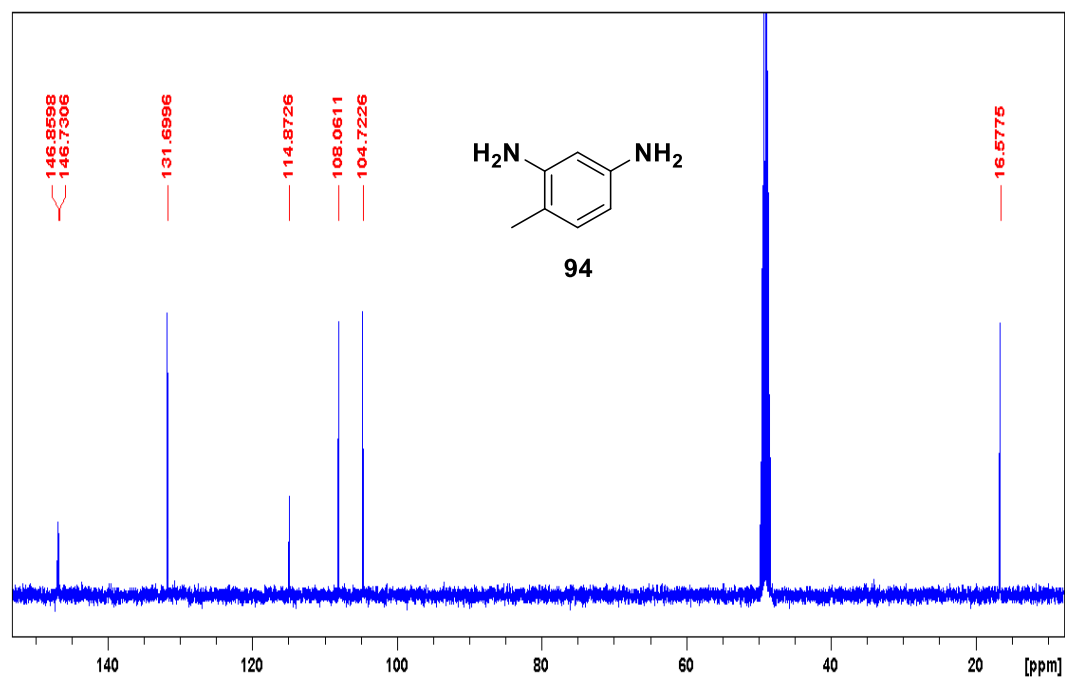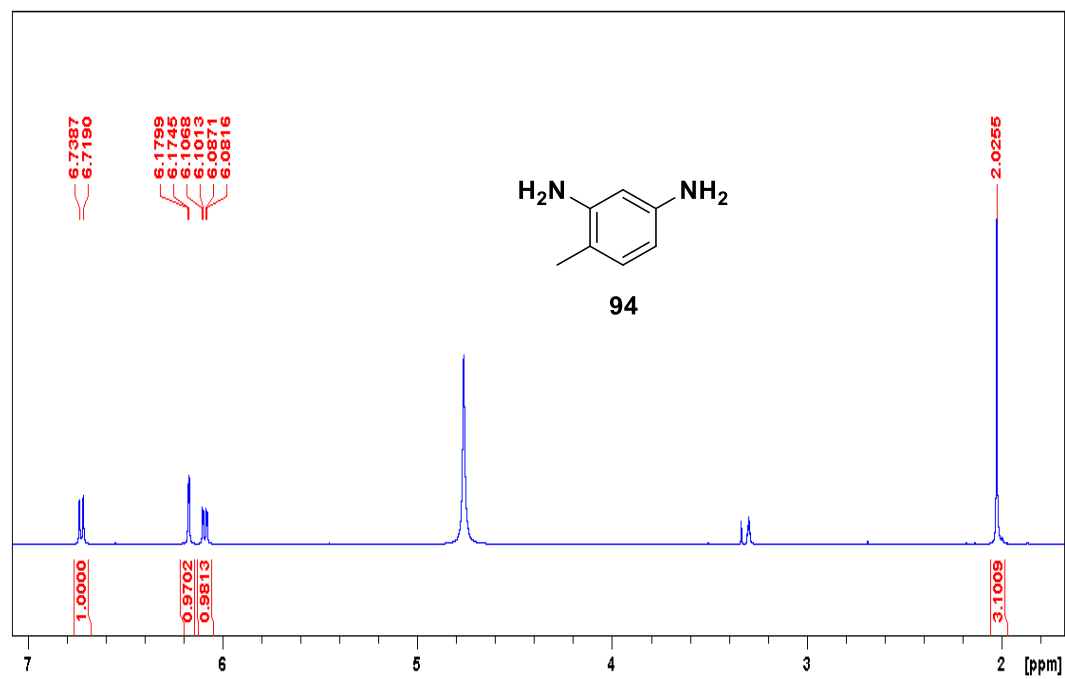
Figure A17. ^{1}H and ^{13}C NMR of 4-Methylbenzene-1,3-diamine (94)
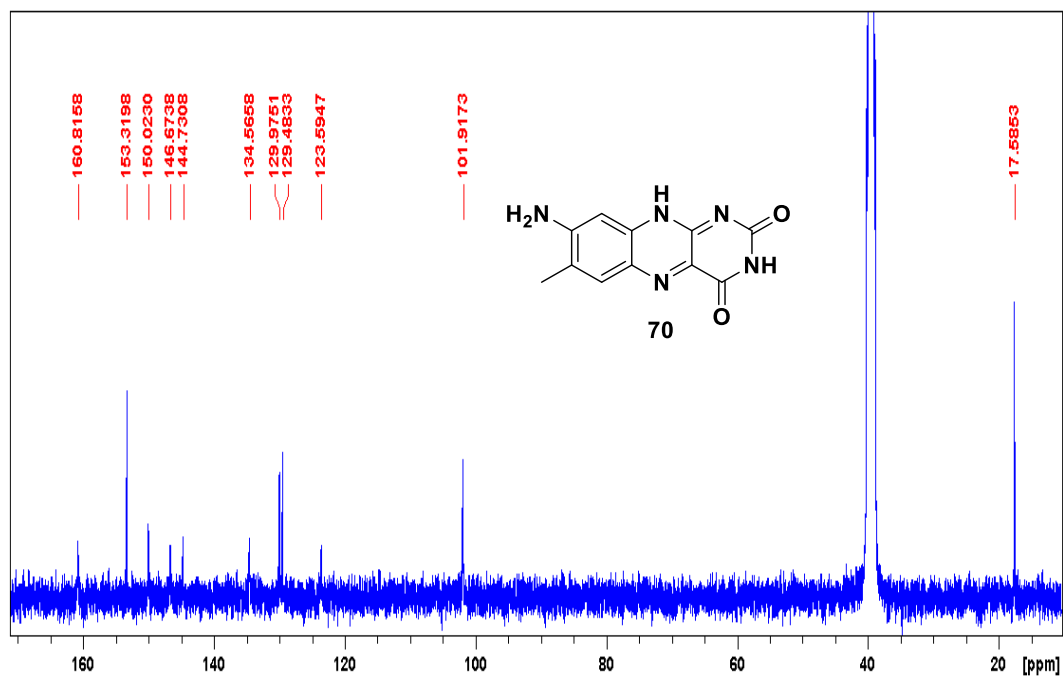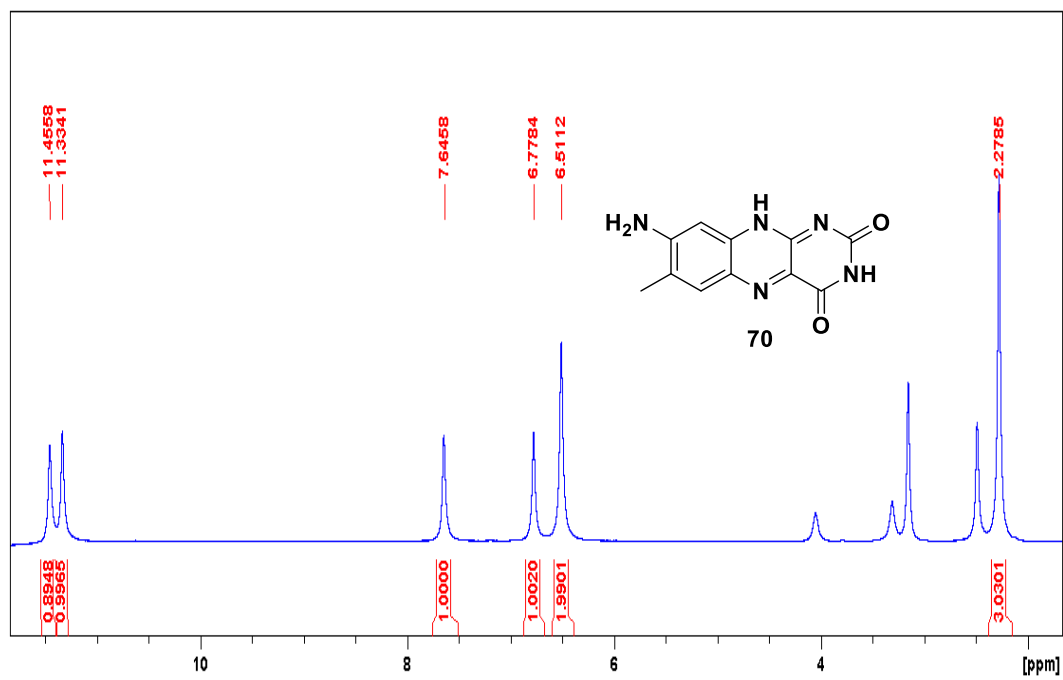
Figure A18. ^{1}H and ^{13}C NMR of 8-NH$_2$ lumichrome (70)
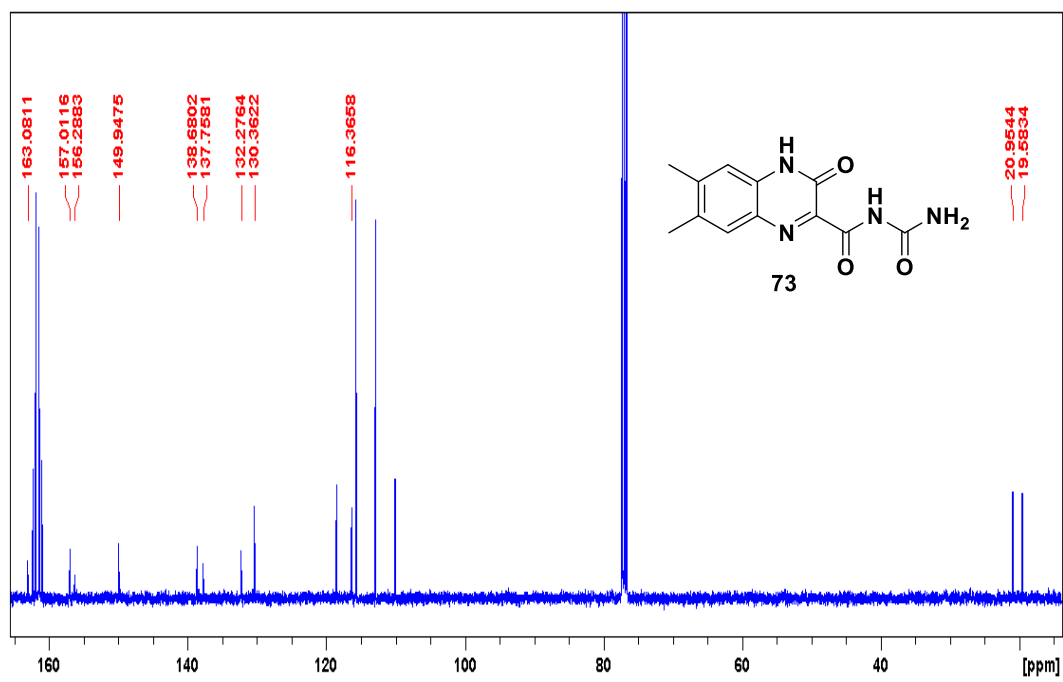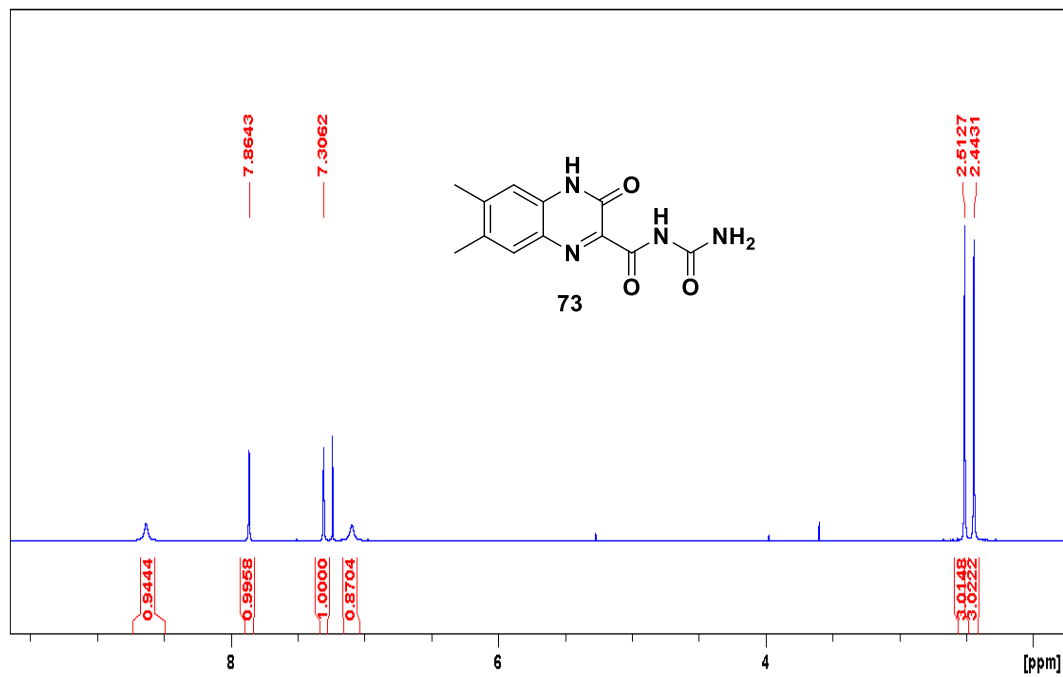
Figure A19. ^{1}H and ^{13}C NMR of 73
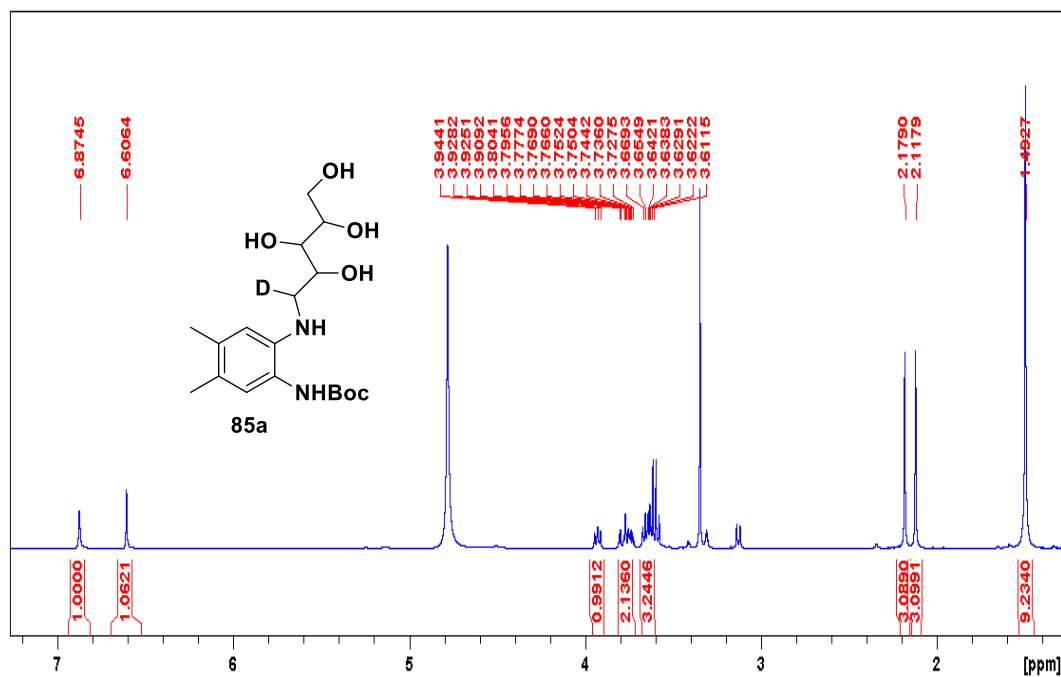
Figure A20. ^{1}H NMR of 85a
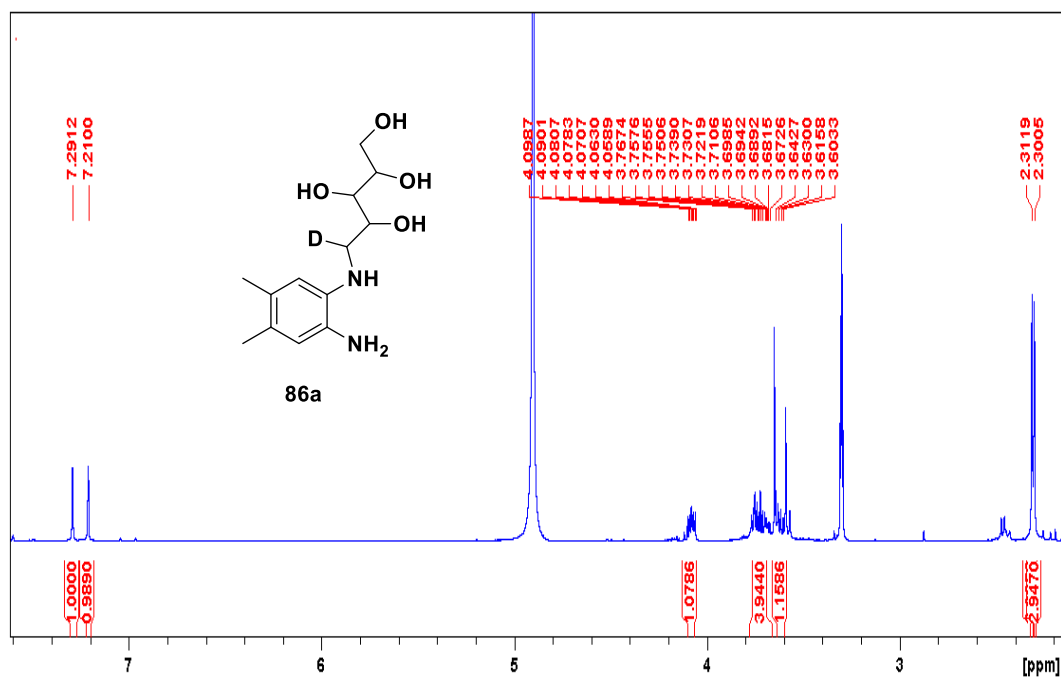
Figure A21. ^{1}H NMR of 86a
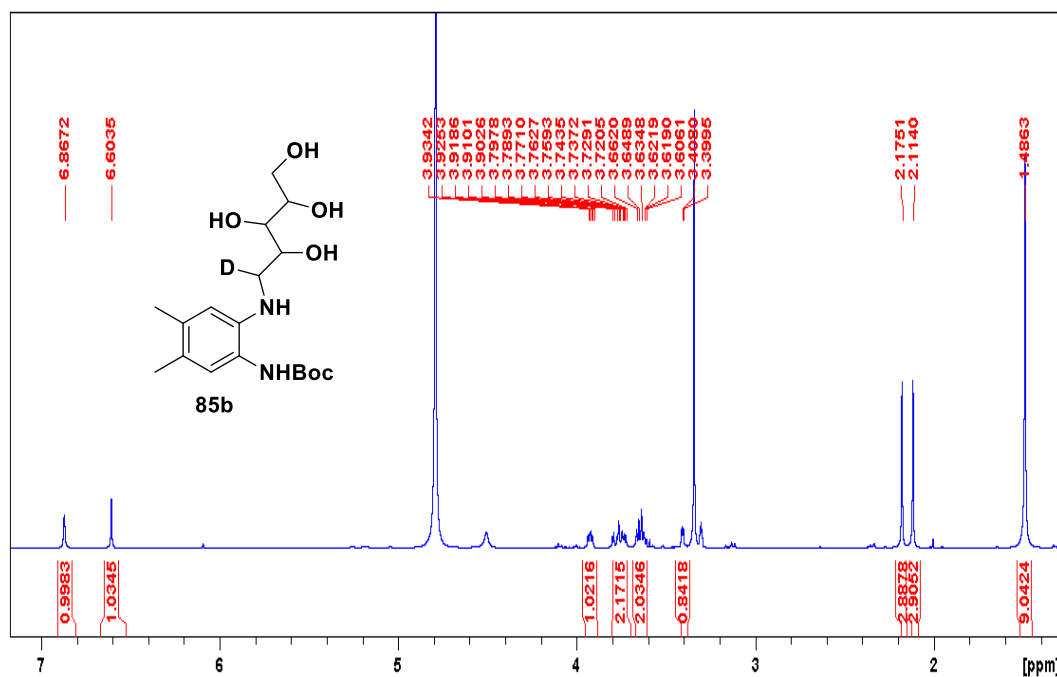
Figure A22. ^{1}H NMR of 85b
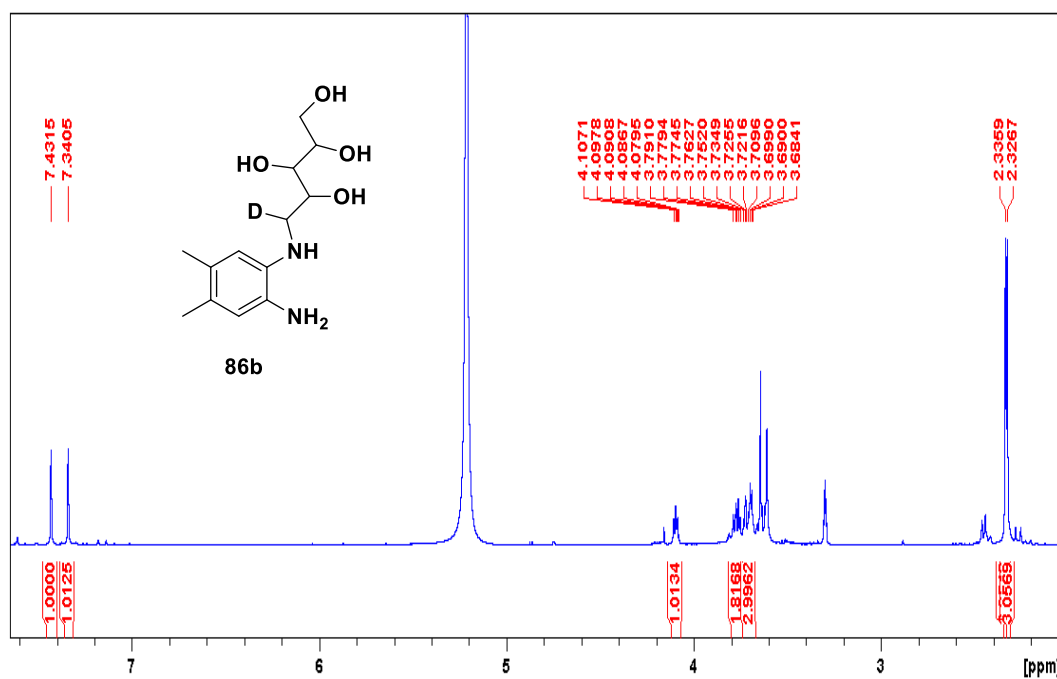
Figure A23. ^{1}H NMR of 86b
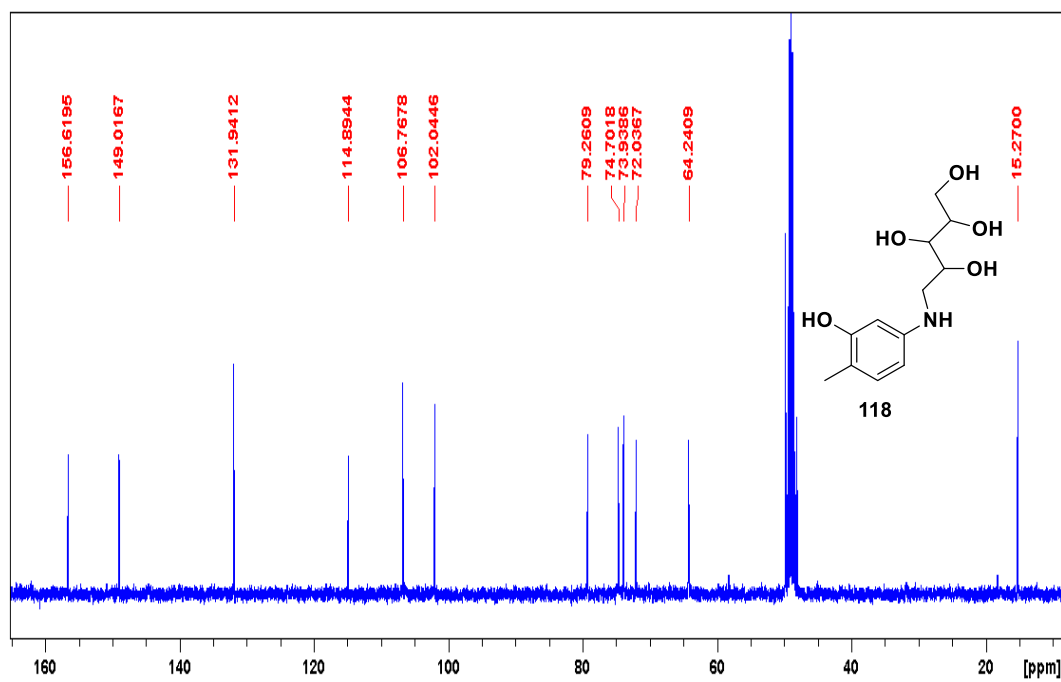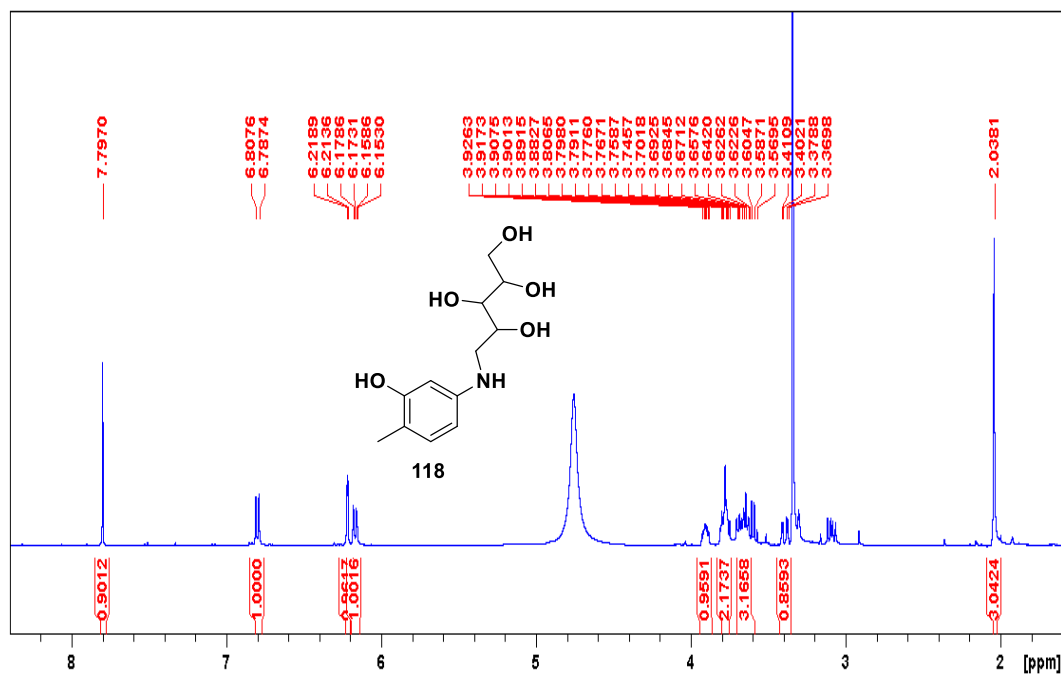
Figure A24. ^{1}H and ^{13}C NMR of 118
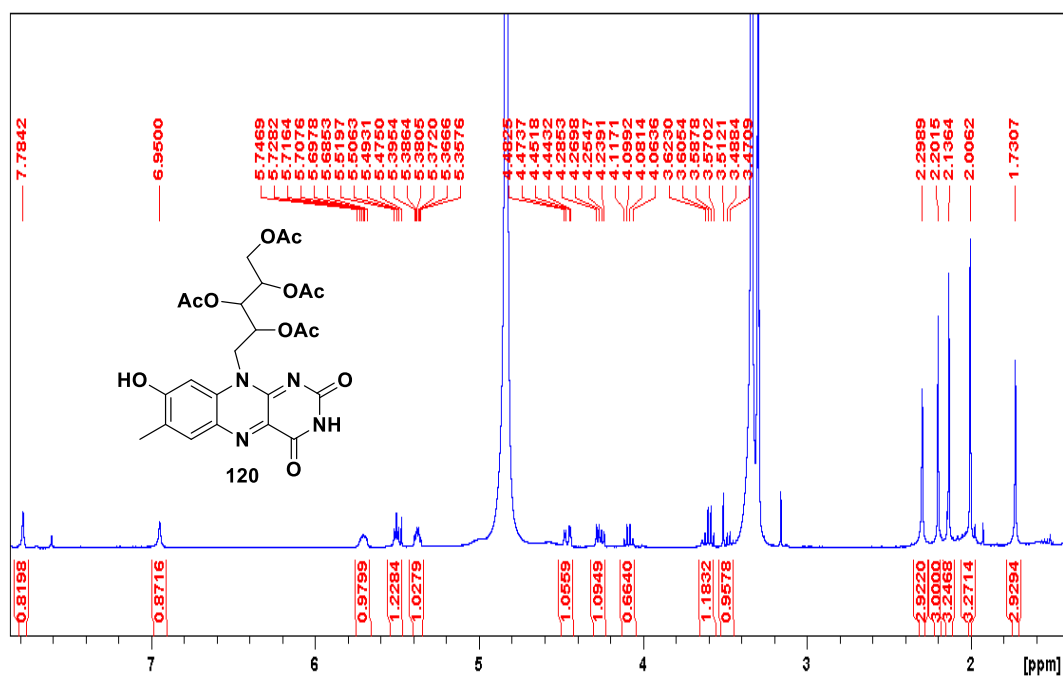
Figure A25. ^{1}H and ^{13}C NMR of 8-Hydroxyriboflavintetraacetate (120)
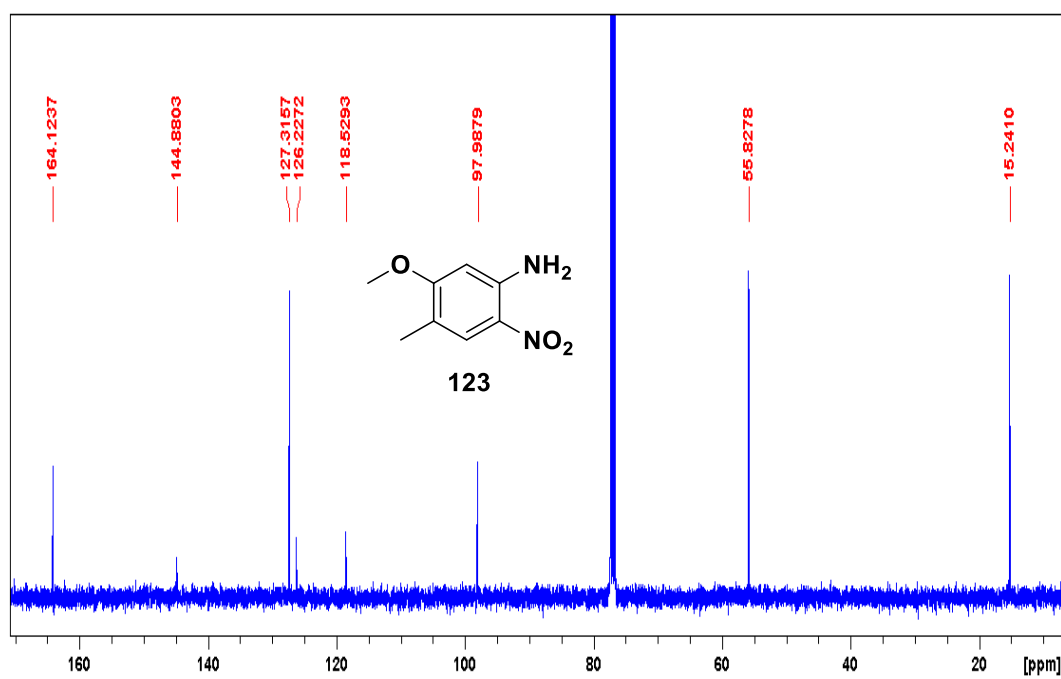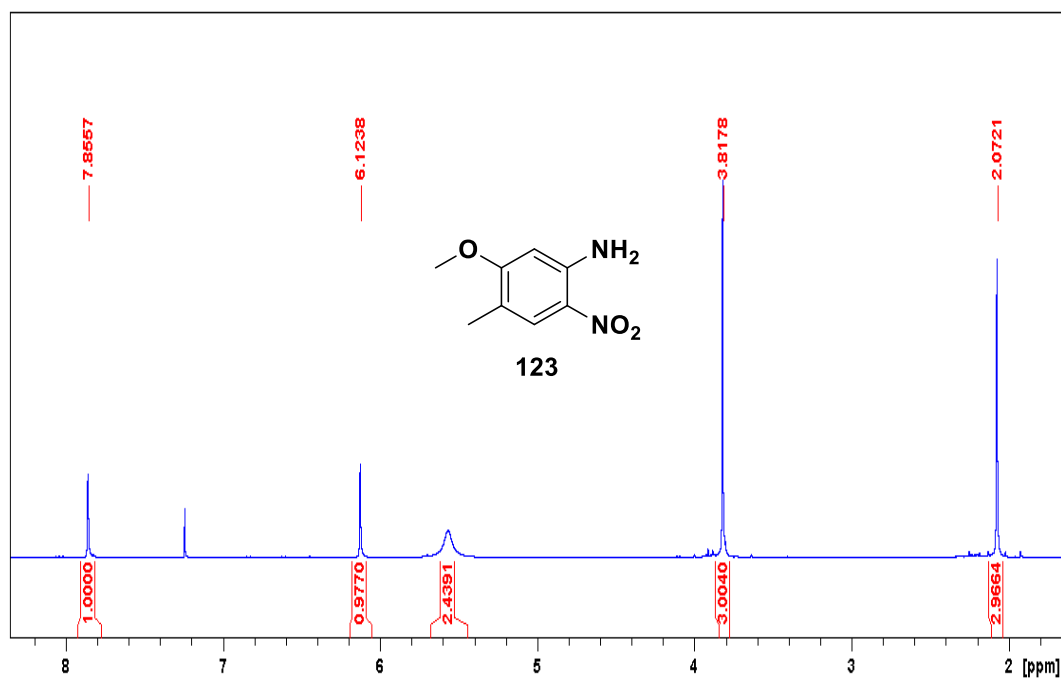
Figure A26. ^1H and ^{13}C NMR of 5-Methoxy-4-methyl-2-nitroaniline (123)
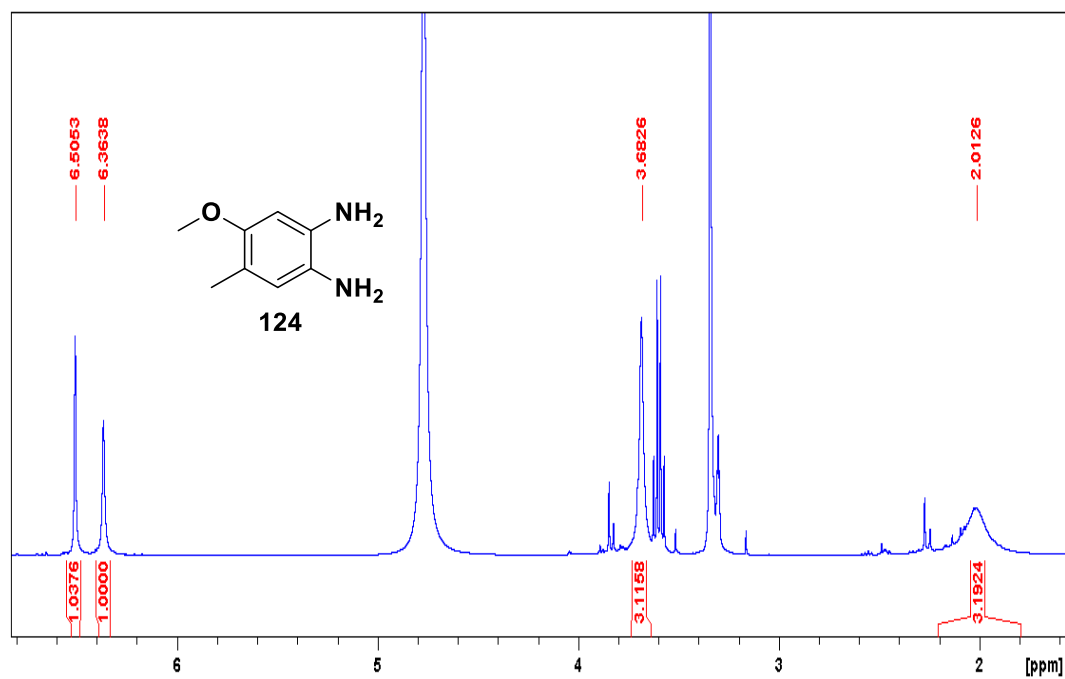
Figure A27. ^{1}H NMR of 4-Methoxy-5-methylbenzene-1,2-diamine (124)
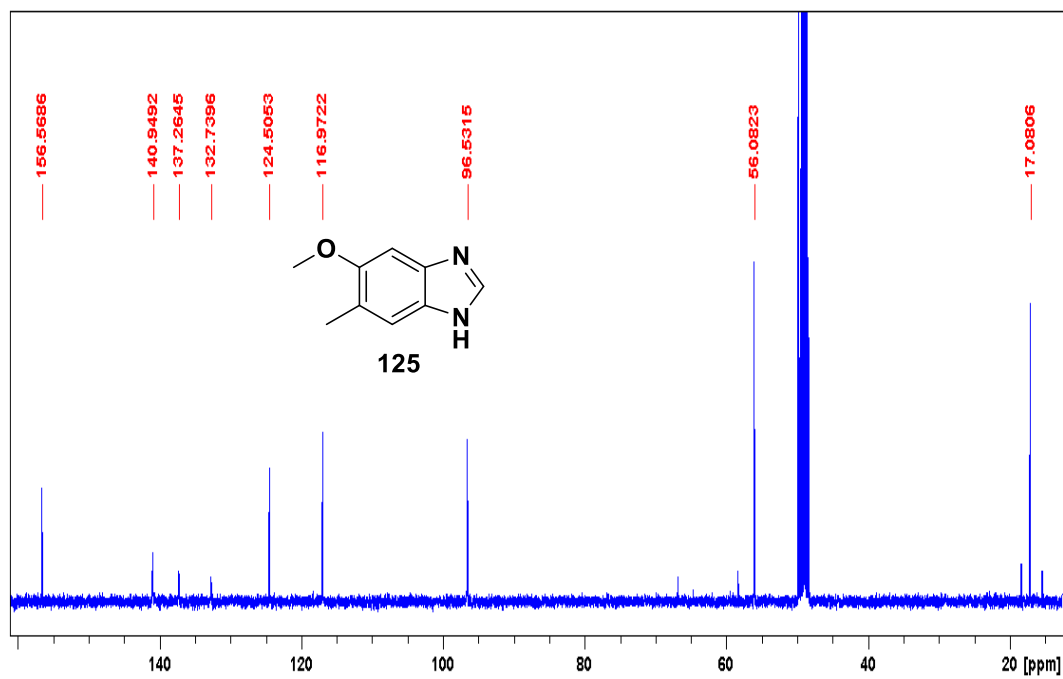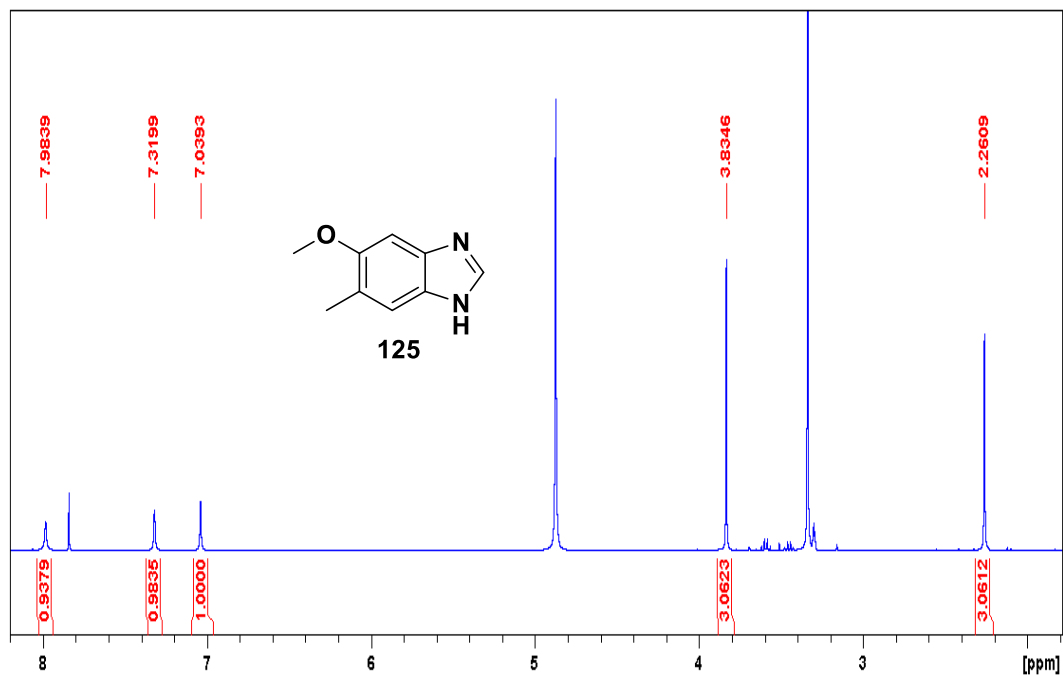
Figure A28. ^{1}H and ^{13}C NMR of 5-Methoxy-6-methylbenzimidazole (125)
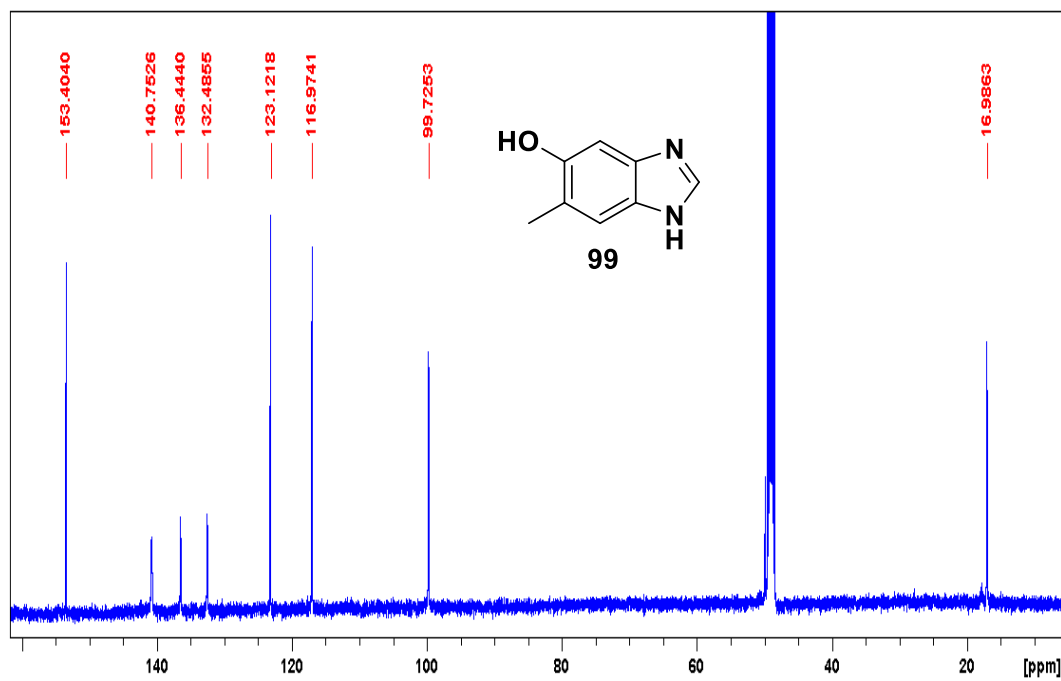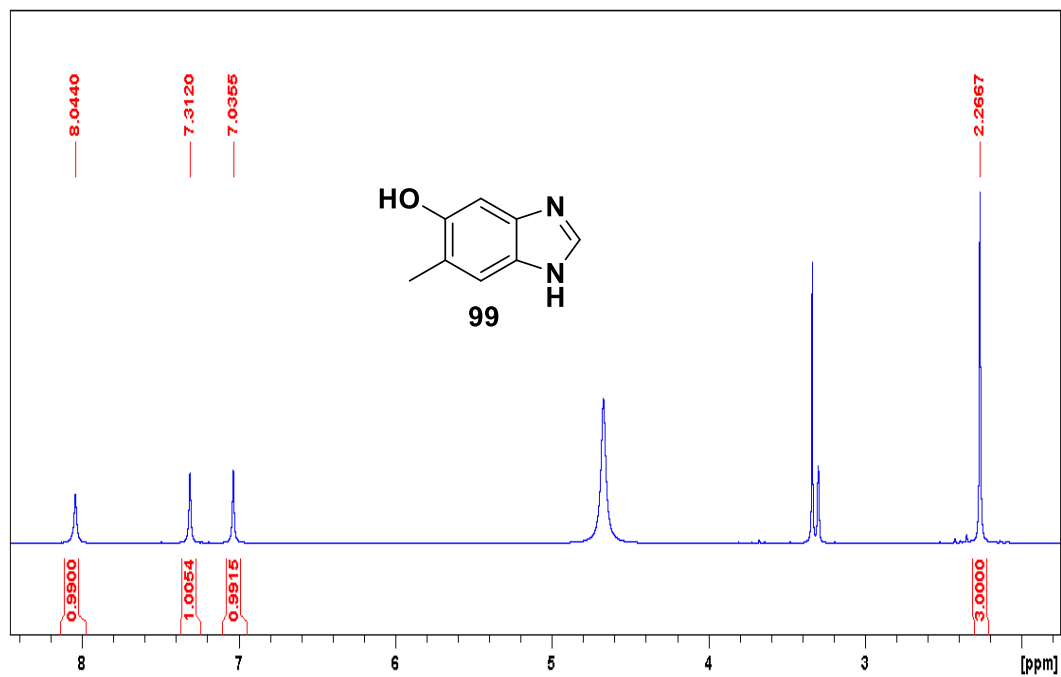
Figure A29. ^{1}H and ^{13}C NMR of 5-OH DMB (**99**)
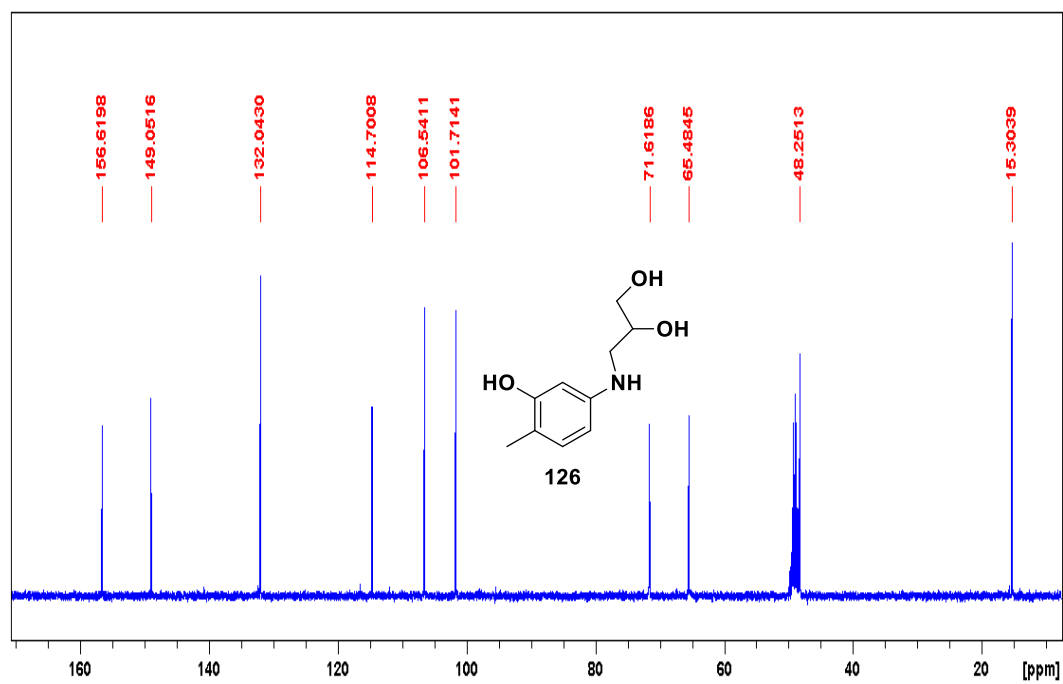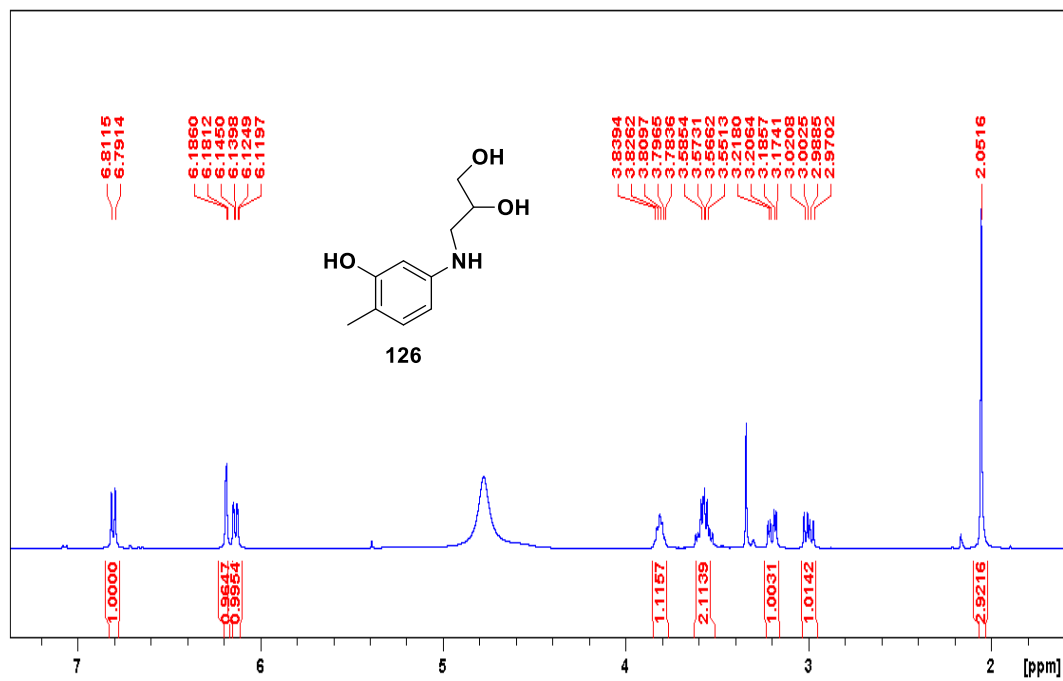
Figure A30. ^{1}H and ^{13}C NMR of 126
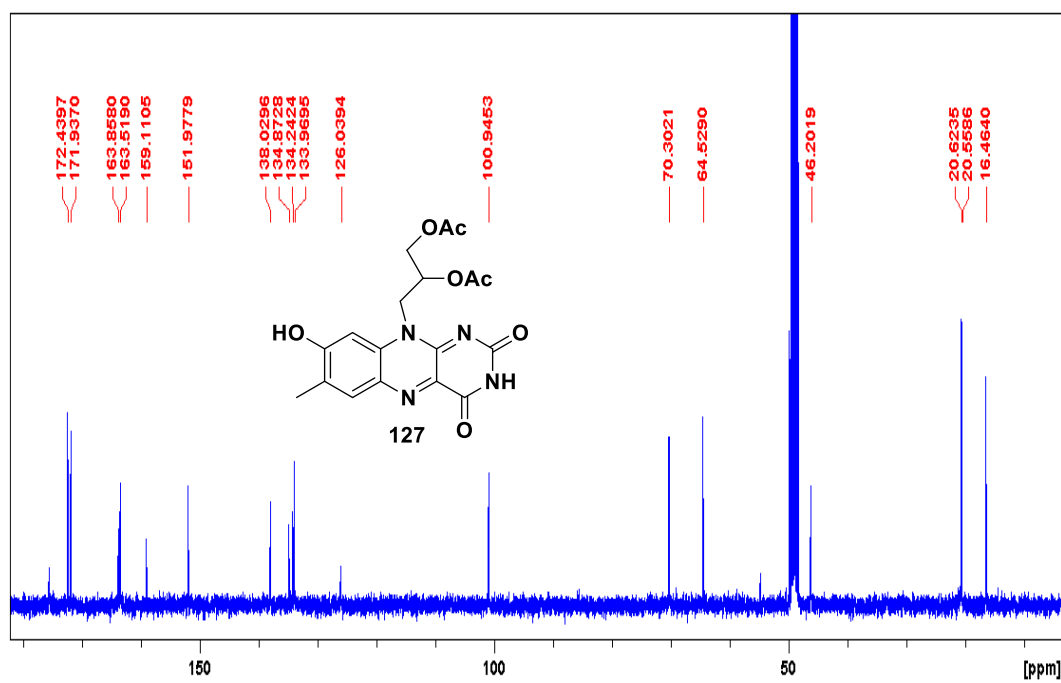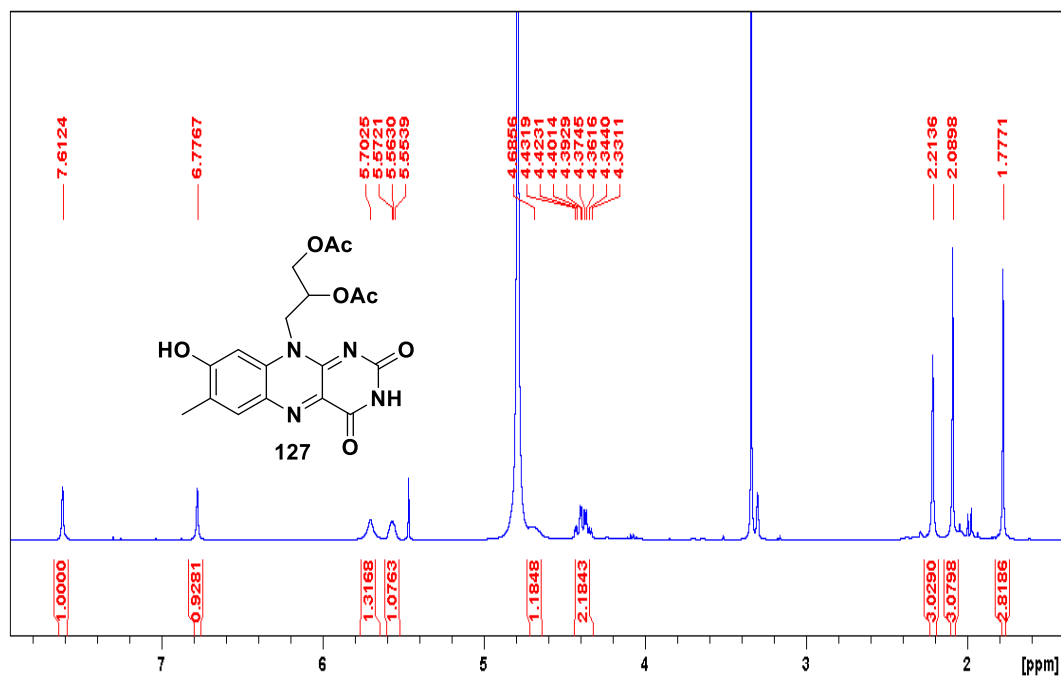
Figure A31. ^{1}H and ^{13}C NMR of 127